REMARKS

Claims 1-14, 19 and 20 are pending. Claims 2 and 10 are amended herein. Claims 15-18 are withdrawn. Reconsideration and further examination is respectfully requested.

On December 12, 2007, Applicant's representative conducted an interview with Examiner Suzanne Lo and Supervisory Examiner Kamini Shah. In this interview, the pending rejections of claims 1, 2 and 10 were discussed in view of Optimal Technologies ("Operations Review of June 14, 2000 PG&E Bay Area System Events Using Aempfast Software"). Agreement regarding claims 1, 2 and 10 was not reached.

During the interview, Applicant's representative explained differences between the prior art method of load flow analysis of electric power networks and the claimed method of analyzing an electric power network by "integrating the model of the transmission-level buses with the model of the distribution-level buses, wherein the single mathematical model further models the interdependency of the plurality of transmission lines and the plurality of transmission electrical elements included in the model of the transmission level buses and the plurality of distribution lines and the plurality of distribution electrical elements included in the model of the distribution-level buses." In particular, Applicant's representative pointed out that conventional electric power modeling methods separately model transmission-level buses and distribution level-buses, that transmission-level models at most, incorporate a simplified approximate of all distribution-level buses into a model of transmission-level buses, and that distribution models do not also incorporate upstream transmission. The Examiner and the Supervisory Examiner requested that Applicant's representative submit disclosures describing conventional load-flow analysis of power networks and any available reports on the use of the Aempfast software disclosed in the Optimal Technologies reference. Accordingly, to advance prosecution of this

application, Applicant has submitted the requested disclosures describing conventional load-flow analysis.

Additionally, Examiner recommended amending claims 2 and 10 to remove "load flow analysis." As suggested by the Examiner, claims 2 and 10 have been amended to remove "load flow analysis" and to more clearly describe the claimed invention.

It is understood that the allowance of the claims is subject to any further searches conducted by the examiner. When conducting any further search and/or application of prior art, the examiner is urged to consider that the claimed feature of "integrating the model of the transmission-level buses with the model of the distribution-level buses, wherein the single mathematical model further models the interdependency of the plurality of transmission lines and the plurality of transmission electrical elements included in the model of the transmission level buses and the plurality of distribution lines and the plurality of distribution electrical elements included in the model of the distribution-level buses," is distinguishable from conventional load-flow analysis of electric power networks.

Claims 1-14 and 19-20 have been rejected under 35 U.S.C. §102(a) as being anticipated by Optimal Technologies. This rejection is respectfully traversed.

Claims 1, 2, 10 and 19 variously recite "generating a single mathematical model by integrating the model of the transmission-level buses with the model of the distribution-level buses, wherein the single mathematical model further models the interdependency of the plurality of transmission lines and the plurality of transmission electrical elements included in the model of the transmission level buses and the plurality of distribution lines and the plurality of distribution electrical elements included in the model of the distribution-level buses."

These aspects of the claimed invention promote comprehensive assessment of the effects of an electric power network by analyzing both transmission system and distribution system effects using a single mathematical model including effects caused by the interdependency of a plurality of transmission lines and a plurality of transmission electrical elements with a plurality of distribution lines and a plurality of distribution electrical elements. These aspects of the claimed invention permit interdependencies between transmission-level effects from transmission lines and transmission electrical elements and distribution-level effects from distribution lines and distribution electrical elements to be included in energy network analysis, improving the accuracy of the evaluation. Further, these aspects of the claimed invention enable assessment of the behavior of the entire electric power network at multiple distribution-level buses. These aspects are submitted not to be disclosed or suggested by the cited reference.

Specifically, Optimal Technologies is understood to disclose analyzing a power network (page 7, §1, ¶¶ 1-4). Optimal Technologies discloses identifying loads that contribute to voltage collapse and ranking generators according to their output ability. (page 13, § 3, ¶ 1) However, there is no disclosure of the type of modeling used to perform this ranking. Merely ranking devices does not disclose a "single mathematical model" that "models the interdependency of the plurality of transmission lines and the plurality of transmission electrical elements included in the model of the transmission level buses and the plurality of distribution lines and the plurality of distribution electrical elements included in the model of the distribution-level buses," as use of separate models for transmission and distribution networks permits the same ranking. Hence, the analysis disclosed in Optimal Technologies does not specify whether a distribution-level model, transmission-level model or other type of model is used to identify loads or rank generators.

In contrast, Optimal Technologies discloses a conventional power network analysis technique receive a dataset from a Cal ISO data file, reformat the dataset and perform conventional load flow analysis on the dataset (page 19, §§ 6.1-6.1.2; page 19, table 3). It is respectfully noted that, as known in the art, Cal ISO regulates and plans high-voltage transmission and does not integrate any data describing a plurality of distribution electrical elements into a dataset (*See* www.caiso.com). In comparing Tables 3 and 4, it is noted that there is no difference in the number of buses, branches, generators or loads analyzed. Hence, examination of Table 4 indicates that Aempfast does not add one or more distribution electrical elements to the original data set (page 20, § 6.2; Table 4). As Optimal Technologies does not disclose that the "ranking of possible additions to system resources" based on "contribution to system stability and power flow" cited by the Examiner uses a modeling technique other than conventional techniques which separately model transmission and distribution systems. Thus, Optimal Technologies fails to disclose the claimed element of "generating a single mathematical model by integrating the model of the transmission-level buses with the model of the distribution-level buses, wherein the single mathematical model further models the interdependency of the plurality of transmission lines and the plurality of transmission electrical elements included in the model of the transmission level buses and the plurality of distribution lines and the plurality of distribution electrical elements included in the model of the distribution-level buses." (emphasis added)

To clarify the preceding arguments, disclosures describing conventional load-flow analysis techniques, as requested by the Examiner and the Supervisory Examiner a telephone interview on December 12, 2007, are attached as an appendix to this amendment and response. Included in the appendix are "Distributed and Electric Power System Aggregation Model and Field Configuration Equivalency Validation Testing" by Davis et al., (NREL/SR-560-33909 and

published in 2003, hereinafter "Davis"), "Knowledge Representation for Power System Modeling" by A. deVos et al. (published 2001, hereinafter "deVos") and U.S. Patent No. 7,096,175 to Rehtanz et al. (hereinafter "Rehtanz"). Additionally in the Appendix, an ISBN number identifying "Distribution System Modeling and Analysis" by Kersting (published 2001, hereinafter "Kersting") is provided, so that the Examiner may review the disclosure in its entirety. To aid in advancement of prosecution, these disclosures are briefly discussed below.

Kersting draws a clear distinction between both a distribution system and a transmission system and the tools or techniques used for modeling transmission systems or distribution systems. As described in Kersting, a distribution system starts with a distribution substation that is fed by one or more sub-transmission lines. According to this description, a transmission network addresses a segment of the electric power network which provides power to the distribution substation; a distribution network then, in turn, distributes the received power from the distribution substation to one or more users (Kersting, page 2). Further, Kersting clearly distinguishes between modeling tools for distribution systems and transmission, or "interconnected," systems. In particular, Kersting explicitly provides that: "The operation of these large interconnected networks required the development of new analysis and operational techniques. Meanwhile the distribution systems continue to deliver power to the ultimate user's meter with little or no analysis" (Kersting, page 9). Hence, Kersting describes a clear difference in the computation necessary to model transmission systems or distribution systems.

Davis similarly distinguishes between transmission systems and distribution systems, describing transmission systems as including large, central-station plants interconnected via a high voltage transmission system which delivers power to end-users through separate, lower-voltage, local distribution networks (Davis, page 1). Further, the modeling approach disclosed in Davis is representative of conventional distribution modeling, where individual circuits are

modeled. In contrast, it is noted that the claimed method integrates "the model of the transmission-level buses with the model of the distribution-level buses, wherein the single mathematical model further models the interdependency of the plurality of transmission lines and the plurality of transmission electrical elements included in the model of the transmission level buses and the plurality of distribution lines and the plurality of distribution electrical elements included in the model of the distribution-level buses." The conventional modeling techniques disclosed in Davis select different distribution circuits and develop different models for each selected distribution circuit. Rather than combine multiple data into a single model, Davis describes the conventional method of individually modeling multiple distribution circuits independent of transmission systems (Davis, pages 3-4).

Further, deVos distinctly describes different factors associated with modeling transmission systems and distribution systems. In particular, deVos discloses that multiple overlapping models must be created and coordinated to model transmission systems while the constant expansion and rearrangement of distribution networks must be accounted for in distribution system modeling. DeVos further provides that transmission system models are ill-suited to model this expansion and rearrangement of distribution networks (deVos, page 1, col. 2 ¶ 3; page 2, FIGS. 1,-3; page 1, col. 2, ¶ 4). Additionally, the modeling approach described in deVos, uses two models having a limited number of common elements. One of the models relates to the SCADA control tier, which is commonly associated with transmission and/or sub-transmission networks. DeVos goes on to disclose a separate model related to substation management, which is commonly associated with distribution control. At most, deVos describes concurrently managing updating the two separate models rather than generating a single mathematical model including both models and interdependencies between various elements in each model (deVos page 5, col. 2, ¶ 8).

Finally, Rehtanz, which was cited in the prior office action by the Examiner, clearly shows conventional load-flow analysis of a power transmission network. Specifically, Rehtanz discloses modeling the stability of an electric power transmission network (Rehtanz, col. 1, lines 6-10). The modeling disclosed in Rehtanz approximates the effects of a distribution network by including only load parameters indicating the static or stationary behavior of loads such as distribution networks by representing the distribution network as a single element, generating a gross approximation of the distribution network as a whole (col. 5, lines 32-34; col. 3, lines 11-27). Hence, the conventional modeling technique disclosed in Rehtanz merely provides an approximation of an entire distribution network when modeling a transmission network. In contrast, the claimed invention includes "a plurality of distribution lines and a plurality of distribution electrical elements" and "the interdependency of the plurality of transmission lines and the plurality of transmission electrical elements included in the model of the transmission level buses and the plurality of distribution lines and the plurality of distribution electrical elements included in the model of the distribution-level buses," in a single mathematical model. Rather, the conventional modeling technique disclosed in Rehtanz, at most, models a relationship between electrical elements in the transmission model with an approximation of an entire distribution network, which fails to model the interaction between a plurality of electrical elements in the model of the distribution level buses and a plurality of electrical elements in the model of the transmission level buses, as claimed. Hence, the conventional modeling in Rehtanz is only capable of modeling interactions between the entire distribution network modeled as a single element and the plurality of transmission level electrical elements, and cannot simulate "interdependency of the plurality of transmission lines and the plurality of transmission electrical elements included in the model of the transmission level buses and the plurality of distribution

lines and the plurality of distribution electrical elements included in the model of the distribution-level buses," as claimed.

Should the Examiner have additional questions or require further information regarding conventional load-flow analysis techniques or if the Examiner believes that for any reason direct contact with Applicants' representative would help to favorably dispose this case, the Examiner is invited to telephone the undersigned at the number given below. It is respectfully noted that additional disclosures further describing the Aempfast software disclosed in Optimal Technologies could not be obtained at this time.

Hence, in view of conventional power network distribution techniques at the time the Application was filed, there is no disclosure or suggestion of "generating a single mathematical model by integrating the model of the transmission-level buses with the model of the distribution-level buses, wherein the single mathematical model further models the interdependency of the plurality of transmission lines and the plurality of transmission electrical elements included in the model of the transmission level buses and the plurality of distribution lines and the plurality of distribution electrical elements included in the model of the distribution-level buses" as variously recited in claims 1, 2, 10 and 19.

Dependent claims 3-9, 11-14 and 20 variously recite additional patentable features such as: "integrating models of theoretical transmission-level real and reactive energy sources connected to one or more of the plurality of transmission level buses into the single mathematical model," or "integrating additional models of theoretical transmission-level loads into the single mathematical model," or "adding to the single mathematical model the models of the energy sources at one of the distribution-level buses and transmission-level buses, wherein the models of real energy sources are added subject to actual limits appropriate for dispatchable demand reductions available on the electric power network, and the real energy sources with

reactive energy sources are added subject to actual limits appropriate for generation at load sites within the electric power network," or "calculating impacts and effects across the simulated electric power network of the theoretical distribution-level real and reactive energy sources connected on one or more of the plurality of distribution level buses."

These aspects of the claimed invention are not disclosed in Optimal Technologies, which is understood to disclose identifying loads that contribute to voltage collapse and ranking generators according to their output ability without describing the type of model used to rank generators or identify loads (page 13, section 3, paragraph 1). Therefore, Optimal Technologies does not anticipate these claims that are, accordingly, submitted to be patentably distinguishable over the cited art.

Favorable consideration is solicited. Should the Examiner wish to discuss the above Remarks, or if the Examiner believes that for any reason direct contact with Applicants' representative would help to favorably dispose this case, the Examiner is invited to telephone the undersigned at the number given below.

Respectfully submitted,
PETER B. EVANS, ET AL.

Dated: January 17, 2008

By: /Brian G. Brannon/

Brian G. Brannon, Reg. No. 57,219
Fenwick & West LLP
Silicon Valley Center
801 California Street
Mountain View, CA 94041
Tel.: (650) 335-7610
Fax.: (650) 938-5200

23990/08225/DOCS/1845428.1

APPENDIX

Knowledge Representation for Power System Modelling

A. deVos, Member IEEE
Langdale Consultants
Elanora Heights, NSW 2101, Australia

C.T. Rowbotham
Langdale Consultants
Elanora Heights, NSW 2101, Australia

Abstract: Modelling power systems is an area of ongoing interest in the transmission management and control systems community. Continuing development is driven by two forces. The traditional tasks of model maintenance and management must be achieved with fewer resources. At the same time, model exchange and coordination has become a priority. The latter force arises from the disaggregation of utility functions and the introduction of power markets.

This paper begins by identifying some of the power system modelling tasks that have become important, but are ill served by current tools and techniques.

Among these are model versioning and version control, migration of models between different schema, the transformation of models for different purposes or applications, and the merging of models from different sources. These tasks are typically handled by semi-manual methods or heavily customized software.

The paper then describes the application of knowledge representation to power system modelling. In particular, the power of this approach to provide generic solutions to the foregoing problems is explored.

Knowledge representation is contrasted with more common data representations and put into context with current industry initiatives, EPRI CIM, UMS DAF and XML/CIM.

Finally, the feasibility of using knowledge representation for power system models is illustrated with a case study from a major Australian distribution utility.

Keywords: power system modelling, knowledge representation, electronic data interchange, data models, power system control, transmission control, data management, data communication, software standards

I. INTRODUCTION

Models are essential to the operation of modern power systems. Simulation of the power system is necessary for both planning and operations and depends on appropriate models. In the operations arena models are typically more comprehensive than those used for planning. Operational models support analysis of incoming SCADA data as well as simulation of expected and unexpected operational scenarios.

An operational power system model is a relatively complex set of information, involving between 100 and 1000 different classes of information. Moreover, these models are closely tied to telemetry models and loosely tied to a range of other information throughout the utility. Creation, maintenance and verification of models are significant activities for most transmission operators.

The disaggregation of utility functions and the introduction of power markets in many national power systems has increased the model maintenance burden. For example, the split between Regional Transmission Operators (RTO's) and Independent System Operators (ISO's) in the United States means that many overlapping models must be created and coordinated with each other where previously there was a single model. This introduces new problems of model information exchange, and exacerbates old problems of version control and verification.

Distribution authorities also face new modelling tasks with the increasing deployment of Distribution Management Systems (DMS). While the DMS capabilities vary from system to system, all require models of the sub-transmission and feeder network that an earlier generation of control systems did not. In the distribution environment, model maintenance solutions developed for Energy Management Systems (EMS) are rarely suitable. Unlike most main transmission systems, a typical distribution system is subject to constant expansion and rearrangement.

In this context, it is worth revisiting the traditional modelling approaches to find improvements. As an aim, new techniques should enable existing teams to meet the greater challenges they now face. The best techniques would relieve the tedious and error prone aspects of the task, freeing maintainers to apply their judgment and experience to network and control system problems.

II. MODELLING TASKS

A. Model Versions

Maintenance implies the existence of multiple versions of a power system model. As a first approximation we can

envisage these versions to be created and deployed one at a time. Figure 1 shows this arrangement. Each version is created by editing the previous version and deployed simply by committing the edits.

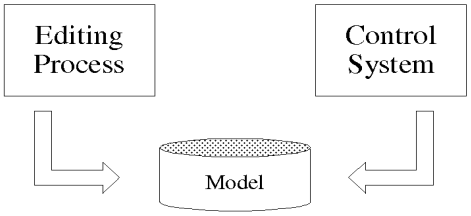

Figure 1

Practical modelling sub-systems are more elaborate than this. There is generally a verification step and the opportunity to make corrections before a model is placed in service. This leads to a data flow more like figure 2.

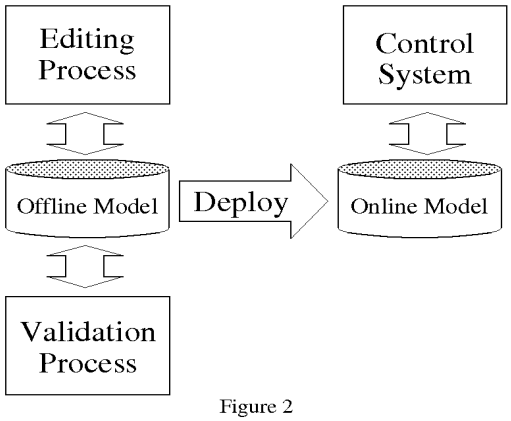

Figure 2

Many modelling sub-systems provide a limited form of parallel development. A typical architecture resembles figure 2 with the addition that the offline model database supports multiple users. In this approach, several maintainers work on the same model version until it is "frozen" for validation and deployment.

It is a methodology best suited to original system configuration or infrequent deployment of large packages of changes. None of the maintainers can validate or deploy their changes until everyone is ready. If, for example, an urgent model change is required, it may not be possible to fit it into the model release schedule.

In a distribution system, changes are deployed on a daily basis and fully parallel development is required. With disaggregation, this may become a requirement for transmission operators as well. In this scenario, several versions of the model are created and validated in parallel as shown in figure 3. (We call them projects.)

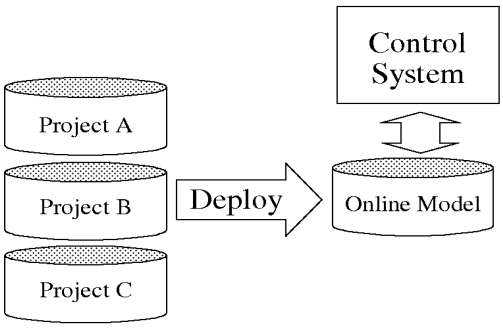

Figure 3

A system that supports parallel development must deal with the "lost update problem". Projects A and B start from the same baseline and develop in parallel. If A is deployed before B, updates that were made in A are apt to be lost, unless they are somehow merged with B.

In practice, modelling systems deal with fully parallel development and the lost update problem with varying degrees of ease and reliability. Ad hoc and semi-manual systems are common.

B. Model Transformations

Power system models and the control systems that use them do not exist in isolation. Frequently, the models used in disparate control systems must be coordinated with each other and with other information systems. This generally requires the transformation of models from one representation and schema to another.

In a distribution system there may be different tiers of control, with a main control system at the top tier and substation or feeder automation at lower tiers. Asset management or geographic information systems may also be coordinated with the control systems. Each will support a different power system model representation, hence the need arises for model transformations. This is illustrated in figure 4.

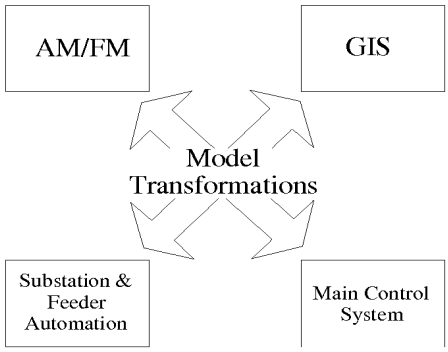

Figure 4

Similarly, the ISO/RTO case involves exchanging models between transmission system operators with disparate control systems and different model schema, see figure 5. In this case, native models are first transformed into a common representation and schema. The proposed standard in the US is a schema [5] derived from the EPRI CIM [4] and represented as XML. This is called the CIM XML language [7].

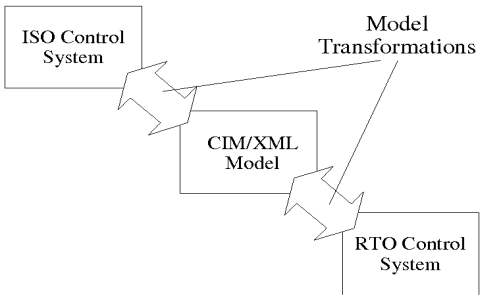

Figure 5

Model transformation solutions are frequently ad hoc, although vendors are beginning to develop converters (sometimes called filters) from their native format to the CIM XML model exchange language. In many cases model transformations remain labour-intensive and error-prone. Maintenance of hard-coded transformation software to track schema changes could also become a burden.

C. Partial Models

Another aspect of the ISO/RTO problem might be termed "the stitching problem", meaning the problem of joining regional models together. Each regional model includes information that must be stripped away before it is stitched into the system model. That includes any overlap or reduced equivalent of the neighbours, the low-voltage network, and attributes that are only relevant to the regional operator.

Because of this overlap stripping, an ISO and an RTO will actually exchange a partial model. Figure 6 shows the whole and partial model for a region, B, with neighbours, A and C.

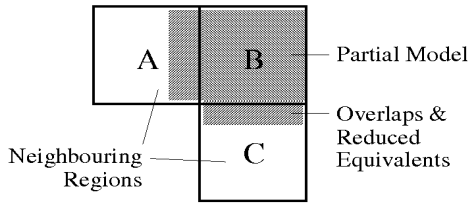

Figure 6

In general, a partial model is one that is incomplete for the intended application. The difference between two versions of a model is another form of partial model. Such difference models can form the basis of a version management strategy within a utility. Difference models are also well suited to the ISO/RTO model exchange scenario.

Partial models, including difference models, represent a challenge for a modelling subsystem. They are nominally invalid because required relationships may be missing. Moreover, the modelling subsystem must preserve information about each partial model even after it is stitched into a complete model. This permits further editing or stitching operations to be performed correctly.

D. Database Solutions

Some of the facilities outlined above prove difficult to implement with the usual modelling vehicle: the database management system. Mainstream database systems employ an interpretation of the relational model of data. In the next section, we will introduce a more flexible alternative for dealing with versions, transformations and partial models.

Here we list the aspects of the relational model, as implemented in mainstream database systems, that tend to limit modelling systems. These observations also apply to object databases although their diversity makes it harder to generalise.

1 Records

The smallest, indivisible unit of information is the tuple or record, which embodies several data fields. While it is possible to make associations between tuples, there is no general mechanism to qualify the fields within a tuple with information about their source or version. Nor is there a general mechanism to provide alternative versions of individual field values.

2 Keys, Table Names and Column Names

Keys, table names and column names are unique only within their respective scopes, local to a database. However, a concept of universal, identity is desirable when dealing with models that span different administrative domains. In other words, keys, table names and field names are likely to be ambiguous when models are exchanged between utilities or between different systems within a utility.

3 Schema Migration

Schema migration is the process of transforming a model to comply with a different schema. In an isolated system, this is required only when the software is upgraded. In the current environment, however, such transformations may occur regularly.

Database systems make dealing with schema differences a difficult task because of their strict enforcement of a single, monolithic schema. For example, this prevents the original and migrated populations from residing in the same system.

Moreover, a complex, multiple pass migration strategy is required to avoid schema constraint violations.

Traditionally, the foregoing issues have been dealt with on a case by case basis by combination of schema design techniques and supporting software. A comprehensive solution requires a new framework layered above the database system. Knowledge Representation provides such a framework.

III. KNOWLEDGE REPRESENTATION

Knowledge representation (KR) is a theory of data that can be applied to modelling tasks. KR concepts can be implemented in markup languages, programming interfaces, data transformation functions and data repositories. Two utility industry standards already use KR concepts to represent power system models:

- The CORBA Data Access Facility (DAF) [6] is an API based on a KR formulation of the EPRI CIM [5] schema.
- The CIM XML language, mentioned in the previous section, is a language for exchanging models. It uses the same KR schema as the DAF.

The attraction of the KR approach to standards is its generality. It can be applied equally well to a variety of control systems with different native model representations. Moreover, it is straightforward to create a concrete KR schema from the abstract EPRI CIM schema, currently formulated in UML. An equivalent relational database schema is not as obvious to derive and not as broadly applicable.

A. Resource Description Framework

The KR framework used in these standards was supplied by a W3C recommendation, the Resource Description Framework (RDF) [1]. RDF contains a KR data model, a syntax for encoding data in XML, and a vocabulary [2] for expressing schema information.

In the RDF data model, a *resource* is anything that can be identified. A Uniform Resource Identifier (URI) [3] is used to designate a resource. A *property* is any characteristic of a resource that can be described with a *value*. The triple: (resource, property, value) is the atomic unit of information in RDF and is called a *statement*. The parts of a statement are its *subject*, *predicate*, and *object* respectively. Figure 7 shows a statement diagrammatically.

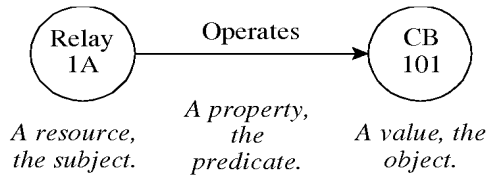

Figure 7

Figure 8 shows a collection of statements forming a small model. Because the value of some of the statements is a resource, which is in turn the subject of another statement, this model forms a directed, labelled graph (DLG).

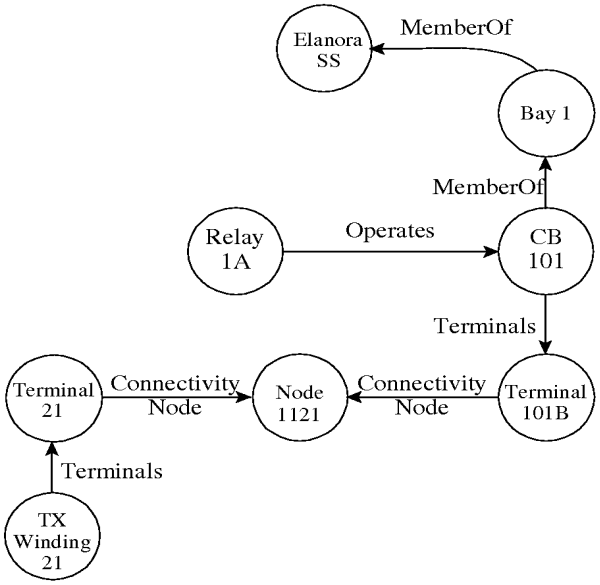

Figure 8

The labels in figure 8 are abbreviated for clarity. The full identification of a each resource and each property is a URI that embodies schema and version identification. A URI is unambiguous in any context, for example:

http://iec.ch/TC57/2000/CIM-schema-cimu09a#Bay.MemberOf_Substation

The *http:* in this URI indicates the use of the http naming scheme and not that any document is available at this address via the http protocol.

Schema information is introduced into this graph in two ways. First, any resource may have a *type* property that designates its *class*. Secondly, both properties and classes are themselves resources and can be described by further statements. Statements about classes and properties form the schema. This is illustrated in figure 9.

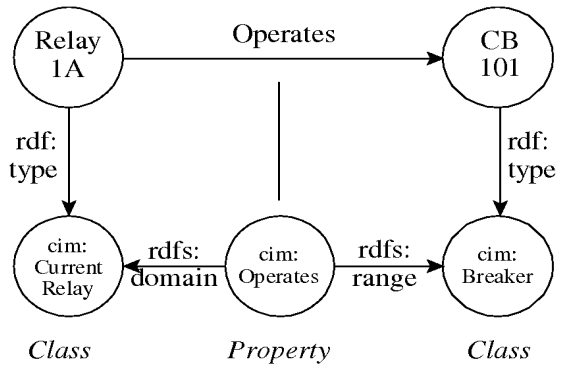

Figure 9

The picture is completed by another category of information: second order statements. A second order statement describes or qualifies another statement. This is a vehicle for conveying version, authorship, accuracy or similar qualifications, as shown in figure 10. Here the statement about Relay 1A has been reified, that is, made concrete as a resource. It then serves as the object of two other, second order, statements.

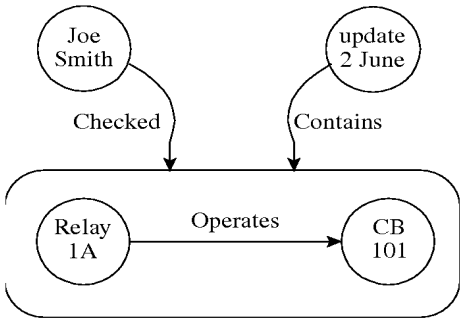

Figure 10

B. Comparison

Comparing the RDF information model to that of conventional databases, several differences emerge:

(i) The statement is a fundamental unit of information, sometimes called a *fact*. In contrast, tuples and objects are composite structures.

(ii) Schema is descriptive not prescriptive. A schema can be enforced, by modifying the population to conform, but this is not mandatory as it is in a database system.

(iii) Schema is flexible. A set of statements can stand alone, without a schema. It is also possible to have a partial schema or multiple schema. The schema can support functions other than validation, including inference and transformation.

(iv) Schema is extensible. Generic RDF software might be expected to interpret public schema vocabularies such as [2] and [8]. However, applications may define and use additional application-specific schema information.

(v) Second order statements can qualify individual facts (corresponding to individual fields in a tuple or object). Several conflicting facts can be represented at once, distinguished by second order statements.

(vi) Universal identification enables one model to extend, qualify or describe another. The models could reside in different systems in different administrative domains.

IV. AN APPLICATION

The foregoing KR framework is a promising environment in which to formulate power system modelling tasks. We will briefly describe a case study that demonstrates the advantages of this approach in solving the modelling problems outlined in chapter II: versioning, transformations, and partial model stitching.

The case study answers the question: can these techniques work in practice where highly proprietary systems are involved?

A. The Problem

One of Australia's largest distribution utilities, Integral Energy, operates a distribution network with an installed capacity of 5,300 MVA.[9]. Its network is under continuous expansion and the task of maintaining the control systems is significant.

The power system model used by the control system includes an equipment model, electrical topology, display layout information, and telemetry and local control configuration data.

The control system has two tiers: a main SCADA system with replicated control centres and a network of substation management systems. The two tiers require different models although the same source information is used for their configuration. Model transformations are necessary both for efficiency and to eliminate manual errors in coordinating the two tiers.

The control system team must work in a fully parallel fashion, with model updates for different substations under concurrent development. This leads to the creation of partial models representing a set of changes or an area of interest. These must be stitched (merged) with each other and the complete model.

The original tools for editing and maintaining the model were ad-hoc. They did not anticipate a) the scale of the task, b) the complexity of the task or c) the present, reduced size of the SCADA team. As with many ad-hoc approaches these tools were arcane and somewhat error-prone.

Given the tools available and the extent of the power system augmentation work, there was considerable pressure on the SCADA team. Skilled staff were spending many hours editing, testing and correcting low-level data files rather than using their expertise to solve more important network issues.

B. Solution

The authors developed a general-purpose KR-based tool, called I-Builder, that performs data capture, display, editing, merging, transformation and export of KR models. Figure 11 is a block diagram of I-Builder. The multiple, concurrent project approach illustrated in figure 3, is used, and figure 11 shows I-Builder in the context of one such project.

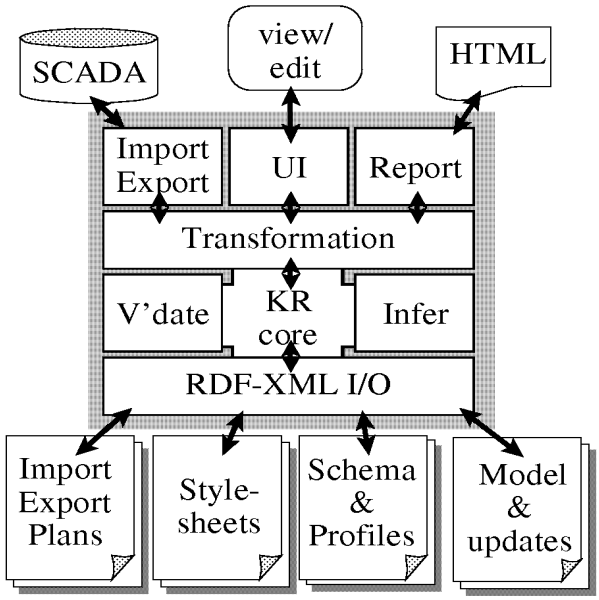

Figure 11

A project lifecycle consists of:

- Capturing the relevant baseline power system model segments from the SCADA systems (Import/Export).
- Updating or extending the model the via the user interface (UI). Profiles are used, which are pre-built templates ranging in size from a single point to a whole substation.
- Exporting the updates and new sections of the model back to the SCADA system(s).

The following sections consider how this architecture deals with the problems of versioning, transformation, and partial models posed in section II.

1 Versioning and Partial Models

Version management relies on reducing the model to atomic units, the statements, in the KR core. Each model statement is qualified by a second order statement (in the manner of figure 10) that records its origin.

Editing does not change existing statements but adds new statements to the KR core. These are allowed to contradict existing statements. The new statements are also qualified with details of their origin.

The lost update problem described in chapter II is avoided because only the new statements are exported back to the SCADA system. These are identified by their second order statements.

During the lifetime of a project, unfinished work may be saved many times. Rather than commit the project back to an offline SCADA system database, the changed contents of the KR core are saved in XML files. A simplified RDF syntax similar to [10] is used. The origin of all information, embodied in second order statements, is therefore preserved. (For convenience, the contents of the KR core is split among XML files based on origin.)

Infrequently, the segment of the baseline model captured in the project may be updated in some other project or in the SCADA system. In this situation, the baseline model may be recaptured without losing updates already made in the project. The updated can then be validated against the new baseline and adjusted as required.

The KR core is responsible for stitching updates to baselines. It does this based on the universal identification scheme (URI's) used in RDF. This type of stitching also takes place between models and the schema, between related schema and between schema and import/export plans.

2 Transformation and Inference

The two tiers of Integral's control system use different model representations and different schema. This creates a requirement for model transformations. The transformation infrastructure in I-Builder serves as the I/O or query sub-system. It drives the import/export function, the user interface and generates reports.

I-Builder implements a general purpose mapping between KR graph models found in the KR core and the hierarchical

XML Information set. Transformation results are presented to the other modules through the Simple API for XML (SAX) [11].

Transformations are directed by stylesheets, which are themselves KR models. These are a KR equivalent to the XML transformation language, XSLT [12]. The stylesheet models are intimately linked with schema information because properties and classes are the most important criteria to select and process statements. They are, in effect, schema extensions.

Figure 12, illustrates rules coupled to schema (compare to figure 9). In the figure, a rule is associated with the Operates property. The rule specifies an action to be performed when that property is encountered in the model, and a context in which this rule applies.

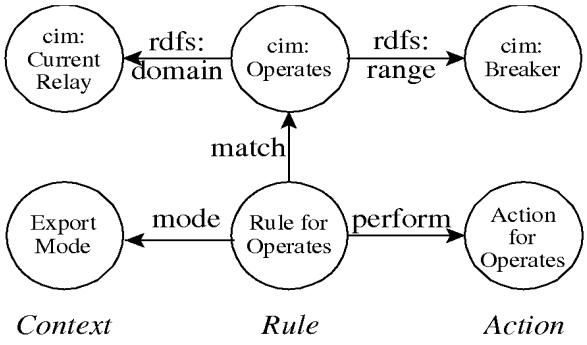

Figure 12

The import/export module shown in figure 11 also forms part of the transformation chain. It is responsible for converting XML to SQL and rowsets back to XML. The chief challenge is to order the SQL queries correctly. The correct order depends on relationships found in the schema. Thus the import/export plan is also a KR model that extends the schema.

Finally, inference is a process related to transformation. Inference adds statements to the model based on other statements found in the model and a set of rules (often the schema itself). For example, inference is used when profiles (ie templates) are copied into the power system model. Statements must be added to the profile based on inference rules that are formulated as a schema extension.

3 Experience

I-Builder is now the vehicle for all model maintenance at Integral and clear improvements in speed and accuracy have been achieved. Creating and validating a new substation, for example, is many times faster. We attribute this to the features that the KR techniques enabled.

One important observation is that interactive performance is satisfactory. We expected the richness of the data model implemented in the KR core to mitigate against performance. We attribute the performance achieved to the use of partial models, relying on stitching process to coordinate with the overall model. This is an inherently scalable approach.

The architecture has produced a few other bonuses: because the user interface is driven by the KR based transformation infrastructure, it is immune to schema changes. Only the stylesheets need be updated. We have tested this by implementing the EPRI CIM schema [5].

Another bonus is that the models, the related transformation rules and the schema are kept in XML with a straightforward vocabulary. These are corporate assets and locking them away in hard-coded software and more proprietary forms of data storage would be undesirable.

V. CONCLUSION

This paper has outlined some of the issues with typical power system modelling solutions. The difficulty of making progress with these issues in a conventional database framework was discussed. Knowledge Representation techniques were introduced as a potentially more fruitful approach. Although KR techniques are unfamiliar to most practitioners, the case study we describe demonstrates that they are feasible, at least as formulated in the Resource Description Framework.

Several features of RDF including its unit-of-data, the second order statements and universal identification make it scalable to large data handling problems. It is particularly useful where multiple systems and administrative domains are involved. (The originators of RDF intend it to work at the scale of the web.) Those qualities have seen RDF incorporated into several power industry standards [5,6,7]. Going beyond that, we have found RDF and KR techniques can be incorporated into a software framework to solve significant real-world problems.

VI. REFERENCES

[1] *Resource Description Framework (RDF) Model and Syntax Specification*, W3C Recommendation, 22 February 1999, Ora Lassila, Ralph R. Swick.

[2] *Resource Description Framework (RDF) Schema Specification*, W3C Candidate Recommendation 27 March 2000, Dan Brickley, R.V. Guha, Netscape

[3] *Uniform Resource Identifiers (URI): Generic Syntax*; Berners-Lee, Fielding, Masinter, Internet Draft Standard August, 1998; RFC2396.

[4] *Guidelines for Control Center Application Program Interfaces*, EPRI Technical Report TR-106324, Project 3654-01, Final Report, June 1996.

[5] *CIM RDF Schema Exported from Ccapi.mdl Version: CIMU09a*, Leila Schneberger. OMG TC Document dtc/2000-11-10.

[6] *Utility Management System Data Access Facility,* Arnold deVos. OMG TC Document dtc/2000-11-09.

[7] *Simplified RDF Syntax for Power System Model Exchange*, Arnold deVos, November 2000. http://egroups.com/group/cimxml

[8] *DARPA Agent Markup Language* http://www.daml.org/

[9] Integral Energy Annual Report, 1999

[10] *A Strawman Unstriped Syntax for RDF in XML*, Tim Berners-Lee, November 1999

[11] *Simple API for XML (SAX),* David Megginson http://www.megginson.com/ SAX/

[12] *XSL Transformations (XSLT) Version 1.0,* W3C Recommendation 16 November 1999, James Clark et al

VII. BIOGRAPHIES

Arnold deVos (M' 96) received his BE(Elec.) from the NSW Institute of Technology, Sydney, Australia in 1981. He worked in system operations at the NSW Electricity Commission and developed software for load forecasting and operational data handling. He also developed inter-utility data exchange standards for the S.E. Australian interconnection. Subsequently he joined Megadata P/L (now part of Logica, UK) where he was the architect of the MOSAIC SCADA system, and developed its distributed database and user interface. In 1995 he joined ALSTOM ESCA where he developed EMS power system modelling tools. He is now a partner in Langdale Consultants where he consults on system integration issues and develops software to address this area. He is active in several utility forums and is the author of the CORBA standard interface for EPRI CIM models.

Christopher Rowbotham received his BE(Elec) from University of NSW in 1975. In 1981 he joined Megadata P/L (now part of Logica, UK) where he became Technical Director. In this role he oversaw the companies product development. In 1995 he founded Langdale Consultants, who develop software and advise clients in the area of realtime system integration.

July 2003 • NREL/SR-560-33909

Subcontractor Report

Distributed and Electric Power System Aggregation Model and Field Configuration Equivalency Validation Testing

M. Davis
DTE Energy Technologies
Farmington Hills, Michigan

D. Costyk
DTE Energy
Detroit, Michigan

A. Narang
Kinectrics
Toronto, Ontario

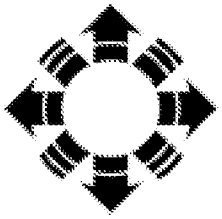

National Renewable Energy Laboratory
1617 Cole Boulevard
Golden, Colorado 80401-3393

NREL is a U.S. Department of Energy Laboratory
Operated by Midwest Research Institute • Battelle • Bechtel

Contract No. DE-AC36-99-GO10337

July 2003 • NREL/SR-560-33909

Distributed and Electric Power System Aggregation Model and Field Configuration Equivalency Validation Testing

M. Davis
DTE Energy Technologies
Farmington Hills, Michigan

D. Costyk
DTE Energy
Detroit, Michigan

A. Narang
Kinectrics
Toronto, Ontario

NREL Technical Monitor: Thomas Basso

Prepared under Subcontract No. AAD-0-30605-09

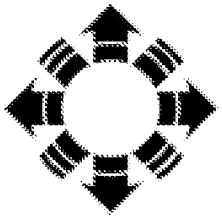

National Renewable Energy Laboratory

1617 Cole Boulevard
Golden, Colorado 80401-3393

NREL is a U.S. Department of Energy Laboratory
Operated by Midwest Research Institute • Battelle • Bechtel

Contract No. DE-AC36-99-GO10337

NOTICE

Available electronically at http://www.osti.gov/bridge

Available for a processing fee to U.S. Department of Energy
and its contractors, in paper, from:

U.S. Department of Energy
Office of Scientific and Technical Information
P.O. Box 62
Oak Ridge, TN 37831-0062
phone: 865.576.8401
fax: 865.576.5728
email: reports@adonis.osti.gov

Available for sale to the public, in paper, from:

U.S. Department of Commerce
National Technical Information Service
5285 Port Royal Road
Springfield, VA 22161
phone: 800.553.6847
fax: 703.605.6900
email: orders@ntis.fedworld.gov
online ordering: http://www.ntis.gov/ordering.htm

Printed on paper containing at least 50% wastepaper, including 20% postconsumer waste

Foreword

DTE Energy, which includes the regulated electric utility Detroit Edison, and DTE Energy Technologies, the unregulated subsidiary of DTE Energy, recognized a need to encourage the use of distributed resources to mitigate future generation capacity shortages, improve reliability, and provide a lower-cost energy-delivery system. DTE Energy Technologies is the prime contractor for this study.

Kinectrics, an unregulated subsidiary of Ontario Hydro, is a recognized authority in determining whether harmonics exceed IEEE 519 and evaluating both the steady-state and transient stability of distributed resources connected to distribution circuits. Kinectrics was also a major contributor to the EEI Planning, Operations, and Interconnection DR Task Force 29-issue report issued in September 1999. This company was selected as a subcontractor for DTE Energy.

The study team consisted of:

DTE Energy

- Murray Davis, vice president and chief technology officer
- Ronald A. Fryzel, retired
- David M. Costyk, principal engineer, Relay Engineering
- Raluca Capatina-Rata, engineer, Relay Engineering
- Kenneth J. Pabian, engineer, Relay Engineering

Kinectrics

- E. Peter Dick, principal engineer, Transmission and Distribution Technologies
- Arun Narang, principal engineer, Transmission and Distribution Technologies.

Table of Contents

Table of Figures

Table of Tables

1. Introduction

The focus of this study was to determine the magnitude of distributed resources (DR) that can be added to a distribution circuit without causing undesirable voltage regulation, power quality, stability, or reliability conditions or equipment damage.

The step-by-step process for interconnecting DR to a utility distribution system is shown in Figure 1. The figure shows that after a review of the interconnection requirements in Step 1, there is an exchange of information between the generating customer and the utility, which is shown in steps 2 and 3. Detailed lists of the types of information exchanged here are given in Appendix A.

This study involves the next three steps:

- Developing equivalent circuits and models (Step 4)
- Running simulations (Step 5)
- Determining the boundaries of DR penetration (Step 6).

The results of this study can therefore be used by utilities and generating customers to expedite the interconnection process.

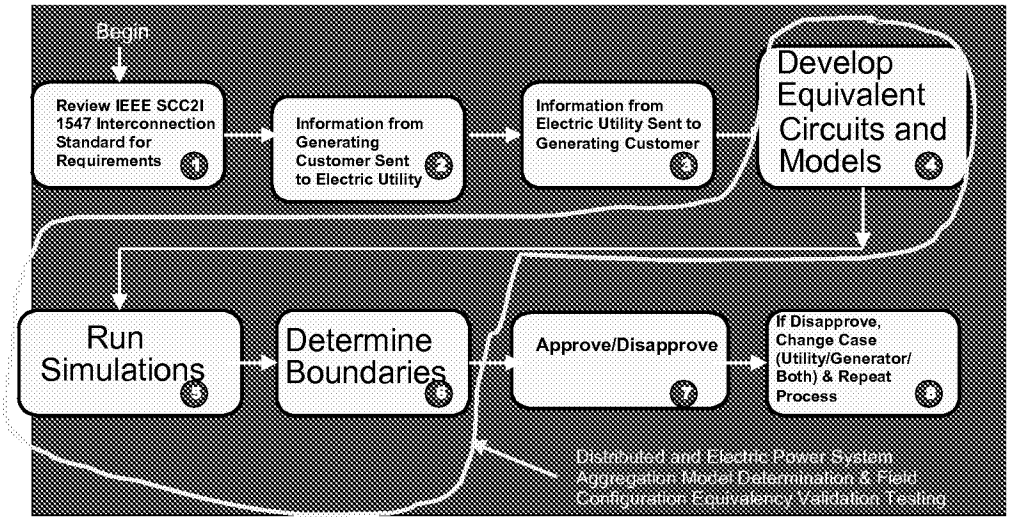

Figure 1. Step-by-step process for interconnecting DR to the distribution system

1.1 Background

In the 20th century, the United States developed an electric power system (EPS) that became the envy of the world for its reliability and low-cost power. Today, the US electric power system consists primarily of large, central-station plants interconnected via a high-voltage transmission system that delivers power to end-users through lower-voltage, local distribution networks. However, interest in the use of distributed generation (DG) and storage has increased substantially over the past 5 years because of the

potential to increase reliability and lower the cost of power through the use of on-site generation. The advent of competition in the electric power industry, through which customers can shop for the ideal solution for any situation, has been a stimulus for this increased interest. The development of small, modular generation technologies such as photovoltaics, microturbines, wind turbines, Stirling engines, and fuel cells has also contributed to this trend.

DG and storage can have many benefits. However, the technologies and operational concepts needed to properly integrate them into the power system must be further developed to achieve these benefits while avoiding negative effects on system reliability and safety. The current power distribution system was not designed to accommodate active generation and storage at the distribution level. Compatibility, reliability, power quality, system protection, and safety issues must also be addressed before the benefits of distributed power can be fully realized.

Although existing literature addresses the requirements of DR operation and interconnection to the distribution system, the cumulative effect of numerous types of DR on a given feeder is less understood. The extent of the eventual integration of DR into the electrical distribution system will depend on the limits imposed by the local grid. These, in turn, are determined by a number of utility coordination issues, including the proper performance of utility fuses, reclosers, and protective relays.

This research into the interaction between DG and distribution lines is one example of ongoing efforts to develop the data and analytical tools necessary to assess the reliability and performance of the transmission and distribution system and promote the deployment of new transmission and distribution system technologies. The detailed modeling, simulations, and analyses presented in this report provide repeatable methods and procedures to evaluate the effects of DR as well as quantitative conclusions and recommendations concerning DG penetration limits and protection equipment requirements.

1.2 Issues

Murray W. Davis presented 29 issues and solutions related to the connection of DR to distribution circuits in "EEI Method for Determining Electric Utility Requirements for Interconnecting Distributed Resources to the Distribution System" September 27–30, 1999. These 29 issues are listed in Table 1.

Of the 29 issues, 10 were considered critical in defining penetration limits and were identified for inclusion in this study. Five of these issues were assigned to Detroit Edison, which evaluated system protection problems. These are listed in Table 1 as issues 1, 2, 15, 16, and 27. Five of the issues were assigned to Kinectrics. These were issues 8, 11, 20, 21, and 22.

Table 1. EEI 29 Issues

Assigned To	Issue	Issue
Detroit Edison	1	Improper coordination
Detroit Edison	2	Nuisance fuse blowing
	3	Reclosing out of synchronism
	4	Transfer trip
	5	Islanding
	6	Equipment overvoltage
	7	Resonant overvoltage
Kinectrics	8	Harmonics
	9	Sectionalizer miscount
	10	Reverse power relay malfunctions
Kinectrics	11	Voltage regulation malfunctions
	12	Line drop compensator fooled by DR
	13	LTC regulation affected by DR
	14a	Substation load monitoring errors
	14b	Cold load pickup with and without DR
Detroit Edison	15	Faults within a DR zone
Detroit Edison	16	Isolate DR for upstream fault
	17	Close-in fault causes voltage dip – trips DR
	18	Switchgear ratings
	19	Self-excited induction generator
Kinectrics	20	Steady-state stability
Kinectrics	21	Transient stability
Kinectrics	22	Loss of exciters causes low voltage
	23	Inrush of induction machines causes voltage dips
	24	Voltage cancelled by forced commutated inverters
	25	Capacitor switching causes inverter trips
	26	Flicker from windmill blades
Detroit Edison	27	Upstream single-phase fault causes fuse blowing
	28	Underfrequency relaying
	29	Distribution automation studies

1.3 Study Procedure

The study procedure consisted of:

1. Selecting two existing Detroit Edison distribution circuits
2. Developing equivalent circuits and models of the distribution circuits
3. Validating the models
4. Classifying contingencies
5. Conducting simulations
6. Determining DR penetration limits.

The major tasks and subtasks, including the project schedule, are given in Appendix B.

Two existing circuits on the Detroit Edison system were selected for study. The circuits selected were typical configurations used at Detroit Edison and at many other electric utilities, so the results can be applied across a range of circuits. They were also selected

because they actually have DR units operating in parallel with the Detroit Edison electric distribution system.

The procedures of specific issue studies are described in subsequent sections.

1.4 Major Findings

1. System voltage has a significant effect on the maximum DR size (or aggregated size) that can be connected to a circuit. The size ratio is near the ratio of system voltages.

   For example, Issue 1: Improper Coordination

4.8 kV	**13.2 kV**
0.47 MVA	**1.25 MVA**

2. The type of fault (three-phase versus line-to-ground) has a heavy influence on determining the size of DR.

   For example, Issue 1: Fault Detection Sensitivity

Mid-point	**3Φ fault**	**L-G fault**
on Pioneer circuit	**80 MVA**	**5.3 MVA**

3. Nuisance fuse blowing tends to limit DR sizes to less than 2 MVA for compact circuits fed from 15-MVA substation transformers (high system fault current = 7,600 A at substation).

4. Harmonic analysis may be required for inverters because of the wide range of acceptable DR sizes (i.e., 870 kVA–9.2 MVA).

5. Active voltage regulation using both real and reactive injection tends to allow larger sizes of DR than DR that track system voltage.

6. The location of DR on the circuit is very important in determining the voltage limits for loss of excitation DR limits.

   For example:

	Bus	**Far End**
Argo	**6.5 MVA**	**0.5 MVA**
Pioneer	**16.2 MVA**	**3.9 MVA**

7. If critical clearing time is 0.1 s or less, then stability should be maintained; the larger the machine inertia, the more stable the unit.

1.5 System and DR Characterizations

Figures 2 and 3 are geographic one-line diagrams of the two circuits selected for study. The node numbers identify changes in line impedance or circuit configuration (i.e., phase spacing and wire size) and junction points of circuit elements. Details of the circuit elements are provided in Appendix C.1.

The distribution circuit DC 326 Argo is a 4.8-kV, ungrounded delta distribution circuit fed from Argo Substation in the Ann Arbor, Michigan, area. DC 9795 Pioneer is a 13.2-kV, multi-grounded wye distribution circuit fed from Pioneer Substation in the Ann Arbor area.

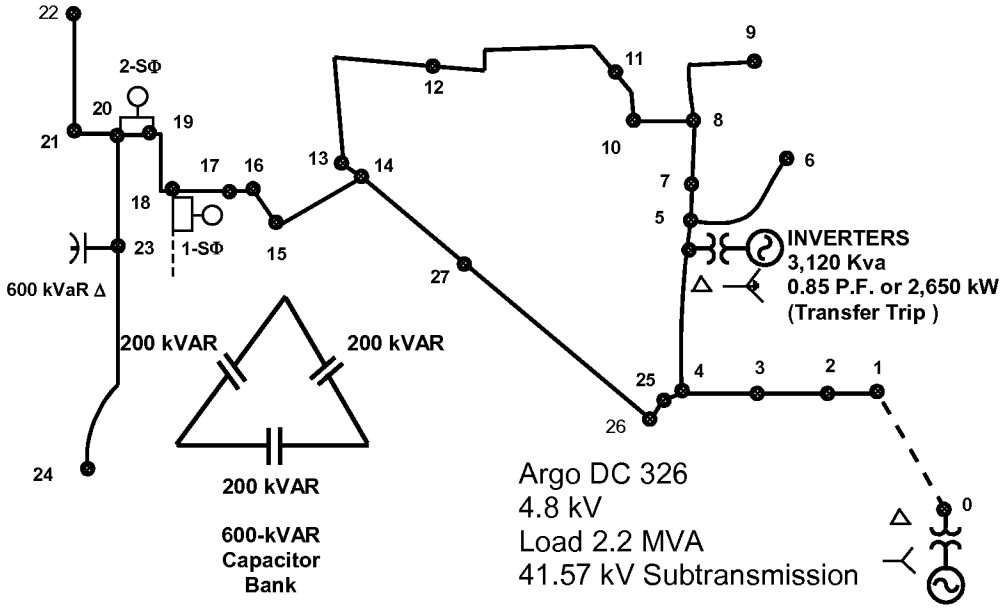

Figure 2. 4.8-kV, ungrounded delta distribution circuit with looped primary

The DC 326 Argo, which has all its load connected line to line, contains a ring, or "loop," that allows power to flow in either direction on that portion of the circuit. The circuit also has the following characteristics:

- A 6-MVA, 41.57–4.8-kV substation transformer (a three-transformer substation)
- A peak load of 2.2 MVA
- A customer with a total of 2,650-kW, 480-V, three-phase inverter-based generation connected to the system through a three-phase wye-delta transformer (generator to line)
- One set of two single-phase 200-A reclosers (between nodes 19 and 20)
- One single-phase 70-A recloser at Node 18
- One 600-kVAR overhead capacitor bank consisting of three 200-kVAR capacitors connected in a delta at Node 23
- 4.4 circuit miles of three-phase conductor
- 1.7 circuit miles of single-phase conductor (two of the three-phase conductors are installed to provide single-phase service on an ungrounded delta system).

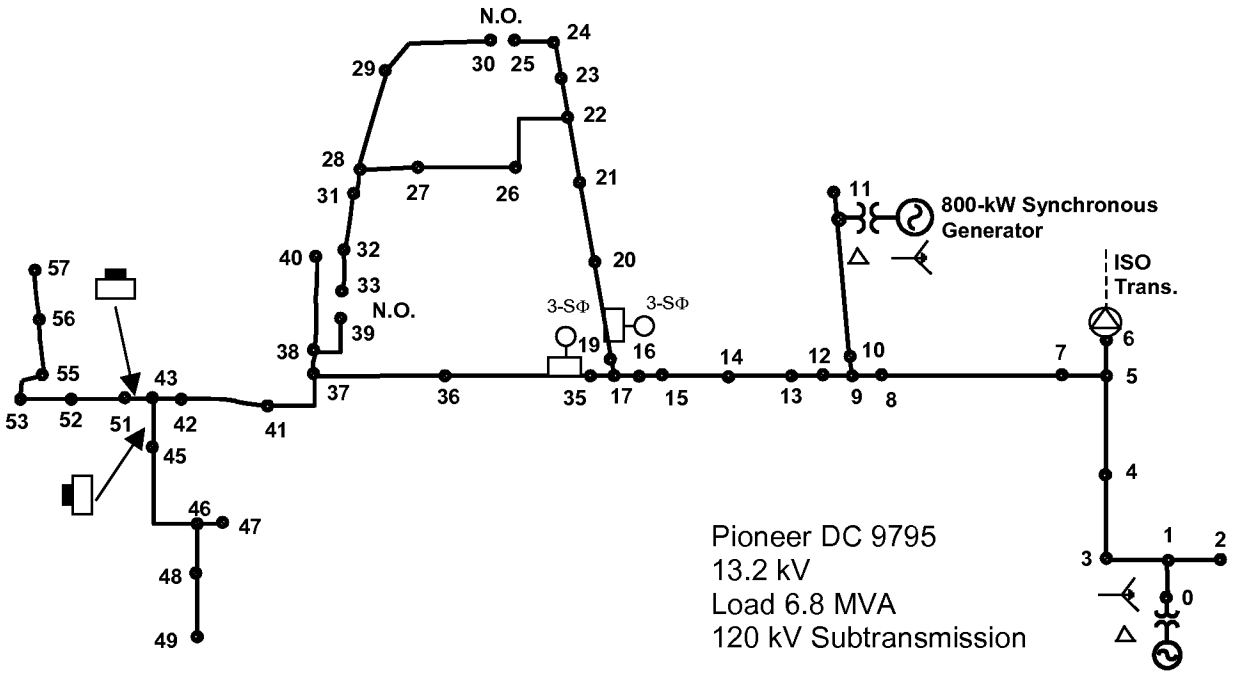

Figure 3. 13.2-kV, multi-grounded wye radial distribution circuit

The 9795 Pioneer radial distribution circuit, which has loads typically connected line to ground, has the following characteristics:

- A 15-MVA, 120–13.2-kV substation transformer (two-transformer substation)
- A peak load of 6.8 MVA
- One 800-kW, 4,160-V, four-wire synchronous generator connected to the system through a wye-grounded delta three-phase transformer (generator to line)
- Two sets of three single-phase 200-A reclosers between nodes 19 and 20 and 35 and 36
- Two sets of three single-phase 200-A sectionalizers between nodes 43 and 51 and 43 and 45
- One single-phase, 7.62–4.8-kV stepdown transformer to serve older 4.8-kV area loads at Node 6
- 6.7 circuit miles of three-phase conductor
- 0.6 circuit miles of two-phase conductor (two phases and neutral)
- 2.5 circuit miles of single-phase conductor (one phase and neutral).

The DR characterizations are summarized below. Details are given in Appendix C.1.

On the 326 Argo distribution circuit, the inverter modeled has the following characteristics:

- Rated voltage = 480 V Y
- Rated kilovolt-amperes = 500 kVA
- Rated power factor = ±0.8
- Maximum current @ 50% V = 1,200 A
- Voltage regulator time constant = 10 ms
- Operating modes = current and voltage source.

The synchronous generator connected to the 9795 Pioneer distribution circuit has the following characteristics:

- Rated voltage = 4,160 V Y
- Rated kilovolt-amperes = 1,000 kVA
- Rated speed = 6 pole, 1,200 rpm
- Rated power factor = ±0.8
- Transient saturated
  Direct axis reactance Xd.' = 0.2342 pu (0.2 pu used for study)
- Zero sequence Xo = 0.0733 pu (0.063 pu used for study)
- Inertia constant H = 1.0 (used for study).

2. Part I: System Protection Issues

2.0.1 Equivalent Circuits and Validating Models

The models used in fault current calculations for generators are those included in the ASPEN One Liner software package, which Detroit Edison has been using for more than 7 years. The One Liner generator models consist of a voltage source behind an impedance. This software is used by more than 100 other users.

One Liner fault calculations can be verified using classical symmetrical component methods. These include manual calculations with a calculator or Excel spreadsheet entries. Results of this study have been spot-checked to verify database accuracy.

Preliminary results were also compared with results from the EPRI-developed product Distribution Engineering Workstation (DEW). Results from both studies were in agreement for those cases tested.

Circuit models have been created from a land-based circuit map database to determine distances between nodes on the circuits studied. Wire type and construction configuration were drawn from input records and not verified from a separate source. Spot checks were made to ensure accuracy of the circuit segment lengths noted in the network model. For example, hand measurements on circuit maps agree with total length as summed in the network model.

2.0.2 Classifying Contingencies

This report provides a sufficient number of contingencies to demonstrate the effects of varying the values of parameters that affect the performance of protective devices. The methods used in the report can be used to determine penetration limits for typical distribution circuits. Replacing the values of the parameters used in this report with those that apply to the selected circuit would allow the user to determine penetration limits for a specific application. However, this report does not provide a comprehensive set of formulae, protective device characteristics, and associated methods to determine the penetration boundaries for any randomly selected circuit.

The following parameters affect the performance of protective devices:

- The fault current available at the substation bus
- The fault current available from each DR
- The circuit configuration (wye or delta, grounded or ungrounded)
- The circuit topology (radial or ring)
- The impedance of wire or cable between protective devices
- The location of protective devices and DR on the circuit
- The location of any type of fault
- The time-current characteristic of each protective device.

To be useful, this report shows the effects of changing the values of various parameters over a reasonably wide range. Including an exhaustive set of parameter values would

require that thousands of sets be studied and would not provide a more useful report. Therefore, the number of contingencies was held to the minimum that would demonstrate the effect of changing each parameter value.

Also, a method was developed that indicates the effectiveness of protective device pairs (i.e., recloser/fuse, breaker/recloser, etc.) over typical ranges of the fault currents. Charts indicate the effective area of these pairs for all typical values of fault currents provided from the substation and a DR. This method provides a very complete set of contingencies for any selected pair of protective devices. It has helped produce a useful report without requiring that thousands of unique combinations of parameter values be studied as individual sets.

Appendix C.2 provides a listing of the contingencies that were studied for each issue.

2.1 EEI Issue 1: Improper Coordination – Protective Device Operates for Fault on Adjacent Circuit

2.1.1 Description

As shown in Figure 4, faults on Distribution Circuit 1 (DC 1) may cause protective devices to operate on Distribution Circuit 2 (DC 2). Typically, this is undesirable because it interrupts service to customers that otherwise would have remained in service.

2.1.2 Scenario

- A fault occurs on DC 1.
- Fault current contributions are from the substation transformer (I_{fs}) and the DR (I_{fDR}).
- The circuit breakers (CB 1 and CB 2), the recloser, and the fuse sense the fault current.
- If CB-1 does not trip soon enough, the fuse, the recloser, or both may also trip.

2.1.3 Question

What is the limit of DR size for any specific combination of protective devices?

The study will provide limits of DR penetration for various protective device combinations as applied to the two Detroit Edison circuits.

2.1.4 Study Results

The method used to determine limits of penetration can be applied to systems having a wide range of stiffness ratios. The study showed specific DR size limits for near-point, mid-point, and far-point locations on each circuit. The results can be generalized to show how they can be used in various locations.

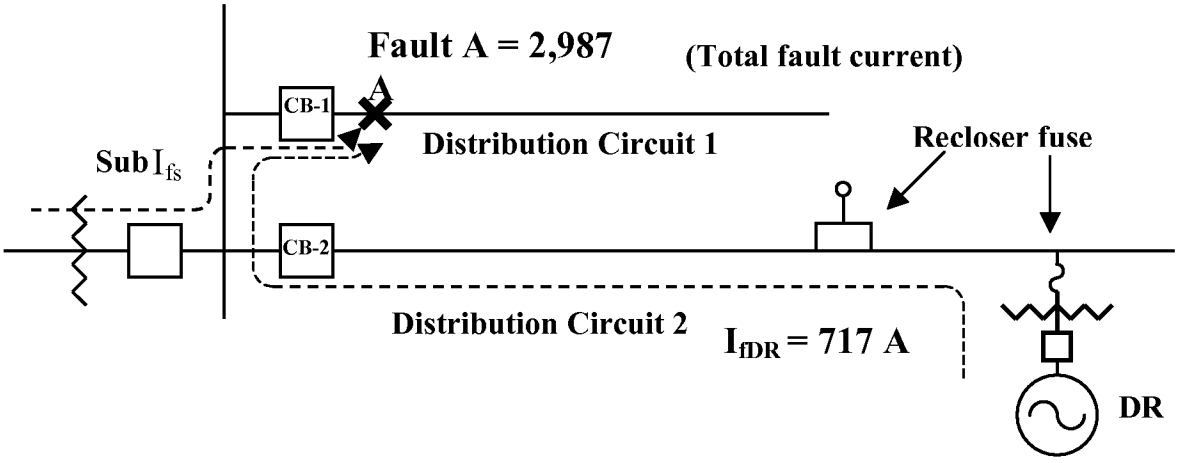

Figure 4. 13.2-kV radial distribution system – improper device coordination fault current paths

If sufficient current flows for enough time through the recloser on DC 2, it will operate. This result is undesirable because the fault is not on DC 2. The circuit breaker on DC 1 will be in the process of tripping based on the relay setting applied to the protective relays on the breaker.

If CB-1 trips before the recloser operates, then the DR and other load downstream of the recloser remain in service. If the recloser operates first, then load downstream of the recloser will be interrupted. If the fuse blows first, then the DR will be interrupted.

Figure 5, shows the time-current curve of a CO-8 relay on CB 1 and a 140-A recloser. Fault currents shown will produce nearly equal trip times of 1.68 s and 1.69 s. These results were obtained from ASPEN by using a fault impedance of 2.4 Ω (resistive) and a DR generator size of 11 MVA. (The fault resistance and DR size were varied using a cut-and-try process until the trip times were essentially equal for a fixed substation transformer size of 15 MVA.)

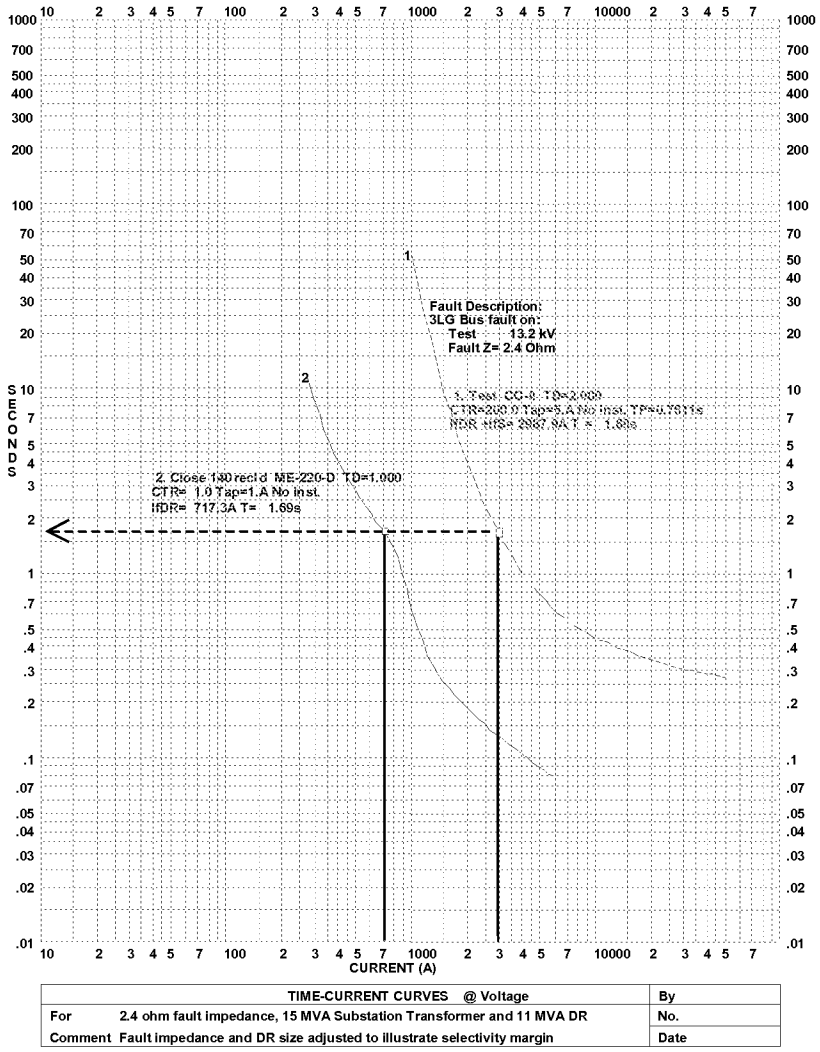

Figure 5. Plot of time-current curves for substation breaker relay and 140-A recloser, showing equal times

This plot shows the curves as separate entities. The current through each device must be known to determine if the devices are selective. If system protection devices (such as a recloser and a fuse) are located on the same circuit and are not on the faulted circuit, then these devices should not operate before the device protecting the faulted circuit operates. This is the desired sequence of operation because it minimizes the amount of load interrupted. Therefore, devices are considered selective when there is enough margin in their time to operation to prevent loads from being unnecessarily interrupted.

In reference to figures 4 and 5, when the recloser current is 717 A and the CB 1 breaker current is 2,987 A, then the trip times are equal, or 1.69 s. To determine the margin of time between the operation of the recloser and the CB 1 breaker, the recloser (Curve 2) is intentionally shifted (to the right) until it intersects the CB 1 curve of Figure 6 at 2,987 A so that the vertical difference between the two curves represents the time margin between the devices. In this case, the margin is only 1.69 – 1.68 = 0.01 s.

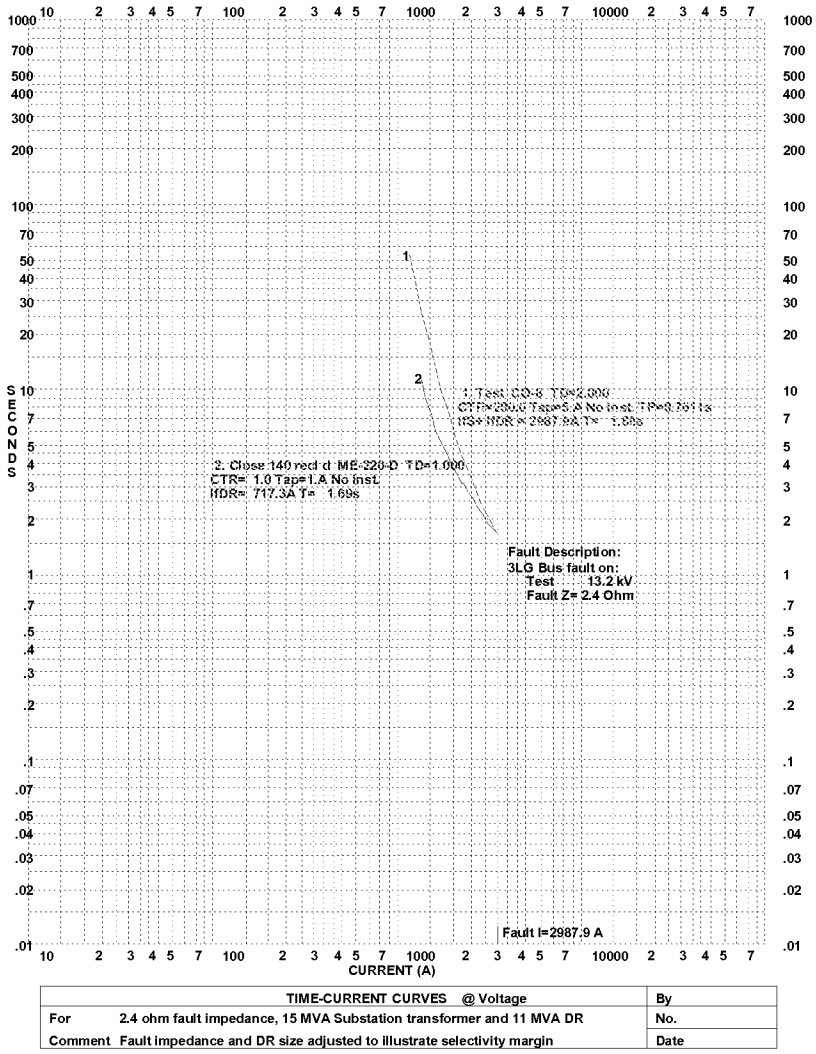

Figure 6. Plot of time-current curves for substation breaker relay and 140-A recloser

Notice that when the recloser curve is translated to the right to intersect the CB 1 curve at 2,987 A, the recloser curve can no longer be used to read the recloser current but can only be used in conjunction with the CB 1 curve to read the difference in time between the two curves on the vertical scale. In other words, a fault study must be run to determine the fault currents through CB 1 and the recloser. The plots can then be used individually to determine if the recloser will trip before CB 1 trips.

The respective current levels are entered on the horizontal axis of Figure 5. When 717 A flow through the recloser and 2,987 A flow through CB 1, the respective trip times would be 1.69 s and 1.68 s (nearly equal). Notice that there is literally no time margin between the recloser and CB 1 for this study case, where the substation transformer is 15 MVA, the DR size is 11 MVA, and the fault is 2.4 Ω resistive. The recloser and substation relay settings are defined in Figure 5. Therefore, this process is very limiting (one substation

transformer impedance, one fault impedance, etc.) in determining DR penetration values, and it is desirable to develop a method of viewing multiple parameter values simultaneously to determine DR penetration limits.

2.1.5 A Diagram to Show a Range of Selectivity

Typically, modern fault-analysis programs will generate composite plots that show all related time-current curves for any one particular situation or fault current. The two plots above become superimposed and accurately shifted to permit selectivity (time margin) to be easily determined on one plot. However, each scenario must be dealt with individually. To determine the effect of different system fault current capabilities and different size DR or DR fault contributions, separate studies are required. Individual studies do not lend themselves to easily determine the effects of varying the DR fault current capabilities.

It would be desirable to see the range of DR current and system current for which selectivity is maintained. This is accomplished by developing a curve that, for each value of system current on the X axis, shows the corresponding maximum DR current on the Y axis while maintaining selectivity for protective devices.

To determine the maximum DR current for a specified recloser and substation relay setting, the following process is used:

1. For a specific value of recloser current, determine the trip time.
2. Determine the corresponding breaker current to trip the breaker for the same trip time.
3. Plot the DR current (recloser current) on the Y axis, opposite the breaker current on the X axis.
4. Develop a curve of maximum DR current and breaker fault current by plotting a range of recloser and breaker currents.
5. Plot a second curve showing system current. (Breaker current is the sum of the system current and recloser current.) Refer to Figure 7.

For specific system fault current, recloser size, and substation relay settings for the CB 1 breaker, this curve describes the penetration limit or the DR size. As an example, for a 2,080-A system fault current, the maximum DR fault current contribution is 600 A, which corresponds to a maximum DR unit size of 2.74 MVA, or:

$$I_{fDR} = 600 \text{ A},$$

$$\text{base 3-}\varnothing \text{ MVA} = \frac{\sqrt{3}\ kV_{Base}\ I_{Base}}{1000}\ , \qquad \text{Equation 1}$$

$$\text{transient fault current} = \frac{\text{pu voltage}}{\text{pu impedance}} \times I_{Base}\ ,$$

$$\text{pu voltage} = 1.0 \text{ and}$$

pu impedance = X'_d = 0.20 pu, then

$$DR\ I_{BASE} = \frac{\text{pu impedance}}{\text{pu voltage}} \times \text{transient fault current}$$

$$DR\ I_{BASE} = \frac{0.20}{1.0} \times 600\ A$$

$$DR\ I_{BASE} = 120\ A.$$

From Equation 1, the maximum DR penetration limit is then:

$$DR\ MVA = 3\text{-}\varnothing\ MVA = \frac{\sqrt{3} \times 13.2\ kV \times 120\ A}{1000}$$

$$= 2.74\ MVA$$

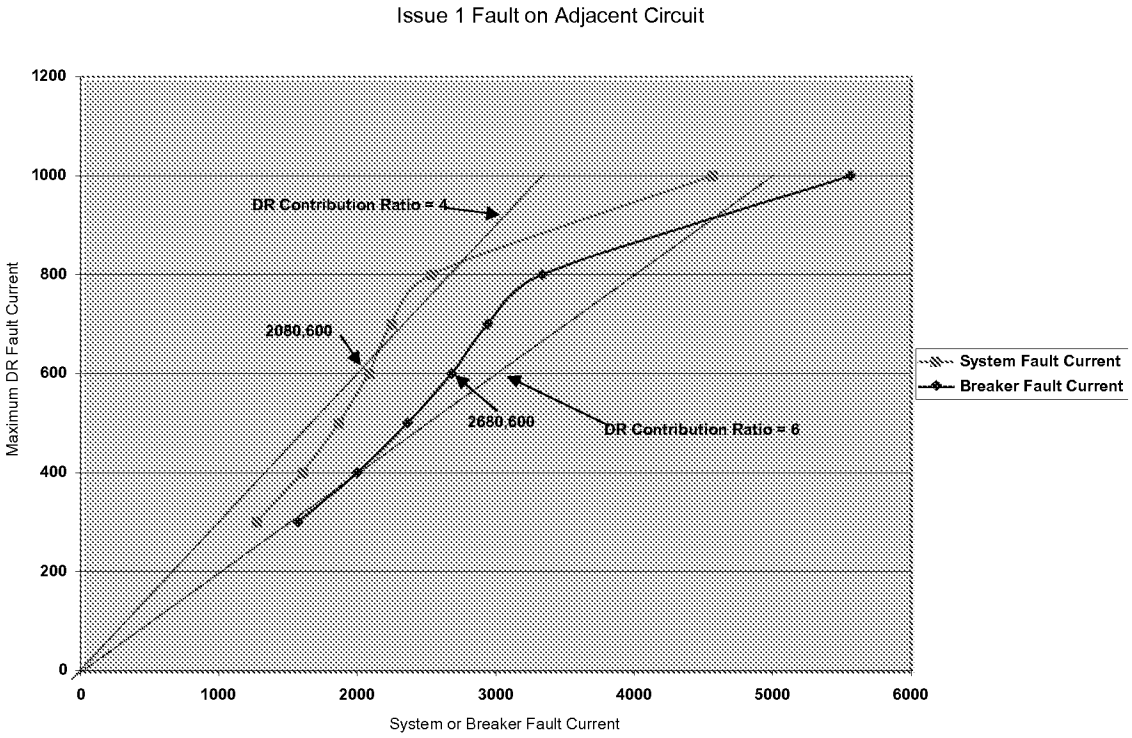

Figure 7. Maximum DR current penetration limit (fault current) for different system fault currents

2.1.6 Limitations

Because the selectivity margin was set to zero by design, or for simplicity, the results displayed in Figure 7 represent the upper boundary of DR size limits. Because margins are required to compensate for the effects of relay overtravel, breaker operating time,

current transformer error, and setting calibration error, margins must be included in any final fault study used to determine the protection required when a DR is added to a system. However, the selectivity diagrams that do not include margins can be very useful in quickly determining "go" or "no go" situations.

Also, for simplicity, the last step assumed the system current and recloser currents are in phase, and algebraic subtraction was used. Although the currents are not necessarily in phase, this is not a limitation because the angle between the two fault currents is very small. As the angle increases, less DR current can be tolerated. (As they become more in phase, more current will be sensed by the relay on CB 1, and the breaker will trip faster.) To accurately determine system current, vector subtraction must be used. A different curve would be required for a different angle, but this is not necessary for most practical applications. Details of this procedure are given in Appendix D.1.

Values of DR current above the breaker current curve will cause the recloser to operate for faults on the adjacent circuit. Notice that breaker fault current and system fault current curves are shown on the same chart. Either the breaker fault current or system fault current can be used to determine the maximum DR size, but because system fault current is readily available, this is the preferred method.

A plot of maximum DR current for a range of system current was added to Figure 7 by plotting X axis values equal to the breaker current minus the recloser current. For example, the maximum DR current for a breaker current of 2,680 A is 600 A on the breaker current curve. For a recloser current of 600 A on the Y axis, the corresponding breaker current is 2,680 A, and the corresponding system current is 2,080 A. (The node equation at the substation bus is: system current + DR current = breaker current.)

Plotting system fault current versus DR fault current permits adding straight lines that indicate the DR contribution ratio, which is similar to the stiffness ratio. The DR contribution ratio as plotted in this figure is determined at the point of fault, or:

$$\text{DR contribution ratio @ point of fault} = \frac{I_{fS} + I_{fDR}}{I_{fDR}}, \qquad \text{Equation 2.}$$

The stiffness ratio is defined at the point of common coupling (PCC) and is given as:

$$\text{stiffness ratio @ PCC} = \frac{I_{fS} + I_{fDR}}{I_{fDR}}, \qquad \text{Equation 3}$$

The difference between these ratios is typically small because their difference is due to the line impedance between the PCC and the fault location.

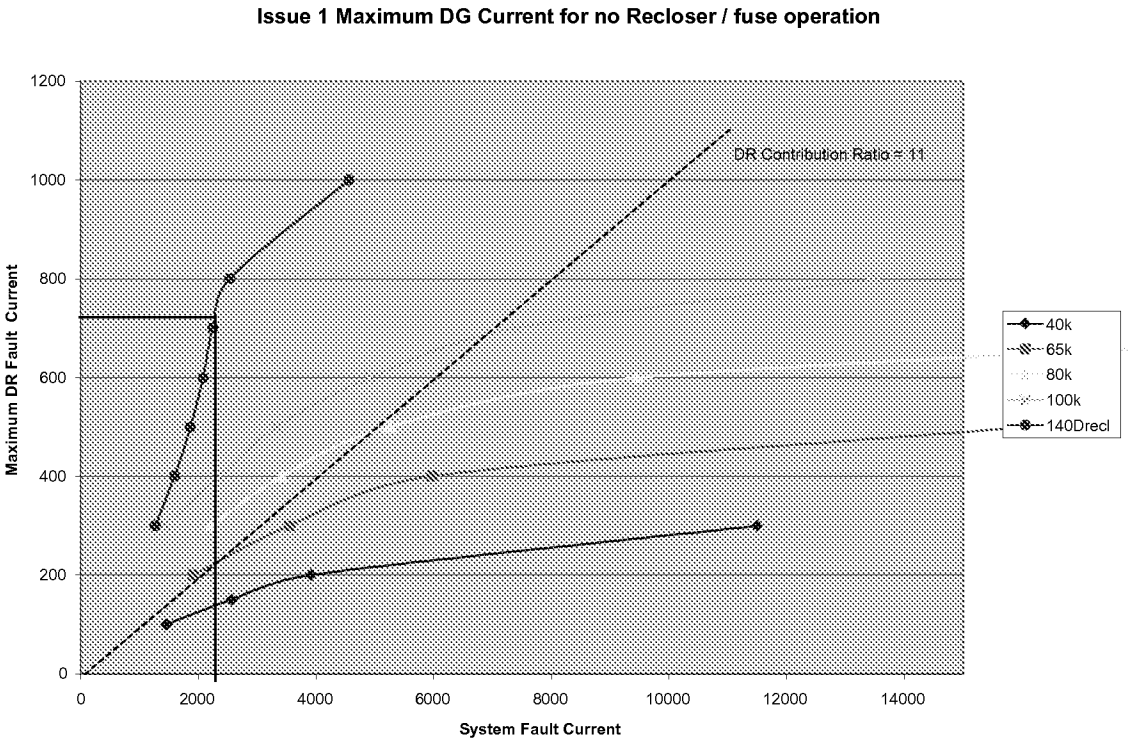

Figure 8. Maximum DR fault current versus system fault current
(Note: The worst-case condition is represented because the line impedance between the DR and the fault is considered to be zero.)

Figure 8 is a composite showing the selectivity boundaries of several fuse sizes and a 140-A "D" recloser. Figure 8 shows the maximum DR fault current (717 A) for an associated system fault current of I_{fS} = (2,987 A – 717 A) = 2,270 A, for the fault condition shown in Figure 4. This figure was produced as described in Appendix D.1 using an Excel spreadsheet.

Figure 8 is in agreement with Figure 5, which shows the condition of 2,270 A from the system and 717 A from the DR such that CB 1 opens at the same time as the recloser. (Other points were similarly checked to verify the accuracy of the data and algorithms used in the spreadsheets.)

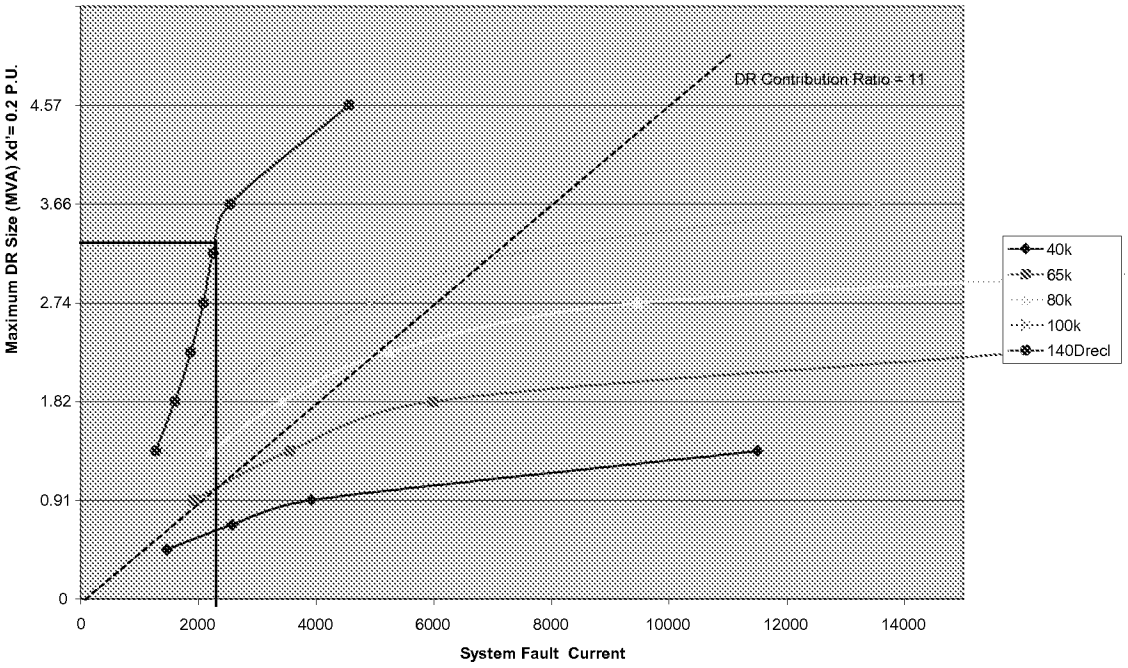

Figure 9. Maximum DR megavolt-amperes versus system fault current
(Note: The data given in Figure 9 for the maximum DR penetration limit is based on a transient reactance of Xd' = 0.20 pu)

To obtain the maximum DR megavolt-amperes rather than the maximum DR fault current, it is only necessary to apply the transient reactance as shown in the example calculation of Equation 1.

2.1.7 Study Results

ASPEN studies on DC 326 Argo indicate that the DR penetration size limits are as follows:

Table 2. Maximum DR Sizes on DC 326 Argo (4.8 kV)

	Maximum Size (MVA) Distance from Substation		
Fuse Size	Near End	Mid Point	Far End
40k	0.47	0.5	0.55
100k	1.25	1.42	2.5
140-A recloser	1.9	2.5	See note

Note: The line impedance limits current to a value such that any size generator will not cause inselectivity.

Table 3. Maximum DR Sizes on DC 9795 Pioneer (13.2 kV)

	Maximum Size (MVA) Distance from Substation		
Fuse Size	Near end	Mid point	Far end
40k	1.25	1.3	1.35
100k	3.3	3.6	4
140-A recloser	5.1	5.9	7.2

For EEI Issue 1, the tables in Appendix H show the DR sizes, associated currents, and trip times for the system shown in Figure 4.

Also refer to Appendix C.1 for circuit and substation parameters used in these studies.

2.1.8 Conclusions and Recommendations

As seen in tables 2 and 3, distance has a minimal effect on the maximum DR size. It is possible for the line impedance to limit the current contributed from the DR to a value less than that required for inselectivity for even an infinitely large generator. For example, with small wire sizes (e.g., #4 copper) and a far-end fault on DC 326, the current is limited such that even for very large generators, there is no inselectivity with a 140k fuse or 140-A recloser.

Note that the DR sizes listed in Table 3 for the DC 9795 Pioneer circuit are larger than those in Table 2 for the 4.8-kV circuit. The ratio is very close to the ratio of the system voltages: 13.2 ÷ 4.8 = 2.75. The protective devices are all current-sensitive. For the same fault current in amperes, a generator connected to the system at 13.2 kV will be 2.75 times the megavolt-ampere rating of a generator connected to the system at 4.8 kV, assuming the line impedance and generator impedance are the same. Based on this analysis, the process for determining the maximum DR penetration megavolt-ampere limit has been simplified into the straightforward approach shown in Figure 9. Notice that only the system fault current and the protective device sizes are needed to determine the maximum DR size that can be interconnected to the circuit.

This result is independent of circuit voltage because all input parameters are current-based. For example, from figures 8 and 9, a system fault current of 6,000 A and a 65k fuse results in a 400-A maximum DR fault current limit or the maximum DR size of:

$$400 \text{ A} \times 0.2 \text{ pu} = 80 \text{ A} \times \sqrt{3} \times 13.2 \text{ kV} = 1.83 \text{ MVA at 13.2 kV system voltage.}$$

Similarly, at 4.8 kV, the maximum DR fault current limit is:

$$400 \text{ A} \times 0.2 \text{ pu} = 80 \text{ A} \times \sqrt{3} \times 4.8 \text{ kV} = 0.665 \text{ MVA.}$$

The ratio of the results is 2.75, as mentioned above.

Selectivity studies should be performed to determine if faults on adjacent circuits may cause protective devices to operate on an unfaulted circuit with which the DR is interconnected. This condition, although generally undesirable, may be permissible. The utility's operating practices and power quality requirements and the likelihood of occurrence would be typical factors involved in deciding if this condition is indeed permissible. Also, this study should be performed as part of the general study described in Appendix I.

2.2 EEI Issue 1: Improper Coordination – Reduced Fault Detection Sensitivity

2.2.1 Description

The addition of DR on the distribution circuit will reduce the fault detection sensitivity of the substation protective relays.

This aspect of Issue 1 was not listed in the original statement of work. However, it is a key issue for determining the maximum penetration limit of DR on a distribution circuit.

2.2.2 Scenario

- As shown in Figure 10, the relay protection of CB 1 must sense the lowest fault current of the three fault locations (A, B, or C). Reclosers sense faults beyond the zone (i.e., Location D).

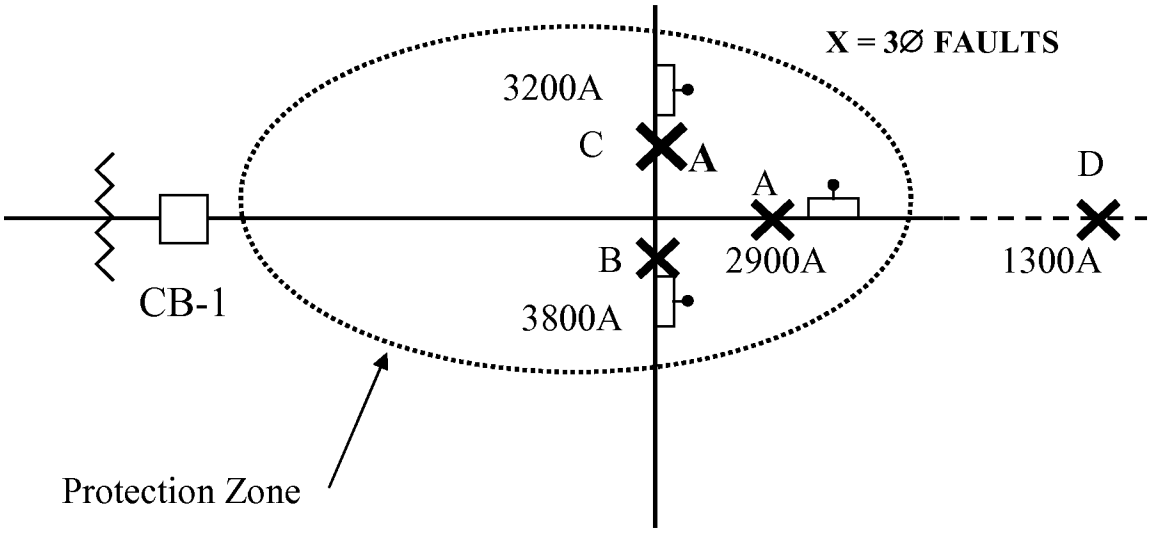

Figure 10. Breaker system protection zone

- In Figure 11, the DR is located near the substation breaker because this represents the worst-case infeed condition. (See infeed effects in Appendix G.)

- Assume a fault at Point A, as shown in Figure 10.

- The fault in Figure 10 is near the line protection device that has the least available system fault current (Location A). The substation breaker will typically not be required to sense faults beyond this line protective device.

- The fault current contribution from DR reduces the fault current contribution from the substation.

- The protective device at the substation takes longer to trip because of fault current contribution or infeed from DR, or it does not trip until the DR trips, at which time the system fault current increases.

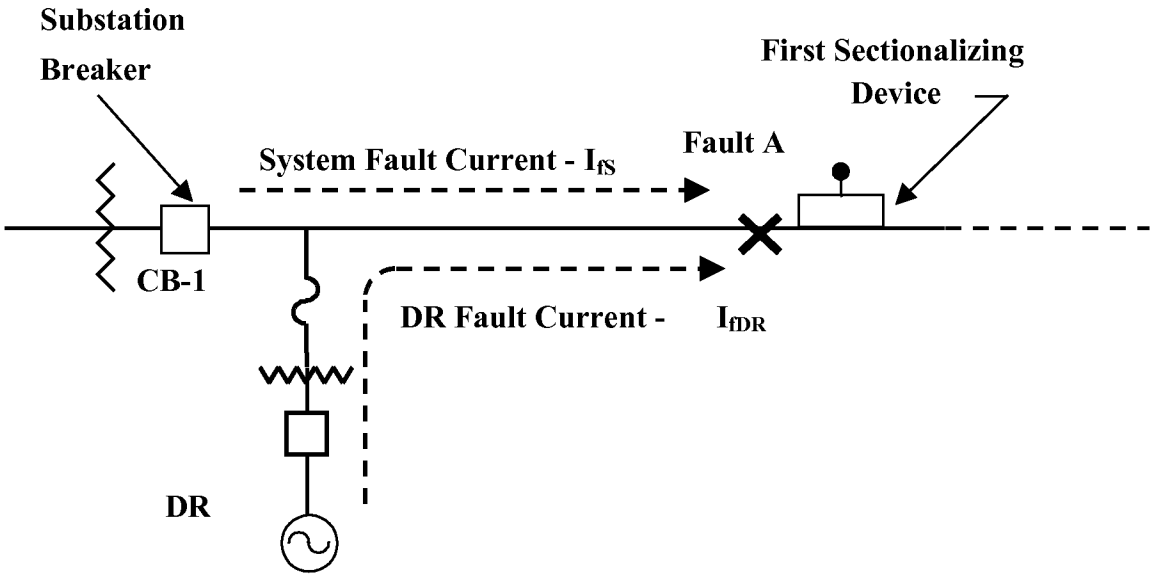

Figure 11. Infeed from DR reduces substation breaker relay fault current detection sensitivity

2.2.3 Question

For the existing protective settings on the two circuits studied (i.e., DC 326 Argo and DC 9795 Pioneer), what is the maximum DR generation size that can be added without violating existing sensitivity guidelines?

2.2.4 Study Results

2.2.4.1 Three-Phase Faults

1. For DC 9795 Pioneer, the maximum generation size that can be added and still have 2,000 A flowing through the substation breaker is 80 MVA. The minimum acceptable fault current is 2,000 A, which is two times the relay setting. It is common relay practice to require the relay to sense faults that are 50% of the fault current for a bolted fault condition. A 50% margin for 2,000 A is 1,000 A.

2. For DC 326 Argo, the maximum generation size that can be added and still have 2,000 A flowing through the substation breaker is 2.5 MVA.

2.2.4.2 Line-to-Ground Faults

For DC 9795 Pioneer, the maximum generation size that can be added to still have 2,000 A flowing through the substation breaker is 5.3 MVA for a line-to-ground fault.

2.2.4.3 Ground Faults on Ungrounded Systems

DC 326 Argo is an ungrounded circuit. Ground faults for the ungrounded 4.8-kV system will not be analyzed in this report for the following reasons:

1. Ground faults on ungrounded distribution circuits will typically have only about 5–20 A flowing at the fault. These low levels are too small for most protective devices to sense and operate.

2. Ground detection voltage transformers or other schemes such as zinc oxide arrester leakage current are employed to sense this fault condition.

3. Ground faults on ungrounded systems are normally not considered during protective relay coordination studies.

A solid ground fault elevates the unfaulted phases to the phase-to-phase voltage with respect to ground. Current flows from the unfaulted phase conductors through the line-to-ground capacitance to the ground fault and then to the faulted phase conductor.

2.2.5 Conclusions and Recommendations

2.2.5.1 DC 9795 Pioneer (13.2 kV)

Node 17 of Figure 3 was selected for the fault location because it is the location of the first sectionalizing device. Normally, the substation breaker relay setting would not be required to sense faults beyond Node 17. For DC 9795 Pioneer, a maximum size of 80 MVA was determined for a three-phase fault condition. An 80-MVA generator would not be located on a distribution circuit similar to this one because the distribution circuit elements are not designed to carry this high level of power and the step-up transformer on the high side would be at least 115 kV or higher to reduce the current. Therefore, there is no fault current detection sensitivity issue for this condition. Of note is the much smaller-size generator (5.3 MVA) that reduces the substation current to below 2,000 A for ground faults. This is due to the relatively low zero sequence impedance of the DR and the relatively high zero sequence impedance of the line.

Node 57 was selected as a more distant node for comparison purposes. At Node 57, the line-to-ground fault current falls to a level that does not provide sufficient margin for sensing ground faults from the substation breaker. The additional line impedance between nodes 17 and 57 also reduces the three-phase fault current level considerably. At Node 57, three-phase faults can still be sensed by the substation breaker relay until at least 10

MVA or more of DR generation has been introduced to the circuit, at which time the current will drop down to a level below 2,000 A. (See Appendix H.1 for results.)

Appendix G contains a spreadsheet, related chart, and discussion of a range of DR sizes and the effects of infeed on relay detection sensitivity. Calculations are based on a range of DR sizes for a unique substation size and several lateral lengths. The method outlined in Appendix G describes a procedure for determining the maximum size of DR for a range of line impedances for a unique 15-MVA substation transformer size.

2.2.5.2 DC 326 Argo

A value of 2,000 A was selected for DC 326 Argo to provide a comparison with DC 9795 Pioneer results. At Node 19 of DC 326, less than 2,000 A flow for three-phase faults. Therefore, the fault was moved closer to the substation source to increase the fault current to greater than 2,000 A, which occurs at Node 15. Node 15 was selected to show the effect of added DR current located at Node 1. For a bolted three-phase fault at Node 15, a maximum of 2.5 MVA can be added near the substation to have 2,000 A flowing from the substation to the circuit.

2.2.6 General

Fault detection sensitivity studies should be performed to determine if the addition of a DR to a circuit will reduce the fault detection sensitivity of existing protective devices to a level that violates the fault detection sensitivity limits used by the utility. The DR should be modeled at the proposed interconnection point. This study should be part of the general study described in Appendix I.

A table similar to Table G-1 in Appendix G may be used to determine if penetration limits are being approached by the addition of a DR.

The studies used in this report are instructive but should not be used as a substitute for studies that model the specific configuration of a DR interconnection to the EPS.

2.3 EEI Issue 2: Nuisance Fuse Blowing Because of DR Fault Current

2.3.1 Description

As shown in Figure 12, faults on a lateral may cause the sectionalizing fuse to operate without being saved by the "fast" curve of the recloser. Typically, this is undesirable because many faults that are temporary in nature can be cleared by momentarily de-energizing the system with the recloser and then immediately reclosing the line.

2.3.2 Scenario

- A fault occurs on a lateral at Location A.
- Current flows from the substation transformer (I_{fs}) and from the DR (I_{fDR}) to the fault.
- The fuse senses the fault current through the recloser plus the fault current from the DR.

- Under normal operating conditions (without DR), when a temporary fault occurs at A, the recloser will open for about 100 cycles to allow the temporary fault to clear. The recloser and fuse operating times are normally coordinated such that the recloser will open first to prevent the fuse from blowing and avoid unnecessary loss of load downstream from the fuse.

- The added current from the DR may cause the fuse to blow. If the DR were not present, the current through the fuse would have been supplied only through the recloser.

- If the recloser does not trip soon enough because of the temporary fault, then the fuse will blow, causing loss of load beyond the fuse.

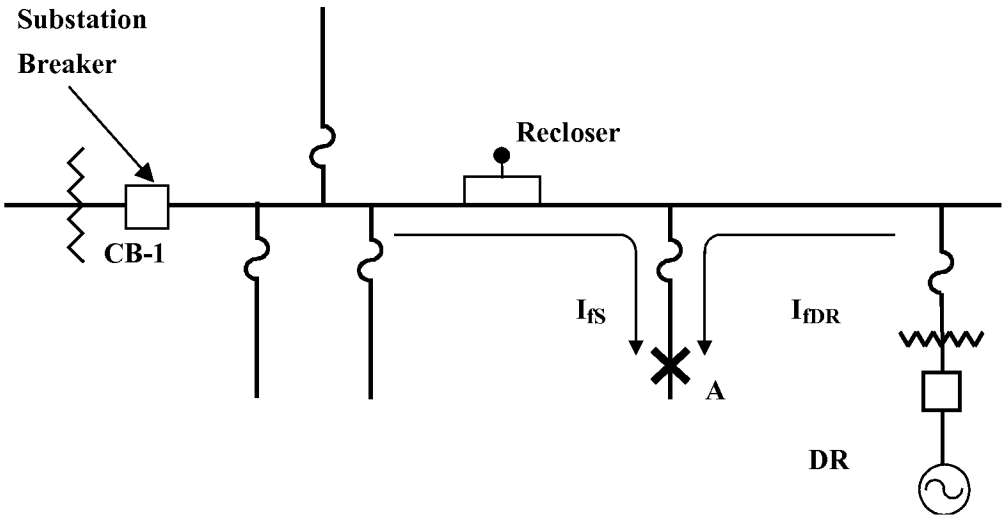

Figure 12. Nuisance fuse blowing because of DR fault current

The single-phase reclosers involved in this study have a fast-tripping characteristic and a slow-tripping characteristic, as shown in Figure 13. The fast-tripping time is intended to clear a temporary fault downstream of a fuse without blowing the fuse. The fast and slow characteristics are shown for a 140-A Cooper V4L recloser.

Upon sensing the fault current, the recloser first trips according to the fast, or "A," curve (see Curve 2 in Figure 13). If the fault current is within certain limits, the fault will be interrupted by the recloser, and the fuse will not blow. The recloser will then reclose automatically. Because the fault was temporary and has now been removed, the recloser will automatically reclose and will remain closed. Also, the fuse will remain intact, and all customers downstream of the recloser will have service automatically restored.

For permanent faults, the recloser will trip four times and lock out unless the fault is downstream of a sectionalizing fuse. The recloser will normally operate one time on the fast, or "A," curve and three times on the slow, or "D," curve. The "D" curve is slower to permit faults that are downstream of fuses to be cleared by those same fuses without locking out the recloser.

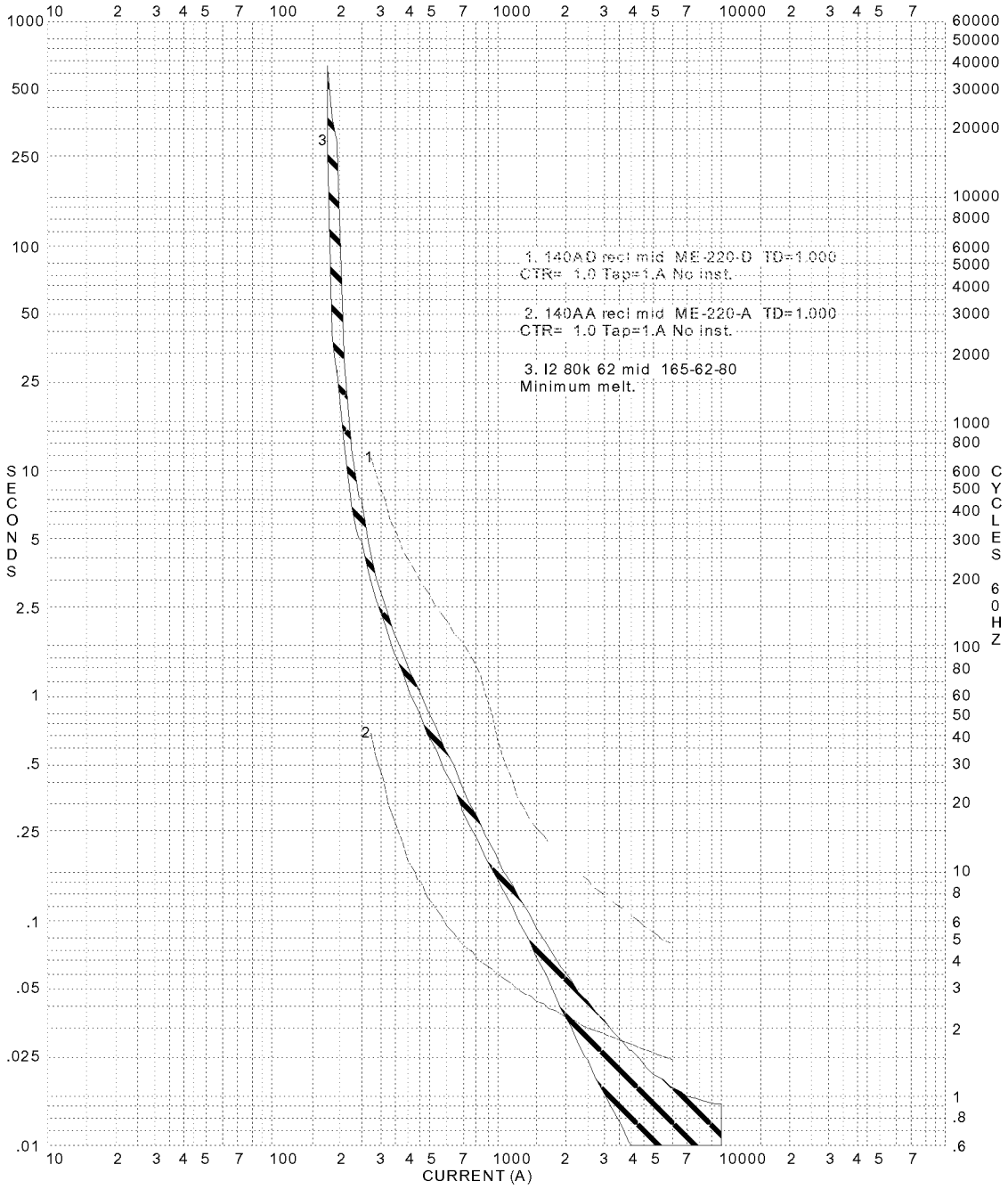

Figure 13. 140-A recloser fast and slow time-current characteristic and 80k fuse time-current characteristic

Figure 14 shows the time-current characteristic (TCC) for the fast, or "A," curve for a 140-A single-phase recloser and an 80k fuse. If the total fault current is less than about 2,000 A, the recloser will interrupt fault current at the same time the fuse will blow (i.e., at 2,000 A of fault current, the "A" curve of the recloser and the minimum melt time curve of the 80k fuse intersect). If the tripping time of the recloser is held to 75% of the time it takes to blow the fuse, then a current maximum of about 1,600 A would be permitted in this case. The fuse can be expected to blow if the current is greater than 1,600 A. Within a certain current range, both the fuse and recloser will open. Fault current that flows from a DR through the fuse will tend to cause the fuse to blow before the recloser operates.

Figure 13 also shows the "D" curve for the recloser as Curve 1. As previously noted, the slower "D" curve will permit permanent faults to be cleared by the fuse without any additional operations of the recloser.

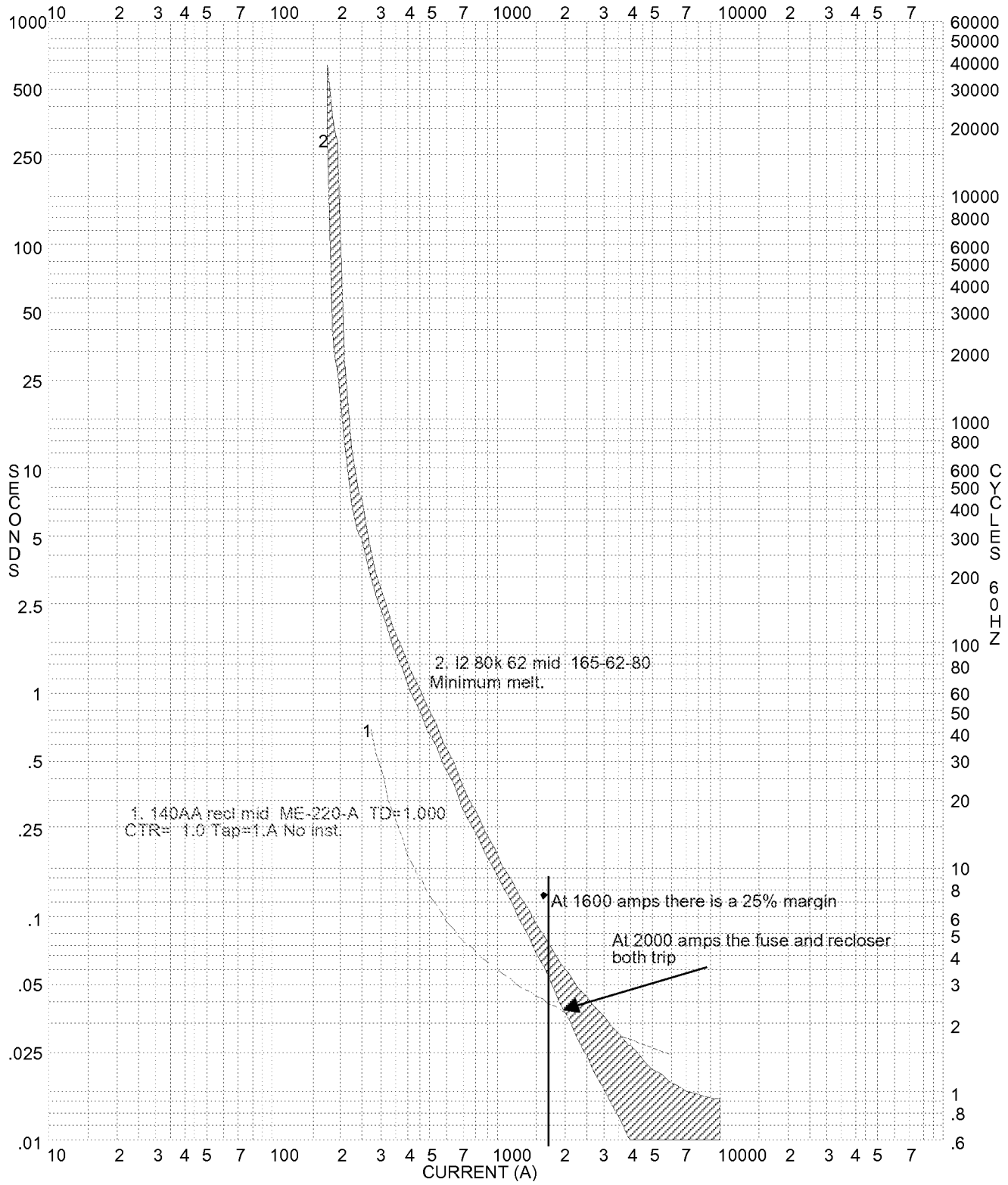

TIME-CURRENT CURVES @ Voltage	By
For	No.
Comment	Date

Figure 14. 140-A recloser fast time-current characteristic and 80K fuse time-current characteristic

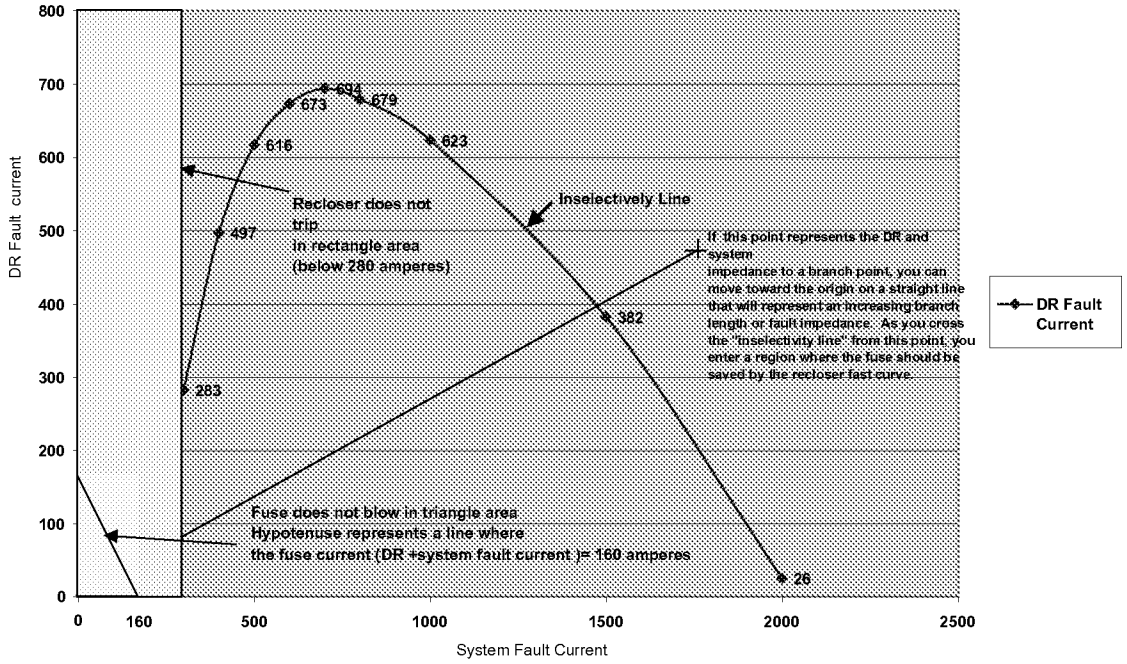

Figure 15. Maximum DR fault versus system fault current for fuse saving (140-A V4L recloser and 80K fuse)

Figure 15 is a plot of the maximum DR fault current that can be added through an 80k fuse, as shown in the configuration of Figure 12. Maximum DR fault current is plotted for a range of system fault current. This curve was developed similarly to Figure 8 in Issue 1.

Note that as the system fault current approaches 2,000 A, the amount of permissible DR fault current approaches zero. This is in agreement with Figure 14, which indicates that at about 2,000 A, the fuse and the recloser will operate at the same time even without any DR fault current contribution.

See Appendix D.2 for additional information about the development of Figure 15.

2.3.3 Question:

What is the limit of DR size for a specific combination of fuse and recloser sizes?

2.3.4 Study Results

The study provided limits of DR penetration for various protective device combinations as applied to the two Detroit Edison circuits.

ASPEN studies indicate the DR size limits are as follows:

Table 4. Maximum DR Size on DC 326 Argo

Fuse Size	Maximum DR Size (MVA) Distance From Substation Near End	Mid Point	Far End
65k	See note	See note	0.3
80k	See note	See note	1.0
100k	See note	See note	2.0

Note: The system fault current is too high to save the fuses even without the DR on line.

Table 5. Maximum DR Size on DC 9795 Pioneer

Fuse Size	Maximum DR Size (MVA) Distance From Substation Near End	Mid Point	Far End
65k	See note	See note	See note
80k	See note	See note	See note
100k	See note	See note	1.0
140k	See note	2.0	8.0

Note: The system fault current is too high to save the fuses even without the DR on line.

See Appendix H.3 for details of the study results.

2.3.5 Conclusions and Recommendations

The protection engineer should perform selectivity studies to determine if the fault current contribution from a DR will reduce the effectiveness of the fuse-saving capability of the recloser-fuse combinations on the Area EPS. In some cases, the fault current may already be too high to save fuses even without the DR connected. In that case, the addition of the DR is not reducing the power quality or reliability of the Area EPS. This study should be performed as part of the general study described in Appendix I.

The fuse-saving practices of the utility should determine the relative significance of any detrimental effects caused by the addition of DR. For example, if a utility uses many sectionalizing fuses to protect lines in remote areas, fuse saving will have high priority. For utilities that have rather high fault currents that make fuse saving marginally effective, the effects of the addition of DR may not be such a high priority.

2.4 EEI Issue 15: Faults Within the DR Zone

2.4.1 Description

The primary concern of the utility is to not have faults within the DR zone (local EPS containing the DR) that cause disruption of service to other loads on the circuit. Related concerns also will be addressed in this section.

2.4.2 Scenario 1

- Faults within the DR zone should be cleared by local protective devices, as shown in Figure 16.

- The fault on the 480-V bus should be cleared by the secondary of the transformer breaker CB 2 and the generator breaker CB 3 without any other protective device operating on the EPS.

- Coordination studies are conducted without the DR, and selectivity is maintained for all protective devices from the substation line breaker to the fault.

- With the DR operating, selectivity needs to be maintained between these same devices such that the protective devices nearest the fault clear first.

- Fault current flowing through CB 1 will always equal fault current flowing through CB 2 for the configuration shown in Figure 17, assuming the transformer turns ratio is included. For example:

  5,011 A @ CB 2 = 182 A x $\left(\frac{13.2}{0.48}\right)$ @ CB 2 when the generator is off, and

  3,160 A @ CB 2 = 115 A x $\left(\frac{13.2}{0.48}\right)$ @ CB 1 when the generator is on.

  This is true whether the generator is on or off. Because the generator *reduces* the system fault current contribution through CB 1 and CB 2, selectivity will normally be improved for this pair of breakers when the generator is on (compared with when it is off).

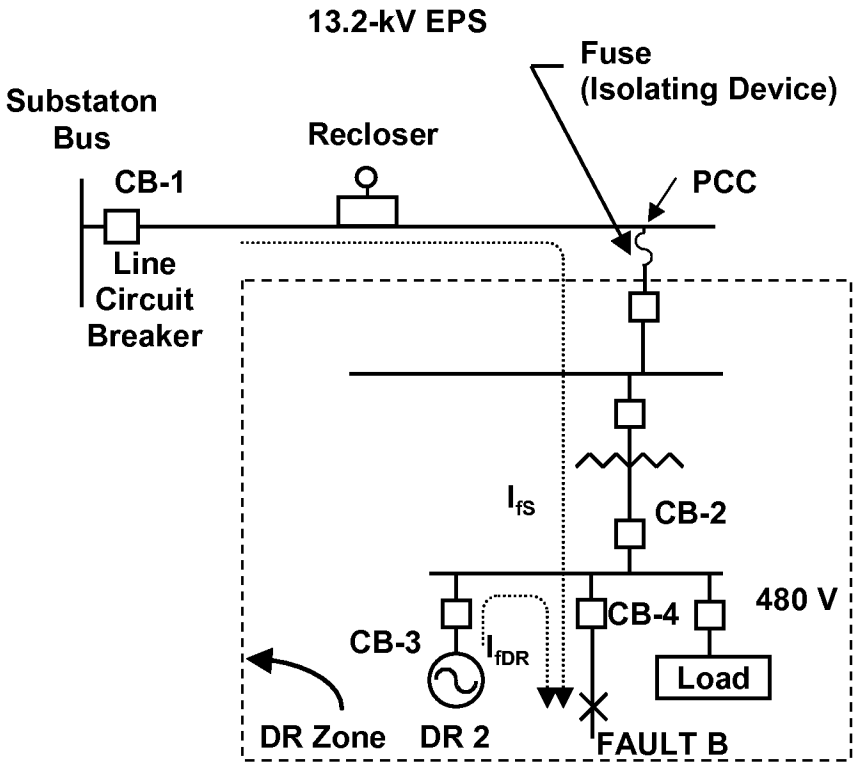

Figure 16. Faults within the DR zone are cleared with local protective devices

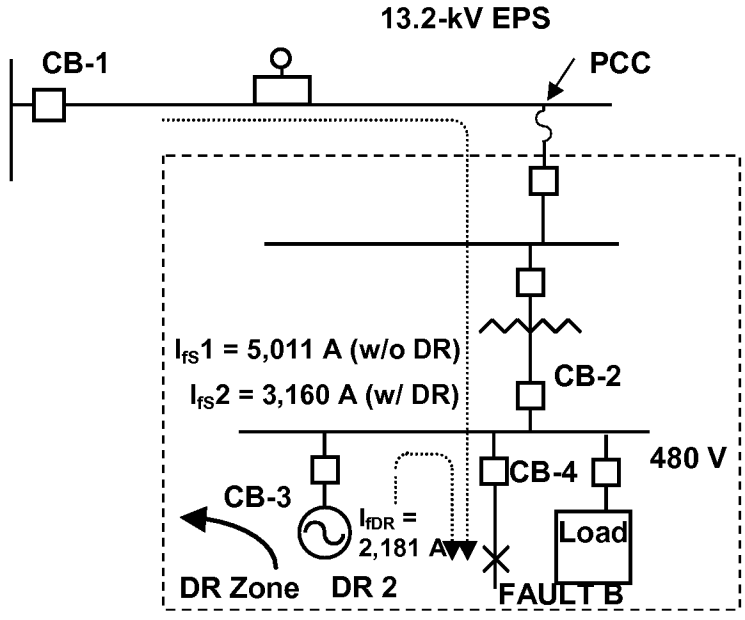

Figure 17. Effects of infeed on system fault current

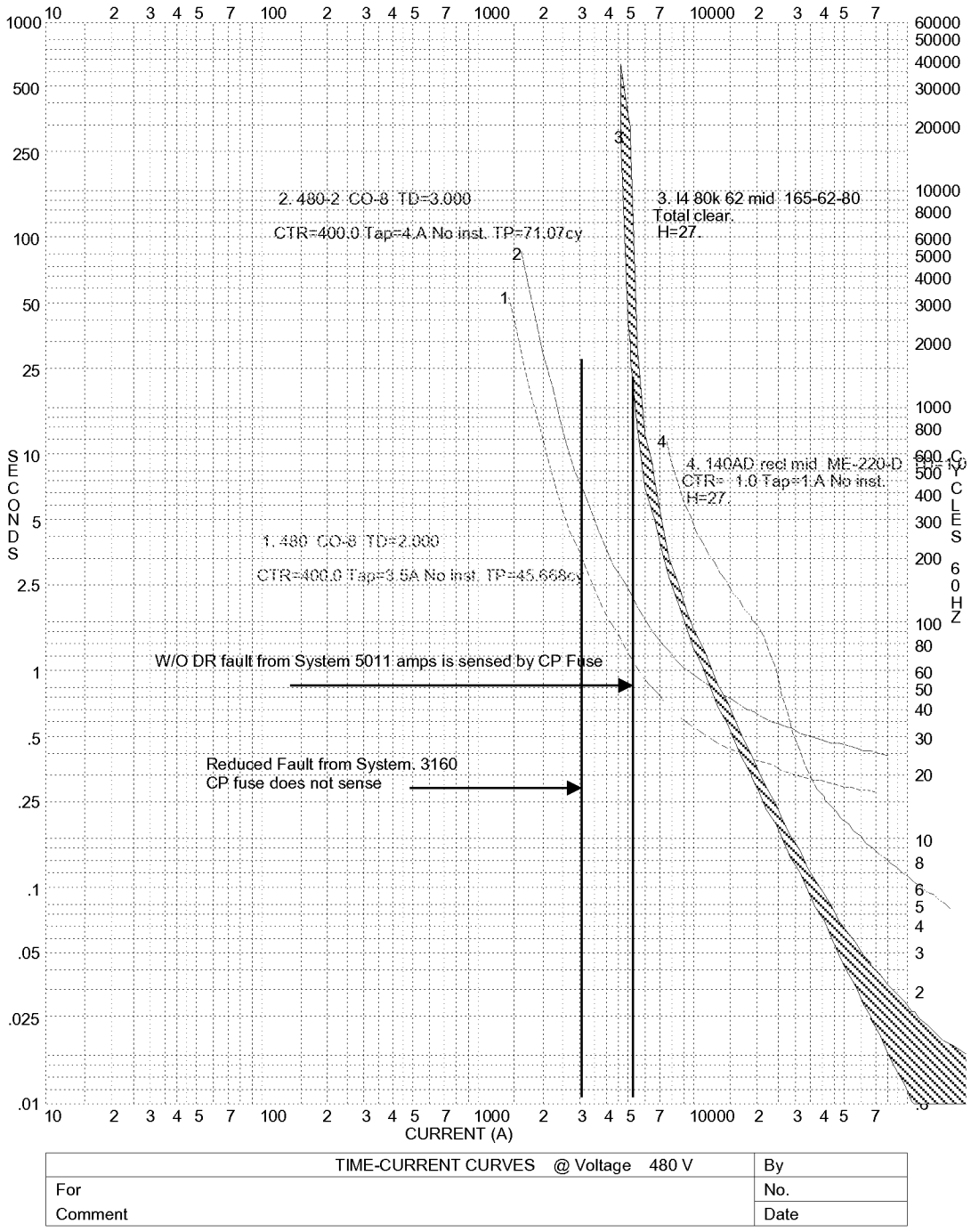

Figure 18. Selectivity coordination of EPS devices and DR zone devices

2.4.3 Question 1: *Selectivity – Between System Protection Devices on the EPS*

Will selectivity be maintained between system protection devices after the DR is added?

2.4.4 Study Results

In Figure 17, two conditions are represented. First, the system fault current without the DR is given. Second, the system fault with the DR added is shown. Figure 18 shows the TCC of the cable pole fuse, the 140-A recloser, and the protective relays for CB 2. Note that these curves are plotted at 480 V, and the 80k cable pole fuse and the 140-A recloser curves have been shifted to show the operate (blowing) time for the fuse and recloser with respect to the operate time for the CB 2 breaker.

Notice the system fault current is lower when the DR is connected. This is because the voltage at the fault is now higher because of the DR current flowing through the fault impedance. See Appendix G for an example of infeed effects and the reason the system fault current will be lower when a DR is connected.

2.4.4.1 Infeed Effect

The desensitizing effects of infeed within the DR zone will normally be small for faults in which DR and Area EPS current only flow through lines or buses. Because typical line lengths within the DR zone will be short, infeed effects will be small for lines and buses that do not have a transformer fed from the Area EPS and the DR. In cases in which the infeed effect is appreciable — such as a transformer secondary fault whose primary source is the Area EPS, and the DR is on the transformer secondary — the fault current from the EPS may be reduced appreciably, and fault current sensitivity can become an issue. Selectivity with other devices on the Area EPS will not be compromised.

DR 1 will typically have little effect on the fault current flowing from the 13.2-kV EPS (I_{fS2}) to Fault A. However, DR 2 can have a significant effect on the fault current flowing from the EPS to Fault B. The increased effect of DR 2 is caused primarily by the impedance of the 13.2-kV–480-V transformer, which is in series with the EPS source.

An example ASPEN study was made on DC 9795. DR 2, a 2-MVA generator, reduced I_{fS2} fault current from 181 A to 115 A when changed from offline to online operation. For similar conditions, DR 1, also a 2-MVA generator, reduced the fault current from 181 A to only 164 A when changed from offline to online operation. A fault impedance of 0.05 Ω was used for these studies. See Appendix H.4 for details.

Note that while selectivity on the utility system is not affected by infeed, fault detection sensitivity is affected. For cases in which infeed effects are appreciable, the current flowing from the Area EPS will be smaller. This will typically cause any protective devices on the EPS to operate more slowly or not at all. For most bus arrangements in which infeed effect is appreciable, a separate protective device will be installed (e.g., a transformer primary fuse). See Figure 19, Fuse F-2. For this situation, the Area EPS protective device (cable pole fuse F-1) would operate as a back-up protective device. If back-up protection is critical, then fault studies should be conducted to model infeed effects to determine if adequate protection is provided.

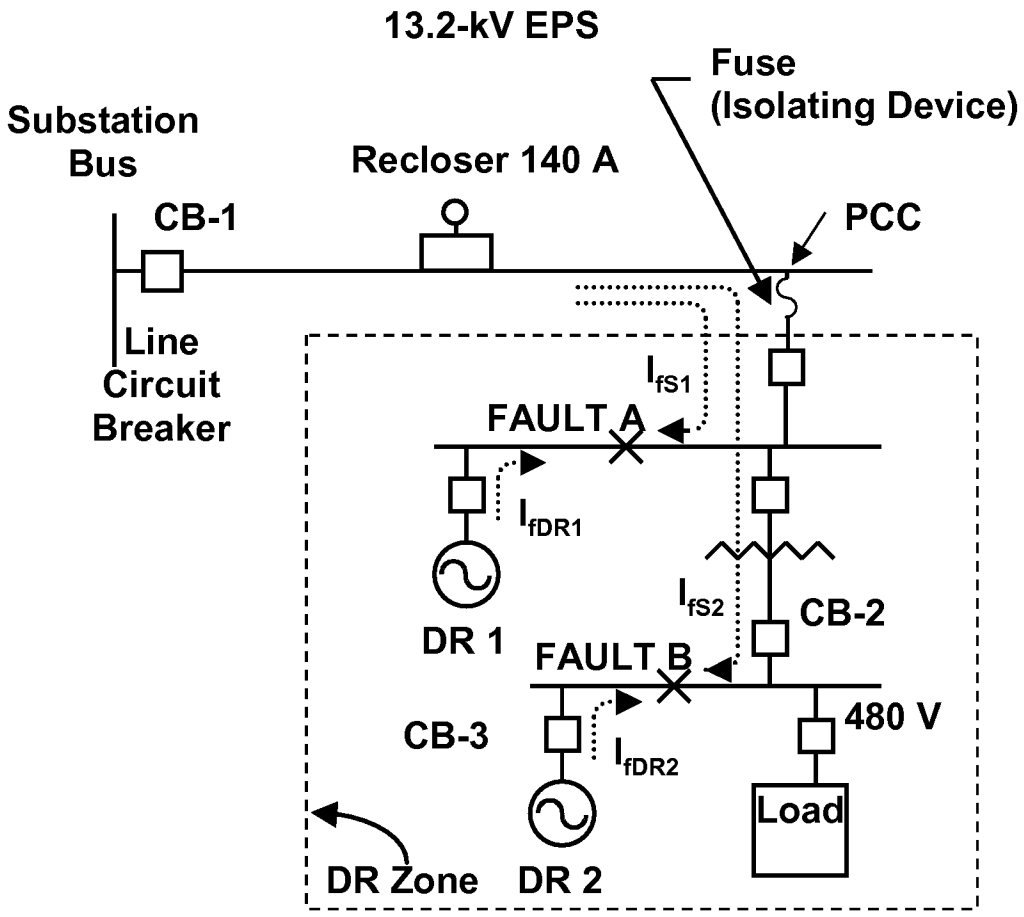

Figure 19. Faults within a DR zone

2.4.5 Scenario 2

- The fault current has increased at the point of fault such that the devices within the DR zone do not coordinate.

- Faults within the DR zone should be cleared selectively by devices nearest the fault.

- With the addition of DR 1 of Figure 20, the fault current at "A" increases through the 65K, F-1 and 25K, F-2 fuses. Although I_{fS} decreases, the total fault current at "A" increases. The point of this scenario is not to demonstrate the selectivity of the devices on the EPS (this was covered in Scenario 1) but to demonstrate the selectivity of the devices within the DR zone.

- As the fault current increases, the selectivity margin among the protective devices decreases within the DR zone.

2.4.6 Question 2: Selectivity – Between Protection Devices in the DR Zone

Will the addition of a DR increase the fault levels to a point at which the selectivity of devices between the DR and the fault is affected?

2.4.7 Study Results

2.4.7.1 Effects of Increased Fault Current on Selectivity

For fuse coordination, increased fault current can cause fuses to become inselective. An additional local DR or changes to the EPS can increase fault current. The replacement of the substation transformer with a unit of larger size or load transfer to a new substation are also typical reasons for significant increases in fault current.

To explain the effect fault current has on DR zone device coordination, refer to the fuse coordination table in Appendix H.3, Cooper Table 2A3, and Figure 20. Notice from Cooper Table 2A3 that the fault currents above 2,200 A will cause the 65k fuse and 25k fuse to blow at the same time and thus do not coordinate. An added DR that will supply 200 A of fault current, as shown in Figure 20, increases the total fault current to 2,300 A. This would further decrease the selectivity margin to a point at which the 65k and 25k fuse will blow for the fault shown. Refer to Figure 21, which shows the inselectivity of devices when the fault current is 2,000 A or greater.

This problem can be addressed several ways. For example, the 65k fuse may be replaced with a larger, 80k fuse if other constraints of selectivity and sensitivity are not violated. If extensive system changes are needed to resolve the problem, budget constraints may not allow the problem to be solved. At the least, operators should be alerted to the problem so they can react accordingly should both fuses blow during a fault.

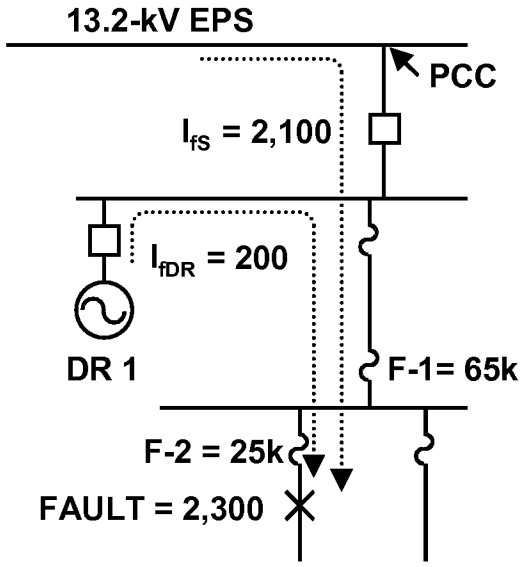

Figure 20. Selectivity coordination within the DR zone

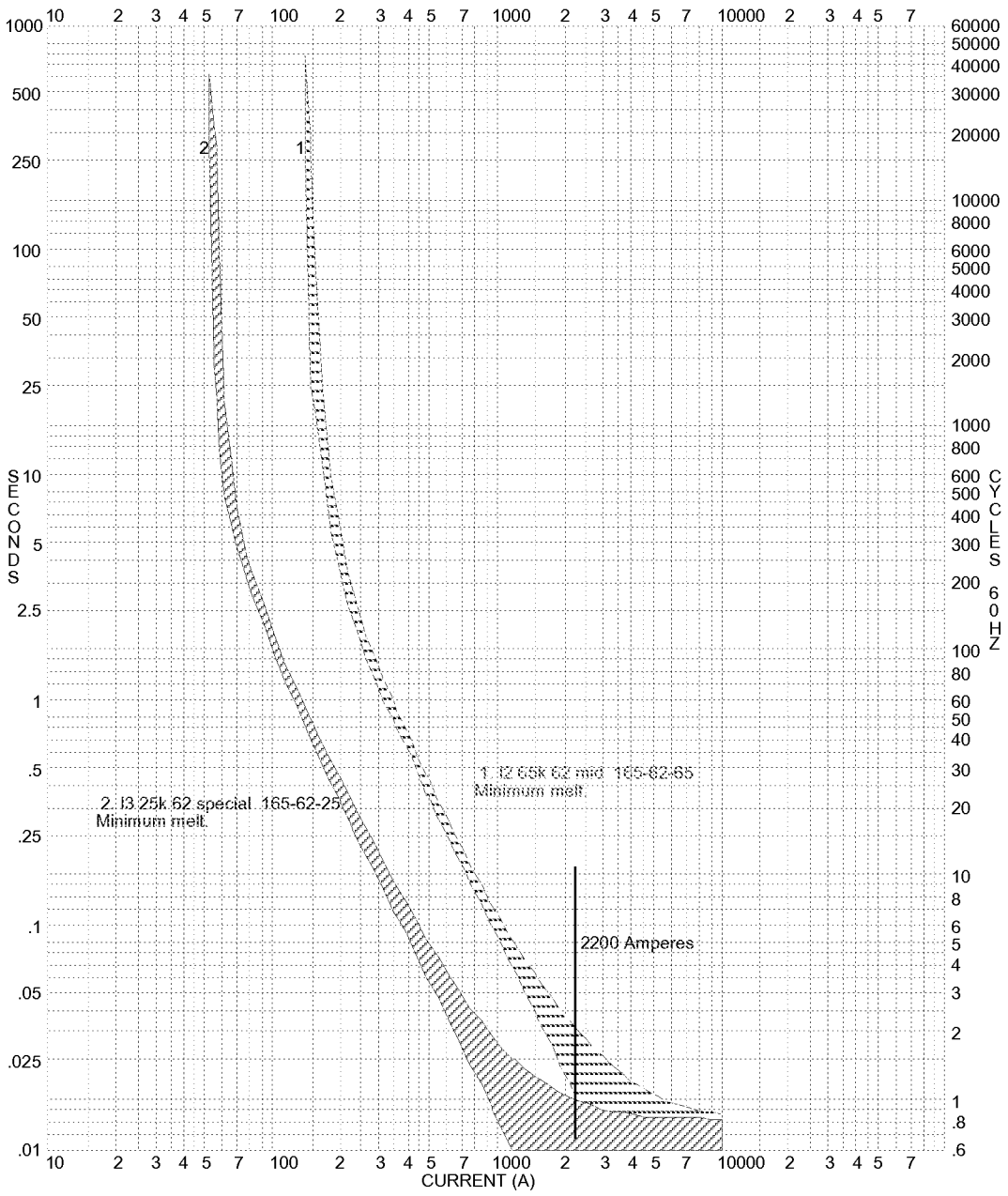

Figure 21. Coordination between devices is compromised when the fault current exceeds a limit of 2,200 A

2.4.8 Other Considerations Not Addressed in Detail in This Report

The following possibilities are not treated extensively in this report. However, they should be taken into consideration when adding any DR equipment to a local EPS.

1. Effects of Increased Fault Current on Equipment Ratings

   As explained earlier, within the DR zone, fault current levels will be increased with the addition of a DR. The interrupting, fault-closing, and momentary fault current ratings of all EPS electrical equipment and equipment within the DR zone should be reviewed before the addition of a DR that increases fault current.

2. Directional Overcurrent Relaying

   Typically, the fault current supplied by the DR is small compared with the fault current supplied by the Area EPS. In many cases, the fault current supplied by the DR may be less than or nearly equal to the local load. To obtain adequate sensitivity and selectivity for faults on the Area EPS, directional overcurrent relaying may be required.

   Shown in Figure 22, the overcurrent relay (51) must be set to a value greater than 2,000 A and cannot sense the 200-A fault current from the DR. Therefore, a more sensitive directional overcurrent relay (67, sensing current flow from the DR to the EPS) is installed to open breaker CB 1, thus retaining the DR to serve the critical load after the fault is cleared.

   The DR generator protection shown in Figure 22 will trip the 100-kW DR for overcurrents above 120 A. Protective devices on the EPS can be expected to interrupt service from the EPS to all equipment in the DR zone. If the DR generator is tripped and the EPS is isolated, then electric service to the critical load is lost. To preserve the critical load and maintain adequate sensitivity and selectivity for faults on the Area EPS, directional overcurrent relaying may be required.

   Note that the local load (2,000 A) is much larger than the capability of the DR (120 A). To maintain uninterrupted service to the critical load, the non-critical load must also be tripped off when CB 1 is tripped. The remaining critical load must not be larger than the DR capability. The details of tripping paths are not shown in Figure 22.

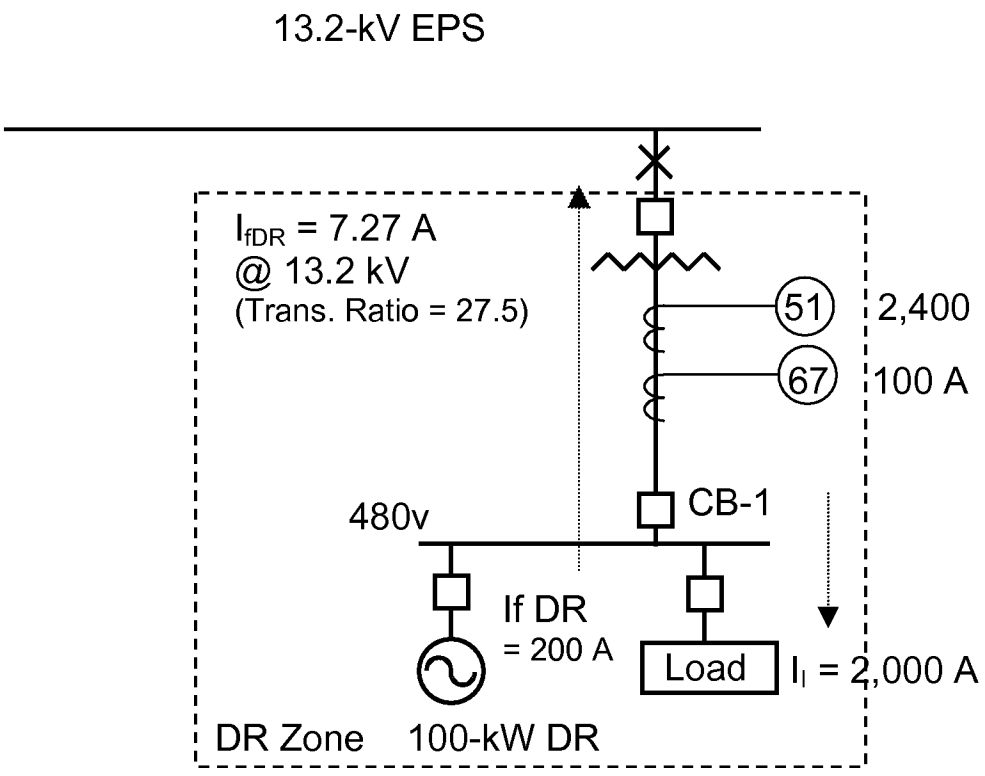

Figure 22. The need for directional overcurrent relaying when the DR fault current is nearly equal or less than the normal load current

3. Generator Protection

   The DR protection as supplied with the purchased package should be reviewed to determine if it has the functions required to protect the DR for all operating conditions.

   One of the many possible conditions that should be reviewed is phase unbalance. Unbalanced load and single-phasing conditions can arise unexpectedly and are more likely in areas with single-phase protective devices. Adequate negative sequence current protection can protect the generator from thermal damage caused by extended periods of unbalanced load operation.

   The generator protection should also be reviewed to determine if it is compatible with the local EPS and with the utility EPS protection schemes.

4. Transformer Delta Connection on Area EPS Side with Line-to-Ground Fault on Area EPS

   Line-to-ground fault conditions on the primary of the interconnection transformer that are cleared from the Area EPS by a single-phase fuse are sometimes overlooked. A study should be done to determine if this fault will be sensed by the DR system relaying and trip the generator. See illustration.

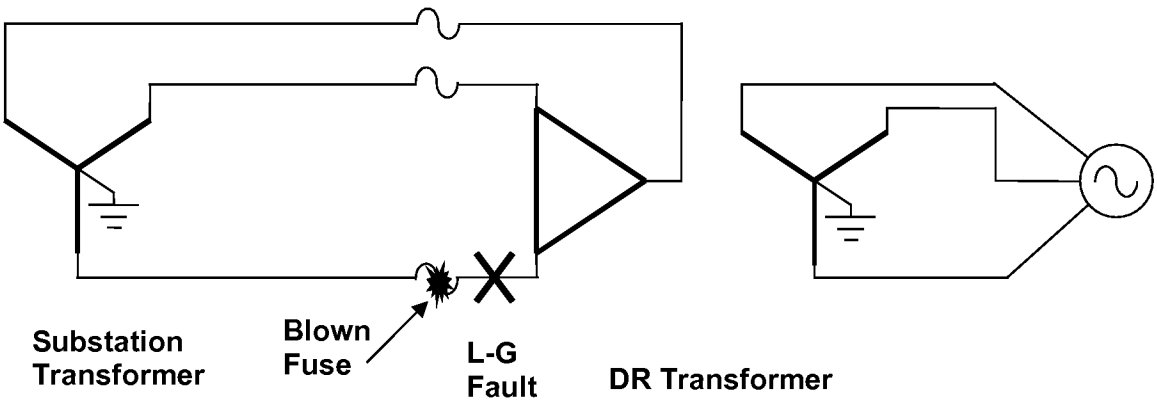

Figure 23. Transformer Delta Connection on Area EPS Side with Line-to-Ground Fault on Area EPS

5. Delta High-Side Transformer Connection

If a delta connection is used on the high side of the interconnection transformer, then line-to-ground faults on a wye multi-grounded system can result in line-to-line voltages (from the delta) being applied across the line-to-neutral loads of the unfaulted phases. In this case, zero sequence overvoltage protection is required on the primary side of the DR interconnection transformer. The illustration below shows the overvoltage condition applied to the loads.

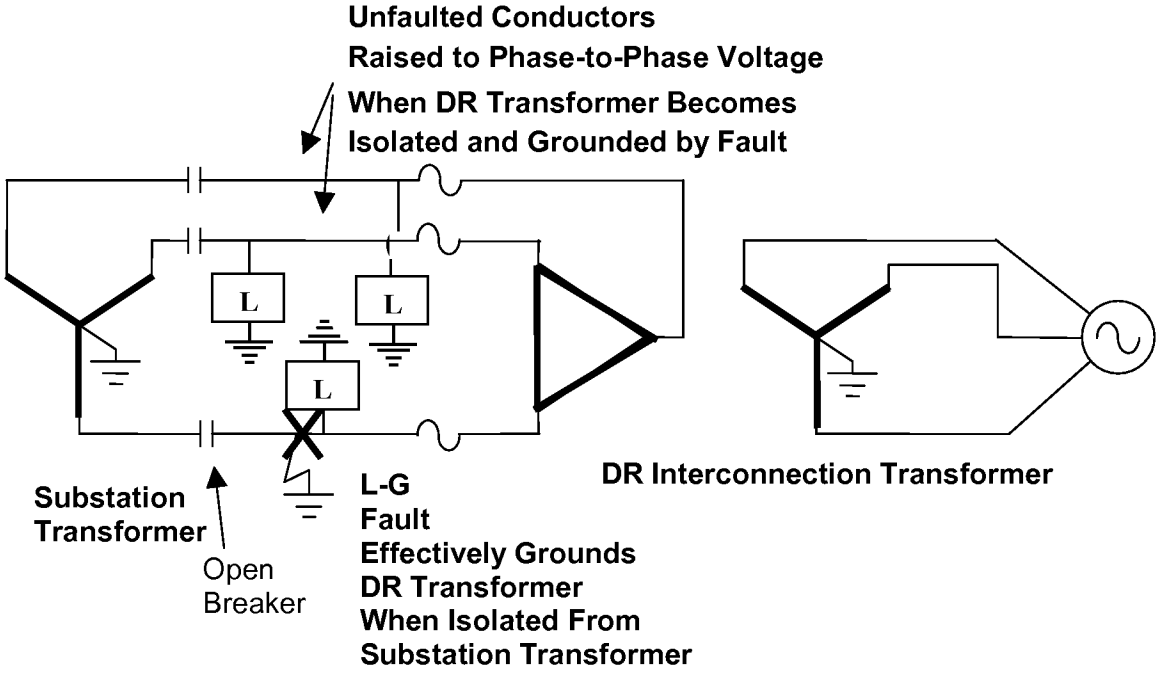

Figure 24. Overvoltage Condition Applied to Delta High-Side Transformer Connection

6. Effect of Variations in DR Size and Area EPS Stiffness

   As fault current through a pair of coordinating fuses increases, the margin for selectivity will decrease. (See Figure 21.) Increasing DR fault current or Area EPS stiffness will have a similar effect.

7. Isolation for Internal Faults

   Typically, if the isolation device (see Figure 16) at the PCC (e.g., cable pole fuse) isolates the fault without the DR running, it isolates the fault with the DR running.

   Note that the DR operator will be concerned that temporary faults on the Area EPS not cause unnecessary or unexpected interruptions of equipment within the DR zone. EEI issues 1, 16, and 27 deal with inselectivity issues that may affect DR operation. This issue is not directly addressed in this report. However, issues 1, 16, and 27 can be applied to determine if the protective device at the interconnection point will operate for faults on the Area EPS.

2.4.9 Conclusions and Recommendations

Protection for faults internal to the DR zone is primarily the concern of the DR operator.

Typically, if an internal fault is properly isolated from the EPS by a protective device on the EPS or by the DR without the DR running, it will be properly isolated for internal faults when the DR is running.

The analysis for faults internal to the DR should include a review of the desired selectivity of devices on the EPS and within the DR zone. At minimum, the Area EPS operator should ensure selectivity with all protective devices on the EPS up to the PCC. Ideally, the selectivity study will include an overlap of one device within the DR zone.

The DR operator should ensure selectivity of devices up to and including the first protective device on the EPS side of the PCC.

The effects of increased fault currents because of the addition of the DR should be reviewed by the Area EPS operator and the DR operator. The primary concern should be the fault duty of equipment. However, selectivity margins may also be reduced because of the increased fault current. Therefore, all parties should remain aware of this effect and perform any necessary studies to determine if equipment or protective device settings require change.

The DR operator should also include studies that provide analysis for those issues not covered in this report. Items of particular importance are:

- Fault duty of all equipment
- Generator protection
- Delta-wye transformer connections causing zero sequence overvoltage during EPS line-to-ground faults
- Possible improvements in operation and fault clearing by adding directional overcurrent relays
- Possible out-of-phase condition caused by EPS reclosing or slow fault clearing
- Line-to-ground faults on primary of a delta-wye transformer cleared by a local fuse on the transformer primary.

2.5 EEI Issue 16: Isolate DR for Upstream Fault

2.5.1 Description

Three-phase faults upstream of a three-phase recloser may cause the recloser to operate because of fault current contribution from a group of DR downstream of the recloser. See Figure 25.

Even though the protection on each individual DR may be selective with the recloser, the added fault current from all DR on the circuit may cause the recloser to operate. If a fault causes system protection equipment to isolate load from the utility source (such as opening the recloser in Figure 25) and causes an island, then the remaining DR may not be capable of serving the islanded load without causing voltage and frequency control problems.

This study considers the operation of a fuse at the PCC of an existing DR. If the operation of the fuse at the PCC were ignored, the total DR current required to operate the recloser of Figure 25 could be simply calculated as any value above the tripping point of the sectionalizing device. Operation of the fuse at the existing PCC will stop the flow of fault current from the existing DR. Then only the additional DR will be supplying current.

If the additional DR were identical to the existing DR in fault current capability and fuse size, the fuse at each DR would blow simultaneously. This study will determine the amount of fault current from the added DR that will cause the recloser to operate on the slow curve.

Operation of the recloser on the fast curve is not considered in this study. Time versus current characteristics for the recloser and fuse are shown in Figure 26. Although undesirable, operation on the fast curve will not cause the recloser to lock out. Therefore, priority was given to the study of tripping on the slow curve. A recloser will typically lock out a minimum of two operations on the slow curve.

Please refer to the "Description" section of Issue 27 for additional details. Paragraphs 3–8 provide details that are essentially the same for single-phase and three-phase faults.

2.5.2 Scenario

- A fault occurs on the circuit at "A" in Figure 25, between the substation circuit breaker CB 1 and the recloser.
- Current flows from the substation transformer and from the DR to the fault.
- The current from DR 1 is sensed by a local device (fuse) and the recloser.
- The current from the additional DR on the circuit may cause the recloser to operate.

2.5.3 Question

Assume the protective devices at an existing DR will isolate the DR from the system prior to the recloser operating. How much additional DR capacity is necessary (assuming the fuses on DR 2 and DR 3 do not exist) to cause the recloser to operate before the protective devices operate on the existing DR 1?

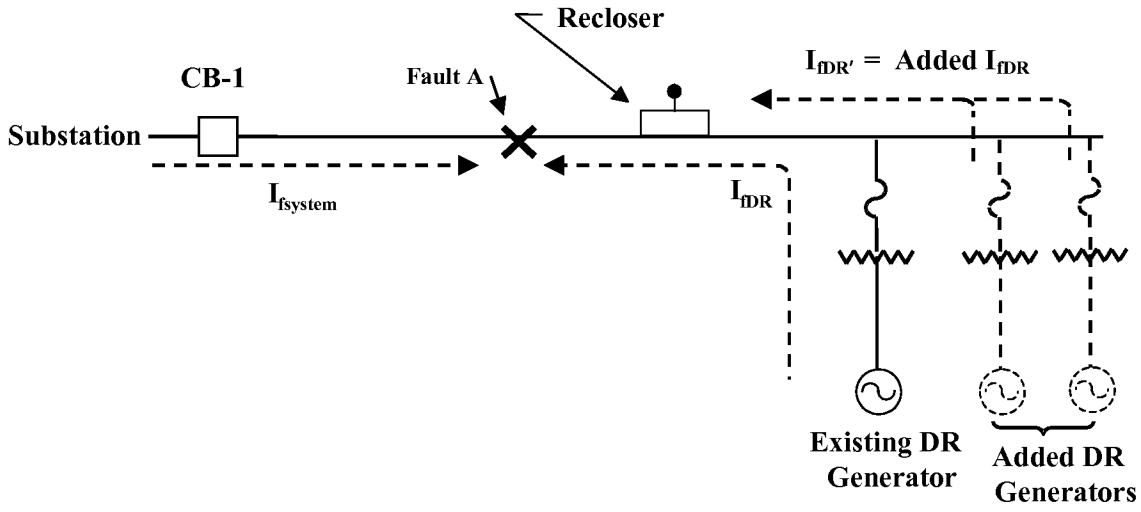

Figure 25. Aggregated DR fault current through a recloser causes recloser to operate

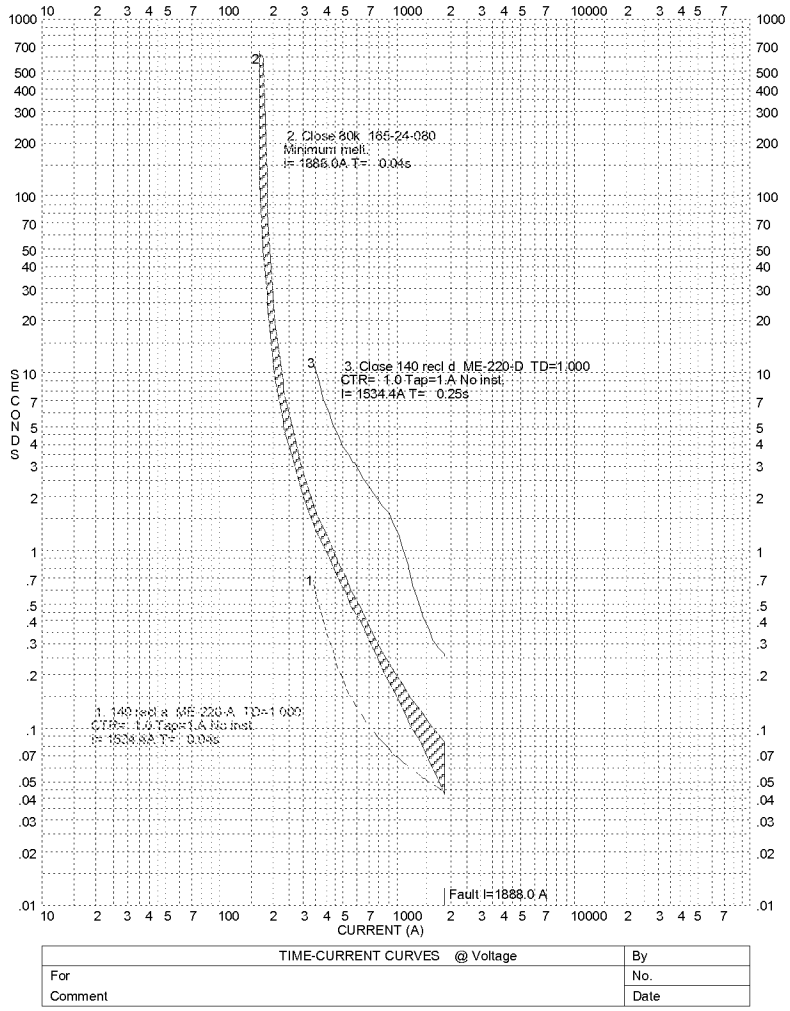

Figure 26. Tripping characteristics for 140-A recloser and 80k fuse showing fast and slow curves for the recloser

2.5.4 Study Results

The studies determined the added DR maximum size for three existing DR sizes: 0.5 MVA, 1 MVA, and 3 MVA, which represent a typical size range for a 4.8-kV circuit. 1-MVA, 3-MVA, and 5-MVA DR sizes were used for the 13.2-kV circuit.

ASPEN studies indicate the DR maximum size limits are as follows:

Table 6. Maximum DR Size on DC 326 Argo (4.8 kV)

Existing DR Size and Fuse Size Combination	Maximum Added DR Size (MVA) Distance From Substation Near End	Mid Point	Far End
40k-0.5 MVA	1.3	1.3	1.3
40k-1 MVA	3.5	3.5	3.5
40k-3 MVA	Greater than 10	Greater than 10	Greater than 10
80k-0.5 MVA	0.3	0.3	0.3
80k-1 MVA	0.75	0.75	0.75
80k-3 MVA	Greater than 10	Greater than 10	Greater than 10

Table 7. Maximum DR Size on DC 9795 Pioneer (13.2 kV)

Existing DR Size and Fuse Size Combination	Maximum Added DR Size (MVA) Distance From Substation Near End	Mid Point	Far End
40k-1 MVA	3.1	3.2	3.2
40k-3 MVA	12	12	12
40k-5 MVA	Greater than 20	Greater than 23	Greater than 23
80k-1 MVA	0.3	0.3	0.3
80k-3 MVA	2.2	2.2	2.2
80k-5 MVA	5	5	5

Tables 6 and 7 indicate that when the existing DR is large, then the additional maximum DR limit is also large. Logic would dictate that as the existing DR size increases for a fixed fuse size for this DR, then the recloser could tolerate less additional DR fault current from the added DR units before tripping. But as the existing DR size gets larger, its fuse is more likely to blow, thus allowing more DR units to be added before the recloser operates. Therefore, the results in tables 6 and 7 are logically confirmed.

Figure 26 shows the additional DR current or MVA that can be added without operating the 140-A recloser before the cable pole fuse or DR 1 breaker opens. The curves in Figure 26 are for a 140-A recloser and an 80k fuse.

The additional scale indicates the current that would be supplied by a 2-MVA generator and the length of overhead line between the DR and the fault that would produce the associated currents.

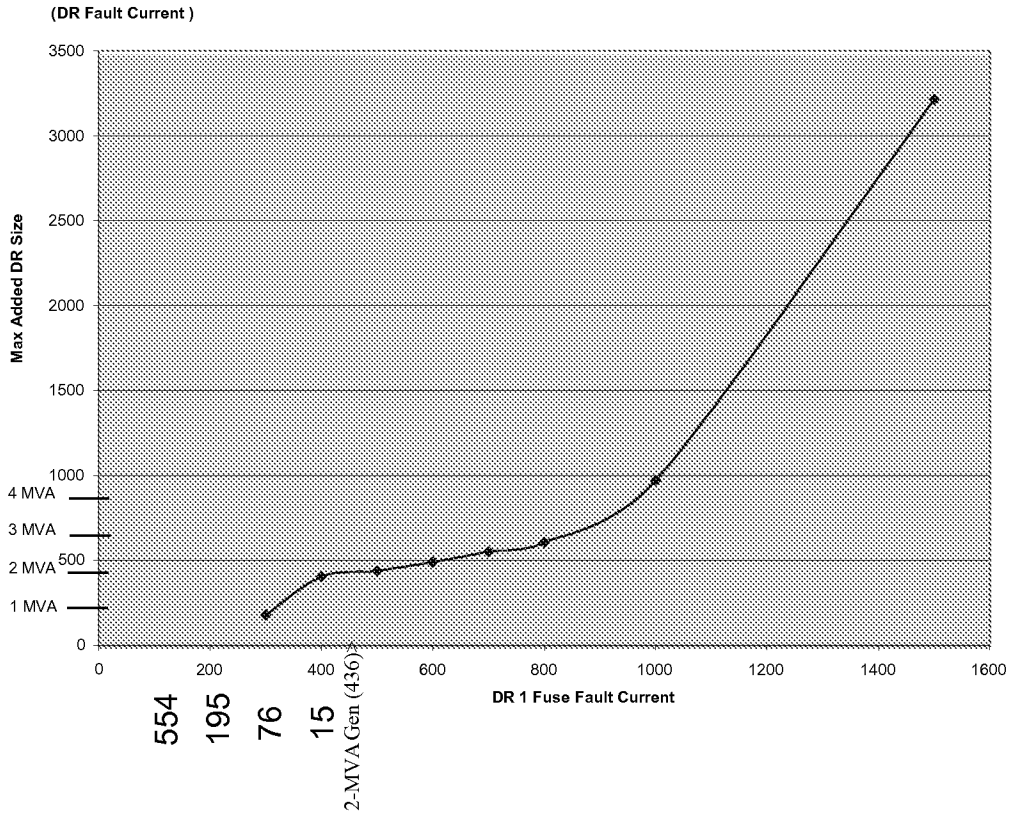

Figure 27. Maximum added DR size as a function of DR fault current

2.5.5 The Unexpected Effect of Increased Current

As the fault current from DR 1 increases, the recloser fuse arrangement can tolerate more current from the additional DR. This seems counterintuitive. It might be expected that as the DR 1 fault current increases, the fault current permitted from the other DR would decrease.

What is happening is the fuse TCC is steeper than the recloser curve for much of the effective range. As current is increased through the fuse of DR 1, the added current will shorten the blowing time of the fuse more than it will shorten the trip time of the recloser. This results in a time margin between the fuse and the recloser, which, in turn, permits the system to tolerate more current from the additional DR.

2.5.6 Conclusions and Recommendations

The distance from the substation has little or no effect on the added fault current from additional DR that will cause the sectionalizing devices to operate. The effect, as analyzed, is a local effect. The faults studied used a value of zero for the fault impedance. Introducing a three-phase fault with zero impedance between the sectionalizing device and the substation effectively separates the distribution circuit into two systems. The first system is the substation and line up to the fault. The second system is all of the distribution circuit beyond the fault, including the DR and the sectionalizing devices. Further study could analyze the effects of introducing fault impedance.

2.6 EEI Issue 27: Upstream Single-Phase Fault Causes Fuse Blowing

2.6.1 Description

Line-to-ground faults upstream from a recloser or sectionalizing fuse (sectionalizing device) may cause the sectionalizing device to operate because of fault current from a group of DR downstream of the device.

This condition is nearly identical to the condition presented in EEI Issue16. Although the effect of these faults is similar to those presented in EEI Issue16, single-phase faults that cause single pole operation are likely to result in unbalanced load currents.

Without the existing DR connected to the circuit, the normal fault-clearing process involves only opening the CB 1 line breaker and eliminating the source of the I_{fS} fault current to fault "A." Because there is no DR connected to the system in this case, no current will flow to the fault through the single-phase recloser on the faulted phase.

When the first DR is added to the circuit (shown as existing DR in Figure 28), the typical system protection scheme includes an overcurrent relay that operates the CB 1 breaker, sectionalizing devices (recloser or fuses), a cable pole fuse for the DR, a transformer secondary breaker, and a DR breaker. For a fault at the generator terminals being supplied fault current from the Area EPS, these devices are coordinated so that the protective devices operate because of overcurrent in the following order:

1. DR breaker
2. Secondary transformer breaker
3. Cable pole fuse
4. Recloser or line fuses
5. CB 1 line breaker.

Proper coordination will result in only the DR breaker operating for a fault at its terminals. The remaining devices operate only if one or more devices fail to operate correctly.

For a fault at location A, I_{fDR} fault current will flow from the DR to the fault at A, and I_{fS} will flow from the substation to the fault at "A." In this case, I_{fDR} current is the same through each protective device from the DR to the fault. It is not important whether the DR breaker or the CB 1 breaker operates first as long as the DR breaker and the CB 1 breaker isolate the fault, but it is important that the DR breaker open before the transformer secondary breaker, cable fuse, and sectionalizing devices open.

If it is desirable to allow the DR to continue to serve its load, then directional overcurrent relays should be installed so the transformer secondary breaker will open this breaker and permit the DR breaker to remain closed and serve the local load.

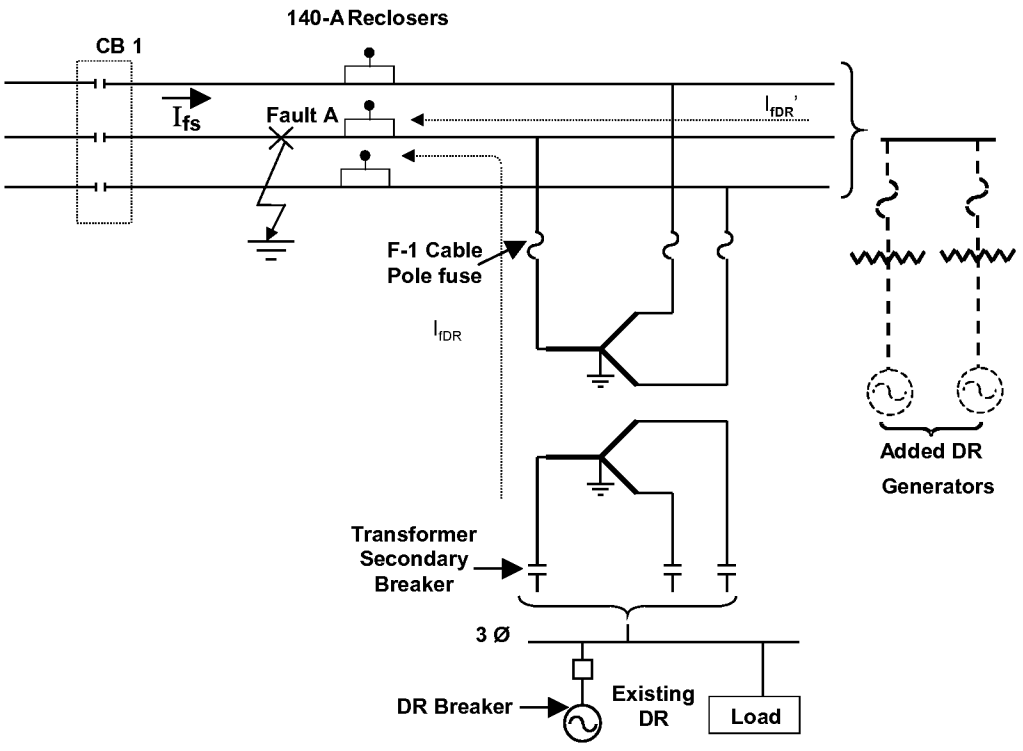

Figure 28. Line-to-ground fault causes single-phase sectionalizing device to open because of DR fault current contribution

When additional DR are connected to this circuit, the total fault current ($I_{fDR} + I_{f'DR}$) through the sectionalizing devices (reclosers or fuses) is now the sum of the existing DR and the additional DR fault contributions, and this additional current may cause the sectionalizing device to open before the DR breaker on any DR opens. This condition could result in the DR serving an islanded load, which may or may not be desirable. If the condition is undesirable, then the DR breaker must be opened. The load is now temporarily lost because of the recloser being open but not locked out (after three to four openings). Now, if the fault condition is removed before the recloser is automatically reclosed, then the recloser can reclose, and CB 1 will automatically reclose (because of the reclosing relay operation), which restores service to the circuit load. Note that the DR have remained offline to permit this desirable operation to occur. The DR can now return to normal operation through re-synchronizing operation with the system.

For a permanent single-phase fault, such that the fault current from the DR causes only one single-phase recloser to lock out (assuming CB 1 is open), then the DR may remain online serving load on the unfaulted phases between the reclosers and the CB 1 breaker and serving all the three-phase load downstream from the reclosers. This situation may cause severe load imbalance for the DR and could result in enough negative sequence current to overheat the DR generators. Normally, DR generators are equipped with negative sequence protection to trip the DR units. Where three single-phase fuses are used in lieu of three single-phase reclosers, the fault current from the DR causes the fuse

on the faulted phase to blow, which permanently results in the loss of loads on the faulted phase from the substation to the fuse, and the DR could continue to serve all of the load (3-phase and single-phase) downstream of the open fuse. If the DR cannot serve the load, and the fault at A is cleared, then the CB 1 could automatically reclose and serve all the load except for the single-phase load on the previously faulted phase downstream from the open fuse. This condition could go undetected until identified by the customers served from the previously faulted phase.

The most desirable case is when the DR breakers open, the fuses are not blown, the fault is temporary, the CB 1 opens and recloses after the fault is cleared, all load (circuit and DR load) is restored, and the DR are re-synchronized.

2.6.2 Scenario

- A fault occurs on the circuit at "A" between the substation line circuit breaker and the sectionalizing device (recloser or fuse).

- Current flows from the substation transformer and from the DR to the location of the fault.

- The current from the existing DR is sensed by a local device (F-1 fuse) and the sectionalizing device (recloser or fuse).

- The current from the additional DR on the circuit may cause the sectionalizing device to open.

2.6.3 Question

Assume the protective devices at an existing DR will isolate the DR from the system prior to the recloser opening (without additional DR). How much additional DR capacity can be added to cause the recloser to open sooner than when the protective device (F-1 fuse) on the existing DR operates?

What concerns are there for single-phase operation of the system?

Determining the additional DR fault current that will cause protective device inselectivity can aid planning and protective relay engineers in quickly estimating if an added DR will cause a problem.

This section will determine levels of fault current from additional DR that will cause operation of the sectionalizing device and also present problems associated with single-phase operation of a system with DR.

2.6.4 Area EPS Line-to-Ground Fault Fed From DR

To provide fault current to line-to-ground faults on the Area EPS, the connection of the DR interconnection transformer on the Area EPS side must be grounded. For three-phase generators, this requires a grounded wye configuration.

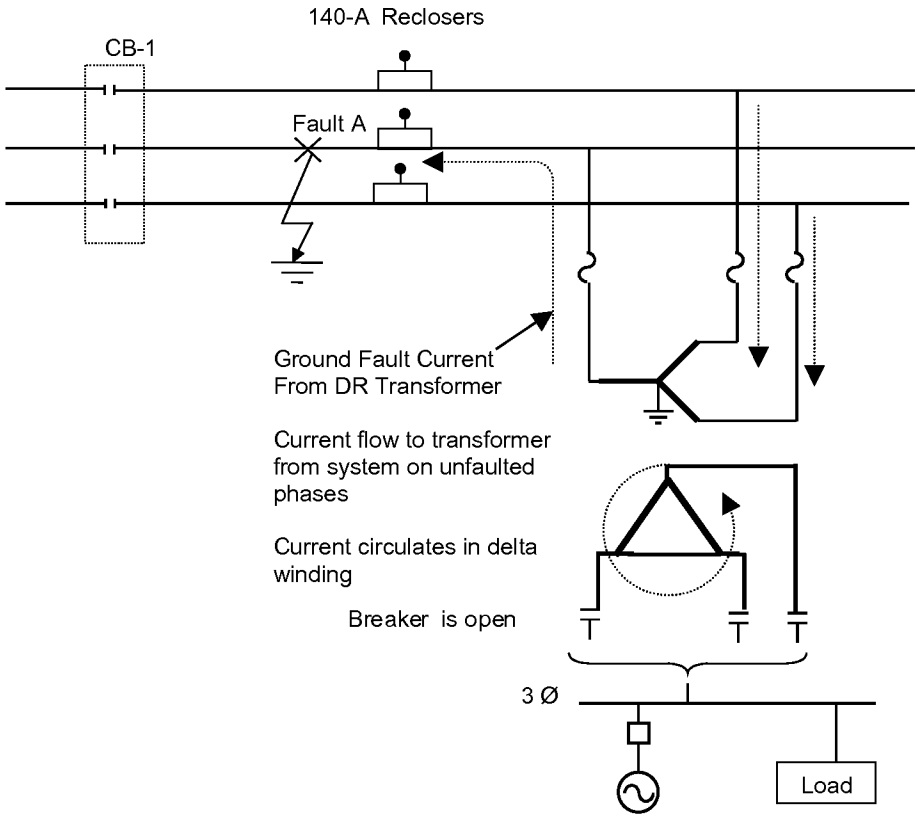

Figure 29. Wye-delta transformer as a ground source

Except for special cases, the transformer will not have a delta connection on the DR side of the transformer because it would then be a source for ground fault current even if the DR is off-line. For a line-to-ground fault on the EPS or primary side of the interconnection transformer, the delta-connected secondary of this transformer provides coupling from the two unfaulted phases on the primary to the faulted phase on the primary and will source ground current to the remote fault. Transformers with grounded wye-delta configurations with grounded wye on the Area EPS side are typically applied in areas in which ground fault current is very weak.

Such transformers have from time to time been misapplied. Misapplication of these transformers is likely to result in unexpected operation of local protective devices for even remote line-to-ground faults on the Area EPS. The Art and Science of Protective Relaying[4] contains information about the protection of grounding transformers. A wye-delta transformer is specifically mentioned as a grounding transformer. Note that the wye winding must have the neutral grounded for a wye-delta transformer to serve as a grounding transformer.

For the purposes of this study, it will be assumed that the transformer is connected wye-wye and solidly grounded on both sides. Resistively grounded transformers or resistively grounded generators will typically limit fault current contribution to line-to-ground faults to the equivalent of a much smaller DR.

2.6.5 Study Results

No studies were done on DC 326 Argo because the system is an ungrounded delta and produces no appreciable ground fault current.

To evaluate the selectivity of DR protective devices and EPS sectionalizing devices, it is necessary to have as a relay source of information the TCC of each device. Figure 30 shows these characteristics for the 140-A single-phase recloser and the 40k and 80k fuses located at the cable pole.

To apply these curves, the following steps are taken, assuming a single DR installation:

1. Determine the desired sequence of operation of devices (i.e., DR breaker opens before cable pole fuse opens, and cable pole fuse opens before recloser opens).
2. Determine the system and DR fault currents of each device.
3. Determine the time to open each device based on that fault current, which will determine actual sequence of operation.
4. Compare the desired sequence of operation with the actual sequence of operation. If the "actual" and "desired" sequences are the same, then selectivity is correct.

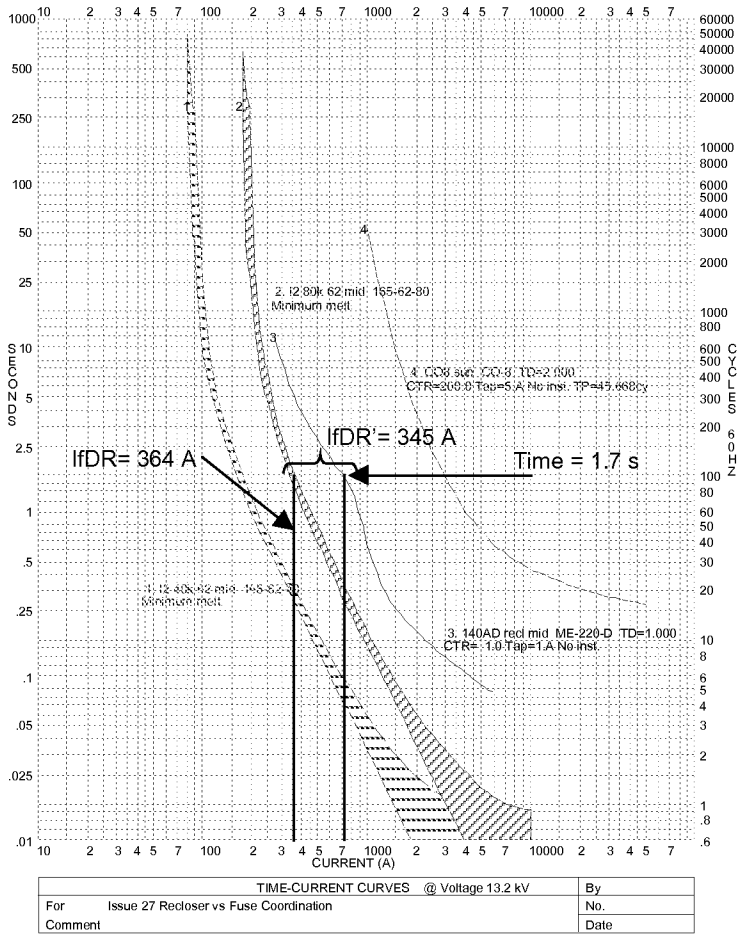

Figure 30. Selectivity analysis time-current characteristics for a 140-A recloser, 80k fuse, and 40k fuse

Using these same steps, additional DR current is added to the circuit until the actual sequence of operation and desired sequence of operation cause an inselectivity problem. As an example, for a 1-MW DR, or I_{fDR} of 364 A, the cable pole fuse opens in 1.72 s, and the recloser opens in 2 s. For existing and additional DR units, the I_{fDR} is 364 A and I_{fDR}' is 345 A. In this case, the cable pole fuse still opens in 1.72 s for the existing DR, but the recloser now opens in 1.71 s because of the added I_{fDR}.

Table 8 shows that for an existing DR size of 1 MVA and with an 80K cable pole fuse and 140-A recloser, the maximum additional DR size is 0.95 MVA. Table 8 shows similar data for 40k cable pole fuses and other locations on the circuit.

Table 8. Maximum DR Size on DC 9795 Pioneer (13.2 kV)

Existing DR size and Fuse Size Combination	Maximum Added DR Size (MVA) Distance From Substation			
	Near End	Mid Point High Z	Mid Point Low Z	Far End
40k-1 MVA	2.5	2.5	2.5	2.5
40k-3 MVA	> 20	14	> 20	> 20
40k-5 MVA	> 20	> 20	> 20	> 20
80k-1 MVA	0.95	1.0	1.0	1.0
80k-3 MVA	3.0	2.5	3.5	3.0
80k-5 MVA	12	7	12	12

Figure 31 shows the additional DR current (or MVA) that can be added without operating the 140-A recloser before the cable pole fuse (80k) or DR 1 breaker opens.

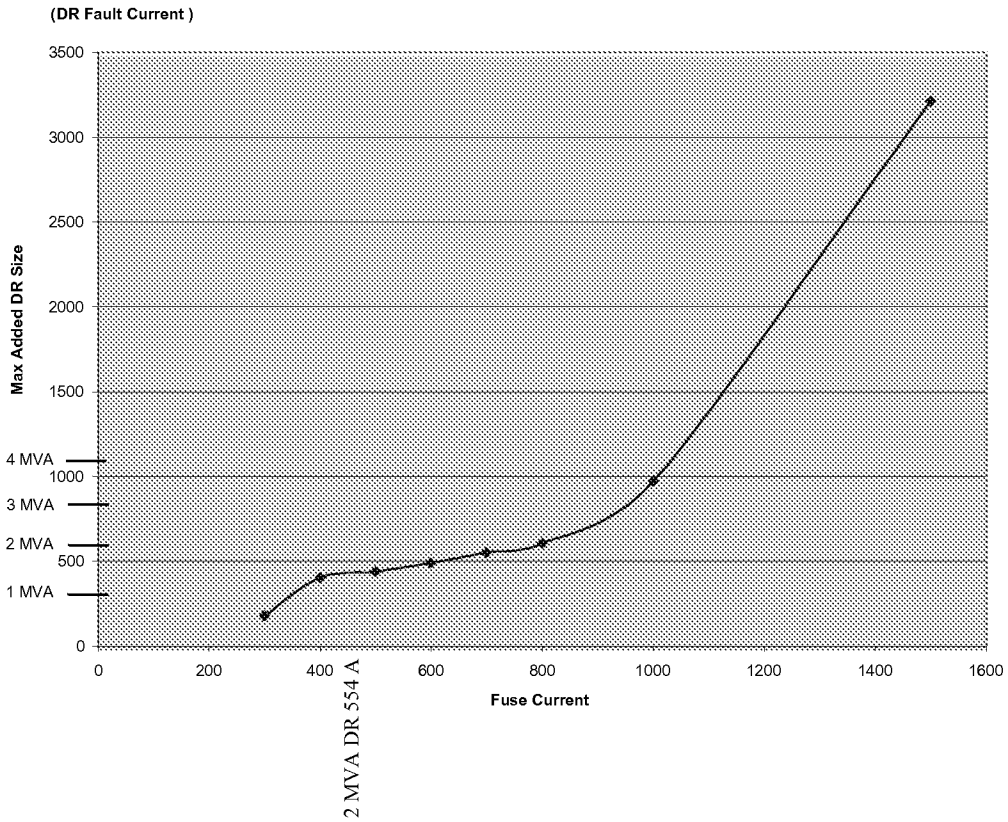

Figure 31. Maximum added DR size as a function of DR (fuse) fault current

2.6.6 Conclusions and Recommendations

A comparison of the results of EEI Issue16 and these results shows that, for most cases, the maximum DR generator size for Issue 16 is smaller than for the single-phase cases shown in Table 8. For most of the studies, an incremental increase in the size of the existing DR would decrease the time of the local fuse blowing. For example, for an 80k fuse and an existing 3-MVA generator, line-to-ground faults (EEI Issue 27) required a 3-MVA generator where the three-phase fault required a 2.2-MVA generator to establish an inselective condition. The reason for this is the I_{fDR} is larger for a line-to-ground fault than for a three-phase fault. This is due to the generator's low zero sequence reactance and the wye-grounded interconnection transformer.

2.6.7 Often Overlooked Results

During line-to-ground faults close to the substation, an appreciable amount of current may flow in the unfaulted phases of the generator. This is due to the substation transformer primary being connected in a delta and reflecting a lower voltage (than before the fault) on the unfaulted phases. Figures 32 and 33 show the unfaulted phase currents are higher than the phase currents before the fault occurred, and this could cause unexpected reclosures or fuse openings. This effect has not been considered.

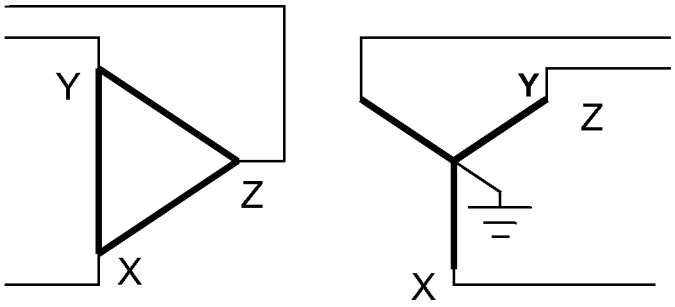

Substation Transformer Connections

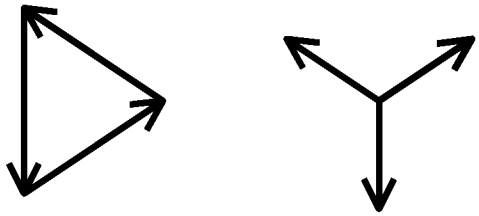

Unfaulted Voltage Vectors

Figure 32. Substation transformer and voltage vectors before fault

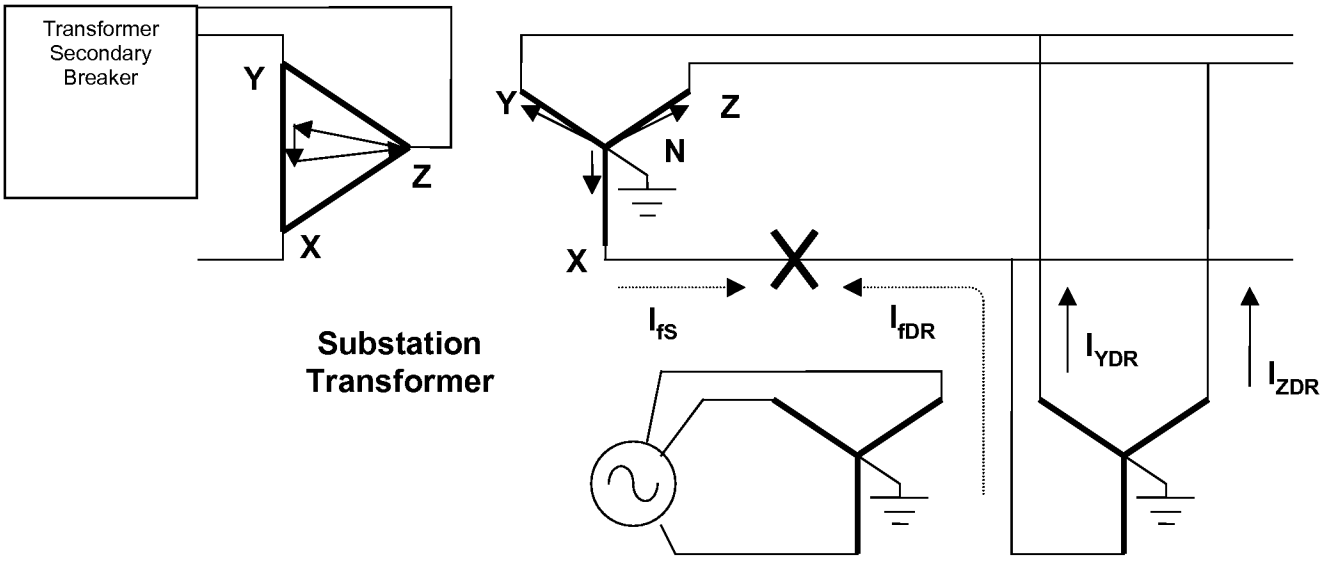

X-N voltage decreases to near zero on secondary
X-Y voltage decreases also on primary
Y-Z voltage and Z-X voltage decrease and change phase angle

DR Current on Y and Z increase because of lower/shifted Y-N and Z-N voltage at substation.

Figure 33. Voltage vectors during X-phase-to-ground fault

Note: The delta-wye substation transformer is an effective grounding transformer. Even without a source to the substation, current will flow in the unfaulted phases from the generator to the substation transformer.

During a line-to-ground fault on X phase, the substation X-N voltage decreases. For faults near the substation, this voltage may approach zero. This low voltage will be reflected in the transformer X-Y primary winding.

This will cause the Y-Z and the Z-X voltages to also decrease and shift in phase because the three primary voltages X-Y, Y-Z, and Z-X must vectorially sum to zero (required by the delta transformer primary connection). These lower voltages will be reflected into the secondary voltages Y-N and Z-N.

Lower and phase-shifted voltages Y-N and Z-N will cause increased current to flow from the DR to the substation because the bus voltage at the DR is higher than the substation voltages.

Note that the X-Y voltage differs from that X-N voltage (neglecting turns ratio) by the voltage drop in the transformer because of the fault current flowing. It will be lower than the unfaulted X-Y voltage because of the voltage drop in the impedance in the line feeding the transformer.

3. PART II: Voltage and Stability Issues

The EEI issues identified for study by Kinectrics were:

1. EEI Issue 8: Harmonics
2. EEI Issue 11: Voltage Regulation Malfunctions
3. EEI Issue 20: Steady State Stability
4. EEI Issue 21: Dynamic Stability During Fault Conditions
5. EEI Issue 22: Loss of Exciters Cause Low Voltage.

3.0.1 Modeling Techniques

3.0.1.1 Harmonics

For harmonic studies, the distribution feeders were modeled by the Electro Magnetic Transients Program (EMTP) using balanced pi-sections, each corresponding to a section of figures 34 and 35. Model parameters (resistance and inductive reactance) were determined from segment lengths and normalized parameters supplied by the host utility. Capacitive reactance values were calculated by taking the speed of propagation to correspond to the speed of light for line modes and half the speed of light for ground modes. Frequency-dependent line models were found to be unnecessary given the relatively short feeder section lengths (typically less than 300 m) and the uncertainty of load damping at harmonic frequencies. Loads were modeled as series R-L branches using specified 60-Hz values and power factor, which produces a reasonable X/R ratio of about 5 near 1 kHz. Cable laterals at service entrance drops were modeled as lumped capacitances at the respective feeder nodes. Synchronous machines were modeled using 0.2 pu subtransient reactance based on the rating of the machine.

The frequency scan feature of the EMTP was used to inject harmonic current sources at selected nodes while computing voltages at various nodes. The ratio of computed voltage to injected current gives a normalized harmonic voltage profile, which taken together with the expected harmonic current spectra from inverter-based DR allows determination of the expected voltage distortion for DR operation.

For voltage impact studies, MATLAB software was used to produce output in a form needed for rapid assessment and formal presentation. A positive sequence feeder model was developed in the same detail and on the same basis as for EMTP studies and included provisions for incorporating generation at specified nodes. Matrix methods were used to solve for the voltage profile for specified generation with loads modeled as constant impedance.

3.0.1.2 Stability

For stability studies, the PTI PSS/E software was used to model generator dynamics for synchronous machines under fault conditions. A positive sequence representation of the feeder was incorporated in the same form as for the analysis using MATLAB. Machine dynamics were modeled using the "GENROU" round rotor model in the PSS/E. Machine parameters were based largely on those provided for an existing DR on the Pioneer feeder, with selected variations in parameters to assess their sensitivity to the solution. Fixed field excitation (fixed field voltage) and prime mover controls were assumed to produce more conservative results.

3.0.2 Validating Models

Models were validated by performing analytical calculations for simplified system representations. Proper feeder representation was confirmed in each case by comparing load flow results provided by DTE using ASPEN Distriview software against results predicted by EMTP, MATLAB, and PSS/E. Agreement was confirmed for the voltage profiles for specific feeder loading. Selected parameters were scaled uniformly up and down to confirm expected model behavior. This was done for feeder loads (real and reactive power), feeder section lengths, and per-unit length parameters defining feeder-section geometry. The MATLAB and EMTP models were built using feeder data assembled in a shared file to reduce effort and ensure modeling consistency.

3.1 EEI Issue 8: Harmonics

3.1.1 Description

Utilities are required by IEEE 519 to limit total harmonic distortion of the voltage waveform to 5% and distortion at any single frequency to 3%. Current harmonics can be produced by rotating machines, by power electronic-based inverters, or by saturation of transformers because of asymmetrical saturation caused by DC injection from unbalanced inverter operation. Emerging standards require injected current harmonics because of nonlinear loads, including inverter-based DR, to be limited to a total harmonic distortion of 5% at the PCC. Limits of harmonics at individual frequencies are 4% for all odd harmonics below the 11th, 2% below the 17th, 1.5% below the 23rd, 0.6% below the 35th, and 0.3% beyond the 35th harmonic. Even harmonics are limited to 25% of the nearest odd harmonic level.

3.1.2 Scenario

An inverter that meets industry standards for harmonic current content may produce harmonic voltages on the EPS that exceed the limit of 3% for any single harmonic. If the inverter is large enough and injects harmonics at the same frequencies for which the EPS has a high resonant impedance, then a high resonant harmonic voltage is produced that may exceed the maximum permissible voltage distortion of 3% at that harmonic frequency.

3.1.3 Question

What are the maximum sizes of inverters that meet permissible industry harmonic limits that can be connected at different nodes on the circuit? The maximum permissible voltage distortion at any single frequency is 3%.

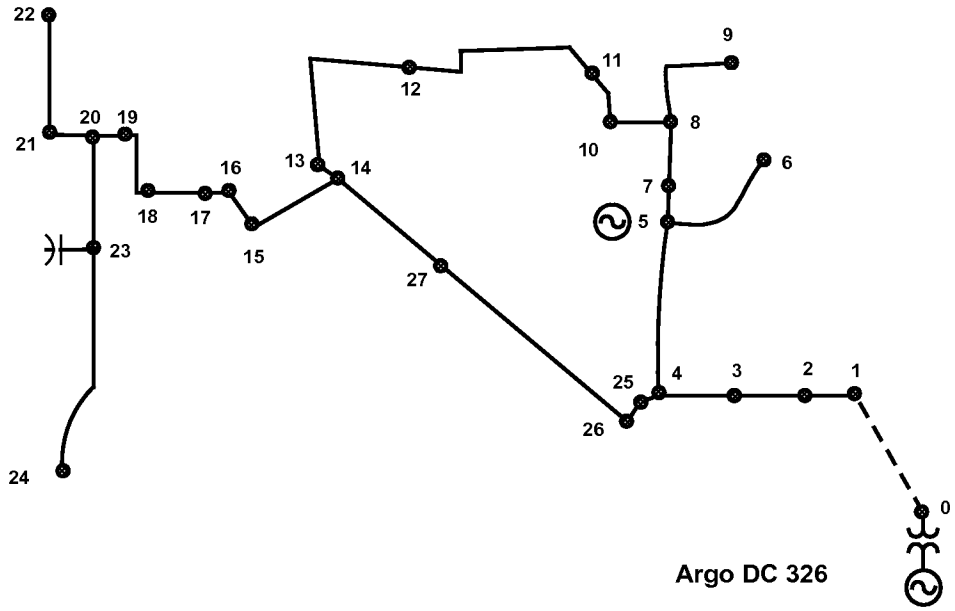

Figure 34. General layout of the three-phase portion of the 4.8-kV Argo feeder

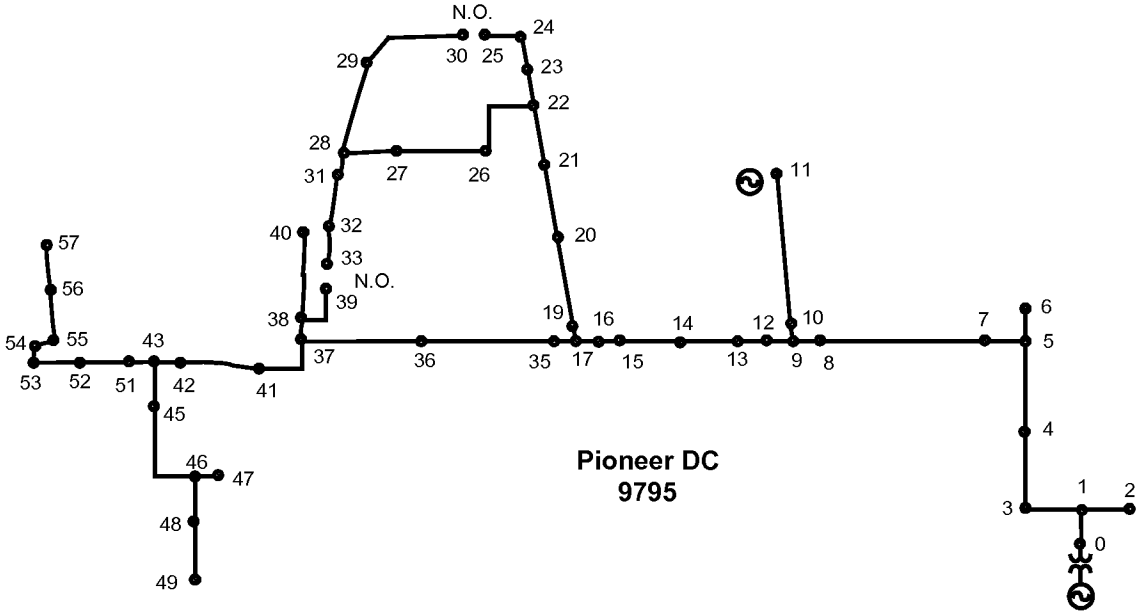

Figure 35. General layout of the three-phase portion of the 13.2-kV Pioneer feeder

3.1.4 Study Results

Figure 36 displays the results of EMTP simulations for the Argo feeder at peak load and shows the predicted voltage for 1 A of harmonic current injected at Node 0 of Figure 34. The plot ordinate accordingly corresponds to an impedance measurement. The following is noted:

- The highest curve on the plot is the driving point impedance at the injected node, indicating that highest harmonic distortion is near the harmonic source at Node 0.

- The first resonant peak, which is about 450 Hz, or near the 7th harmonic, is associated with a parallel resonance condition involving the 600-kVAR capacitor at Node 23 and the inductive source reactance (see Figure 37).

- Beyond this resonance, the capacitor dominates the response, causing harmonic impedance to drop until a series resonance is encountered involving the intervening feeder inductance (10th to 15th harmonic, depending on the node being considered).

- Subsequently, the plot exhibits an inductive response, representing the source impedance in parallel with the inductance of the feeder to the capacitor.

- Modeled loads offer negligible dampening at harmonic frequencies, so the presented findings are independent of diurnal load variations.

The response seen from all nodes upstream of the capacitor (nodes 5, 9, 14, and 22) is remarkably similar, as shown in figures 38–42. However, in case of harmonic injection at Node 24, the capacitor at Node 23 acts as an effective filter to limit voltage distortion upstream (Figure 42). If capacitive compensation at Node 23 is temporarily disconnected, the harmonic impedance plot exhibits a simple inductive response associated with the source and feeder reactance (Figure 43). In this case, the first resonance mode is found near the 200th harmonic, corresponding to quarter wave resonance for a feeder having a 3.9-mile electrical length.

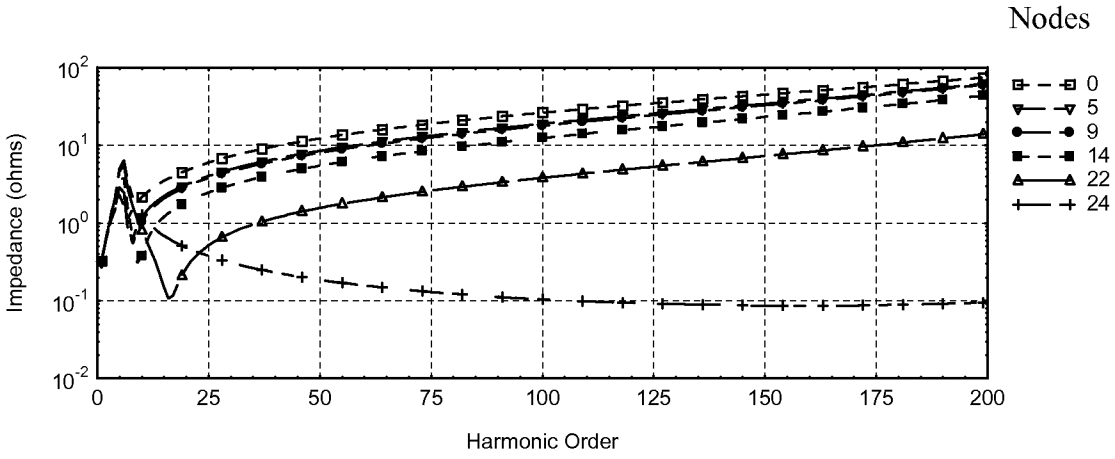

Figure 36. Argo feeder, harmonic injection at Node 0 for the peak load condition at 0.9 PF

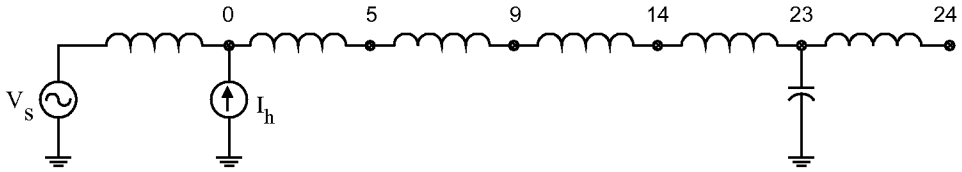

Figure 37. Simplified equivalent circuit representation of Argo feeder
(distributed feeder capacitance not shown)

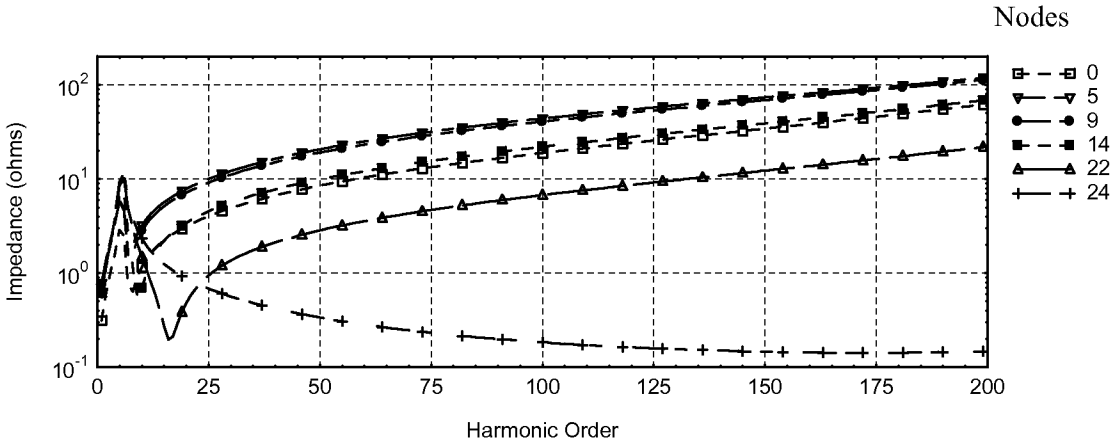

Figure 38. Argo feeder, harmonic injection at Node 5 for peak load at 0.9 PF

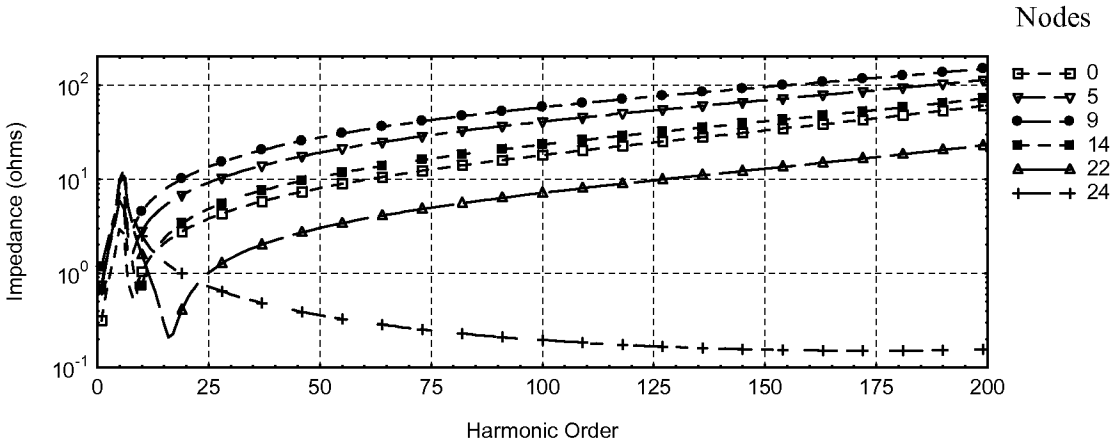

Figure 39. Argo feeder, harmonic injection at Node 9 for peak load at 0.9 PF

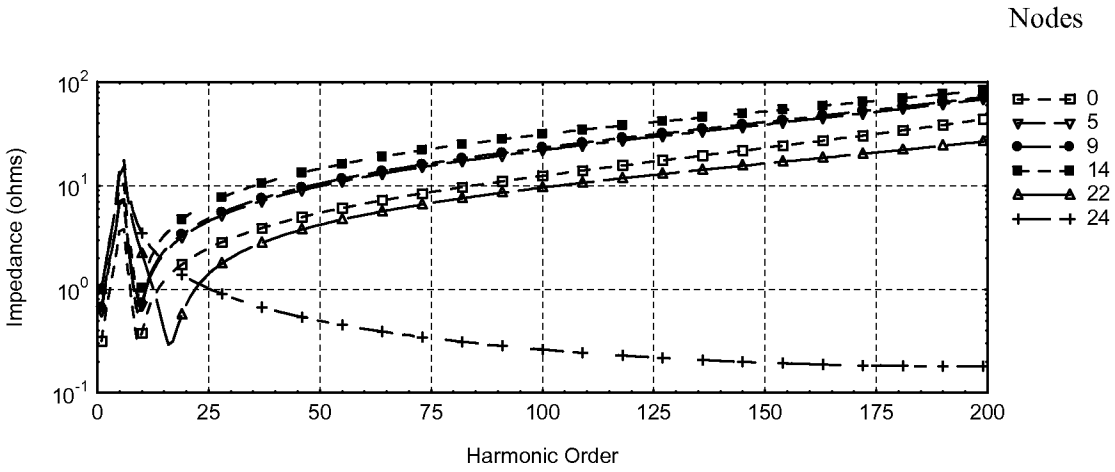

Figure 40. Argo feeder, harmonic injection at Node 14 for peak load at 0.9 PF

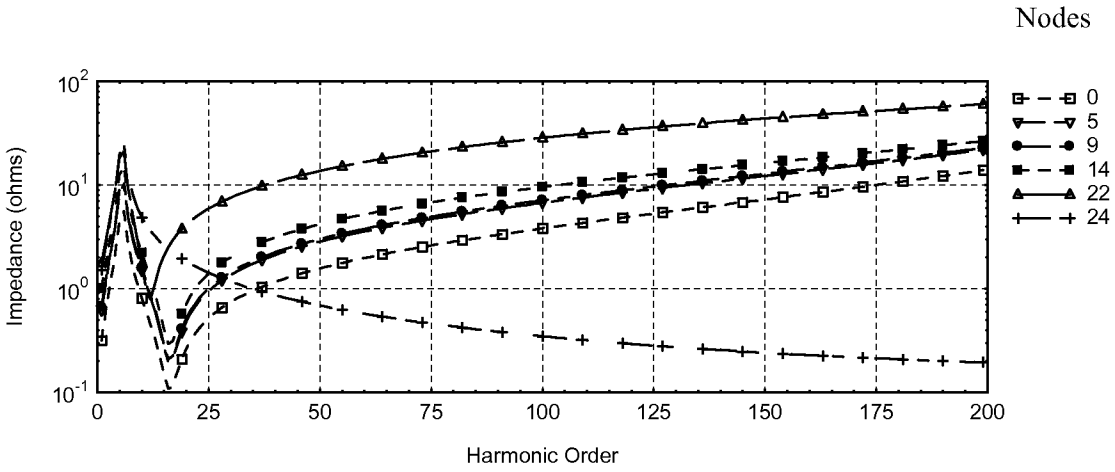

Figure 41. Argo feeder, harmonic injection at Node 22 for peak load at 0.9 PF

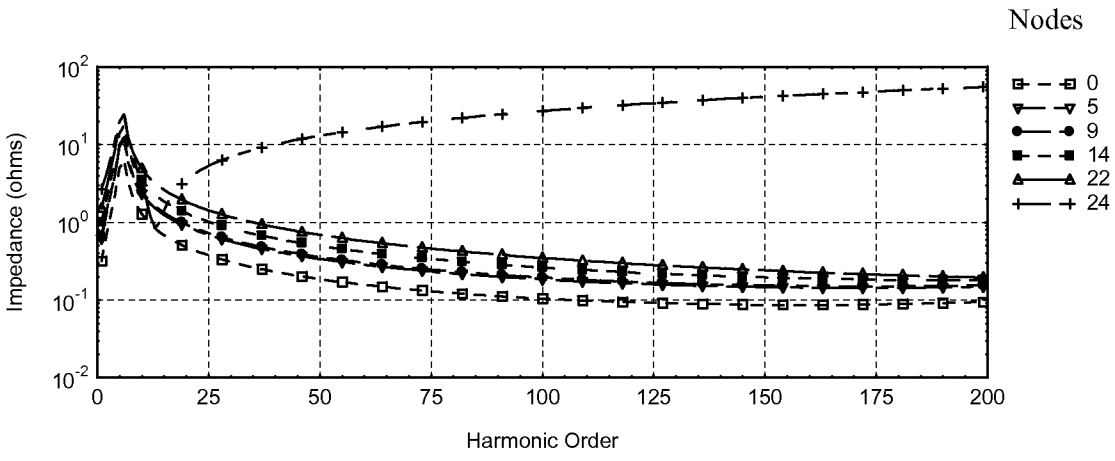

Figure 42. Argo feeder, harmonic injection at Node 24 for peak load at 0.9 PF

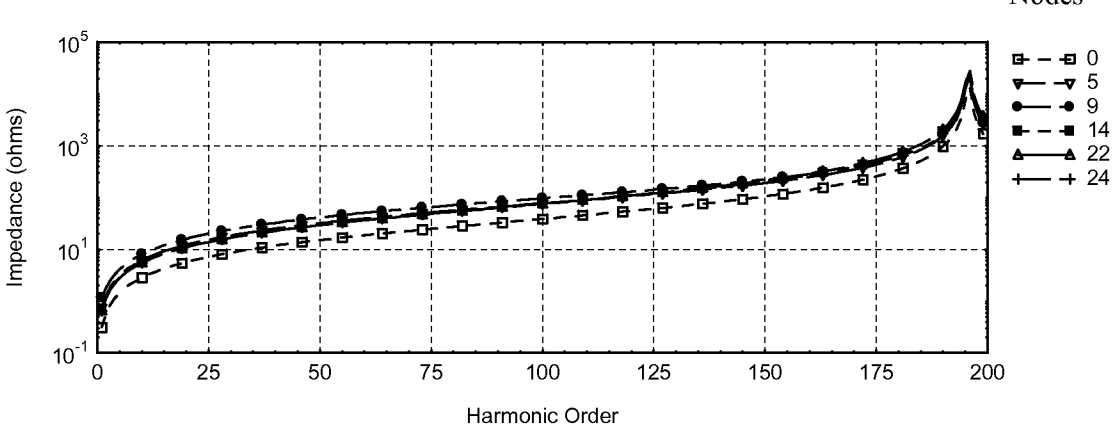

Figure 43. Argo feeder, harmonic injection at Node 9, capacitor bank at Node 23 temporarily disconnected

The results for the Pioneer feeder appear somewhat different (see Figure 35).

- The longer feeder length yields multiple resonances because of standing wave effects near the 45th and 130th harmonics (figures 44 and 45).
- The first quarter-wave resonance mode seen near the 45th harmonic corresponds to an almost 28-mile electrical length — much longer than the feeder's physical feeder length because of the lumped capacitive contribution of the cable laterals.
- With the 3-MVA bus capacitor switched in service, a low-order resonance near the 6th harmonic is introduced (Figure 46), similar to that found for the Argo feeder. When the capacitor is switched out, this harmonic resonance is eliminated (figures 44 and 45).
- Ground-mode harmonic current injection produces similar results, as illustrated in Figure 47. This figure shows the effect of doubling the length of each modeled feeder trunk section. As expected, the first quarter wave resonance occurs at a lower harmonic (near the 35th), although not at half the previous value because of the capacitance of cable laterals.

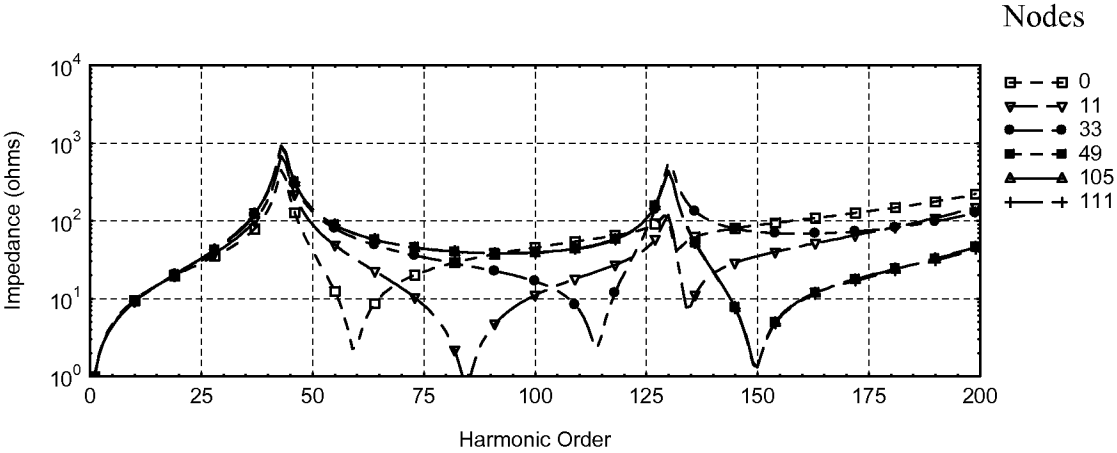

Figure 44. Pioneer feeder for line-mode current injection at Node 0, peak load, 3-MVAR capacitor bank switched out of service

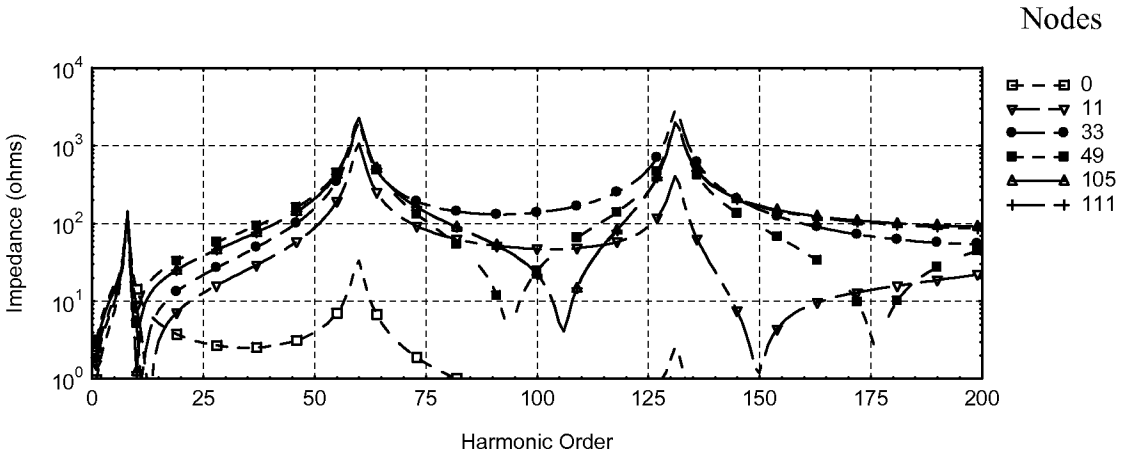

Figure 45. Pioneer feeder for line-mode current injection at Node 49, peak load, 3-MVAR capacitor bank out of service

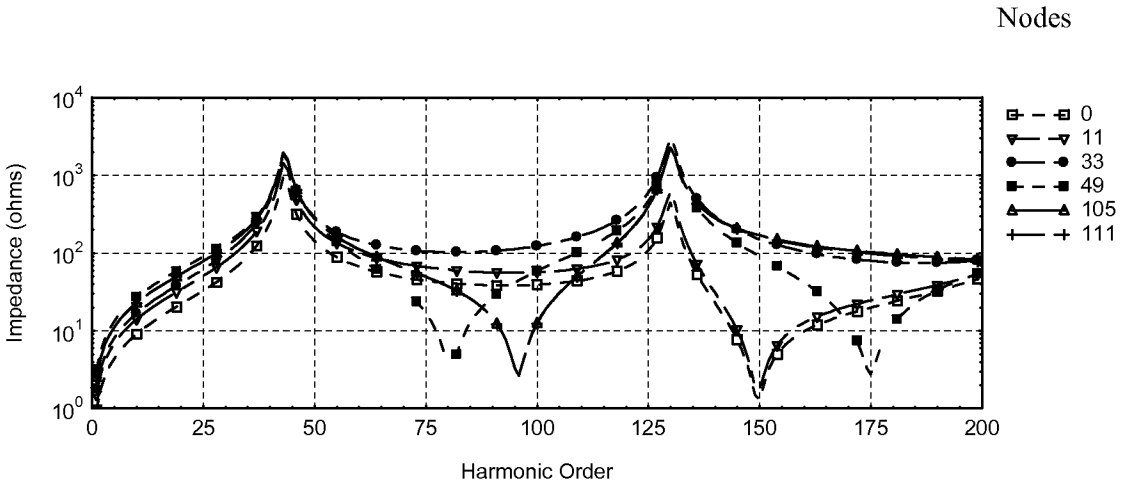

Figure 46. Pioneer feeder for line-mode current injection at Node 49, peak load, 3-MVAR capacitor bank in service

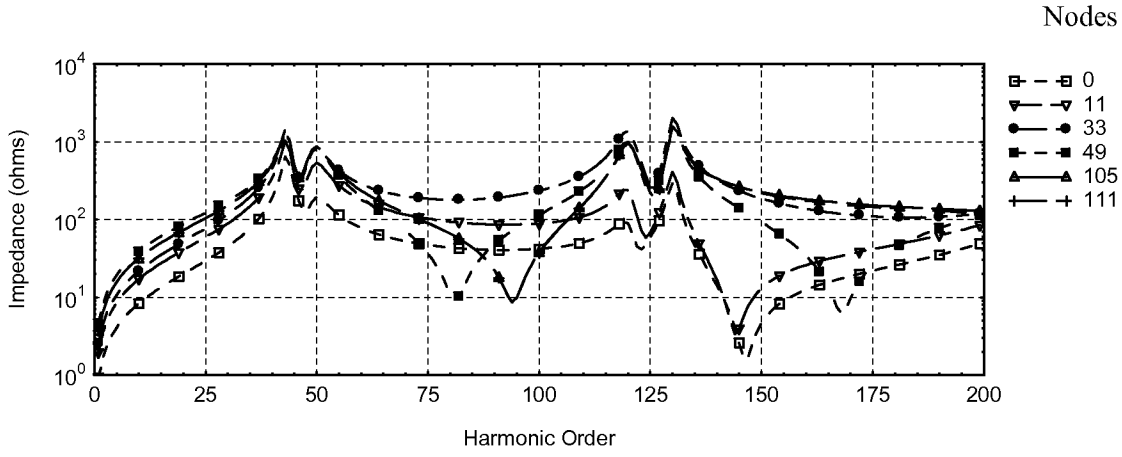

Figure 47. Pioneer feeder at peak load, ground mode harmonic current injection at Node 49, 3-MVAR capacitor bank out of service

3.1.5 Conclusions and Recommendations

Inverters used in DR applications can be grouped into two categories based on their harmonic performance.

1. Those that produce harmonics primarily below the 15th order:
   These inverters tend to be an older design, using a line-commutated switching strategy and incorporating silicon controlled rectifiers as the solid-state switch. Harmonics generated by multiple units add together algebraically. Thus, multiple units are equivalent to a single unit having the same aggregate capacity.

2. Those that produce harmonics largely beyond the 35th order:
   This group includes modern designs employing force-commutated switching using isolated gate bipolar transistors, gate turn-off thyristors, and more recently, integrated gate commutated thyristors. For inverters rated up to a few hundred kilowatts, the use of pulse-width modulation (PWM) switching at frequencies of 2–20 kHz virtually eliminates low-order harmonics. At higher power ratings, the use of multi-level converter designs provides similar harmonic performance even though the switching frequency for individual power switches is reduced. Forced commutation tends to introduce random phase shifts in the harmonics produced by multiple units operating in parallel. Also, the particular harmonics generated by individual units are themselves not in phase. This results in partial cancellation of harmonics produced by multiple units, such that "n" units of approximately equal size may be comparable to a single unit having a rating equal to the square root of "n" times the individual unit size.

To assess the harmonic effect of an inverter-based DR, it is necessary to take into account its expected harmonic spectra, as described by these groupings, and the harmonic impedance characteristic of the feeder, as presented earlier in Issue 8.

For the Argo feeder operating at 4.8 kV, the maximum permissible voltage distortion at any single frequency is 3%, or 144 V line-to-line. Given that the highest harmonic impedances in the two frequency bands (below the 15th order and above the 35th order) are about 25 Ω near the 7th harmonic and approaching 100 Ω at the 200th harmonic, respectively (in normal configuration, with capacitive compensation at Node 23), the associated current injection limits are 5.76 A (25 Ω x 5.76 A = 144 V) and 1.44 A (100 Ω x 1.44 A = 144 V), respectively. Inverters complying with permissible standards may inject up to 4% and 0.3% of rated current over the respective frequency ranges. This translates into inverter current ratings of 144 A (4% x 144 A = 5.76 A) and 480 A (0.3% x 480 A = 1.44 A) and power ratings of 1.2 MVA ($\sqrt{3}$ x 4.8 kV x 144 A) and 4 MVA ($\sqrt{3}$ x 4.8 kV x 480 A), respectively. Thus, line-commutated inverters are limited to 1.2 MVA, which can be taken as the combined capacity of all such units. This is equivalent to about 55% of peak feeder load for the 4.8-kV circuit and a stiffness ratio (at the PCC) of about 60 (given that short circuit contribution of inverter-based DR equals their rating). For PWM-based DR, a single unit rated 2.3 MVA may be accommodated without causing excessive harmonic voltage distortion. Alternatively, 16 PWM units rated a quarter of this value (0.6 MVA) would appear to be acceptable, allowing for some harmonic cancellation. It should be noted that in the absence of capacitive compensation at Node 23, harmonic impedance beyond the 35th harmonic rises by almost an order of magnitude, causing (under worse harmonic

distortion conditions) the permissible PWM inverter rating to be dramatically reduced to 230 kVA (stiffness ratio near 300).

For the Pioneer feeder operating at a nominal 13.2 kV, the maximum voltage distortion is about 228.6 V (3% x 7.620 kV) line-to-ground. Given *peak* computed harmonic impedances of 150 Ω (bus capacitor in service) for below the 15th harmonic and 2,000 Ω for beyond the 35th harmonic, the maximum permissible current injection is 1.52 A (150 Ω x 1.52 A = 228 V) and 0.11 A (2,000 Ω x 0.11 A = 228 V). Working through the same calculations as above, the maximum inverter current ratings are coincidentally 38 A in either case, i.e., (4% x 38 A = 1.52 A) and (0.3% x 38 A = 0.11 A) yielding 870 kVA ($\sqrt{3}$ x 13.2 kV x 38 A = 870 kVA) inverter rating, or about 13% of peak feeder load and a stiffness ratio of about 200.

As a final note, the above limits should be viewed as conservative, given that they assume the inverters to be marginally compliant with harmonic standards.

The conclusions given are specific to the circuit impedances and placement of the inverters on their respective circuits. The penetration limits have taken into account the location of inverters on these circuits, but the results are not generic because circuit impedance may vary considerably.

3.2 EEI Issue 11: Voltage Regulation Malfunctions (Not Actively Regulating System Voltage)

3.2.1 Description

Steady-state operating voltages need to be maintained within permissible limits, as defined in ANSI C84.1. This defines ranges A and B for service voltages at the primary distribution level, corresponding to tolerances of ±5% and ±6% of the nominal value, respectively. Range A is considered the normally permissible limit, while B is acceptable on a temporary basis allowing time for permanent corrective action. At secondary levels, Range A allows tolerances of ±5%, while Range B permits ±5.8% and -8.3%. Synchronizing or tripping generating facilities will inevitably disturb the prevailing voltage profile on the connected feeder, possibly causing service voltages to deviate from permissible limits and requiring coordinated intervention by utility controls. At the same time, DR may actually improve feeder voltage profile if allowed to regulate local voltage. This may counter voltage changes because of large power swings, sudden load changes, and faults on adjacent feeders.

A fundamental constraint on distribution system design is the voltage level at the customer service point. Utilities rely on various equipment such as load tap changing transformers, auto-transformer voltage regulators, and capacitors to regulate this voltage for expected operating conditions. These devices are adjusted or operated based on the assumption of radial power flow from the substation to the loads. However, the introduction of DR can counter these assumptions by reducing or even reversing power flow on sections of the circuit, inevitably affecting the voltage profile. The location and size of DR invariably affect the resulting feeder voltage profile.

A rigorous analysis of the effect of DR can only be performed by carrying out detailed load flow studies that take into account the varied nature of feeder conductor geometry and the dispersed loads. However, simplified analysis can provide a reasonable estimate, as follows.

The phaser voltage drop, ΔV, along a line segment of complex impedance Z = (R + jX) carrying current I is given by:

$$\Delta V = Z I . \qquad \text{Equation 4}$$

For normal feeders operating at relatively small power factor angle, θ, the scalar voltage difference between the sending and receiving end voltage magnitudes Vs and Vr can be approximated as:

$$\Delta V = I R_{Line} \cos\theta + I X_{Line} \sin\theta = R_{Line} \frac{P}{V_S} + X_{Line} \frac{Q}{V_S} , \qquad \text{Equation 5}$$

where the P real and Q reactive components of line current are defined on a per-unit base. This allows determination of the voltage change at any point on the feeder because of the change in real or reactive power flows caused by the introduction of a DR, although load dependence on voltage has been neglected.

With normal feeder conductor impedances providing relatively low X/R ratios (i.e., 2 to 6), the voltage drop associated with active power flow along the circuit can be significant. In addition, the *load* power factor during heavy load conditions can be significantly lower than during normal conditions, and thus, Equation 5 would indicate a higher voltage drop. Under peak load conditions, the maximum voltage drop will exist at remote points on the feeder, assuming uniformly distributed loads and assuming there is no intervention by voltage regulators and capacitors. Similarly, the introduction of DR at points remote from the substation bus will cause greater disruption to the voltage profile.

3.2.2 Scenario

DR connected to distribution circuits can cause significant changes to the voltage profile. Real and reactive injections may cause voltages to exceed the limits specified in ANSI C84.1. Conversely, properly controlled injections may improve the voltage profile.

3.2.3 Question 1

What are the locations on a circuit and the maximum P (real power) injections from DR that will not cause voltage limit violations? Notice this DR is operating at a fixed unity PF. This will allow the DR to track the system voltage and not actively regulate the distribution circuit voltage.

3.2.4 Study Results

A DR supplying power to a feeder displaces about the same amount of infeed from the normal supply. The associated voltage change at the substation bus can be determined from Equation 5. For the Argo feeder, the voltage change is associated with the change in power flow through the positive sequence source impedance 0.0126 pu + j 0.14156 pu (4.8 kV, 10 MVA base). For 1 pu (10 MVA) change in active power, substitute P = 1 pu, Vs = 1 pu, and R = 0.0126 pu in Equation 5. This predicts 0.0126 pu voltage change, indicating that voltage regulation at the substation bus is about

1.26% for a 10-MVA power change, or about 0.28% for a DR output equal to the peak feeder load. A similar calculation for the Pioneer feeder (source impedance 0.00272 pu + j 0.05327 pu on 13.2-kV, 10-MVA base) yields 0.27% voltage change per 10 MVA DR output, or 0.18% at peak feeder load.

Injection of power onto the feeder downstream of the substation bus causes the local voltage to rise with respect to a relatively stiff bus because of an impedance drop given by Equation 5. In the case of the Argo feeder, a conductor resistance of 0.425 pu/mile for the main trunk would suggest a voltage rise at the DR bus of about 4.25% per megawatt output from a DR located 1 mile from the substation bus (P = 0.1 pu, Vs = 1 pu, R = 0.425 pu), or 9.3% (i.e., 4.25% x 2.2 MVA) for a DR output equal to the peak feeder load. A similar calculation for the Pioneer bus yields an estimated 2% per 10 MVA DR output, or 1.4% for a DR equaling peak feeder load located 1 mile from the substation bus.

Detailed load flow solutions expand on these findings.

Figure 48 shows the normal voltage profile and load distribution for the Argo feeder (Figure 34) while serving 2.2 MVA peak load at 0.9 PF. This assumes that the existing DR at Node 5 is not in service. The voltage at all points along the feeder is regulated to within ±2%, or at most 4% below the head-end voltage. This is used as the base case hereafter, and various amounts of generation at different locations along the feeder will be added to determine the effect on voltage profile. Intervention by automatic regulators is not considered because none are present on this feeder.

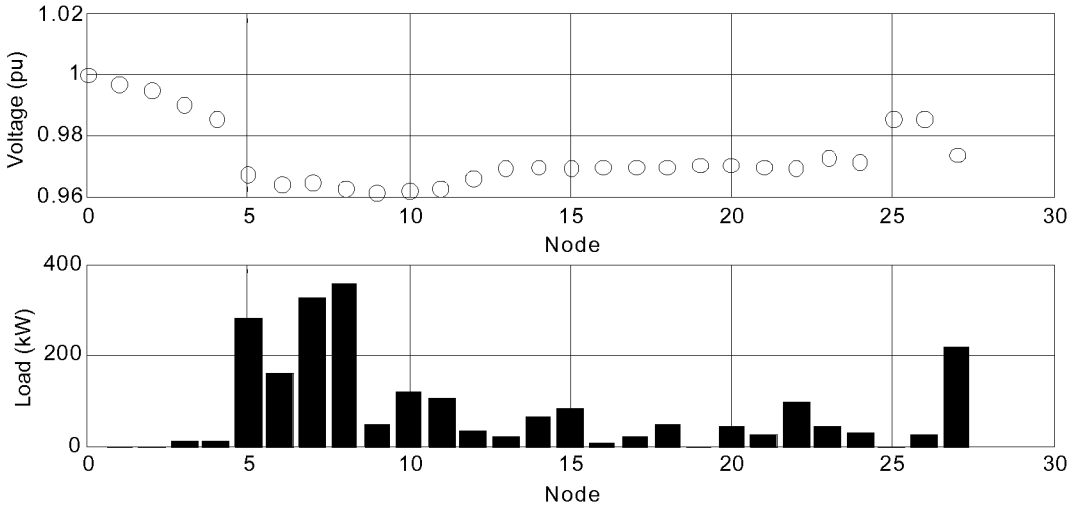

Figure 48. Voltage and load profile for Argo feeder nodes

Figure 49 shows the effect of injecting generation at Node 5 (about 0.55 conductor miles from the substation bus) operating at unity power factor.

- Voltage at the substation bus (Node 0) is only marginally affected even for a DR output at 200% of peak feeder load. This is a consequence of a relatively high 70-MVA substation short-circuit level compared with the 4-MW generator output and a relatively high source X/R ratio compared with the feeder. The associated stiffness ratio[1] is about 4.2 in the case of a synchronous machine with a 0.2 pu subtransient reactance.

- The greatest effect on the voltage is evidently near the machine terminals, yielding about 1.5% change in voltage per megawatt of added generation.

- For a DR located close to the substation bus on this feeder and having capacity equaling twice the peak feeder load (i.e., 4.4 MVA), voltage regulation on the entire feeder can be maintained within required limits without downstream regulators.

- Locating the DR at remote points on the feeder is invariably less desirable, causing greater regulation difficulties. Figure 50, 51, and 52 display results for nodes 9, 22, and 24 on the main trunk. In this case, feeder voltage profile is within ±5% range (Range A) for a DR capacity approaching the peak feeder load of Argo (2.2 MVA).

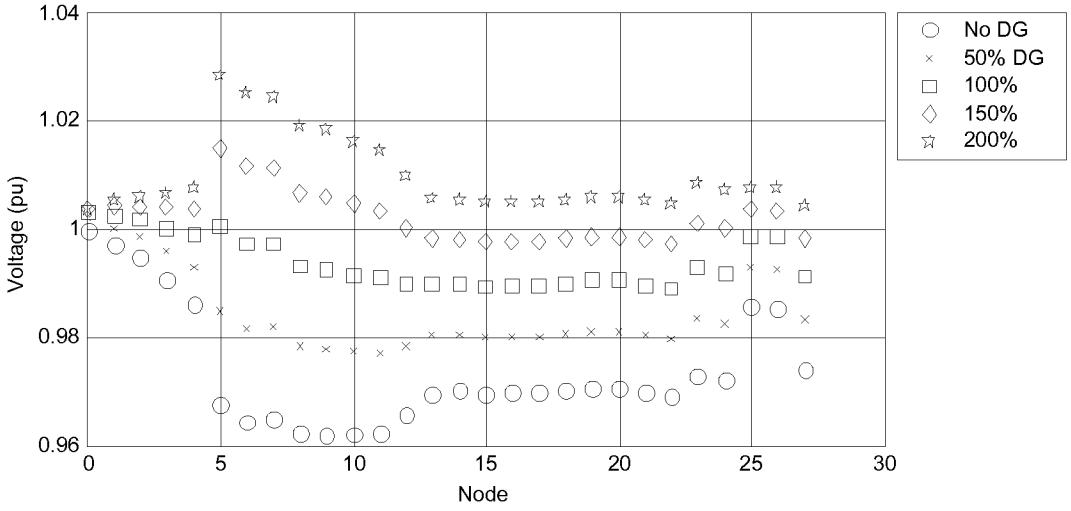

Figure 49. Argo feeder voltage profile because of DR at Node 5

[1] " Stiffness ratio" is defined as the ratio of the combined short circuit capacity of the existing supply, including the DR, to the short circuit capacity contributed by the DR alone.

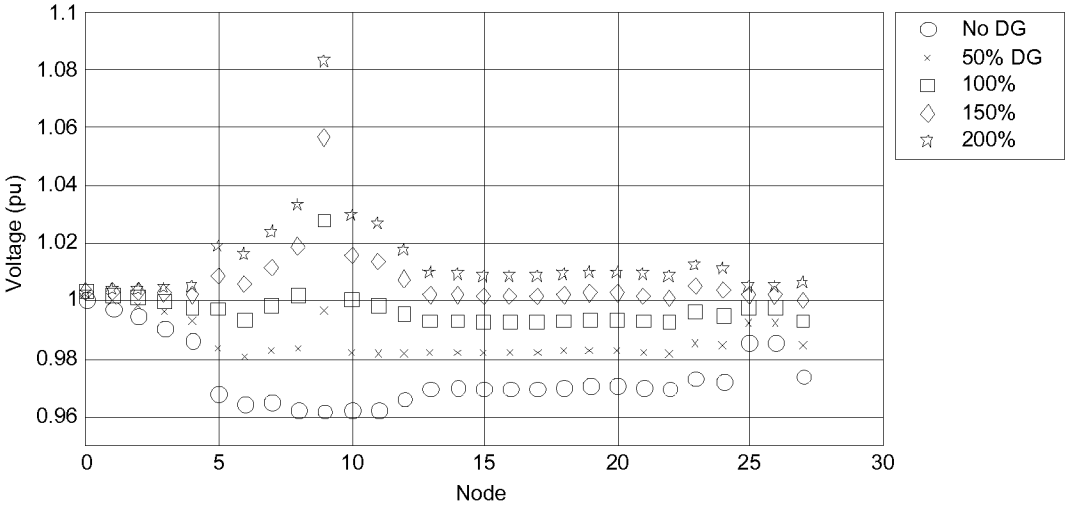

Figure 50. Argo feeder voltage profile because of DR at Node 9

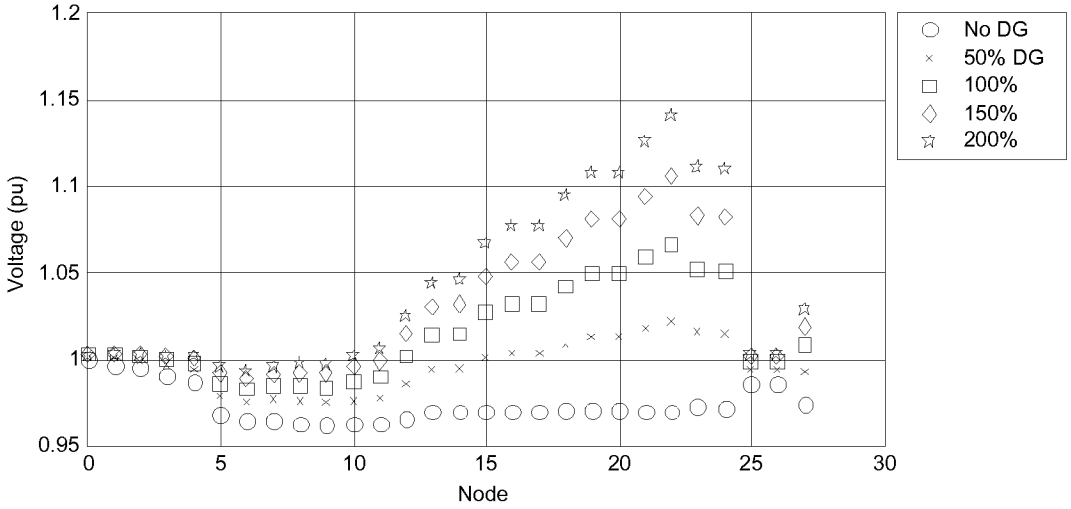

Figure 51. Argo feeder voltage profile because of DR at Node 22

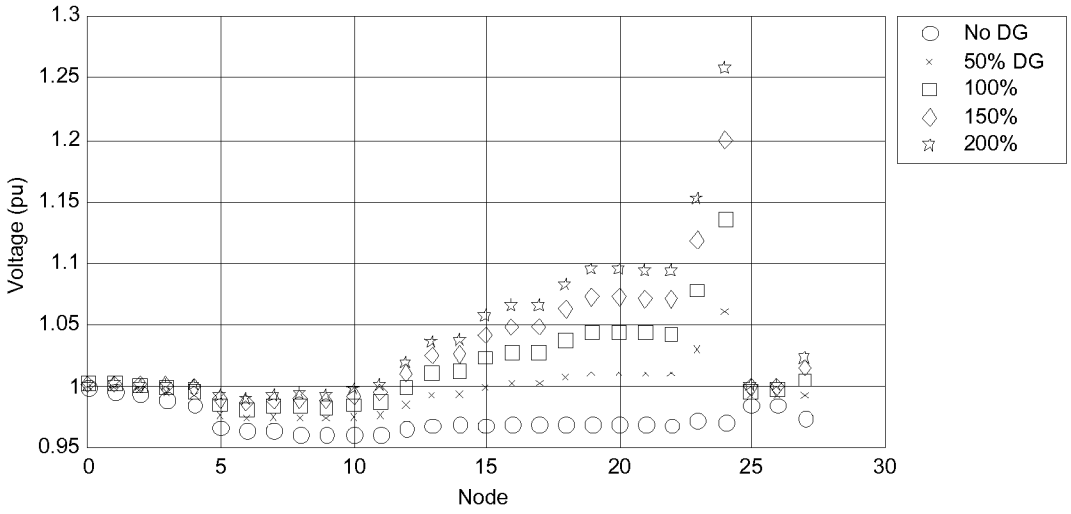

Figure 52. Argo feeder voltage profile because of DR at Node 24

Figure 53 shows the normal voltage and load profiles of the Pioneer feeder. Detailed calculations for this feeder confirm earlier simplified analysis and show that voltage disruption because of DR is more subdued. Figure 54, 55, and 56 show the voltage profiles for DR incorporated near the head end at Node 5, a remote end at Node 57, and at Node 11, corresponding to an actual installation. Substation bus voltage is only marginally affected by a DR. Remote locations tend to be more limiting. However, in this case, a DR rated twice peak feeder load can be accommodated at the far end (Node 57) while maintaining ±5% voltage regulation for all loads (Figure 55). The limiting stiffness ratio is about 3.6.

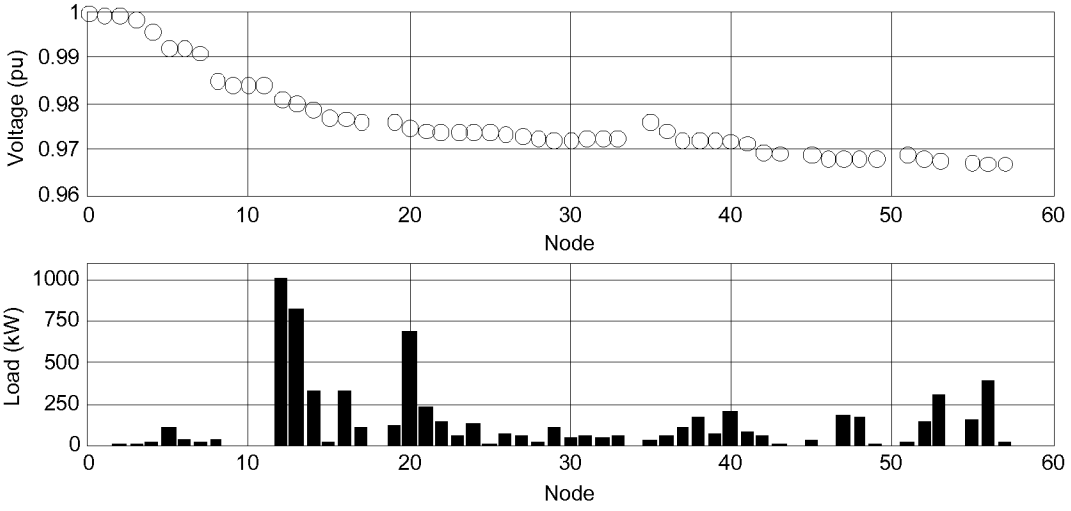

Figure 53. Pioneer feeder, normal voltage and load profile

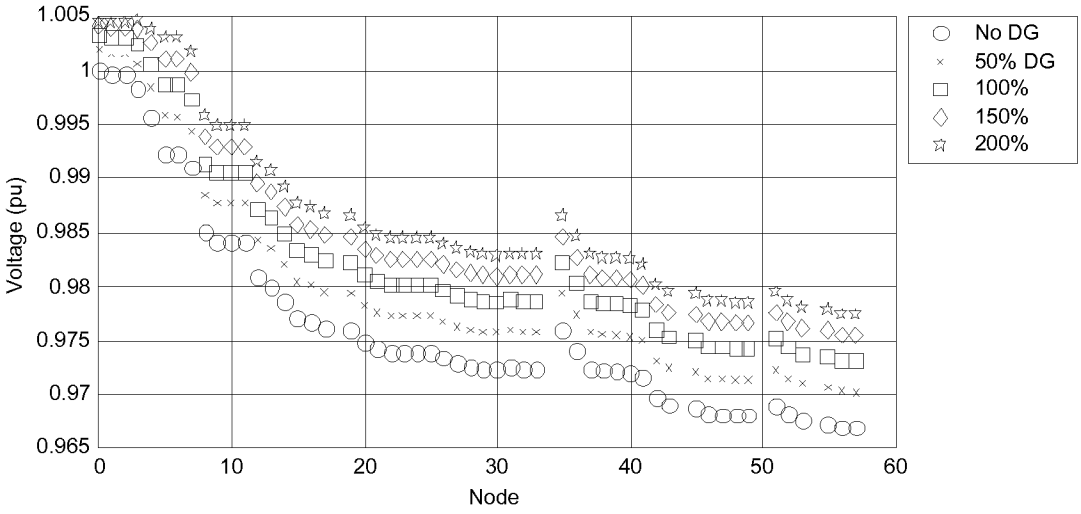

Figure 54. Pioneer feeder voltage profile because of DR at Node 5

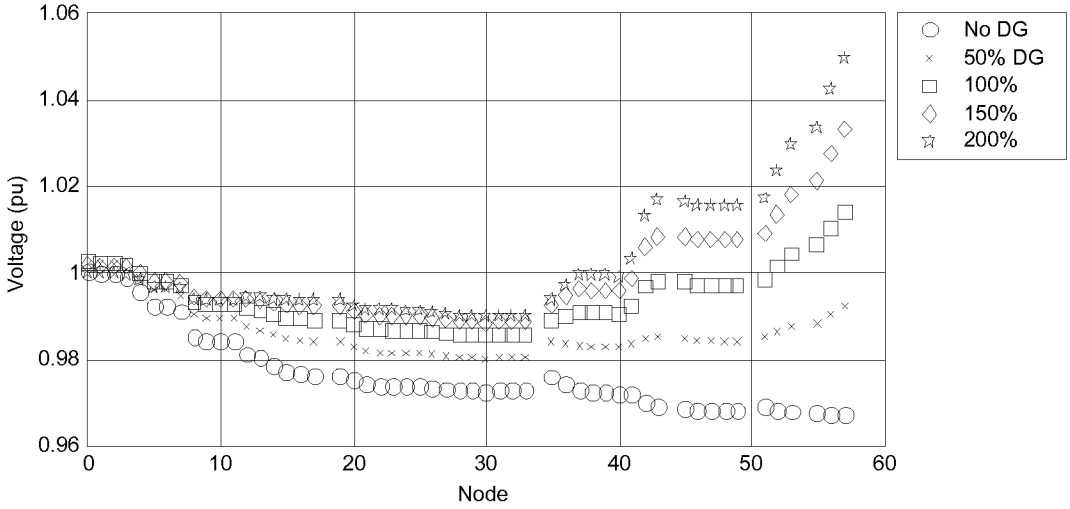

Figure 55. Pioneer feeder voltage profile because of DR at Node 57

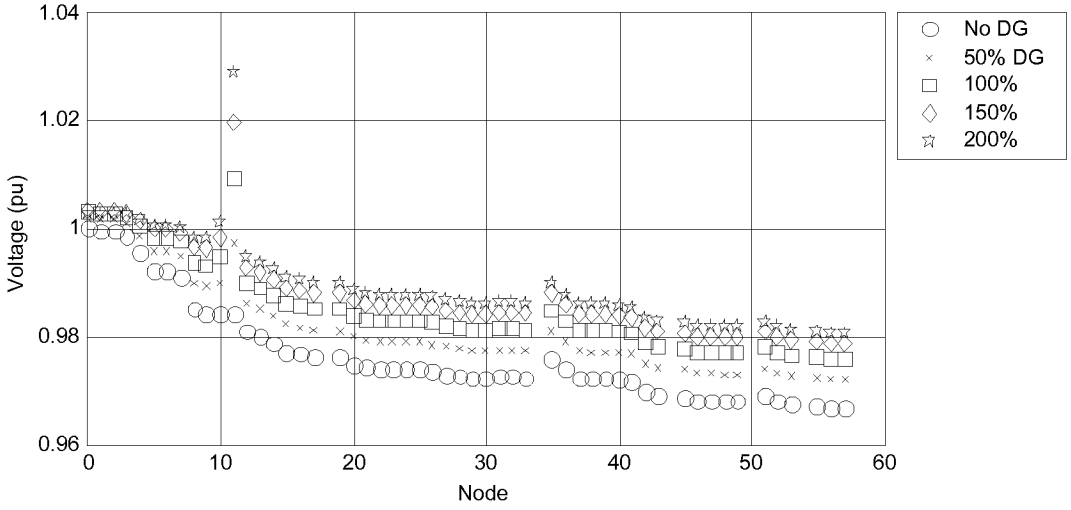

Figure 56. Pioneer feeder voltage profile because of DR at Node 11

3.2.5 Conclusions and Recommendations

1. For generating units located at the substation bus, a 10-MVA DR at unity PF produces only a 0.27% voltage change, or 0.3 V on a 120-V base. For a 10-MVA generator at the 4.8-kV substation bus, the voltage change is 1.26%, or 1.5 V on a 120-V base.

2. However, when the generating unit is located about 1 mile from the Argo substation bus, the voltage change is more dramatic: 4.25% per megawatt. Similarly, for the Pioneer circuit, the voltage change is only 0.206% per megawatt of generation.

3. The limit on the 4.8-kV circuit for DR located at the remote end without DR voltage regulation is approximately 2.2 MVA or equivalent to the circuit peak load for Argo to still maintain the voltage within Range A of ANSI C84.1.

4. The limit on the 13.2-kV circuit for DR located at the remote end without DR voltage regulation is twice the peak feeder load or 6.8 MVA x 2 = 13.6 MVA to still maintain the voltage within Range A.

5. Because the voltage drop calculation includes both real and reactive terms, it is important to include the PF of the load and the PF of the generator when calculating the voltage profile.

3.3 EEI Issue 22: Loss of Exciters Causes Low Voltage

3.3.1 Description

Unplanned outages or abrupt shutdowns of DR facilities can cause voltage sags on the feeder and may disrupt sensitive loads. The effect can be seen from earlier plots for both feeders and is consistent with the simplified analysis presented in the section on voltage regulation malfunctions. According to the ITIC curve, loads should tolerate voltage sags up to 0.8 pu of

normal for 10 s and 0.7 pu for 0.5 s. Voltage swells up to 1.4 pu should be tolerated for 3 milliseconds and 1.2 pu for 0.5 s.

- For the Argo feeder, loss of generation from a unit near the head end, sized at twice peak load, will cause customers to experience a sudden 6% voltage sag (see Figure 50), which coordinates marginally with Range B of the permissible voltage limits under ANSI C84.1. For DR near the far end (Figure 52), voltage sags because of unplanned unit outages range to almost 8% per megawatt, which limits permissible DR size for remote feeder locations. If an occasional 10% voltage dip because of such eventualities were considered permissible, the maximum DR size at the most remote location would be about 1.25 MW, or about 55% of peak feeder load.

- For Pioneer, the voltage dip because of generator trip is less severe. As shown in Figure 55, a DR delivering twice peak feeder load located at Node 57 results in about 8% voltage sag.

3.3.2 Scenario

The loss of excitation (LOE) on a synchronous machine interrupts active power output from the DR while suddenly applying a reactive load on the feeder because of motoring. Although most large synchronous machines are equipped with LOE protection, smaller machines may dispense with such protection because of its cost. The effect of such disturbances on the feeder voltage can be estimated by superposition, taking into account the combined effect of a reduction in active power output and an increase in reactive load, both of which tend to depress feeder voltage.

3.3.3 Question

What is the maximum DR size that can be installed at certain nodes without exceeding the 10% voltage dip created by LOE?

3.3.4 Study Results

According to Equation 5, changes in active power combine with upstream resistance to create a voltage drop (see Issue 11). Similarly, changes in reactive power combine with upstream reactance to cause a voltage drop. (This is estimated as the ratio of the added reactive loading and available short circuit capacity, $\Delta V = -\Delta Q/SCVA$ pu, using consistent units.) Although resistance is contributed almost entirely by the feeder, reactance includes a dominant component from the Thevenin source seen at the substation bus. Thus, a large part of the voltage change because of reactive loading appears directly at the substation bus, as illustrated in Figure 57 for Argo and Figure 58 for Pioneer. This sudden change in voltage is seen at all feeder nodes, augmented further by additional drops because of feeder reactance and the increased reactive load of the DR.

Reactive loading is typically 0.5–1 pu of machine rating, given its inverse relation to the machine's synchronous reactance, which tends to be 1–2 pu of rating. Taking the higher value to be conservative shows that a 1-pu drop in active power because of a machine tripping may be compounded by a 1-pu increase in reactive loading.

- The combined effect for the Argo feeder can be seen from Figure 49 and 57 for a DR near the head end. Voltage drop because of the loss of a 1-MVA unit operating at unity power factor is about 1.5%, and reactive loading because of the generator motoring contributes another 3.5%.

- For the Pioneer feeder, the combined voltage sag is about 2.5% per 1-MW loss of generation at the far end (Figure 55 and 58) and under 1% near the head end (Figure 56 and 59).

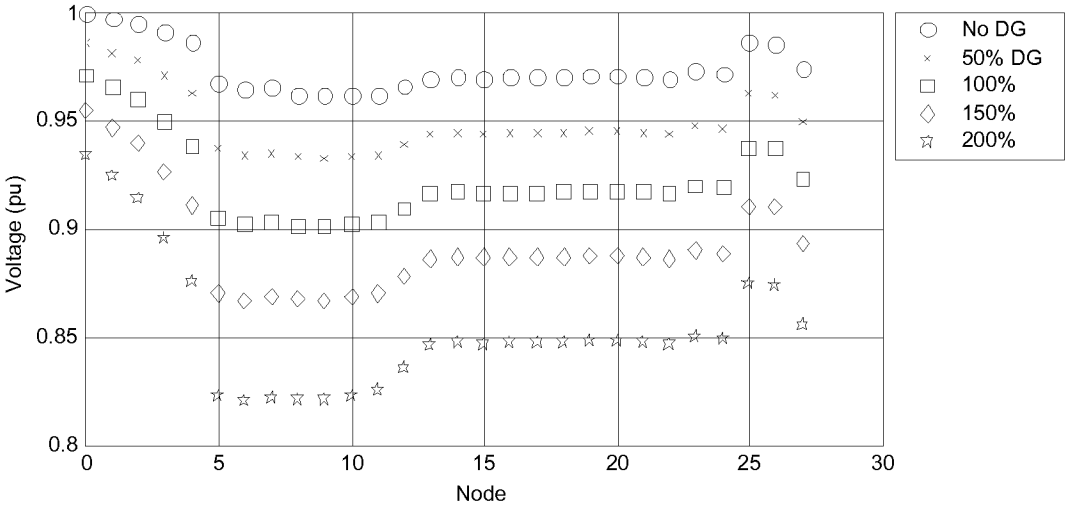

Figure 57. Impact of reactive loading at Node 5 of Argo feeder, expressed in relation to peak feeder load

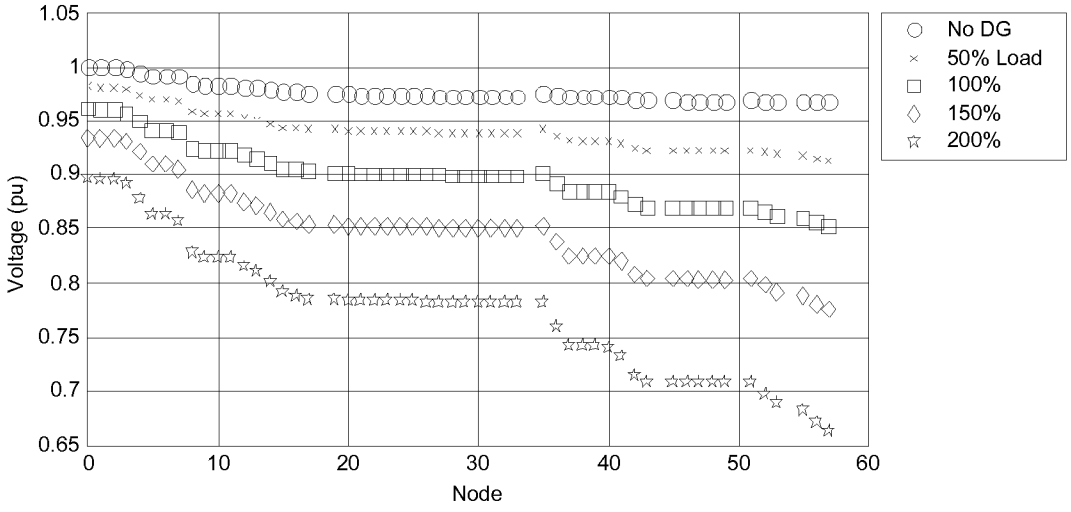

Figure 58. Impact of reactive loading at Node 57 of Pioneer feeder, expressed in relation to peak feeder load

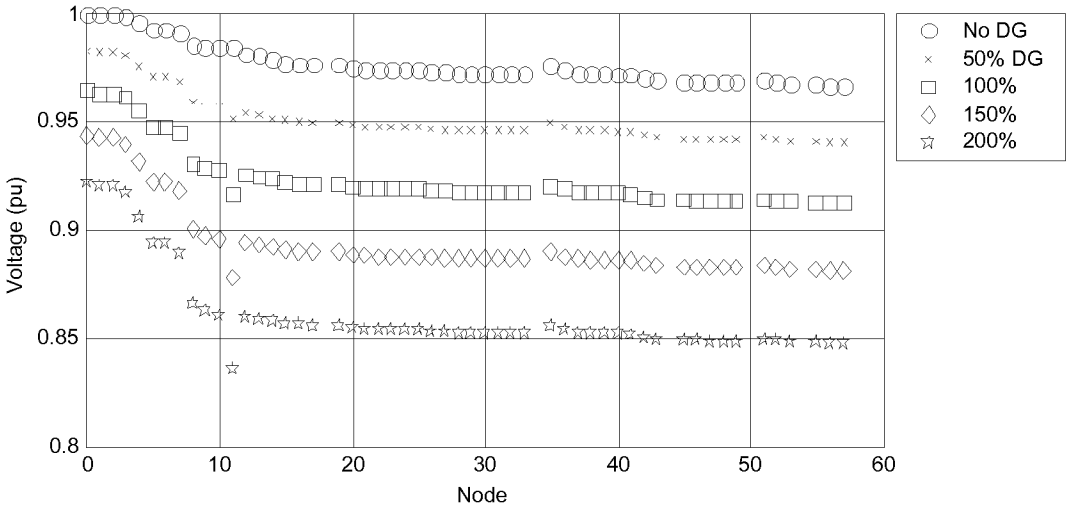

Figure 59. Impact of reactive loading at Node 11 of Pioneer feeder, expressed in relation to peak feeder load

Table 9 displays the results predicted for various nodes on the respective feeders, as determined by using Equation 5 and the Thevenin source impedance values computed using the MATLAB model. Columns 8 and 9 give the maximum permissible DG rating assuming operation at 1.0 and 0.9 leading power factors, respectively, and requiring that the voltage sag resulting from an unplanned outage be limited to 10%. Outages of DG operating at leading power factor are evidently more limiting because they produce deeper voltage sags because of loss of reactive power support. This deficiency must be made up by the system, and the resulting voltage drop is associated with the second term in Equation 5. The results predict, for instance, that at Node 5 on the Pioneer feeder, an outage on a 110-MVA DG operating at unity power factor, or an outage on a 32-MVA DG operating at 0.9 leading power factor, will produce a 10% voltage sag.

The last column in Table 9 gives the maximum permissible DG rating (operated at unity power factor) if voltage sag because of LOE must be limited to 10%. For the Argo feeder, the maximum permissible DG rating is about 6.5 MVA at the station bus. For DG located on the feeder, the maximum permissible rating is about the same as peak station load (about 2 MVA) for DG located close to the station bus at Node 5 and only about 0.7 MVA for remote locations. For Pioneer, the limit is 12 MVA near the head end (175% of peak feeder load) and about 4 MVA at a remote node (about 60% of peak load).

Table 9. Predicted Voltage Dip at Respective Feeder Nodes Because of Changes in Active Power and Reactive Loading

	Thevenin Source Impedance		SC Level	ΔV/MVAr	ΔV/MW	ΔV Combined (LOE)	Max DG for 10% Sag on Outage		Max DG for 10% Dip on LOE
							1.0 PF	0.9 Lead PF	
Node	R (pu)	X (pu)	MVA	%	%	%	MVA	MVA	MVA
Pioneer Feeder, Bases 13.2 kV, 10 MVA									
0	0.00394	0.0575	173.5	0.57	0.04	0.61	254	46	16.3
5	0.00906	0.0722	137.3	0.72	0.09	0.81	110	32	12.3
11	0.03961	0.1080	86.9	1.08	0.40	1.48	25	14.3	6.8
33	0.06952	0.1566	58.4	1.57	0.70	2.26	14.4	8.9	4.4
49	0.08024	0.1619	55.3	1.62	0.80	2.42	12.5	8.1	4.1
57	0.07816	0.1604	56.0	1.60	0.78	2.39	12.8	8.3	4.2
Argo Feeder, Bases 4.8 kV, 10 MVA									
0	0.0126	0.1416	70.4	1.42	0.13	1.54	79	17.8	6.5
5	0.1642	0.3086	28.6	3.09	1.64	4.73	6.1	4.1	2.1
9	0.3359	0.3799	19.7	3.80	3.36	7.16	3.0	2.4	1.4
14	0.2349	0.3719	22.7	3.72	2.35	6.07	4.3	3.0	1.6
22	0.4852	0.5506	13.6	5.51	4.85	10.36	2.1	1.6	1.0
24	0.8013	0.6270	9.8	6.27	8.01	14.28	1.2	1.1	0.7

3.3.5 Conclusions and Recommendations

1. LOE causes a sudden voltage dip because of the loss of real power from the DR and a simultaneous increase in reactive loading because of the generator motoring (assuming the generation breaker remains closed and the LOE protection doesn't operate). This aggravates the voltage drop compared with the case of a simple machine outage.

2. The maximum size of DR for the Argo circuit is 6.5 MVA at the bus and 0.5 MVA at the remote end.

3. The maximum DR size for the Pioneer circuit is 16.2 MVA at the bus and 3.9 MVA at the remote end.

3.4 EEI Issue 11A: Voltage Regulation Malfunctions (Actively Regulating System Voltage)

3.4.1 Description

Utilities are reluctant at this time to allow DR to regulate voltage because of concerns about exceeding voltage regulation limits. Nevertheless, it is instructive to consider the extent to which DR may affect such control if it were permitted.

3.4.2 Scenario

Synchronous machines are rated in terms of megavolt-ampere output at a specified voltage and power factor (generally 0.8 or 0.9 lagging) that they can carry continuously without overheating. The active power (megawatt rating) output is limited by the prime mover capability to a value within the megavolt-ampere rating of the generator. The continuous reactive power capability is limited by three considerations: armature current limit, field current limit, and end iron heating limit. Terminal voltage is regulated by automatic excitation control of the field winding current, which controls the reactive power output by varying the internal generated voltage.

With inverters, voltage regulation is achieved by pulse firing control such that the injected power-frequency (60 Hz) current waveform is phase-shifted relative to the voltage waveform. However, inverters tend to be constrained by the peak current output capability of solid-state switches based on thermal considerations. Thus, active power output must be reduced to deliver additional reactive power, so there is a cost penalty in reducing the real power to have an inverter regulate voltage by reactive power control.

For simplicity, assume the connected DR can be operated continuously from 0.8 leading to 0.8 lagging power factor.

3.4.3 Question

What are the maximum real power and reactive power injections from the DR that will not cause voltage limit violations? Notice that, in this case, the DR is not necessarily operating at a fixed PF and thus would affect the system voltage profile.

3.4.4 Study Results

Consider a DR located at Node 24, the weakest point on the Argo feeder, during light load conditions (25% of peak feeder load). Figure 60 shows the voltage profile for various levels of DR output at unity power factor. Note that the primary voltage is within ±15% along the feeder for a DR delivering twice peak feeder load. This is an unacceptable voltage range. However, when the DR is allowed to regulate the voltage (by absorbing reactive power), the voltage profile reverts to the permissible range for all customers (see Figure 61).

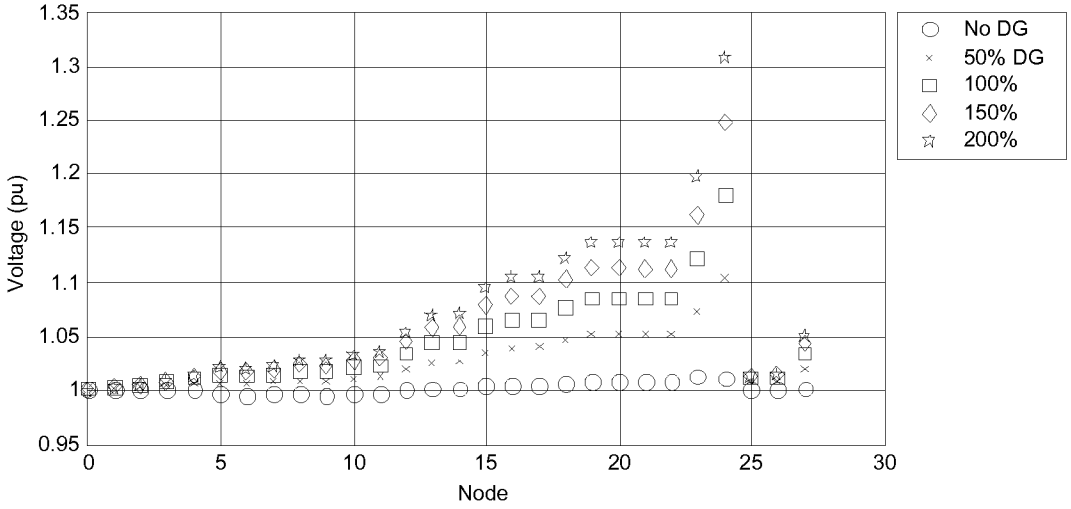

Figure 60. DR at Node 24 operated at unity power factor, Argo feeder at 25% peak load

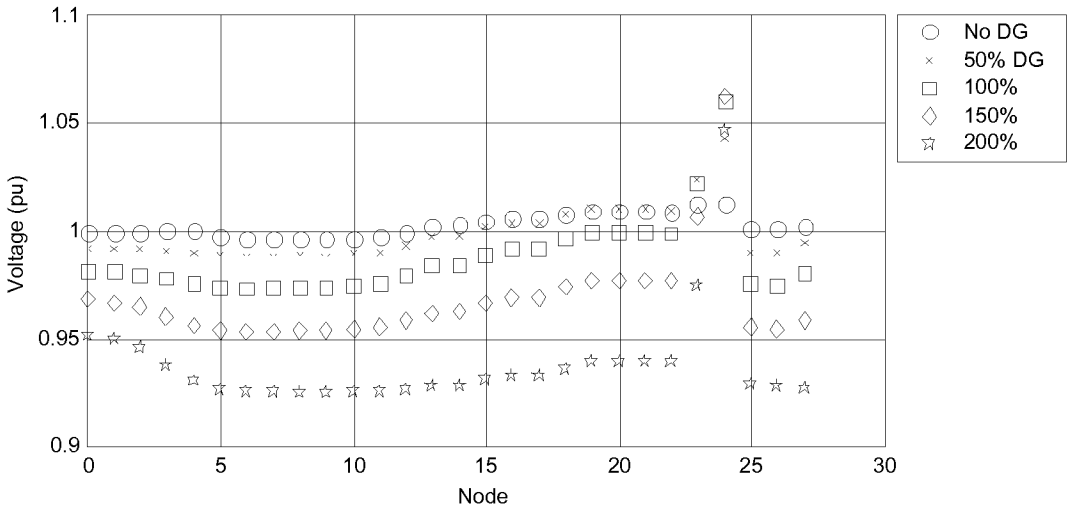

Figure 61. DR at Node 24 operating at 0.8 leading power factor, Argo feeder at 25% peak load

Figures 62 and 63 show the corresponding results for Pioneer, confirming a marked improvement in regulation because of DR reactive control.

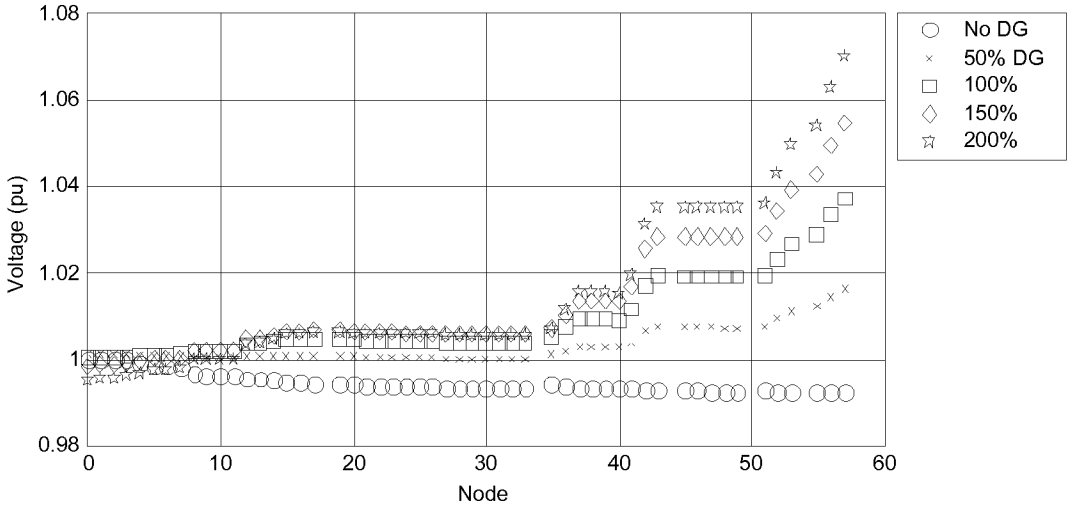

Figure 62. DR at Node 57 operating at unity power factor, Pioneer feeder at 25% peak load

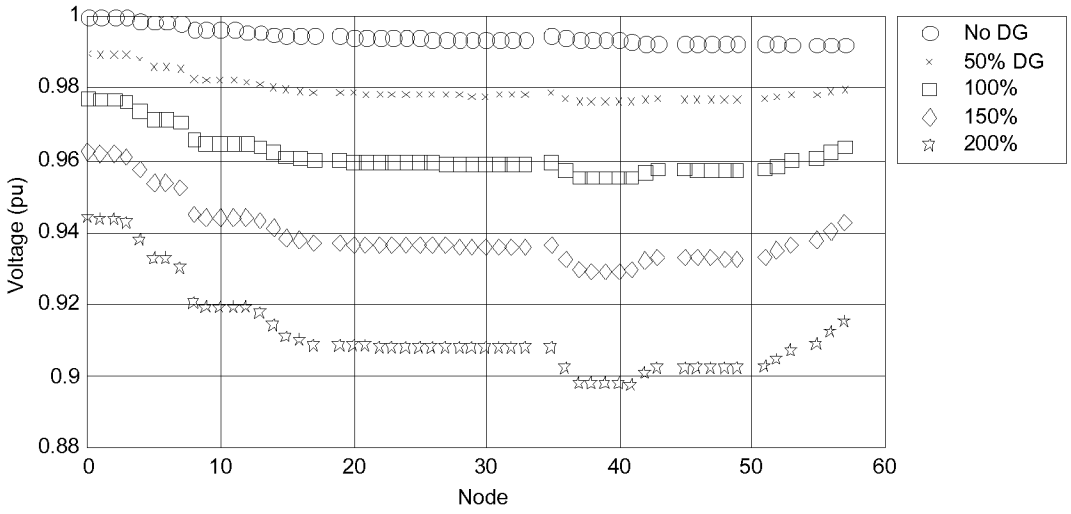

Figure 63. DR at Node 57 operating at 0.8 leading power factor, Pioneer feeder at 25% peak load

Finally, as expected, dispersing a given amount of generation along the entire feeder provides much better voltage regulation than concentrating all such generation at one node. Figures 64 and 65 illustrate this result for both feeders, with the aggregate generation capacity increased in steps to twice peak feeder load.

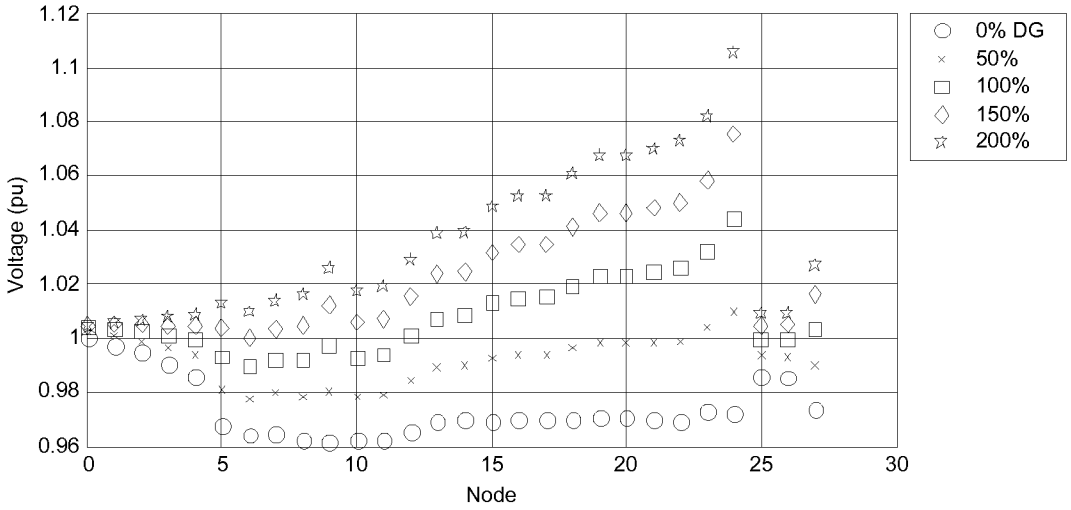

Figure 64. Argo feeder at peak load, with aggregate DR capacity distributed over nodes 5, 9, 14, 22, and 24

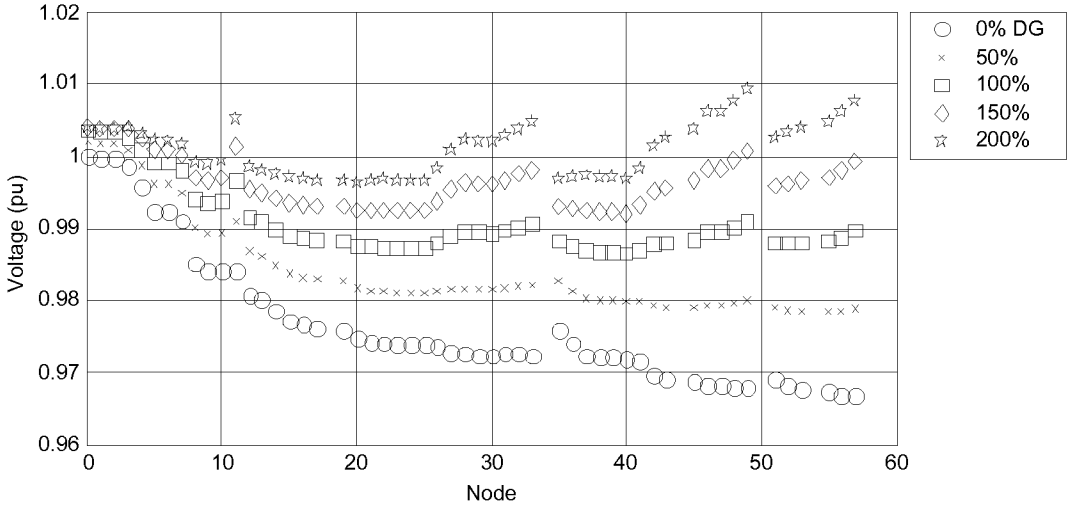

Figure 65. Pioneer feeder at peak load, with aggregate DR capacity distributed over nodes 5, 11, 33, 49, and 57

3.4.5 Conclusions and Recommendations

The steady-state voltage profile along the feeder is affected by both the active power supplied by a DR and the reactive loading of a DR under certain operating conditions (e.g., because of LOE). Simplified methods can provide a good estimate of the expected voltage change. Analysis carried out for the selected feeders reveals the following:

1. For the Argo feeder, serving a 2.2-MVA peak feeder load from a substation with a 70-MVA short-circuit capacity, voltage regulation at the DR terminals ranges from 0.13% per megawatt of generation at the substation bus to 8% per megawatt at remote points on the feeder. Comparable values for the Pioneer feeder are 0.04% and 0.8% per megawatt. This feeder serves a 6.8-MVA peak feeder load from a substation having a 170-MVA short-circuit capacity.

2. Assuming a 10% voltage sag is acceptable for a LOE condition for an infrequent, unplanned DR outage, the maximum permissible DR rating is 6.5 MVA and 16.2 MVA near the head end of Argo and Pioneer feeders, respectively, and about 0.5 MVA and 3.9 MVA at the more remote locations on these feeders.

3. As expected, the voltage profile is affected significantly by changes in reactive loading, such as that caused by LOE on a synchronous machine. If the machine is not tripped by protection, the added load may approach the machine's megavolt-ampere rating. This produces a relatively large drop in voltage at the substation bus and a more gradual decrease in voltage along the feeder length because of the added load. At the substation bus, the voltage drop is about 1.4% per megavolt-ampere of added load (or machine rating) on the Argo feeder, and it is almost 0.6% for Pioneer. At remote points on the feeder, corresponding to a presumed DR location, the predicted voltage drop is 10.2% per megavolt-ampere on Argo and 1.8% per megavolt-ampere on Pioneer.

4. Moving now to locations on the feeder and assuming a 10% voltage sag to be acceptable from an occasional LOE event, the maximum permissible DR rating for the Argo feeder ranges from 0.5 MVA to 1.9 MVA depending on location, or about 20–100% of peak feeder load. For Pioneer, the comparable values of DR ratings located at various locations on the circuit range from 3.9 MVA to 12.2 MVA, or about 60–175% of peak load.

5. Detailed load flow studies confirm the potential for improving voltage profile on feeders by locating DR at remote points on the feeder. Calculations show that voltage on the entire feeder can be regulated to within ±5% of nominal for DR when operated with fixed field voltage control based on prescribed voltage set points, and matching peak feeder load on Argo (2.2 MVA), in excess of twice peak load for Pioneer (>13.6 MVA). Even higher ratings may be accommodated with further improvement in the voltage profile if the DR is allowed to regulate voltage by power factor control.

3.5 EEI Issue 20: Steady-State Stability

Steady-state stability is associated with the ability of a synchronous machine to remain stable while delivering power into an interconnected AC system. Problems can be avoided with proper design and are not an issue in this study.

For a simple radial connection between a single generator and a relatively stiff power system, simple formulas are available to determine the maximum power that may be transmitted. For a multi-machine system with distributed loads, this calculation may produce unrealistically pessimistic results and needs to be evaluated by more rigorous methods.

The real power output of synchronous machines can be controlled independently of the reactive power. It is determined by the applied mechanical power, which produces a change in the power angle, δ. The machine's real power output is given as:

$$P = \frac{V\,E}{X_s}\sin\delta \qquad \text{Equation 6}$$

where V is the terminal voltage, E is the internal generated voltage, and X_S is the machine's synchronous reactance. Figure 66 shows the value of power P plotted against the load power angle for a round rotor generator assuming V and E remain constant. As the value of the power angle is increased, because of increasing mechanical power input, the power output of the generator increases. Maximum power is produced when the power angle is 90°. Any further increase in the value of the power angle results in a reduction of the power produced. The value of the power angle for which maximum power is produced is called the steady-state stability limit of the generator. If the power angle is increased beyond the stability limit, the generator loses synchronism with the power system to which it is connected. For round rotor generators, the theoretical stability limit occurs for a power angle equal to 90°. For salient pole machines, the stability limit occurs at values of slightly less than 90°.

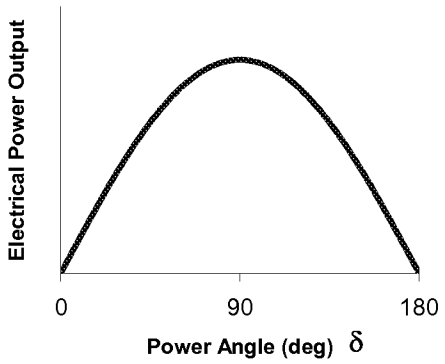

Figure 66. Power output as a function of power angle

In normal operation, a generator must be operated with a power angle much below the stability limit. During a system fault, the terminal voltage is reduced, so the electrical power demand on the machine is greatly reduced. However, the prime mover cannot respond as rapidly to reduce the applied mechanical power. So in the initial moments after fault occurrence, the excess mechanical power input over the electrical power output causes the rotor to accelerate. As a result, the power angle increases, possibly beyond the point at which synchronism is lost.

The actual operating angle will depend on the specific machine design. For typical machine synchronous reactances of 1–2 pu, the operating angle ranges over 30–40° at rated output (see Equation 6). Within this range of power angle, and with constant field voltage (manual excitation control), steady-state stability is generally not an issue because there is sufficient inherent synchronizing torque to maintain steady-state stability. However, the presence of an automatic voltage regulator control and a fast exciter (high gain feedback system) can reduce synchronizing torque, potentially causing oscillatory instability. Again, such problems can be avoided with proper design and are not considered in this study.

3.6 EEI Issue 21: Transient Stability

3.6.1 Description

To determine whether a power system is stable after a disturbance, one can plot and inspect the swing curves. If these curves show that the angle between any two machines tends to increase without limit, the system is unstable. If, on the other hand, after all the disturbances including switching have occurred, the angles between the two machines of every possible pair reach maximum values and thereafter decrease, it is probable, although not certain, that the system is stable. Occasionally in a multi-machine system, one of the machines may stay in step on the first swing and yet go out of step on the second swing because the other machines are in different positions and react differently from the first machine.

In a two-machine system, under the usual assumptions of constant mechanical input and constant voltage behind transient reactance, the angle between the machines either increases indefinitely or, after all disturbances have occurred, oscillates with constant amplitude. In other words, the two machines either fall out of step on the first swing or never. Under these conditions, the observation that the machines come to rest with respect to each other may be taken as proof that

the system is stable. There is a simple graphical method of determining whether the machines come to rest with respect to each other. This method is known as the equal area criterion of stability (see Equation 7). When this criterion is applicable, its use eliminates the need for computing swing curves and thus saves considerable computation effort. It is applicable to any two-machine system based on the above.

The incremental change in power angle for a given drop in electrical output can be approximated by:

$$d\delta = \frac{5{,}400\, t^2\, dP}{H} \qquad \text{Equation 7}$$

where

$d\delta$ = incremental change in power angle (degrees)
t = fault clearing time(s)
dP = change in loading expressed as per unit of machine rating
H = combined generator and turbine inertia constant (kW•s/kVA), corresponding to the time taken by the machine to accelerate from standstill to 0.5 pu rated speed with rated applied mechanical torque.

The value of dP is calculated by multiplying the per unit drop in positive sequence voltage during a fault by the machine power factor (current does not change within the time period of interest). A three-phase short circuit results in the largest drop in loading and thus produces the worst conditions for loss of stability.

3.6.2 Scenario

To illustrate with a simple example, consider a DR operating at rated power. A three-phase fault occurs sufficiently nearby such that the voltage and the electrical output can be assumed to drop to zero. The change in the machine's electrical output is unity, and the power angle starts to increase as the machine accelerates. Assuming a pre-disturbance power angle of 35°, it can be assumed that the machine can be allowed to accelerate until the power angle reaches 90° ($d\delta$ = 55°). At this time, if the fault is cleared such that the original feeder circuit is returned to service, the rotor will decelerate because of the reapplied load. It will advance to the brink of instability at 145° (neglecting damping) before reversing and returning to the pre-disturbance value.

The maximum fault clearing time, according to Equation 7, with $d\delta$ = 55°, dP = 1 pu, for typical machine inertia constant H = 1 to 5 ranges from 100 to 225 ms. A representative computer simulation showing this result is depicted in Figure 67 for a 1-MVA synchronous machine located at Node 5 on the Pioneer feeder (see Appendix C). Table 10 displays the *normalized* machine parameters used throughout, with H taken to be unity unless otherwise indicated. Note that the critical clearing time depends on the machine's inertia constant. Thus, the post-disturbance performance of a DR on a feeder will depend more on its design (e.g., its inertia constant and excitation controls) than its absolute power rating.

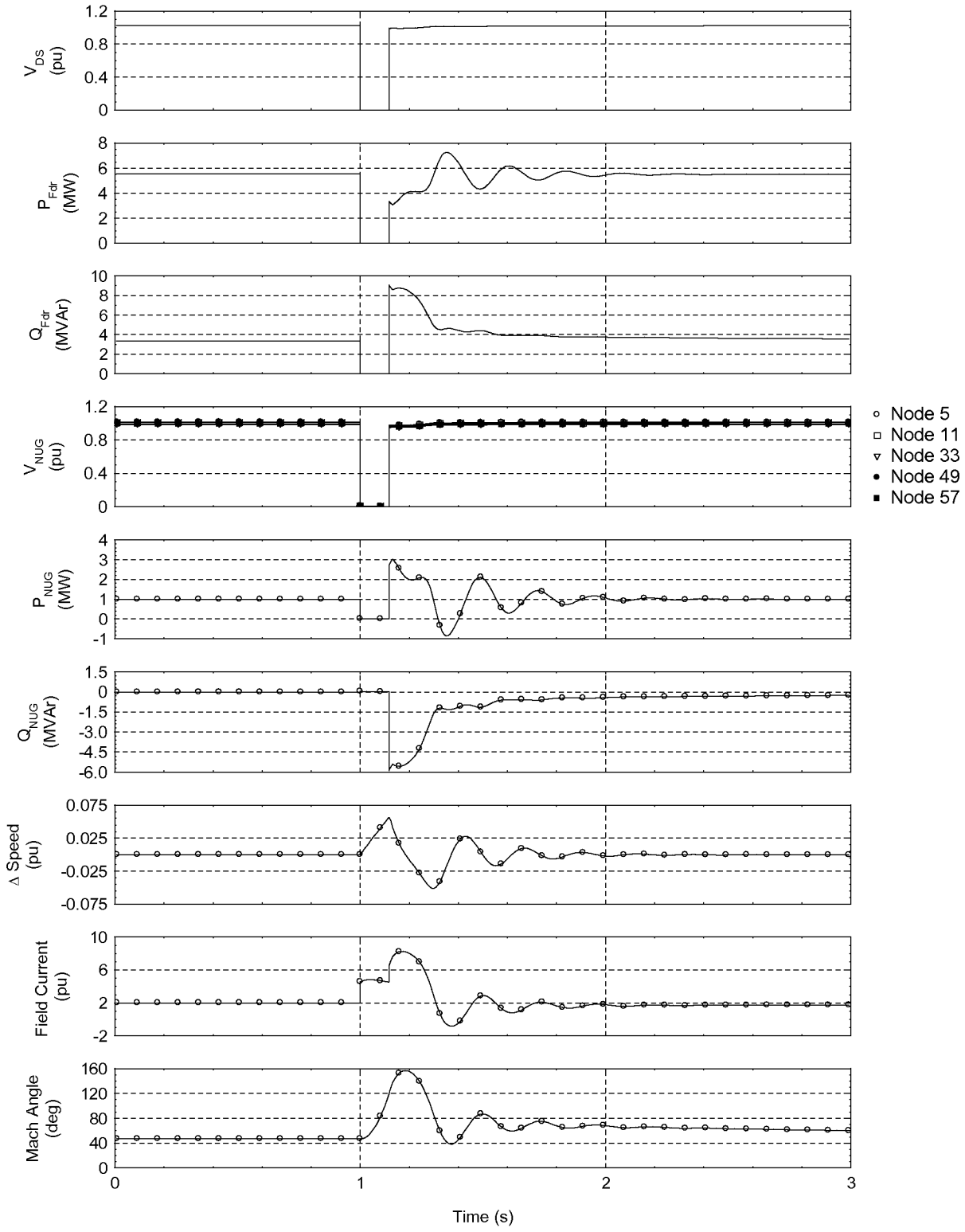

Figure 67. Simulation of three-phase fault at DR terminals on Node 5, Pioneer feeder, cleared in 0.11 s (machine angle referenced to substation bus)

Table 10. Normalized Synchronous Machine Parameters (1-MVA base)

T'do	Xd	X'd	X"d	Xo
2.76	1.595	0.234	0.16	0.07

For faults remote from the machine, the terminal voltage does not collapse completely. This is illustrated in figures 68 and 69 for the two feeders, assuming a three-phase fault at the respective nodes. With the voltage only partially collapsed, the machine's output is only partially reduced, allowing more time for fault clearing before the machine falls out of step. Many factors can determine the outcome of stability studies, including the generator characteristics as defined by its parameters, the short-circuit capacity of the distribution feeder, the fault type and its location, characteristics of the loads and their distribution on the feeder, and generation excitation controls if present. Modern software tools make it easy to take such factors into account in a rigorous fashion, whereas simplified models can be tedious and overly conservative. The following findings are based on results of simulations using the PTI PSS/E software.

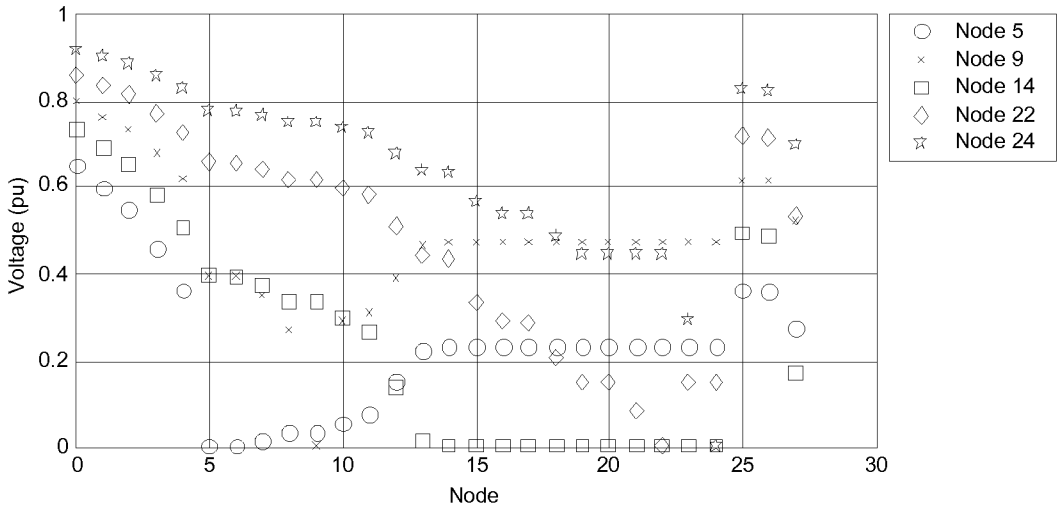

Figure 68. Voltage profile because of three-phase fault at respective nodes on Argo feeder

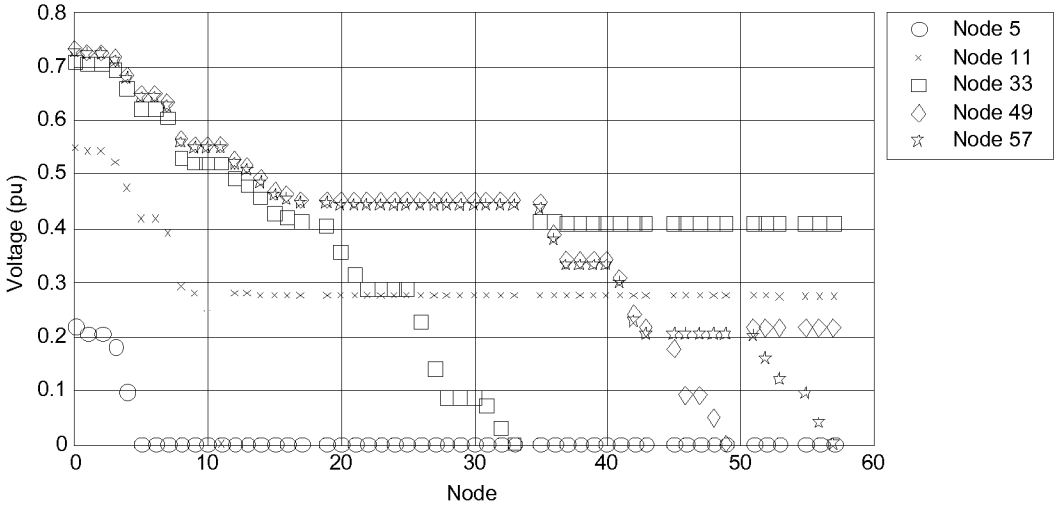

Figure 69. Voltage profile because of three-phase fault at respective nodes on Pioneer feeder

3.6.3 Question

What is the critical clearing time for synchronous generators to remain stable when faults occur close to the DR or remote from the DR?

3.6.4 Study Results

Figure 70 illustrates the result for a DR located at Node 24 of the Argo feeder with a three-phase fault occurring upstream — for example, near the head end of an adjacent feeder.[2] In this case, the limiting fault clearing time has been extended to about 0.25 s, compared with the about 0.1 s limit for faults occurring near the machine terminals. A similar result is obtained for DR located closer to the feeder head end with a fault occurring on an adjacent feeder. For instance, Figure 71 illustrates the result of a DR located at Node 5 with the fault on the adjacent feeder yielding 0.5 pu voltage at the supply bus. The machine is found to remain stable for a fault clearing time of 1 s, apparently helped by a low feeder X/R ratio that allows terminal voltage to remain near its nominal value. Load representation was found not to matter appreciably. For instance, although Figure 72 assumes 50% constant impedance and 50% constant (complex) power loads, Figure 73 shows comparable results for 100% constant impedance load representation.

Multiple DR on a feeder may tend to increase stability by tending to support feeder voltage during upstream faults. For example, Figure 74 illustrates the case for 1-MVA DR connected at five nodes on the Argo feeder. With a solid three-phase fault initiated at the substation bus at t = 1 s, feeder voltages are prevented from collapsing completely, and the machines are able to maintain stability for fault clearing in 0.15 s.

[2] For all Argo feeder plots, the plotted machine angle includes a 30° phase shift because of the supply transformer at the substation bus.

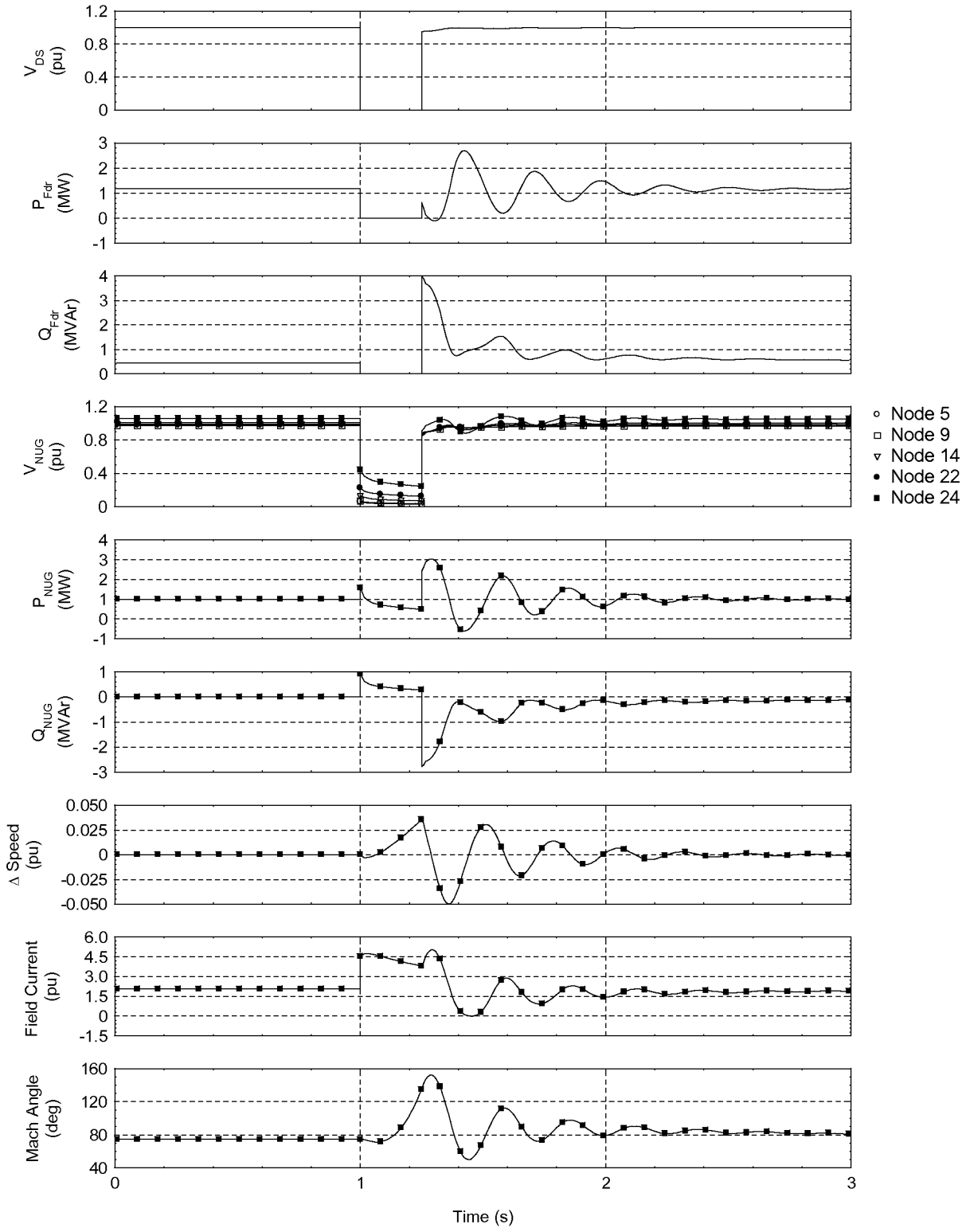

Figure 70. DR at Node 24 of Argo feeder, fault on substation bus cleared in 0.25 s

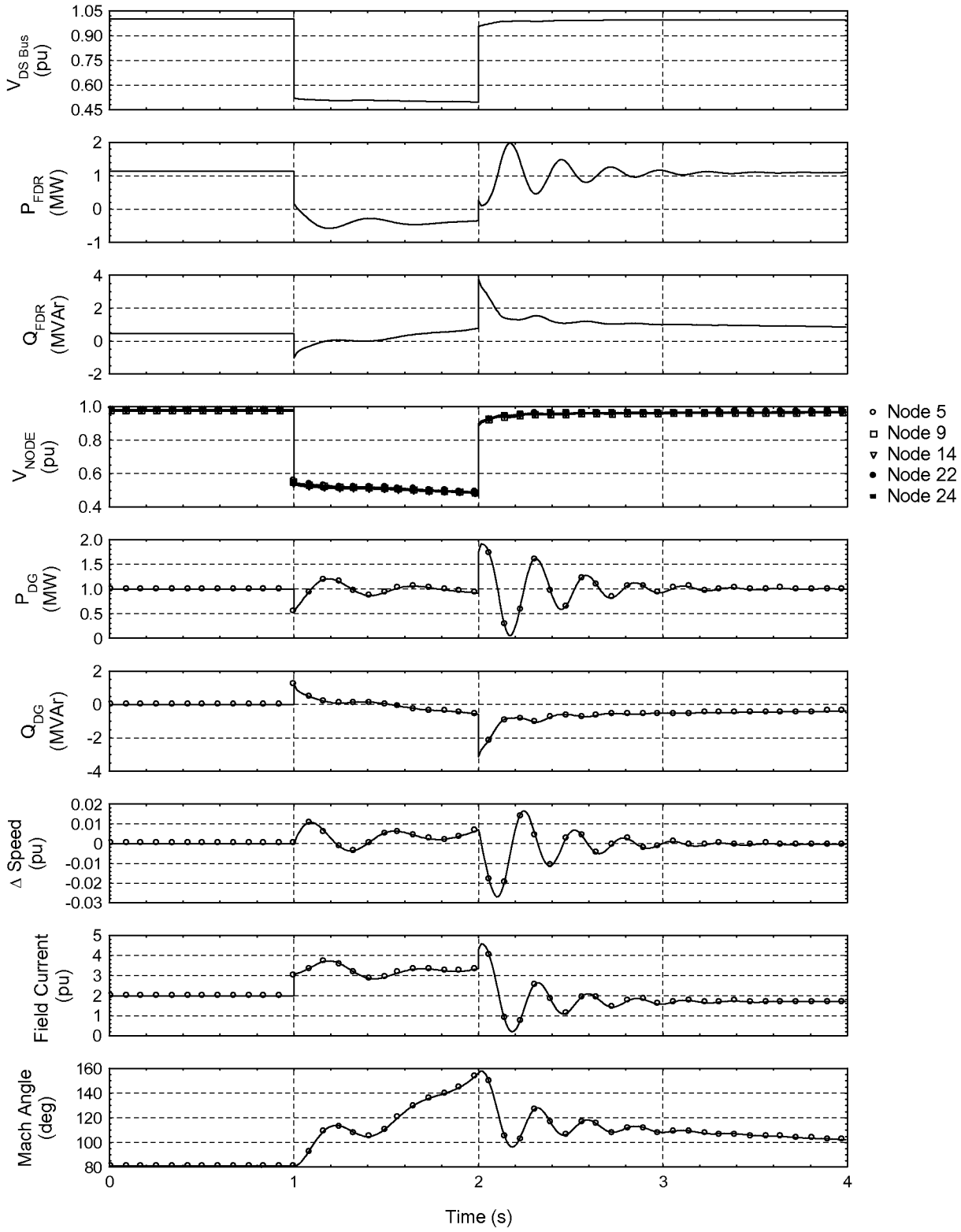

Figure 71. DR at Node 5 on Argo feeder, upstream fault yielding 0.5 pu voltage at substation bus, cleared in 1 s, constant impedance load model

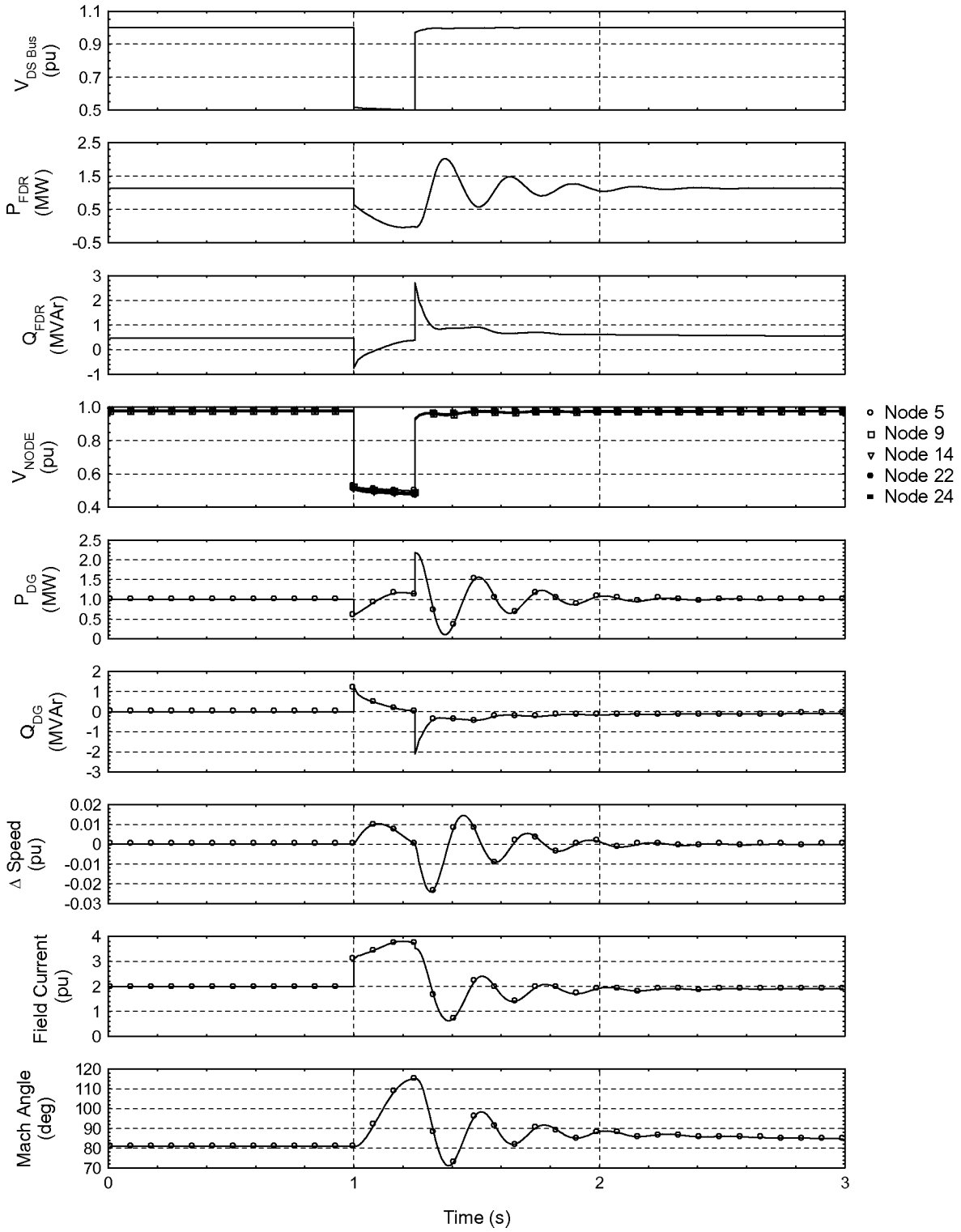

Figure 72. DR at Node 5 on Argo feeder, upstream fault yielding 0.5 pu voltage sag at supply substation, cleared in 0.25 s (load model 50% constant impedance, 50% constant power)

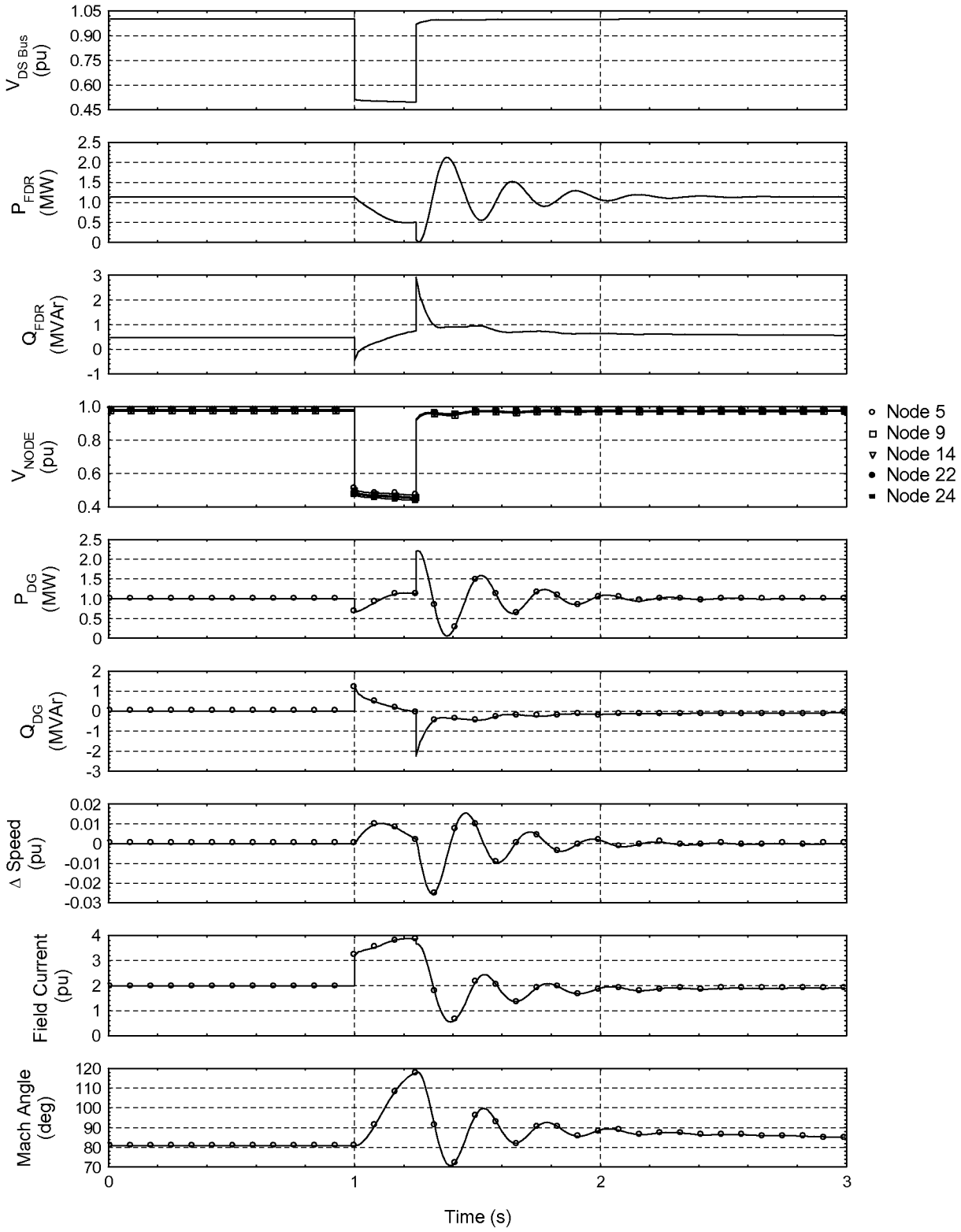

Figure 73. DR at Node 5 on Argo feeder, upstream fault yielding 0.5 pu voltage sag at supply bus, cleared in 0.25 s, constant power load model

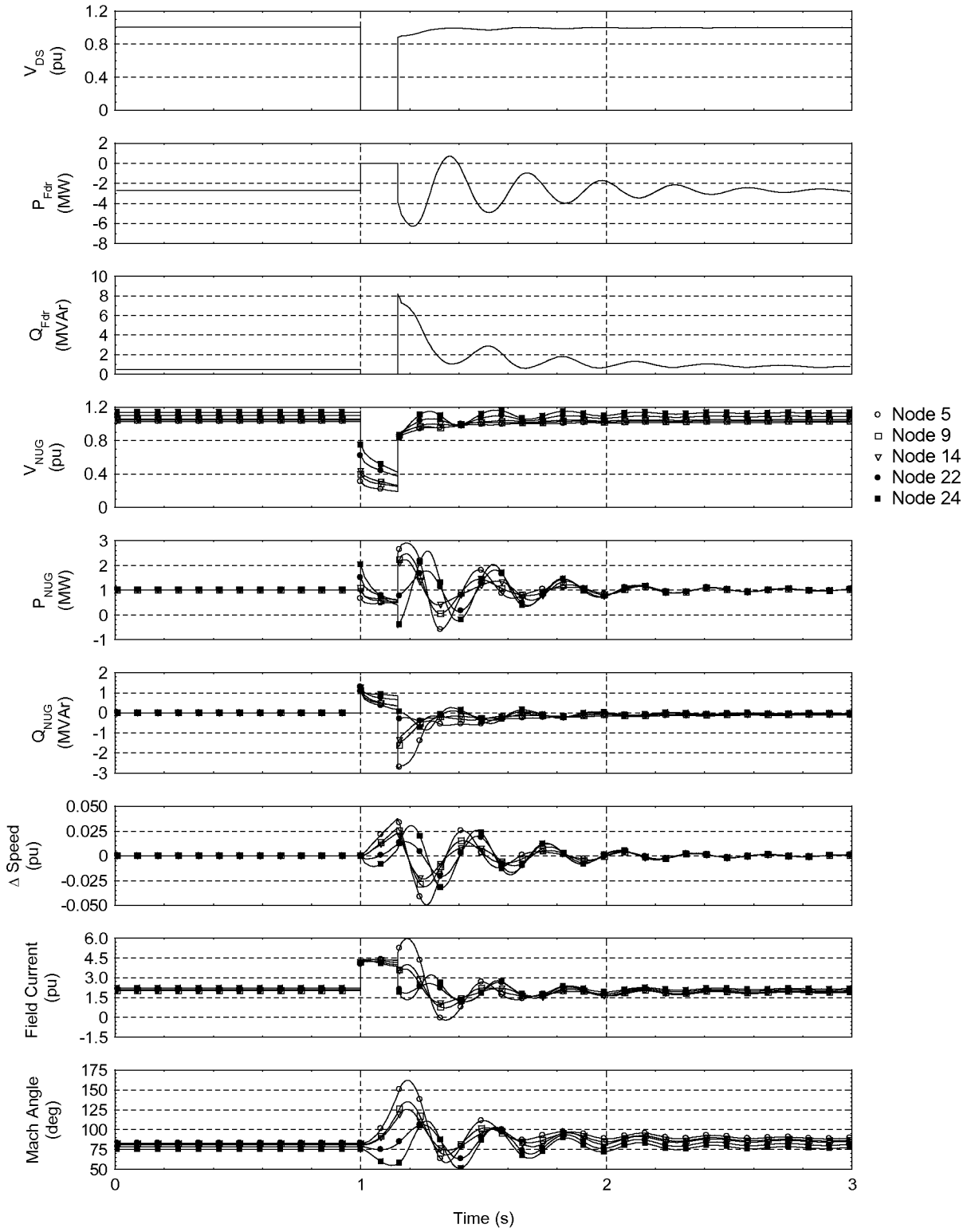

Figure 74. 1-MVA DR at respective nodes on Argo feeder, fault on supply bus cleared in 0.15 s

3.6.5 Conclusions and Recommendations

In summary, findings of simulations carried out for the Argo and Pioneer feeders suggest the following for generators on manual excitation control and an inertia constant H = 1 kW•s/kVA:

1. Faults occurring electrically close to the DR must be cleared within about 0.1 s for the synchronous generator to remain stable and continue in operation.

2. For more distant faults, such that the voltage at machine terminals is more than 0.5 pu, the fault clearing time can be delayed appreciably (to about 1 s) without the DR falling out of step and tripping.

3. Higher machine inertia constants would inevitably extend fault-clearing times proportionately and should be favored to reduce nuisance tripping. Modern excitation controls should also be helpful in extending critical clearing times, though these were not simulated here.

4. Stability considerations are not likely to be a governing factor for determining how much generation capacity may be incorporated on a given feeder without affecting feeder performance or even the maximum rating for an individual unit that may be accommodated. Instead, this issue is important because it defines a limit to the operation of synchronous generator-based DR and determines to what extent such units can support the grid during major disturbances. The analysis suggests:

    - Whether a synchronous machine maintains angular stability during major disturbances depends on both the severity of the disturbance and the machine design. Three-phase faults are the most severe disturbances. Machines incorporating higher rotational inertia can accommodate such faults for proportionately longer durations without falling out of step. It is expected that further improvement in operating performance can be attained through application of fast response time excitation controls.

    - Machines exhibiting a relatively low inertia constant of 1 are likely to lose synchronism for terminal faults unless cleared within 0.1 s. More distant faults, such as those occurring on adjacent feeders, can be tolerated for longer durations. For instance, simulations show that the machine remains stable for up to 1 s in cases of upstream faults yielding 0.5 pu at the substation bus. Evidently, machines displaying a higher inertia constant can tolerate such disturbances for a proportionately longer time.

    - Multiple machines on a feeder may increase stability by tending to support local voltage during upstream disturbances.

Based on these findings, there may be little merit in rapidly isolating a DR based solely on the depth or duration of voltage sags during disturbances. Doing so may unnecessarily isolate a DR that could otherwise continue supporting local loads and the utility system. With proper choice

of machine parameters and excitation controls, it would seem possible to reduce the frequency of such nuisance DR trips while improving supply reliability for customers.

Table 11. Clearing Times To Maintain Stability

Feeder	Location of DR		3Ø Fault Location and Clearing Time	
	Near End	Far End	Near End	Far End
Argo		Node 24	0.25 s	
	Node 5		0.10 s	
	Node 5 0.5 pu voltage			1 s
Pioneer	Node 5		0.11 s	
	Node 5 0.5 pu voltage			1s

Notes:

1. Multiple DR tend to increase the stability or extend critical clearing times.
2. Different load representations of (a) 50% constant impedance and 50% constant power and (b) 100% constant impedance have little effect on results.
3. Results were based on H = 1 kW • s/kVA; higher machine inertia constants would extend fault clearing times proportionately.

Appendix A: Information Required for Interconnection

Appendix A.1 Information Required to Evaluate a Request From a Generating Customer to Install Facilities on the Distribution System

General

1. A detailed drawing showing the proposed location of DR facilities
2. A one-line diagram showing the arrangement of the major equipment, such as overhead lines, underground cables, transformers, breakers, disconnects, arresters, C.T.s, V.T.s, and metering
3. A list of the voltage and normal day-to-day current ratings of each major electric line and equipment component

System Protection

1. System protection one-line diagrams
2. A description of each proposed protection scheme
3. Periodic testing and maintenance plans for the system protective devices and interrupting devices
4. Protective device settings

Prime Mover

1. Type — gas turbine, spark ignition gas, diesel, photovoltaic, fuel cell, Stirling, wind turbine, or other — and description
2. Manufacturer and model
3. Nominal rating and overload rating
4. Inertia constant
5. Percent governor droop, nominal 5%

Power Factor Regulator

1. Range of reactive power (kilovolt-ampere reactive) lagging and leading
2. Accuracy of setting

Generator

1. Type — induction (i.e., self-excited, external-excited), synchronous, inverter (i.e., line-commutated)
2. Manufacturer and model
3. Nominal kilovolt-ampere rating, overload kilovolt-ampere rating
4. Nominal voltage rating and configuration, delta or wye or wye-grounded
5. Speed RPM
6. Percent THD into a linear balanced load
7. Neutral resistance or reactance
8. Synchronizing equipment
9. For synchronous generator, sub-transient Xd", transient Xd', and synchronous Xd reactances
10. Inverter pu short-circuit current
11. Inverter "pull back" (turn down) characteristic

Voltage Regulator

1. Voltage regulator range
2. Accuracy of voltage regulator setting

Voltage Regulation Compensator

1. Compensator resistance
2. Compensator reactance

Transformers

1. Base kilovolt-ampere rating
2. Cooling stages and corresponding ratings
3. Nominal high voltage transformer connection
4. Nominal low voltage transformer connection
5. Tapchanger — no load tap changer or load tap changer
6. Short circuit impedance pu
7. Neutral resistance or reactance
8. Periodic testing and maintenance plans

Instrument Transformers

1. Ratios
2. Accuracy
3. Frequency bandwidth

Breakers

1. Types
2. Nominal current ratings (amperes)
3. Interrupting current ratings (kiloamperes)
4. Interrupting times
5. Periodic testing and maintenance plans

Operating Modes

1. Grid parallel
   (a) Export
   (b) Import
   (c) Base loaded or peaking
2. Isolated operation
3. Capacity factor
4. Availability
5. Dispatchable capacity
6. Transfer trip isolation point (breaker) if required

Equipment Grounding

1. Grounding method grid or ring and spur
2. Grounding impedances

Modeling Data

1. Transient data
2. Steady-state data
3. Flicker-induction generator (motor) inrush current
4. Size of PF correction capacitors

Ancillary Services to be Provided

1. Reactive supply
2. Voltage control (island)
3. Load regulation and frequency control (island)
4. Non-spinning (supplemental reserves)
5. Spinning reserve
6. Losses

Contact Lists, Persons' Names and Addresses

1. Engineering
2. Operating
3. Commercial terms

Appendix A.2 Electric Utility Information Required by a Generating Customer

A. List of site-specific system protection requirements

B. Source impedance and available system fault current

1. Minimum and maximum 60-Hz positive, negative, and zero sequence impedance at the point of interconnection (see Figure A-1) without generation
2. Present and future system fault currents
3. Settings and characteristics for protection devices
4. Clearing and reclosing times for single-phase and multiple-phase faults for various protection and interrupting devices

C. One-line diagrams for typical DR installation

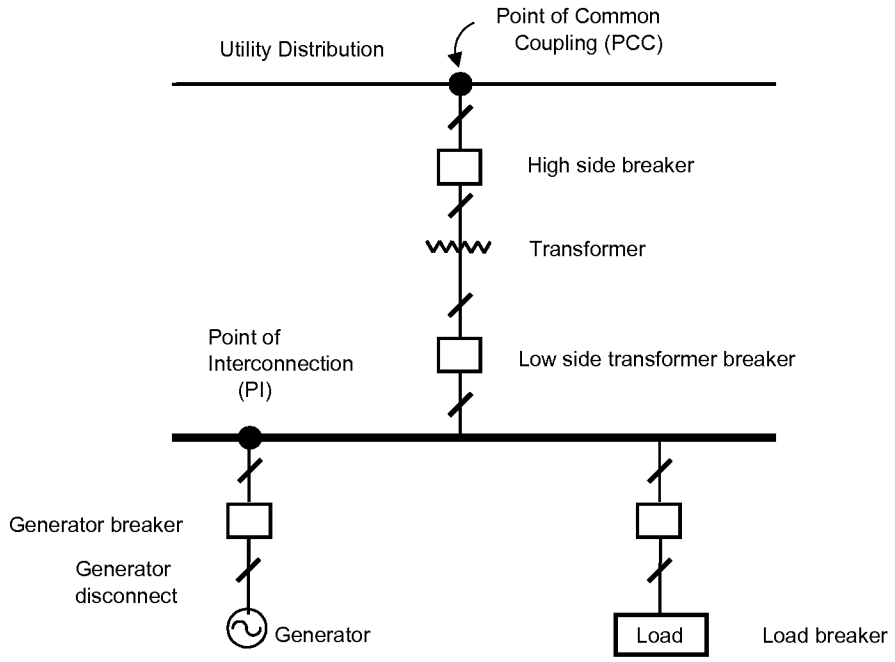

Figure A-1. A one-line diagram of DR installation

D. Maximum and minimum operating voltages for normal and emergency operations

E. Existing harmonics profile at PCC

F. Availability of system capacity

G. Reliability, planning, and operating criteria

H. Technical requirements for interconnecting (protection devices, transformer connections, etc.)

I. Safety and grounding requirements for interconnecting

J. Cost of studies, cost of changes needed to the system to interconnect, and schedule

K. Planned future system modifications

L. Contact list of names and addresses
   1. Engineering
   2. Operating
   3. Commercial terms

M. List of relevant standards such as IEEE, ANSI, NEMA, CSA, and IEC

N. Metering requirements

Appendix B: Tasks, Subtasks, and Schedule

Task 1. Develop Study Requirements

Subtask 1.1: Identify the Distributed Resources
Identify the characteristics of:

- Microturbines and fuel cells up to 4 MW
- Generation types (synchronous, inverter).

Subtask 1.2: Identify the Utility Distribution System and Other Customer Loads

- Screen Detroit Edison distribution circuits, and select two circuits to study.
- Fully characterize two circuits to facilitate dynamic modeling.

Subtask 1.3: Identify the Interface Mechanisms Requiring Study

Subtask 1.3.a: Voltage Dynamics
Identify the issues — such as inverter harmonics, disturbances causing loss of DR, and misoperation of voltage regulation for generator/inverter — that could cause circuits to malfunction.

Subtask 1.3.b: System Protection
Identify system protection schemes/relay issues — such as over/under voltage, over/under frequency, phase and ground overcurrent, and reverse power flow — and issues of coordination with line reclosers and fusing associated with DR operation.

Task 2: Develop Modeling Scenarios

Subtask 2.1: Develop Equivalent Circuits

Subtask 2.1.a: Voltage Dynamics
Build equivalent circuits to study disturbances affecting system voltage.

Subtask 2.1.b: System Protection
Build equivalents for evaluating distribution system and DR protection.

Subtask 2.2: Classify Contingencies
Select the contingencies — such as feeder faults, breaker operations, capacitor switching, and harmonic injection — that will cause interaction between the DR and the distribution system, and group them into those affecting voltage dynamics and those affecting system protection.

Subtask 2.3: Validate Modeling

- Compare the modeling with simplified analytical tools and previous experience.
- Consider preliminary simulations to identify contingencies likely to have a major effect on voltage dynamics and/or system protection.

Task 3: Conduct Simulations Utilizing the Models

- Run numerous simulations to study performance issues associated with interconnection identified in previous tasks.
- Consider sensitivity studies and field experience to verify the reasonableness of results.
- Include plots of voltage and electrical transients and effects on protective devices.
- Tabulate data indicating edges of boundaries for various parameters.

Task 4: Determine Performance Boundaries, Guidelines

- Compare simulation results with performance boundaries associated with each interconnection issue.
- Provide simplified analytical tools (tables, graphs, and simplified analytical expressions) that consultants, DR manufacturers, and utility planners can use to define DR penetration limits and minimum protection requirements.
- Summarize results into conclusions regarding areas needing additional study and the adequacy of analytical tools.

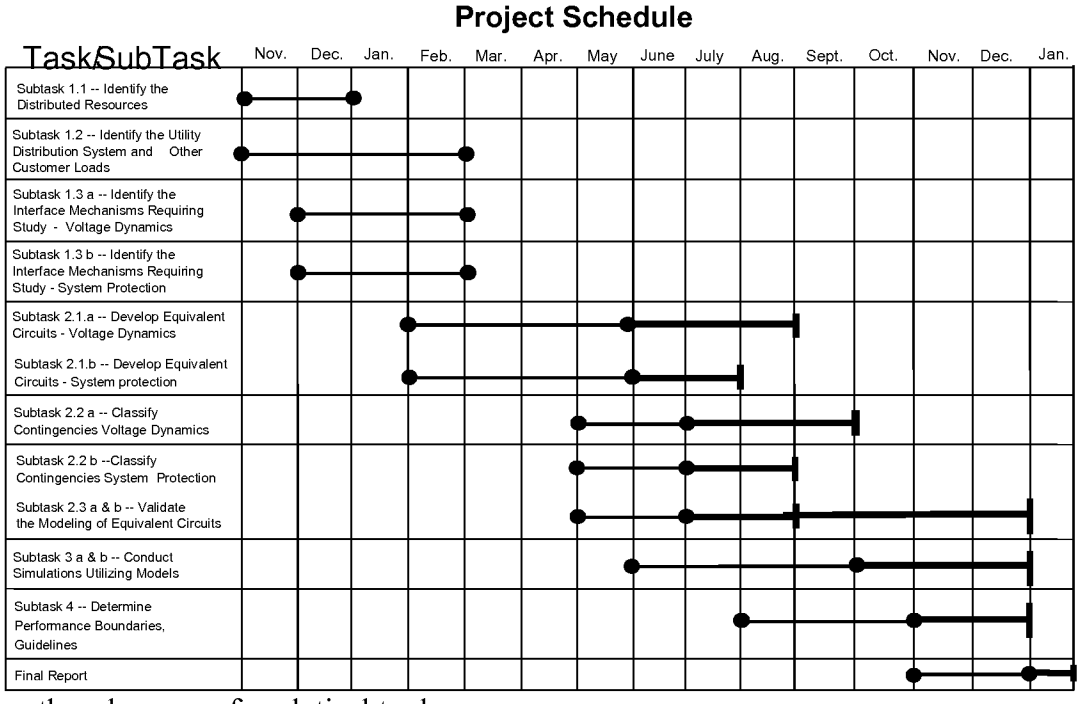

Figure B-1. Project schedule

Appendix C: System Characteristics and Contingencies

Appendix C.1 Generator, Inverter, and Circuit Characteristics

Table C-1. Generator Characteristics

Manufacturer: Lafayette Power Systems		
Arrangement No.	7C-4914	
Generator Parameters		
Ratings		
Line-to-Line Voltage	4,160 V	
Line-to-Neutral Voltage	2,402 V	
Rated kVA	1,000 kVA	
Rated RMS Current	139 A	
Rated Speed	1,200 rpm	
Excitation		
Rated Power Factor	**No Load**	**0.8 PF**
Excitation Voltage	4.8 V	41.3 V
Excitation Current	3.7 A	10.5 A
Inertia Constant H	≅1	
Voltage Regulation and Accuracy		
Voltage Level Adjustment	+/-5%	
Constant Speed	+/-1%	
With 3% Speed Change	+/-2%	

Generator Resistances

Resistances at 25ºC		Generator Impedance
Stator (Ω)	Field (Ω)	Base Ω
0.2008	0.8318	17.3056

Generator Reactances

		Per Unit	Ohms
Subtransient Direct Axis	X"d	0.1587	2.7459
Subtransient Quadrature Axis	X"q	0.1498	2.5190
Transient Saturated	X'd	0.2342	4.0533
Synchronous Direct Axis	Xd	1.5949	27.6012
Negative Sequence	X2	0.1542	2.6689
Zero Sequence	X0	0.0733	1.2683

		Seconds
Open Circuit Transient Direct Axis	T'dO	2.76159
Short Circuit Subtransient Direct Axis	T"d	0.00239
Open Circuit Subtransient Quadrature Axis	T"qO	0.00857
Short Circuit Subtransient Quadrature Axis	T"q	0.00012

Armature Short Circuit	TA	0.02617

Waveform Deviation Line-to-Line No Load	Telephone Influence Factor
Less Than 5%	Less Than 50

For Inertia Data, Refer to TD6502

Table C-2. Inverter Characteristics

	FCE	Turbogenset
Rated Kilovolt-Amperes	250 kVA	500 kVA
Rated Current	300 A	600 A
Rated PF	+/-0.8	+/-0.8
Rated Voltage	480 V Wye	480 V Wye
Transient Voltage Limits	75%–120% for 50 ms	75%–120% for 50 ms
Current Unbalance Limits	50%	50%
Voltage Unbalance Limits	No Limit	No Limit
Maximum Current at 50% Voltage	600 A	1,200 A
Maximum Current at 50% Voltage	600 A	1,200 A
THD	<2%	<2%
Harmonic Voltage Tolerance	2%	2%
Voltage Regulator Time Constant	10 ms	10 ms
Operating Modes	Current Source Voltage Source	Current Source Voltage Source

Protective Trip Settings	Value	Time	Value	Time
Underfrequency	<59.3 Hz	10 Cycles	<59.3 Hz	10 Cycles
Overfrequency	>60.5 Hz	10 Cycles	>60.5 Hz	10 Cycles
D.C. Current Limit	0.5% of Rated Current		0.5% of Rated Current	
Undervoltage	<90%	2 s	<90%	2 s
Undervoltage	<75%	3 Cycles	<75%	3 Cycles
Overvoltage	>110%	60 Cycles	>110%	60 Cycles
Overvoltage	>120%	6 Cycles	>120%	6 Cycles

Table C-3. Circuit Characteristics for DC 326 Argo
40-kV Source Impedance: (0.171+ j0.684)% on 10-MVA Base
Transformer Size 6 MVA, Impedance (2.3 + j13.85)% on 10-MVA Base (8.42% on Own Base)
Generator Transient Impedance X'd = (0.0 + j20.0)% on Own Base

This file shows the impedance of each line of 326 Argo.
The line is defined as the segment between nodes.
The impedances are calculated on a 10-MVA base and 4.8-kV voltage and are given in percent except as otherwise noted.

Node	To Node	Wire Code	Feet	Wire Size	R1/ 1,000 Ft	X1/ 1,000 Ft	R1%	JX1%	Z1 PU	Z1%
0	1	404	1,164	450 M 3/C	1.09	1.17	1.2688	1.3619	0.0186	1.86
1	2	422	332	350 MA, B	2.15	4.92	0.7138	1.6334	0.0178	1.78
2	3	422	160	350 MA, B	2.15	4.92	0.344	0.7872	0.0086	0.86
3	4	414	160	#4/0 Cu	2.27	5.0	0.3632	0.8	0.0088	0.88
4	5	420	3,581	#0A, B	7.98	5.58	28.5764	19.982	0.3487	34.87
5	6	410	991	#6 Cu	18.35	6.07	18.1849	6.0154	0.1915	19.15
5	7	420	313	#0A, B	7.98	5.58	2.4977	1.7465	0.0305	3.05
7	8	420	562	#0A, B	7.98	5.58	4.4848	3.136	0.0547	5.47
8	9	410	733	#6 Cu	18.35	6.07	13.4506	4.4493	0.1417	14.17
8	10	420	531	#0A, B	7.98	5.58	4.2374	2.963	0.0517	5.17
10	11	417	474	#0, ACSR	7.73	6.08	3.664	2.8819	0.0466	4.66
10	11	420	220	#0A, B	7.98	5.58	1.7556	1.2276	0.0214	2.14
11	12	417	1,957	#0, ACSR	7.73	6.08	15.1276	11.8986	0.1925	19.25
12	13	417	1,823	#0, ACSR	7.73	6.08	14.0918	11.0838	0.1793	17.93
13	14	412	202	#2 Cu	7.25	5.61	1.4645	1.1332	0.0185	1.85
14	15	412	10	#2 Cu	7.25	5.61	0.0725	0.0561	0.0009	0.09
15	16	412	375	#2 Cu	7.25	5.61	2.7188	2.1038	0.0344	3.44
16	17	412	10	#2 Cu	7.25	5.61	0.0725	0.0561	0.0009	0.09
17	18	412	697	#2 Cu	7.25	5.61	5.0533	3.9102	0.0639	6.39
18	19	412	514	#2 Cu	7.25	5.61	3.7265	2.8835	0.0471	4.71
19	20	999	10	336 ACSR	2.51	5.47	0.0251	0.0547	0.0006	0.06
20	21	415	284	#4 ACSR	18.42	6.66	5.2313	1.8914	0.0556	5.56
21	22	421	1,018	#3/0A, B	4.3	4.9	4.3774	4.9882	0.0664	6.64
20	23	415	944	#4 ACSR	18.42	6.66	17.3885	6.2870	0.1849	18.49
23	24	415	1,796	#4 ACSR	18.42	6.66	33.0823	11.9614	0.3518	35.18
4	25	422	144	350 MA, B	2.15	4.92	0.3096	0.7085	0.0077	0.77
25	26	422	125	350 MA, B	2.15	4.92	0.2688	0.6150	0.0067	0.67
14	27	412	2,063	#2 Cu	7.25	5.61	14.956	11.5734	0.1891	18.91
26	27	412	2,217	#2 Cu	7.25	5.61	16.0733	12.4374	0.2032	20.32

Table C-4. Circuit Characteristics for DC 9795 Pioneer
120-kV Source Impedance: (0.082 + j0.395)% on 10-MVA Base
Transformer Size 15-MVA, Impedance (0.272 + j5.327)% on 10-MVA Base (8% on Own Base)
Generator Transient Impedance:
X'd = (0.0 + j20.0)% on Own Base, X0 = (0 + j6.3)% on Own Base

This file shows the impedance of each line of 9795 Pioneer.
The line is defined as the segment between nodes.
The impedances are calculated on a 10-MVA base and 13.2-kV voltage and are given in percent or pu.

Node	To Node	Wire Code	Feet	Wire Size	R1/ 1,000 Ft	X1/ 1,000 Ft	R1%	JX1%	Z1 PU	Z1%
0	1	361	134	636 MA, B	0.178	0.583	0.023852	0.078122	0.000817	0.81682
1	2	361	517	636 MA, B	0.178	0.583	0.092026	0.301411	0.003151	0.315147
1	3	365	803	1000 cable	0.138	0.204	0.110814	0.163812	0.001978	0.19773
3	4	361	989	636 MA, B	0.178	0.583	0.176042	0.576587	0.006029	0.602863
4	5	361	1,131	636 MA, B	0.178	0.583	0.201318	0.659373	0.006894	0.689421
5	6	313	413	0 ACSR	1.217	0.909	0.502621	0.375417	0.006273	0.627348
5	7	361	481	636 MA, B	0.178	0.583	0.085618	0.280423	0.002932	0.293202
7	8	361	2,110	636 MA, B	0.178	0.583	0.037558	1.23013	0.012862	1.286188
8	9	361	331	636 MA, B	0.178	0.583	0.058918	0.192973	0.002018	0.201767
9	10	313	199	0 ACSR	1.217	0.909	0.242183	0.180891	0.003023	0.302282
10	11	313	1,926	0 ACSR	1.217	0.909	2.343942	1.750734	0.029256	2.9256
9	12	313	331	0 ACSR	1.217	0.909	0.402827	0.300879	0.005028	0.50279
12	13	361	362	636 MA, B	0.178	0.583	0.064436	0.211046	0.002207	0.220664
13	14	361	704	636 MA, B	0.178	0.583	0.125312	0.410432	0.004291	0.429136
14	15	361	819	636 MA, B	0.178	0.583	0.145782	0.477477	0.004992	0.499236
15	16	361	234	636 MA, B	0.178	0.583	0.041652	0.136422	0.001426	0.142639
16	17	361	292	636 MA, B	0.178	0.583	0.051976	0.170236	0.00178	0.177994
17	18	302	146	350 MA, B	0.32	0.704	0.04672	0.102784	0.001129	0.112904
18	19	999	10	200A OH Recloser	0	0	0	0	0	0
19	20	302	1,184	350 MA, B	0.32	0.704	0.37888	0.833536	0.009156	0.91560
20	21	302	966	350 MA, B	0.32	0.704	0.30912	0.680064	0.00747	0.747022
21	22	302	709	350 MA, B	0.32	0.704	0.22688	0.499136	0.005483	0.54828
22	23	302	479	350 MA, B	0.32	0.704	0.15328	0.337216	0.003704	0.370418
23	24	302	423	350 MA, B	0.32	0.704	0.13536	0.297792	0.003271	0.327112
24	25	305	483	#3/0A, B	0.666	0.752	0.321678	0.363216	0.004852	0.485183
22	26	311	814	#0A, B	1.058	0.79	0.861212	0.64306	0.010748	1.074808
26	27	311	1,169	#0A, B	1.058	0.79	1.236802	0.92351	0.015436	1.543551
27	28	311	691	#0A, B	1.058	0.79	0.731078	0.54589	0.009124	0.912398
28	29	305	1,155	#3/0A, B	0.666	0.752	0.76923	0.86856	0.011602	1.16022
29	30	305	1,307	#3/0A, B	0.666	0.752	0.870462	0.982864	0.013129	1.312907
28	31	305	292	#3/0A, B	0.666	0.752	0.194472	0.219584	0.002933	0.29332
31	32	305	675	#3/0A, B	0.666	0.752	0.44955	0.5076	0.006781	0.678051
32	33	305	559	#3/0A, B	0.666	0.752	0.372294	0.420368	0.005615	0.561527
17	34	302	179	350 MA, B	0.32	0.704	0.05728	0.126016	0.001384	0.138423
34	35	999	10	200A OH Recloser	0	0	0	0	0	0
35	36	302	1,489	350 MA, B	0.32	0.704	0.47648	1.048256	0.011515	1.151466
36	37	302	1,279	350 MA, B	0.32	0.704	0.40928	0.900416	0.009891	0.98907
37	38	308	479	#3/0 ACSR	0.786	0.874	0.376494	0.418646	0.00563	0.563038
38	39	308	626	#3/0 ACSR	0.786	0.874	0.492036	0.547124	0.007358	0.735829
38	40	308	1,070	#3/0 ACSR	0.786	0.874	0.84102	0.93518	0.012577	1.257727
37	41	308	490	#3/0 ACSR	0.786	0.874	0.38514	0.42826	0.00576	0.575968
41	42	311	978	#0A, B	1.058	0.79	1.034724	0.77262	0.012914	1.291354

42	43	311	344	#0A, B	1.058	0.79	0.363952	0.27176	0.004542	0.454219
43	44	311	559	#0A, B	1.058	0.79	0.591422	0.44161	0.007381	0.738105
44	45	999	10	200A Sectionalizer	0	0	0	0	0	0
45	46	311	1,201	#0A, B	1.058	0.79	1.270658	0.94879	0.015858	1.585805
46	47	311	157	#0A, B	1.058	0.79	0.166106	0.12403	0.002073	0.207303
46	48	311	614	#0A, B	1.058	0.79	0.649612	0.48506	0.008107	0.810727
48	49	311	684	#0A, B	1.058	0.79	0.723672	0.54036	0.009032	0.903156
43	50	311	55	#0A, B	1.058	0.79	0.05819	0.04245	0.000726	0.072622
50	51	999	10	200A Sectionalizer	0	0	0	0	0	0
51	52	311	593	#0A, B	1.058	0.79	0.627394	0.46847	0.00783	0.78299
52	53	311	530	#0A, B	1.058	0.79	0.56074	0.4187	0.006998	0.699814
53	54	999	10	100K Fuses	0	0	0	0	0	0
54	55	313	312	#0, ACSR	1.217	0.909	0.379704	0.283608	0.004739	0.47392
55	56	313	625	#0, ACSR	1.217	0.909	0.760625	0.568125	0.009494	0.949377
56	57	313	496	#0, ACSR	1.217	0.909	0.603632	0.450864	0.007534	0.753425

Table C-5. Circuit Characteristics for DC 9795 Pioneer
120-kV Source Impedance: (0.082 + j0.395)% on 10-MVA Base
Transformer Size 15-MVA, Impedance (0.272 + j5.327)% on 10-MVA Base (8% on Own Base)
Generator Transient Impedance:
X'd = (0.0 + j20.0)% on Own Base, X0 = (0 + j6.3)% on Own Base

This file shows the impedance of each line of 9795 Pioneer.
The line is defined as the segment between nodes.
The impedances are calculated on a 10-MVA base and 13.2-kV voltage and are given in percent or pu.

Node	To Node	R0/1,000 Ft	X0/1,000 Ft	R0%	jX0%	Z0 PU	Z0%
0	1	0.906	2.381	0.121404	0.319054	0.003414	0.341371
1	2	0.906	2.381	0.468402	1.230977	0.013171	1.317082
1	3	1.362	0.895	1.093686	0.718685	0.013087	1.308685
3	4	0.906	2.381	0.896034	2.354809	0.025195	2.519524
4	5	0.906	2.381	1.024686	2.692911	0.028813	2.881276
5	6	1.91	2.473	0.78883	1.021349	0.012905	1.290506
5	7	0.906	2.381	0.435786	1.145261	0.012254	1.22537
7	8	0.906	2.381	1.91166	5.02391	0.053753	5.375325
8	9	0.906	2.381	0.299886	0.788111	0.008432	0.843238
9	10	1.91	2.473	0.38009	0.492127	0.006218	0.621818
10	11	1.91	2.473	3.67866	4.762998	0.060182	6.018197
9	12	1.91	2.473	0.63221	0.818563	0.010343	1.03428
12	13	0.906	2.381	0.327972	0.861922	0.009222	0.922212
13	14	0.906	2.381	0.637824	1.676224	0.017935	1.793473
14	15	0.906	2.381	0.742014	1.950039	0.020864	2.086441

15	16	0.906	2.381	0.212004	0.557154	0.005961	0.596126
16	17	0.906	2.381	0.264552	0.695252	0.007439	0.743884
17	18	1.013	2.268	0.147898	0.331128	0.003627	0.362656
18	19	0	0	0	0	0	0
19	20	1.013	2.268	1.199392	2.685312	0.02941	2.940993
20	21	1.013	2.268	0.978558	2.190888	0.023995	2.399493
21	22	1.013	2.268	0.718217	1.608012	0.017611	1.761118
22	23	1.013	2.268	0.485227	1.086372	0.011898	1.189811
23	24	1.013	2.268	0.428499	0.959364	0.010507	1.05071
24	25	1.358	2.317	0.655914	1.119111	0.012972	1.297163
22	26	1.742	2.375	1.417988	1.93325	0.023975	2.397529
26	27	1.742	2.375	2.036398	2.776375	0.034431	3.443134
27	28	1.742	2.375	1.203722	1.641125	0.020352	2.035249
28	29	1.358	2.317	1.56849	2.676135	0.031019	3.101912
29	30	1.358	2.317	1.774906	3.028319	0.035101	3.510129
28	31	1.358	2.317	0.396536	0.676564	0.007842	0.784206
31	32	1.358	2.317	0.91665	1.563975	0.018128	1.812806
32	33	1.358	2.317	0.759122	1.295203	0.015013	1.501272
17	34	1.013	2.268	0.181327	0.405972	0.004446	0.444627
34	35	0	0	0	0	0	0
35	36	1.013	2.268	1.508357	3.377052	0.036986	3.698597
36	37	1.013	2.268	1.295627	2.900772	0.03177	3.176968
37	38	1.47	2.46	0.70413	1.17834	0.013727	1.372692
38	39	1.47	2.46	0.92022	1.53996	0.01794	1.793957
38	40	1.47	2.46	1.5729	2.6322	0.030663	3.066348
37	41	1.47	2.46	0.7203	1.2054	0.014042	1.404216
41	42	1.742	2.375	1.703676	2.32275	0.028806	2.880569
42	43	1.742	2.375	0.599248	0.817	0.010132	1.013206
43	44	1.742	2.375	0.973778	1.327625	0.016465	1.64646
44	45	0	0	0	0	0	0
45	46	1.742	2.375	2.092142	2.852375	0.035374	3.537386
46	47	1.742	2.375	0.273494	0.372875	0.004624	0.462423
46	48	1.742	2.375	1.069588	1.45825	0.018085	1.808456
48	49	1.742	2.375	1.191528	1.6245	0.020146	2.014631
43	50	1.742	2.375	0.09581	0.130625	0.00162	0.161995
50	51	0	0	0	0	0	0
51	52	1.742	2.375	1.033006	1.408375	0.017466	1.746603
52	53	1.742	2.375	0.92326	1.25875	0.01561	1.561045
53	54	0	0	0	0	0	0
54	55	1.91	2.473	0.59592	0.771576	0.009749	0.97491
55	56	1.91	2.473	1.19375	1.545625	0.019529	1.952945
56	57	1.91	2.473	0.94736	1.226608	0.015499	1.549857

Selection of Synchronous Machine Reactances

The synchronous machine per unit reactances for the actual generator on 9795 Pioneer are:

X"d = 0.1587, X'd = 0.2342, Xd = 1.5949, X0 = 0.0733, on its own base.

A more conservative number of 0.2 for X'd was used instead of 0.2342 for the studies in this report because the short circuit is slightly larger. X0 was scaled down from 0.0733 to 0.063 to be consistent with the lower transient reactance (i.e., 0.2342 ÷ 0.2 = 1.17 and 0.733 ÷ 0.063 = 1.17)

Table C-6. Other Circuit Parameters

Item	DC 9795 Pioneer	DC 326 Argo
Peak Load	6.8 MVA	2.2 MVA
Number of Customers (2001 Data)	R = 2,122, C = 268, I = 3	R = 335, C = 42, I = 2
Substation Stepdown Transformer	2 – 15/20/25 MVA	3 – 6 MVA
Subtransmission Voltage	120 kV	41.57 kV
Distribution Voltage	13.2 kV	4.8 kV

NOTE: R = residential, C = commercial, I = industrial

Appendix C.2 System Protection Contingencies

C.2.1 EEI Issue 1: Fault on Adjacent Circuit

Table C-7. Fault on Adjacent Circuit – DC 326 Argo
Substation Transformer Size 6 MVA (All Contingencies)
Breaker Setting at Substation: CO-8 Relay, Pickup 1,000 A @4.8 kV,
Time Dial = 2.0 (All Contingencies)

Contingency	Sectionalizing Device	Distance
1	40k fuse	Near End
2	65k fuse	Near End
3	80k fuse	Near End
4	100k fuse	Near End
5	140k fuse	Near End
6	140-A recloser	Near End
7	40k fuse	Mid Point
8	65k fuse	Mid Point
9	80k fuse	Mid Point
10	100k fuse	Mid Point
11	140k fuse	Mid Point
12	140-A recloser	Mid Point
13	40k fuse	Far End
14	65k fuse	Far End
15	80k fuse	Far End
16	100k fuse	Far End
17	140k fuse	Far End
18	140-A recloser	Far End

Table C-8. Fault on Adjacent Circuit – DC 9795 Pioneer
Substation Transformer Size 15 MVA (All Contingencies)
Breaker Setting at Substation: CO-8 Relay, Pickup 1,000 A @13.2 kV,
Time Dial = 2.0 (All Contingencies)

Contingency	Sectionalizing Device	Distance
1	40k fuse	Near End
2	100k fuse	Near End
3	140-A Recloser	Near End
4	40k fuse	Mid Point
5	100k fuse	Mid Point
6	140-A Recloser	Mid Point
7	40k fuse	Far End
8	100k fuse	Far End
9	140-A Recloser	Far End

C.2.2 EEI Issue 1: Reduced Protective Device Sensitivity

Table C-9. Reduced Protective Device Sensitivity – DC 326 Argo
Substation Transformer Size 6 MVA (All Contingencies)
Breaker Setting at Substation: CO-8 Relay, Pickup 1,000 A @ 4.8 kV,
Time Dial = 2.0 (All Contingencies)

Contingency	Fault location	Fault Type
1	Node 15	Three-phase
2	Node 19	Three-phase

Table C-10. Reduced Protective Device Sensitivity – DC 9795 Pioneer
Substation Transformer Size 15 MVA (All Contingencies)
Breaker Setting at Substation: CO-8 Relay, Pickup 1,000 A @ 13.2 kV,
Time Dial = 2.0 (All Contingencies)

Contingency	Fault location	Fault Type
1	Node 17	Three-phase
2	Node 57	Three-phase
3	Node 17	Line-to-ground
4	Node 57	Line-to-ground

C.2.3 EEI Issue 2: Nuisance Fuse Blowing Because of DR Fault Current

Table C-11. Nuisance Fuse Blowing Because of DR Fault Current – DC 326 Argo
Substation Transformer Size 6 MVA
Breaker Setting at Substation: CO-8 Relay, Pickup 1,000 A @ 4.8kV,
Time Dial = 2.0 (All Contingencies)
Recloser Size 140 A

Contingency	Sectionalizing Device	Distance
1	40k fuse	Near End
2	65k fuse	Near End
3	80k fuse	Near End
4	100k fuse	Near End
5	140k fuse	Near End
6	40k fuse	Mid Point
7	65k fuse	Mid Point
8	80k fuse	Mid Point
9	100k fuse	Mid Point
10	140k fuse	Mid Point
11	40k fuse	Far End
12	65k fuse	Far End
13	80k fuse	Far End
14	100k fuse	Far End
15	140k fuse	Far End

Table C-12. Nuisance Fuse Blowing Because of DR Fault Current – DC 9795 Pioneer
Substation Transformer Size 15 MVA
Breaker Setting at Substation: CO-8 Relay, Pickup 1,000 A @ 13.2 kV, Time Dial = 2.0
Recloser Size 140 A

Contingency	Sectionalizing Device	Distance
1	40k fuse	Near End
2	65k fuse	Near End
3	80k fuse	Near End
4	100k fuse	Near End
5	140k fuse	Near End
6	40k fuse	Mid Point
7	65k fuse	Mid Point
8	80k fuse	Mid Point
9	100k fuse	Mid Point
10	140k fuse	Mid Point
11	40k fuse	Far End
12	65k fuse	Far End
13	80k fuse	Far End
14	100k fuse	Far End
15	140k fuse	Far End

C.2.4 EEI Issue 15: Faults Within the DR Zone (Independent of Circuit Referenced)

Table C-13. Faults Within the DR Zone (Independent of Circuit Referenced)

Contingency	Condition
1	No DR On
2	DR 1 on DR2 Off
3	DR 2 on DR 1 Off

DR 1: size = 2 MVA, Xd'= 0.2 pu on own base
DR 2: size = 2 MVA, Xd'= 0.2 pu on own base
13.2-kV–480-V three-phase transformer: size = 1 MVA, 5.75% Z on own base
System positive sequence Thevenin impedance at DR 1 bus: (0.61172 + j1.77788)% on a 100-MVA base
Fault Impedance: 0.05 Ω resistive, actual

C.2.5 EEI Issue 16: Isolate DR for Upstream Fault

Table C-14. Isolate DR for Upstream Fault – DC 326 Argo
Substation Transformer Size 6 MVA (All Contingencies)
Breaker Setting at Substation: CO-8 Relay, Pickup 1,000 A @ 4.8 kV,
Time Dial = 2.0 (All Contingencies)

Contingency	DR Size (MVA)	Cable Pole Fuse Size	Distance
1	0.5	40k	Near End
2	1.0	40k	Near End
3	3.0	40k	Near End
4	0.5	80k	Near End
5	1.0	80k	Near End
6	3.0	80k	Near End
7	0.5	40k	Mid Point
8	1.0	40k	Mid Point
9	3.0	40k	Mid Point
10	0.5	80k	Mid Point
11	1.0	80k	Mid Point
12	3.0	80k	Mid Point
13	0.5	40k	Far End
14	1.0	40k	Far End
15	3.0	40k	Far End
16	0.5	80k	Far End
17	1.0	80k	Far End
18	3.0	80k	Far End

Table C-15. Isolate DR for Upstream Fault – DC 9795 Pioneer
Substation Transformer Size 15 MVA (All Contingencies)
Breaker Setting at Substation: CO-8 Relay, Pickup 1,000 A @ 13.2 kV,
Time Dial = 2.0 (All Contingencies)

Contingency	DR Size (MVA)	Cable Pole Fuse Size	Distance
1	1.0	40k	Near End
2	3.0	40k	Near End
3	5.0	40k	Near End
4	1.0	80k	Near End
5	3.0	80k	Near End
6	5.0	80k	Near End
7	1.0	40k	Mid Point
8	3.0	40k	Mid Point
9	5.0	40k	Mid Point
10	1.0	80k	Mid Point
11	3.0	80k	Mid Point
12	5.0	80k	Mid Point
13	1.0	40k	Far End
14	3.0	40k	Far End
15	5.0	40k	Far End
16	1.0	80k	Far End
17	3.0	80k	Far End
18	5.0	80k	Far End

C.2.6 EEI Issue 27: Upstream Single-Phase Fault Causes Fuse Blowing

Table C-16. Upstream Single-Phase Fault Causes Fuse Blowing – DC 326 Argo
Substation Transformer Size 6 MVA (All Contingencies)
Breaker Setting at Substation: CO-8 Relay, Pickup 1,000 A @ 4.8 kV,
Time Dial = 2.0 (All Contingencies)

Contingency	DR Size (MVA)	Cable Pole Fuse Size	Distance
1	0.5	40k	Near End
2	1.0	40k	Near End
3	3.0	40k	Near End
4	0.5	80k	Near End
5	1.0	80k	Near End
6	3.0	80k	Near End
7	0.5	40k	Mid Point
8	1.0	40k	Mid Point
9	3.0	40k	Mid Point
10	0.5	80k	Mid Point
11	1.0	80k	Mid Point
12	3.0	80k	Mid Point
13	0.5	40k	Far End
14	1.0	40k	Far End
15	3.0	40k	Far End
16	0.5	80k	Far End
17	1.0	80k	Far End
18	3.0	80k	Far End

Table C-17. Upstream Single-Phase Fault Causes Fuse Blowing – DC 9795 Pioneer
Substation Transformer Size 15 MVA (All Contingencies)
Breaker Setting at Substation: CO-8 Relay, Pickup 1,000 A @ 13.2 kV,
Time Dial = 2.0 (All Contingencies)

Contingency	DR Size (MVA)	Cable Pole Fuse Size	Distance
1	1.0	40k	Near End
2	3.0	40k	Near End
3	5.0	40k	Near End
4	1.0	80k	Near End
5	3.0	80k	Near End
6	5.0	80k	Near End
7	1.0	40k	Mid Point
8	3.0	40k	Mid Point
9	5.0	40k	Mid Point
10	1.0	80k	Mid Point
11	3.0	80k	Mid Point
12	5.0	80k	Mid Point
13	1.0	40k	Far End
14	3.0	40k	Far End
15	5.0	40k	Far End
16	1.0	80k	Far End
17	3.0	80k	Far End
18	5.0	80k	Far End

Appendix D: Maximum DR Penetration Limits Curve Development

Appendix D.1 Development for EEI Issue 1

The manufacturer's published trip times (in seconds) for the recloser and protective relay at the CB 1 breaker are arranged in a table. The trip times for the relay are in one row. The trip times for the recloser are in the next row. The columns are aligned such that the 2,000 column indicates the respective current for the times of the relay and the recloser to be 4.074 s and 0.19 s, respectively.

Within a desired range of current, the breaker current that will trip the recloser in the same time that the recloser trips is entered in the last row.

Table D-1. Current and Trip Times of Protective Devices

	Current Through Protective Device and Their Trip Times							
Current for Breaker or Recloser (A)	4,000	**3,000 (e)**	**2,000 (f)**	1,500	1,000	800	**700 (a)**	600
Relay Time (s)	1.022	**1.668 (c)**	**4.074 (d)**	9.996				
Recloser Time (s)	0.105	0.132	0.19	0.259	0.682	1.393	**1.738 (b)**	2.137
Relay Current for Same Time as Recloser					5,562.8	3,334	**2,944.5**	2,680

A second table, Table D-2, is developed. A partial table is shown here. Rows are established for each protective device current. For each row headed by its respective current [e.g., 700 (a)], the respective recloser trip time from Table D-1 [e.g., 1.738 (b)] is used to calculate the breaker current that is required to cause the relay to trip in that same time.

An interpolation is required because the recloser trip time (i.e., 1.738 s) falls between the relay trip time values listed in Table D-1 (i.e., 4.074 s and 1.668 s). Note that the recloser trip time of 1.738 s falls between 1.668 (c) and 4.074 (d). Interpolation is used to determine the value of relay current corresponding to the trip time of 1.738 s. Note that the current value must be between 3,000 (e) and 2,000 (f) A because the trip time lies between the corresponding data points of 1.668 (c) and 4.074 (d). The logarithmic method of interpolation used is described in Appendix F. A result of 2,944 A is produced by this interpolation. This value is placed in the appropriate cell of Table D-2, which is below the rightmost value of current of 2,000 A.

Note that there are other values of current in this same row. These other values are the interpolated values based on other trip relay times. For example, the value to the left of 2,944 (or 2,928) is based on interpolating the recloser trip time of 1.738 "between" 1.022 and 1.668 and the current values of 4,000 and 3,000. This interpolation would not be expected to be very accurate because 1.738 does not fall between the values of 1.022 and 1.668. These cells were filled to produce a useable mathematical tool in Excel. Note that only the correct interpolated value is carried down to the next row, where all values except 2,944 are blank or zero.

The value of 2,944 is carried to Table D-1 by summing all the values in this lower Row 5.

Table D-2. Breaker Current Required to Cause Relay to Trip in Same Time as Recloser

		Breaker Current							
1	Recloser Current	4,000	3,000	2,000	1,500	1,000	800	700	600
2	600	2,288	2,593	2,680	2,459.4				
3		0	0	2,680	0	0	0	0	0
4	**700 (a)**	2,676	2,928	**2,944**	2,627.9				
5		0	0	**2,944**	0	0	0	0	0
6	800	3,164	3,334	3,255	2,821				
7		0	3,334	0	0	0	0	0	0
8	1,000	5,432	5,072	4,502	3,546.7				
9		0	0	0	0	0	0	0	0
10	1,500	11,302	8,956	6,988	4,37.2				
11		0	0	0	0	0	0	0	0
12	2,000	14,288	10,744	8,044	5,342.2				
13		0	0	0	0	0	0	0	0

Appendix D.2 Use of Maximum Penetration Curve for Issue 2

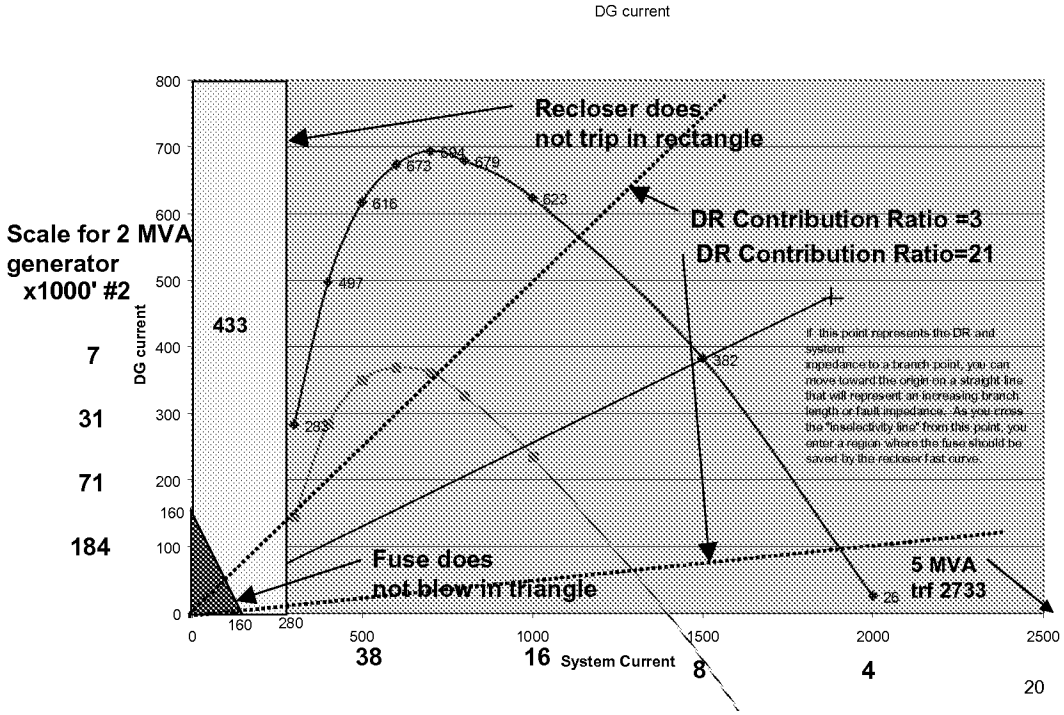

Figure D-1. Maximum DR penetration curve for Issue 2

This plot represents the maximum DR fault current, as noted in Issue 2, that can be provided from a DR while maintaining the fuse-saving ability of the fast curve of a 140-A single phase (i.e., three single-phase reclosers). The maximum DR fault current is plotted as a function of system fault current flowing through the recloser. Refer to Figure 12 in the body of this report for the electrical system configuration.

The upper curve is to be used for an 80k fuse; the lower curve is for a 65k fuse.

A variety of information can be obtained from this plot.

- **Maximum DR fault current (primary purpose of plot)**
  The maximum DR fault current is obtained directly from the upper curve. Ampere values of 283, 497, 616, etc., are noted along the curve and indicate the DR fault current that will cause the fuse to blow with the first operation of the recloser. Note that the curve reaches a peak as the system fault current value increases and then decreases to zero at about 2,000 A. At 2,000 A of system current, the fuse will not be saved by the recloser even without any DR fault current.

- **Area in which recloser does not trip**
  The clear, vertical rectangular area at the left of the plot represents the area in which the system fault current is too low to operate the recloser (less than 280 A). The 140-A recloser requires 280 A or more to trip.

- **Area in which fuse does not blow**
  The dark triangular area at the lower left of the plot represents the area in which the fuse does not blow. The 80k fuse requires 160 A to blow. Current through the fuse is equal to the sum of the DR fault current and the system fault current. The hypotenuse of the triangle represents the values at which this sum equals 160 A. Thus, the area under the hypotenuse is an area in which the sum of the DR fault current and the system fault current is less than the 160 A required to blow the fuse.

- **Stiffness lines**
  Assume the DR contribution ratio is defined as (DR fault contribution + system fault contribution)/DR fault contribution measured at the specific fault location. Then the straight lines drawn from the origin represent values of constant DR contribution ratio. Two such lines have been shown: one for a ratio of 3 and the other for a ratio of 21. Note that increasing this ratio does not necessarily increase the DR size that can be added.

- **Lines representing moving a fault location out on a lateral**
  Straight lines drawn from the origin can be used to determine the effect of moving a fault farther down a lateral from its connection to the circuit "backbone." One such line is shown. This is done as follows:

  - Determine the DR fault current and system fault current at the point where the lateral is connected to the backbone.
  - Plot these values as a point on this plot. (See the point labeled "+.")
  - Draw a line from this point to the origin.
  - Moving along this line to the origin represents moving the fault out on the lateral away from the connection point. The point at which the line and the curve intersect is the point at which fuse saving is marginal. Moving farther toward the origin improves the fuse-saving capability. Moving away from the intersection decreases the fuse-saving capability.

- **Rescaling the X and Y axes to read DR size, line length, and system transformer size**
  The X axis has a second scale (bold numbers) that represents different lengths of lines connected to a 5-MVA substation transformer. A typical 5-MVA transformer will have a fault current at the bus of about 2,700 A, shown on the plot as 2,733 A. If the circuit conductor is specified, the axis can be rescaled to read in conductor length rather than system fault current. For this case, the rescaling was done for #2 Al and reads in 1,000 values. Similarly, if a specific DR size is specified, including its short-circuit reactance, the Y axis can be re-scaled.

In this case, it was done for a 2-MVA synchronous generator with an Xd' of 0.2 pu. The Y scale also reads how many feet of #2 ACSR are needed to obtain comparable fault current contribution from the DR (see bolded numbers).

Appendix E: Ratio of Fault Currents Flowing Into a Lateral

Does the ratio of fault current from the DR to the system fault current stay the same no matter what the fault impedance is? Nodal analysis can be used to show that the ratio of these currents is determined only by the ratio of the Thevenin impedances.

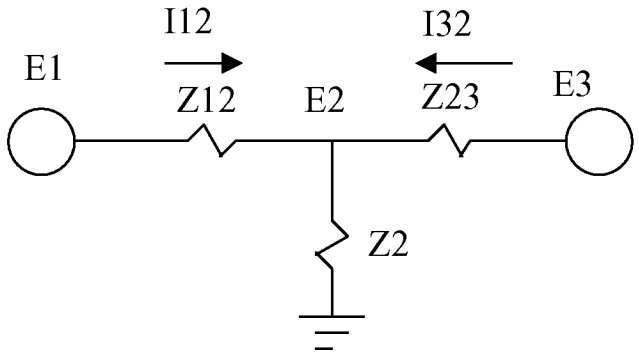

The current in each of the two sources is:

I12 = (E1 - E2) / Z12
I32 = (E3 - E2) / Z23

Assume E1 = E3, and substitute E1 for E3 in the second equation.

I12 = (E1 - E2) / Z12
I32 = (E1 - E2) / Z23

The ratio of the two currents = I12 / I32 = [(E1 - E2) / Z12] / [(E1 - E2) / Z23] = Z23 / Z12,

or the ratio of the currents in those two branches is inversely proportional to the ratio of the impedances.

Also, the ratio of the current in one branch to the total current is proportional to the ratio of the impedance of the opposite branch to the sum of the two impedances, or:

I12 / (I12 + I32) = Z23 / (Z12 + Z23).

This means that the current split will remain constant for any length of lateral or magnitude of fault impedance on a lateral fed from the two sources.

ASPEN studies confirm this for simple networks.

Appendix F: Logarithmic Interpolation

Following is a discussion of straight-line interpolation using log scales for both X and Y axes (log-log graph or plot).

This discussion is based on the fact that horizontal and vertical distances on log–log paper are proportional to the differences of the logs of the respective X and Y values of the two points.

To interpolate values on a log–log plot along a straight line, use the following procedure:

Determine the log values of X1, Y1, X2, Y2, and X. (Any base can be used; for this discussion, the base 10 is used.)

Calculate Y from the formula (using Excel notation):

Y =10^(LOG10(Y1)+(LOG10(X)-LOG10(X1))*(LOG10(Y2)-LOG10(Y1))/(LOG10(X2)-LOG10(X1)))

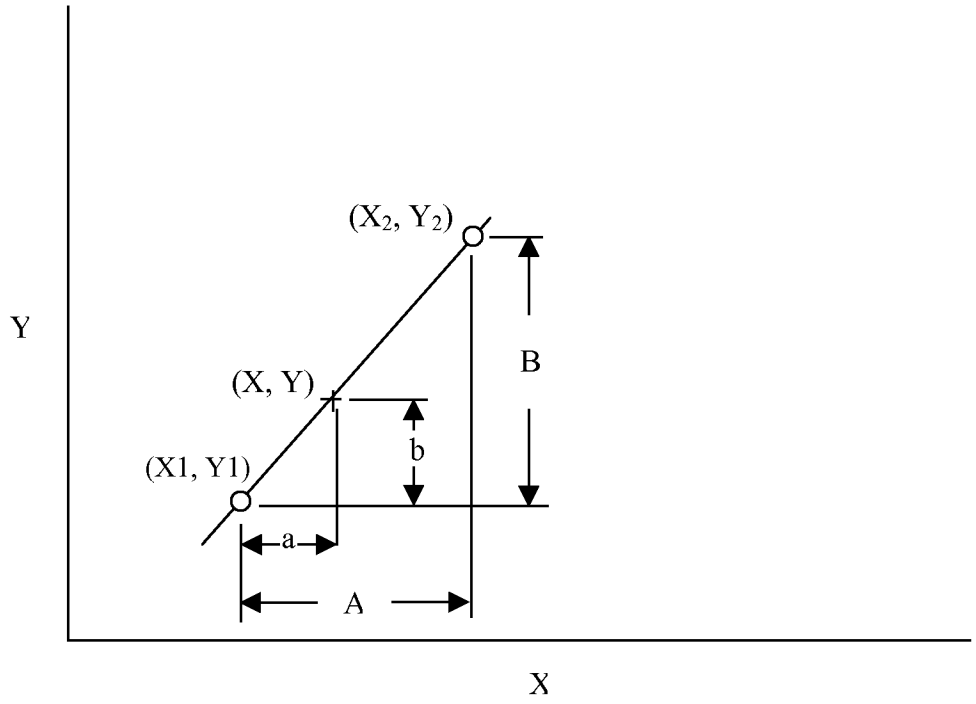

Figure F-1. Logarithmic Interpolation

For right triangles with equal angles:

b / a = B / A
b = a * B / A

because distances can be measured by the differences between the logs of the respective numbers.

(Refer to the L and C scales on a slide rule. The L scale is the log of the C scale; the L scale is linear. The C scale is similar to the scale on log-log paper.)

a=LOG10(X)-LOG10(X1)
b=LOG10(Y)-LOG10(Y1)
A=LOG10(X2)-LOG10(X1)
B=LOG10(Y2)-LOG10(Y1)

Rearranging b=LOG10(Y)-LOG10(Y1),
LOG10(Y)=LOG10(Y1) + b.

Substituting for b,
LOG10(Y)=LOG10(Y1) + a*B/A.

Substituting for A, B, and A,
LOG10(Y)=LOG10(Y1) +(LOG10(X)- LOG10(X1))* (LOG10(Y2)-LOG10(Y1))/ (LOG10(X2)-LOG10(X1)).

Performing exponentiation on both sides (Base 10),
Y=10^(LOG10(Y1) +(LOG10(X)- LOG10(X1))* (LOG10(Y2)-LOG10(Y1))/ (LOG10(X2)-LOG10(X1))).

Appendix G: Infeed Effects

The effects of infeed can be seen in the simple circuit below. Two sources are connected to a single node through separate impedances. This node is then connected to ground through a single impedance.

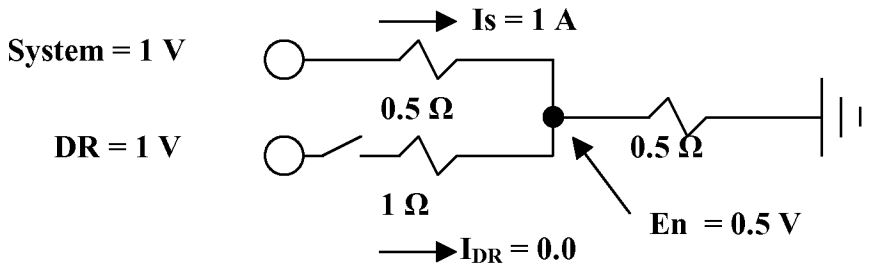

Figure G-1. Infeed circuit with DR "off"

With the DR off, 1 A flows from the system source through the two 0.5-Ω impedances. The voltage at the node is 0.5 volts.

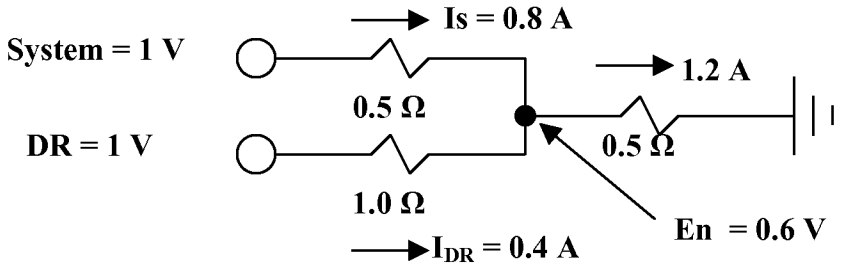

Figure G-2. Infeed circuit with DR "on"

With the DR on, the total current increases to 1.2 A, with 0.8 A contributed by the system source and 0.4 A contributed by the DR source. The voltage at the node has increased to 0.6 V (or 1.2 A x 0.5 Ω).

Calculation Notes:

- Because the source voltages are equal, the sources can be treated as a single node, and the source impedances can be treated as a parallel combination of impedances.
- The combined parallel impedance of 1/2 Ω and 1 Ω = 1/3 Ω.
- 1/3 Ω in series with 1/2 Ω equals a total of 5/6 Ω.
- Total current = 1 V / (5/6 Ω) = 6/5 A = 1.2 A.
- System current = (1 V – 0.6 V) / 0.5 Ω = 0.8 A.

A helpful way of visualizing this effect is to note that additional current from the DR will raise the voltage at the node. This is due to additional current flowing through the grounded impedance. A higher voltage at the node will cause less current to flow from the system source. This is due to a lower voltage drop across the system source impedance.

Because the current contributed by the system source is less with the DR on, protective devices will become "less sensitive" to faults (represented by the ground on the system in figures G-1 and G-2). The DR can, in this way, desensitize protective devices at the system source.

A more detailed description of infeed effects can be found in Protective Relaying Theory and Applications.[1]

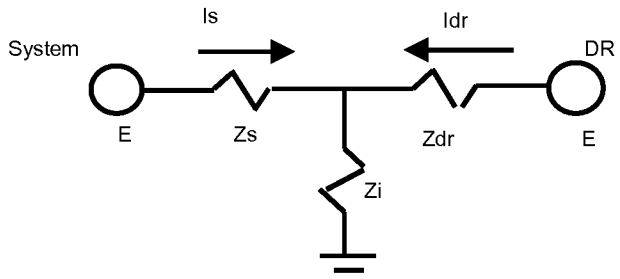

Figure G-3. The effect of infeeds

Table G-1 shows source current (I_S) and DR current (I_{DR}) of various per unit source and DR impedances (three-phase faults only).

Table G-1. Source Current and DR Current of Impedances

MVA Base=	10								
kV Base =	13.2								
I Base =	437.3866								
Z Base =	17.424								
DR pu Z =	0.2	(to calculate DR size)							
All Z in pu				E=	1.0				
Zs =	**0.057**								

Is = Zdr / (Zdr + Zs) E / ((Zdr * Zs)/ (Zdr + Zs) + Zi)
Id = Zs / (Zdr + Zs) E / ((Zdr * Zs) / (Zdr + Zs) + Zi)
Zdr = (Zi * Zs) / ((E / Is - (Zs + Zi))

		Charted			Charted			Charted	Charted
	Zi ->	**0.030**	**0.050**	**0.060**	**0.054**	**0.080**	**0.090**	**0.127**	**0.200**
DR MVA size	**Zdr**					**Is**			
80	**0.025**	2814.6	1979.1	1723.4	1881.4	1369.4	1241.9	923.6	613.4
66.66666667	**0.03**	3037.4	2165.3	1893.4	2061.7	1513.4	1375.4	1028.4	686.6
50	**0.04**	3371.0	2453.8	2159.9	2342.3	1742.6	1589.1	1198.4	807.0
10	**0.2**	4577.6	3607.3	3261.6	3478.3	2737.1	2533.4	1986.4	1393.0
4	**0.5**	4837.3	3881.0	3531.9	3751.2	2993.3	2781.3	2203.7	1563.2
2	**1**	4930.5	3981.7	3632.2	3851.9	3089.8	2875.1	2287.1	1629.6
0.2	**10**	5017.6	4076.9	3727.5	3947.4	3182.0	2965.1	2367.8	1694.4

						Idr			
	0.025	6417.3	4512.4	3929.2	4289.6	3122.2	2831.5	2105.8	1398.7
	0.03	5771.1	4114.0	3597.6	3917.2	2875.6	2613.3	1954.0	1304.6
	0.04	4803.7	3496.6	3077.9	3337.7	2483.2	2264.4	1707.7	1150.0
	0.2	1304.6	1028.1	929.6	991.3	780.1	722.0	566.1	397.0
	0.5	551.4	442.4	402.6	427.6	341.2	317.1	251.2	178.2
	1	281.0	227.0	207.0	219.6	176.1	163.9	130.4	92.9
	10	28.6	23.2	21.2	22.5	18.1	16.9	13.5	9.7

This table shows the effects of infeed for various lateral (Zi) impedances
and various DR impedances (Zdr). Currents are in amperes for a 13.2-kV system.
The upper table shows the source current. Each column represents a different
line impedance (Zi). Each row represents a different DR impedance (Zdr).
The lower table shows the DR current (Idr).
All calculations are for a fixed source impedance (Zs).

Spreadsheet to verify last equation

	Enter P.U. E Zs Zi	Enter Desired Is (amps)
Is	**4.573**	**2000.000**
E	**1.000**	
Zs	**0.057**	
Zi	**0.127**	
Zdr=	0.209 Calculated DR Impedance	

Is = Zdr / (Zdr + Zs) E / ((Zdr * Zs) / (Zdr + Zs) + Zi)
Id = Zs / (Zdr + Zs) E / ((Zdr * Zs) / (Zdr + Zs) + Zi)
Zdr = (Zi * Zs) / ((E / Is - (Zs + Zi))

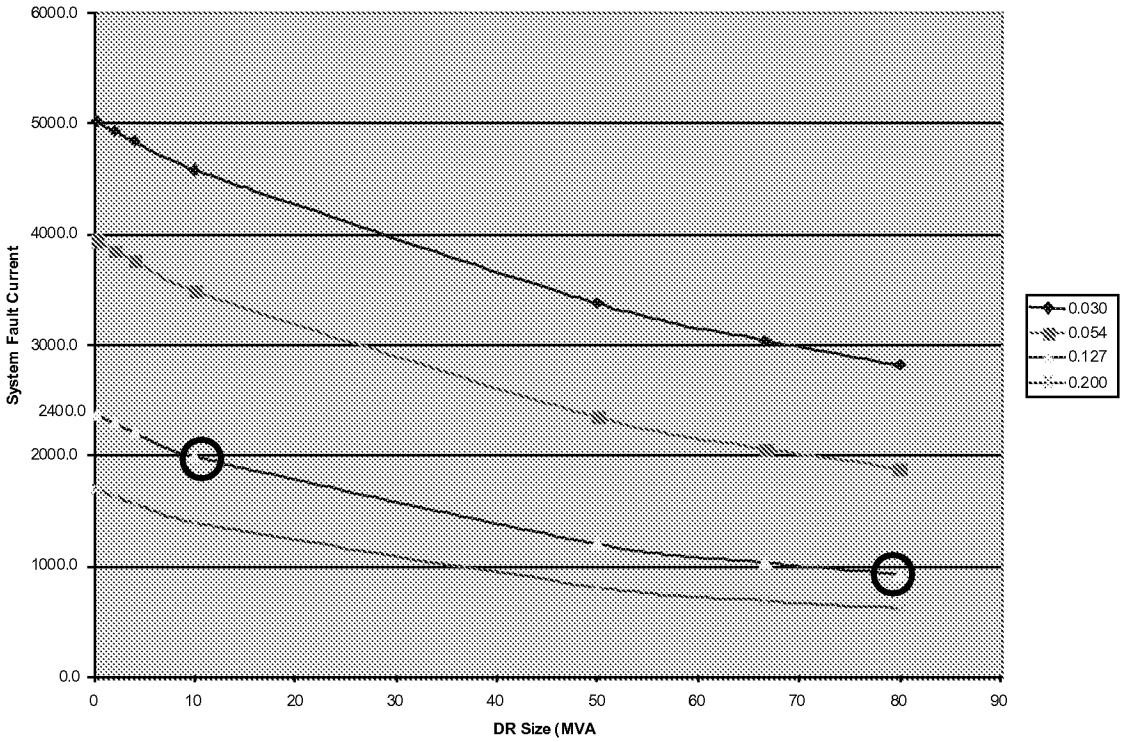

Figure G-4. The effect of DR size on system fault current

The above chart and previous table indicate the effect of adding various-sized DR generators to a circuit similar to DC 9795 Pioneer. Each line represents a different per unit impedance from the substation. The second line from the top (0.054 pu Z) represents the impedance to Node 17, the first sectionalizing point. The third line (0.127 pu Z) represents the impedance to Node 57.

As the DR size increases, the current through the substation breaker (system current) decreases. The chart is consistent with ASPEN results that show an 80-MVA DR will reduce the system current to 2,000 A for faults at Node 17. A 10-MVA DR generating unit will reduce the system current to 2,000 A for faults at Node 57.

Table Use and Restrictions

The table uses a fixed source impedance of 0.057 pu based on a 10-MVA base and a fixed DR impedance of 0.2 pu based on the actual DR sizes shown on the abscissa. For different impedances, Zs and Zdr must be re-entered.

The spreadsheet and chart use the magnitudes only for voltage, current, and impedance. Therefore, they will not produce results identical to ASPEN, which uses the magnitude and angle of all parameters. Circled areas represent the ASPEN results of 10 and 80 MVA. However, because the angles of the impedance of the DR, system, and lines are generally not more than 30° apart, reasonable results can be obtained by using only magnitudes. Results can be used for training and rough estimates. Final analysis for

actual DR connections should be done with software that includes the angle of the impedances.

Also note that the table and chart are meant to be used only for three-phase faults. Line-to-ground faults require that the zero sequence impedance be included. This was not done for this table or chart.

Appendix H: Study Results

Appendix H.1 EEI Issue 1 – Improper Coordination

For EEI Issue 1, the tables show the generator size, associated currents, and trip times for the system shown in Figure 2.

Table H-1. EEI Issue 1 – Table of Near-End Results on DC 326 Argo

	DR Size (MVA)	Fuse or Recloser Fault Current (A)	System Fault Current (A)	Total Fault Current (A)	Breaker Trip Time (s)	Fuse/Recloser Operation Time (s)
40k	0.47	281	8,416	8,693	0.48	0.49
65k	0.75	446	8,416	8,857	0.48	0.49
80k	0.95	564	8,416	8,973	0.47	0.48
100k	1.25	738	8,416	9,146	0.47	0.46
140k	2.1	1,226	8,415	9,631	0.46	0.46
140-A Recloser	1.9	1,113	8,415	9,518	0.46	0.48

Table H-2. EEI Issue 1 – Table of Mid-Point Results on DC 326 Argo

	DR Size (MVA)	Fuse or Recloser Fault Current (A)	System Fault Current (A)	Total Fault Current (A)	Breaker Trip Time (s)	Fuse/Recloser Operation Time (s)
40k	0.5	284	8,416	8,698	0.48	0.48
65k	0.82	448	8,416	8,863	0.48	0.48
80k	1.07	569	8,416	8,984	0.47	0.47
100k	1.42	725	8,416	9,142	0.48	0.47
140k	2.75	1,217	8,415	9,633	0.46	0.46
140-A Recloser	2.5	1,136	8,415	9,552	0.46	0.45

Table H-3. EEI Issue 1 – Table of Far-End Results on DC 326 Argo

	DR Size (MVA)	Fuse or Recloser Fault Current (A)	System Fault Current (A)	Total Fault Current (A)	Breaker Trip Time (s)	Fuse/Recloser Operation Time (s)
40k	0.55	280	8,416	8,697	0.48	0.49
65k	1.0	443	8,416	8,851	0.48	0.48
80k	1.5	574	8,416	8,970	0.47	0.46
100k	2.5	737	8,416	9,095	0.47	0.47
140k	See Note					
140-A Recloser	See Note					

Note: Line impedance limits current to a value such that any size generator will not cause inselectivity.

Table H-4. EEI Issue 1 – Table of Near-End Results on DC 9795 Pioneer

	DR Size (MVA)	Fuse or Recloser Fault Current (A)	System Fault Current (A)	Total Fault Current (A)	Breaker Trip Time (s)	Fuse/Recloser Operation Time (s)
40k	1.25	272	7,615	7,887	0.51	0.52
100k	3.3	719	7,614	8,332	0.49	0.49
140-A Recloser	5.1	1,110	7,614	8,722	0.48	0.48

Table H-5. EEI Issue 1 – Table of Mid-Point Results on DC 9795 Pioneer

	DR Size (MVA)	Fuse or Recloser Fault Current (A)	System Fault Current (A)	Total Fault Current (A)	Breaker Trip Time (s)	Fuse/Recloser Operation Time (s)
40k	1.3	274	7615	7889	0.51	0.51
100k	3.6	718	7614	8333	0.49	0.49
140-A Recloser	5.9	1,114	7,614	8,728	0.48	0.48

Table H-6. EEI Issue 1 – Table of Far-End Results on DC 9795 Pioneer

	DR Size (MVA)	Fuse or Recloser Fault Current (A)	System Fault Current (A)	Total Fault Current (A)	Breaker Trip Time (s)	Fuse/Recloser Operation Time (s)
40k	1.35	274	7,615	7,889	0.51	0.51
100k	4	711	7,614	8,324	0.49	0.50
140-A Recloser	7.2	1,106	7,614	8,712	0.48	0.49

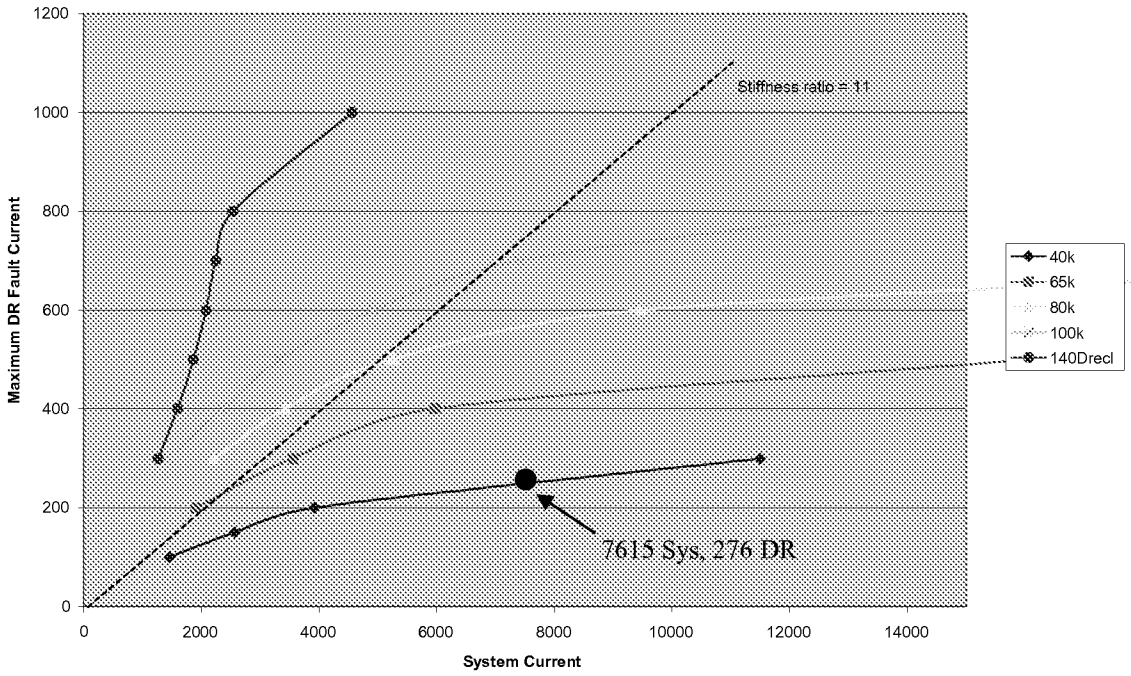

Figure H-1. Issue 1 – Maximum DR fault current for no recloser/fuse operation

Appendix H.2 EEI Issue 1 – Reduced Protective Device Sensitivity

For EEI Issue 1, the tables show the maximum DR size and associated currents.

Table H-7. EEI Issue 1 – Maximum DR Size on DC 9795 Pioneer

	DR Size (MVA)	DR Fault Current (A)	System Fault Current (A)	Total Fault Current (A)
Line-to-ground at Node 17	5.3	956	2,013	2,967
Three-phase at Node 17	80	4,464	1,943	6,406
Line-to-ground at Node 57	See Note	0	1,580	1,580
Three-phase at Node 57	10	571	1,966	2,538

Note: At Node 57, L-G fault current is less than 2,000 A with no DR current.

Table H-8. EEI Issue 1 – Maximum DR Size on DC 326 Argo

	DR Size (MVA)	DR Fault Current (A)	System Fault Current (A)	Total Fault Current (A)
Three-phase at Node 15	2.5	407	1,990	2,391
Three-phase at Node 19	See Note	0	1,786	1,786

Note: At Node 19, three-phase fault current is less than 2,000 A with no DR current.

Appendix H.3 EEI Issue 2 – Nuisance Fuse Blowing Because of DR Fault Current

Table H-9. EEI Issue 2 – Near-End Results on DC 326 Argo

	DR Size (MVA)	Fuse Fault Current (A)	Recloser Fault Current (A)	DR Fault Current (A)	Recloser Trip Time (s)	Fuse Operation Time (s)
40k	See Note					
65k	See Note					
80k	See Note					
100k	See Note					
140k	See Note		8,416			

Note: System fault current is too high to save fuse even without DR on line. System fault current is too high for interrupting rating of V4L reclosers (6,000-A rating).

Table H-10. EEI Issue 2 – Mid-Point Results on DC 326 Argo

	DR Size (MVA)	Fuse Fault Current (A)	Recloser Fault Current (A)	DR Fault Current (A)	Recloser Trip Time (s)	Fuse Operation Time (s)
40k	See Note					
65k	See Note					
80k	See Note					
100k	See Note					
140k	2 MVA	3,858	2,528	1,503	0.03	0.04

Note: System fault current is too high to save fuse even without DR.

Table H-11. EEI Issue 2 – Far-End Results on DC 326 Argo

	DR Size (MVA)	Fuse Fault Current (A)	Recloser Fault Current (A)	DR Fault Current (A)	Recloser Trip Time (s)	Fuse Operation Time (s)
40k	0.0 – See Note	1,066	1,066	0.0	0.06	0.03
65k	0.3	1,184	1,066	180	0.06	0.06
80k	1.0	1,507	1,066	601	0.06	0.07
100k	2.0	2,032	1,066	1,202	0.06	0.06
140k	3.7	2,990	1,066	2,224	0.06	0.07

Note: System fault current is too high to save 40k fuse even without DR on line. Cooper Power Publication R240-30-3 page 7 [2] shows the 40k fuse is not listed as a fuse selective with a 140-A recloser.

Table H-12. EEI Issue 2 – Near-End Results on DC 9795 Pioneer

	DR Size (MVA)	Fuse Fault Current (A)	Recloser Fault Current (A)	DR Fault Current (A)	Breaker Trip Time (s)	Fuse/Recloser Operation Time (s)
40k	See Note					
100k	See Note					
140k	See Note		7,705			

Note: System fault current is too high to save fuse even without DR on line. System fault current is too high for interrupting rating of V4L recloser (6,000-A rating).

Table H-13. Mid-Point Results on DC 9795 Pioneer

	DR Size (MVA)	Fuse Fault Current (A)	Recloser Fault Current (A)	DR Fault Current (A)	Recloser Trip Time (s)	Fuse Operation Time (s)
40k	See Note					
65k	See Note					
80k	See Note					
100k	See Note					
140k	See Note	4,374	3,758	650	0.03	0.04

Note: Fault current in this area is too high for the recloser to save these fuses unless the fuse is protecting a long lateral and the fault is near the end of the lateral. The fault would have to be nearly 5,000 feet away (down the lateral) from the fuse for the recloser to marginally save the 100k fuse.

Table H-14. EEI Issue 2 – Far-End Results on DC 9795 Pioneer

	DR Size (MVA)	Fuse Fault Current (A)	Recloser Fault Current (A)	DR Fault Current (A)	Recloser Trip Time (s)	Fuse Operation Time (s)
40k	See Note					
65k	See Note					
80k	See Note					
100k	1.0	2,566	2,367	219	0.03	0.04
140k	8.0	4,016	2,366	1,748	0.03	0.04

Note: Fault current in this area is too high for the recloser to save these fuses unless the fuse is protecting a long lateral and the fault is near the end of the lateral. The fault would have to be nearly 5,000 feet away (down the lateral) from the fuse for the recloser to marginally save the 100k fuse.

Appendix H.4 EEI Issue 15 – Faults Within the DR Zone

Table H-15. Faults Within a DR Zone

Condition	Total Fault Current	DR Contribution	System Fault Contribution
No DR on	5,011 A @ 480 V	0	181 A @ 13.2 kV
DR 1 on, DR2 off	5,033 A @ 480 V	18 A @ 13.2 kV	164 A @ 13.2 kV
DR 2 on, DR 1 off	5,338 A @ 480 V	2,181 A @ 480 V	115 A @ 13.2 kV

DR 1: size = 2 MVA, X´d = 0.2 pu on own base
DR 2: size = 2 MVA, X´d = 0.2 pu on own base
13.2-kV–480-V transformer: size = 1 MVA , 5.75% Z on own base
System positive sequence Thevenin impedance at DR 1 bus: 0.61172 + j1.77788 100-MVA base
Fault impedance: 0.05 Ω resistive, actual

Table H-16. EEI-NEMA Type K Fuse Links

Protecting Fuse link Amperes	Protected Link Amperes							
	30k	40k	50k	65k	80k	100k	140k	200k
	Maximum Fault-Current Protection Provided by Protecting Link – Amperes							
20k	500	1,100	1,700	2,200	2,800	3,900	5,800	9,200
25k		660	1,350	2,200	2,800	3,900	5,800	9,200
30k			850	1,700	2,800	3,900	5,800	9,200
40k				1,100	2,200	3,900	5,800	9,200
50k					1,450	3,500	5,800	9,200
65k						2,400	5,800	9,200
80k							4,500	9,200
100k							2,400	9,100
140k								4,000

This table shows maximum values of fault currents at which EEI-NEMA Type K fuse links will coordinate with each other. The table is based on maximum clearing-time curves FL2B for protecting links and 75% of minimum melting–time curves FL1B for protected links.

Appendix H.5 EEI Issue 16 – Isolate DR for Upstream Fault

Table H-17. EEI Issue 16 – Near-End Results on DC 326 Argo

Existing Fuse-Gen Combination	Maximum Added Generator Size (MVA)	Total Recloser Fault Current (A)	Existing DR Fault Current (A)	Added DR Fault Current (A)	Recloser Trip Time (s)	Fuse Operation Time (s)
40k–0.5-MVA gen	1.3	1,082	300	782	0.52	0.50
40k–1-MVA gen	3.5	2,705	601	2,104	0.14	0.14
40k–3-MVA gen	Greater than 10 MVA	7,810 See Note	1,803	6,007	0.08	0.03
80k–0.5-MVA gen	0.3	481	300	180	2.99	3.02
80k–1-MVA gen	0.75	1,052	601	451	0.57	0.55
80k–3-MVA gen	Greater than 10 MVA	7,810 See Note	1,803	6,007	0.08	0.07

Note: The added DR must be greater than 10 MVA for the 80k or 40k fuse at an existing DR of 3 MVA. Currents and times are for a 10 MVA added DR with existing 3 MVA DR.

Table H-18. EEI Issue 16 – Mid-Point Results on DC 326 Argo

Existing Fuse-Gen Combination	Maximum Added Generator Size (MVA)	Total Recloser Current (A)	Existing DR Fault Current (A)	Added DR Fault Current (A)	Recloser Trip Time (s)	Fuse Operation Time (s)
40k–0.5-MVA gen	1.3	1,082	300	782	0.52	0.50
40k–1-MVA gen	3.5	2,705	601	2,104	0.14	0.14
40k–3-MVA gen	Greater than 10 MVA	7,809 See note	1,802	6,007	0.08	0.03
80k–0.5-MVA gen	0.3	481	300	180	2.99	3.02
80k–1-MVA gen	0.75	1,052	601	451	0.57	0.55
80k–3-MVA gen	Greater than 10 MVA	7,809 See note	1,802	6,007	0.08	0.07

Note: The added DR must be greater than 10 MVA for the 80k or the 40k fuse at an existing DR of 3 MVA. Currents and times are for a 10 MVA added DR with existing 3 MVA DR.

Table H-19. EEI Issue 16 – Far-End Results on DC 326 Argo

Existing Fuse-Gen Combination	Maximum Added Generator Size (MVA)	Total Recloser Current (A)	Existing DR Fault Current (A)	Added DR Fault Current (A)	Recloser Trip Time (s)	Fuse Operation Time (s)
40k–0.5-MVA gen	1.3	1,082	300	782	0.52	0.50
40k–1-MVA gen	3.5	2,705	601	2,104	0.14	0.14
40k–3-MVA gen	Greater than 10 MVA	7,809 See note	1,802	6,007	0.08	0.03
80k–0.5-MVA gen	0.3	481	300	180	2.99	3.02
80k–1-MVA gen	0.75	1,052	601	451	0.57	0.55
80k–3-MVA gen	Greater than 10 MVA	7,809 See note	1,802	6,007	0.08	0.07

Note: The added DR must be greater than 10 MVA for the 80k or the 40k fuse at a DR of 3 MVA. Currents and times are for a 10 MVA added DR with existing 3 MVA DR.

Table H-20. EEI Issue 16 – Near-End Results on DC 9795 Pioneer

Existing Fuse-Gen Combination	Maximum Added Generator Size (MVA)	Total Recloser Current (A)	Existing DR Fault Current (A)	Added DR Fault Current (A)	Recloser Trip Time (s)	Fuse Operation Time (s)
40k–1-MVA gen	3.1	896	219	678	1.02	1.00
40k–3-MVA gen	12	3,276	656	2,621	0.12	0.12
40k–5-MVA gen	More than 20	5,456 See Note 1	1,092	4,364	0.08	0.05
80k–1-MVA gen	0.3	284 See Note 2	218	66	10.53	16.45
80k–3-MVA gen	2.2	1,136	656	481	0.45	0.46
80k–5-MVA gen	5	2,186	1,093	1,093	0.17	0.16

Note 1: To trip the recloser before the fuse blows, this scenario requires more current than the recloser is capable of interrupting. This scenario is not practical on an actual system. The currents and times shown are for a 20-MVA additional DR that supplies a fault current of 4,364 A.

Note 2: Current through the recloser must be reduced to a level below the recloser minimum trip level. The currents and times shown are for a 0.3-MVA generator. A 0.2-MVA generator would not supply enough current to cause the recloser to trip at all. Less than 265 A will flow through the recloser with the 0.2-MVA DR added.

Table H-21. EEI Issue 16 – Mid-Point Results on DC 9795 Pioneer

Existing Fuse-Gen Combination	Maximum Added Generator Size (MVA)	Total Recloser Current (A)	Existing DR Fault Current (A)	Added DR Fault Current (A)	Recloser Trip Time (s)	Fuse Operation Time (s)
40k–1-MVA gen	3.2	884	210	673	1.07	1.09
40k–3-MVA gen	12	2,852	573	2,279	0.14	0.15
40k–5-MVA gen	More than 23 See Note 2	4,719	851	3,868	0.09	0.08
80k–1-MVA gen	0.3	281 See Note 1	216	65	11.0	18.42
80k–3-MVA gen	2.2	1,085	626	459	0.52	0.51
80k–5-MVA gen	5	1,997	1,000	997	0.19	0.19

Note 1: Current through the recloser must be reduced to a level below the recloser minimum trip level. The currents and times shown are for a 0.3-MVA generator. A 0.2-MVA generator would not supply enough current to cause the recloser to trip at all. Less than 265 A will flow through the recloser with the 0.2-MVA DR added.

Note 2: To trip the recloser before the fuse blows, this scenario requires more current than the recloser is capable of interrupting. This scenario is not practical on an actual system. The currents and times shown are for a 23-MVA additional DR that supplies a fault current of 3,868 A for a total of 4,719 A through the recloser.

Table H-22. EEI Issue 16 – Far-End Results on DC 9795 Pioneer

Existing Fuse-Gen Combination	Maximum Added Generator Size (MVA)	Total Recloser Current (A)	Existing DR Fault Current (A)	Added DR Fault Current (A)	Recloser Trip Time (s)	Fuse Operation Time (s)
40k–1-MVA gen	3.2	918	218	699	0.94	1.00
40k–3-MVA gen	12	3,275	656	2,619	0.12	0.12
40k–5-MVA gen	More than 23 See Note 2	6,103	1,091	5,011	0.08	0.05
80k–1-MVA gen	0.3	284 See Note 1	219	66	10.53	16.45
80k–3-MVA gen	2.2	1,137	656	481	0.45	0.46
80k–5-MVA gen	5	2,185	1,093	1,092	0.17	0.16

Note 1: Current through the recloser must be reduced to a level below the recloser minimum trip level. The currents and times shown are for a 0.3-MVA generator. A 0.2-MVA generator would not supply enough current to cause the recloser to trip at all. Less than 265 A will flow through the recloser with the 0.2-MVA DR added.

Note 2: To trip the recloser before the fuse blows, this scenario requires more current than the recloser is capable of interrupting. This scenario is not practical on an actual system. The currents and times shown are for a 23-MVA additional DR that supplies a fault current of 3,868 A for a total of 4,719 A through the recloser.

Appendix H.6 EEI Issue 27 – Upstream Single-Phase Fault Causes Fuse Blowing

Table H-23. EEI Issue 27 – Near-End Results on DC 9795 Pioneer

Existing Fuse-Gen Combination	Maximum Added Generator Size (MVA)	Total Recloser Current (A)	Existing DR Fault Current (A)	Added DR Fault Current (A)	Recloser Trip Time (s)	Fuse Operation Time (s)
40k–1-MVA gen	2.5	1,248	357	891	0.36	0.36
40k–3-MVA gen	More than 20	7,288	954	6,335	0.08	0.06
40k–5-MVA gen	More than 20	See Note 2 7,979	1,580	6,289	0.08	0.03
80k–1-MVA gen	0.95	See Note 1 709	364	345	1.71	1.72
80k–3-MVA gen	3	2,084	1,042	1,042	0.18	0.18
80k–5-MVA gen	12	5,510	1,623	3,887	0.08	0.08

Note 1: To trip the recloser before the fuse blows, this scenario requires more current than the recloser is capable of interrupting. This scenario is not practical on an actual system. The currents and times shown are for a 20-MVA additional DR that supplies a fault current of 6,289 A.

Note 2: To trip the recloser before the fuse blows, this scenario requires more current than the recloser is capable of interrupting. This scenario is not practical on an actual system. The currents and times shown are for a 20-MVA additional DR that supplies a fault current of 6,335 A.

Table H-24. EEI Issue 27 – Mid-Point Results on DC 9795 Pioneer

Existing Fuse-Gen Combination	Maximum Added Generator Size (MVA)	Total Recloser Current (A)	Existing DR Fault Current (A)	Added DR Fault Current (A)	Recloser Trip Time (s)	Fuse Operation Time (s)
40k–1-MVA gen	2.5	1,205	345	860	0.39	0.38
40k–3-MVA gen	14	3,749	670	3,079	0.11	0.11
40k–5-MVA gen	More than 20	4,733	962	3,771	0.09	0.06
80k–1-MVA gen	1	See note 764	382	382	1.53	1.53
80k–3-MVA gen	2.5	1,708	932	776	0.22	0.22
80k–5-MVA gen	7	2,988	1,250	1,738	0.13	0.13

Note: This scenario is not practical on an actual system. The currents and times shown are for a 20-MVA additional DR that supplies a fault current of 3,771 A.

Table H-25. EEI Issue 27 – Mid-Point Results on DC 9795 Pioneer With Near Zero Branch Impedance*

Existing Fuse-Gen Combination	Maximum Added Generator Size (MVA)	Total Recloser Current (A)**	Existing DR Fault Current (A)	Added DR Fault Current (A)	Recloser Trip Time (s)	Fuse Operation Time (s)
40k–1-MVA gen	2.5	1,394	339	**860**	0.29	0.29
40k–3-MVA gen	More than 20	7,238	962	6,227	0.08	0.06
40k–5-MVA gen	More than 20	See Note 1 7817	1,589	6,228	0.08	0.06
80k–1-MVA gen	1	See Note 2 842	421	421	1.23	1.22
80k–3-MVA gen	3.5	2,404	1,112	1,293	0.16	0.16
80k–5-MVA gen	12	5,550	1,646	**1,738**	0.08	0.08

*Z1 = 0.0 + j0.0001 Z0 = 0.0 + j0.0001

**Midpoint currents slightly higher than near-end and far-end conditions because of I1 I2 support on unfaulted phases from substation. For the near-end condition, high line-to-ground fault depresses voltages on unfaulted phases. For the far-end condition, the added line impedance lowers voltages on unfaulted phases.

Note 1: To trip the recloser before the fuse blows, this scenario requires more current than the recloser is capable of interrupting. This scenario is not practical on an actual system. The currents and times shown are for a 20-MVA additional DR that supplies 6,227 A.

Note 2: To trip the recloser before the fuse blows, this scenario requires more current than the recloser is capable of interrupting. This scenario is not practical on an actual system. The currents and times shown are for a 20-MVA additional DR that supplies 6,228 A.

Table H-26. EEI Issue 27 Far-End Results on DC 9795 Pioneer

Existing Fuse/Gen Combination	Maximum Added Generator Size (MVA)	Total Recloser Current (A)	Existing DR Fault Current (A)	Added DR Fault Current (A)	Recloser Trip Time (s)	Fuse Operation Time (s)
40k–1-MVA gen	2.5	1,293	370	924	0.33	0.33
40k–3-MVA gen	More than 20	6,936	908	6,029	0.08	0.07
40k–5-MVA gen	More than 20	See Note 1 7504	1,505	5,999	0.08	0.03
80k–1-MVA gen	1	See Note 2 798	399	399	1.4	1.38
80k–3-MVA gen	3	2,061	1,031	1,030	0.18	0.18
80k–5-MVA gen	12	5,239	1,543	3,639	0.09	0.09

Note 1: To trip the recloser before the fuse blows, this scenario requires more current than the recloser is capable of interrupting. This scenario is not practical on an actual system. The currents and times shown are for a 20-MVA additional DR that supplies 6,029 A.

Note 2: To trip the recloser before the fuse blows, this scenario requires more current than the recloser is capable of interrupting. This scenario is not practical on an actual system. The currents and times shown are for a 20-MVA additional DR that supplies 5,999 A.

Appendix I: Overview of Typical Analysis Steps by Utility Protection and Planning Engineers

General Approach

The following outline will help ensure that key steps are executed in the determination of the requirements of an adequate interconnection of a DR and an EPS. Because of the nearly infinite variety of configurations and situations, a detailed list of steps cannot cover all situations. A list of steps in a process should never be a substitute for good engineering judgment. Therefore, a list of general steps is presented below to cover most situations.

1. Understand all applicable interconnection guidelines.

2. Understand corporate planning policies concerning DR development.

3. Understand the operating, protection, and power quality requirements.

4. Understand the electrical characteristics of the EPS to which the DR is being connected.

5. Understand the basic operation of the DR and the DR electrical configuration.

6. Perform studies to determine the effects of DR operation on the EPS.

7. Determine the required modifications to the DR, the EPS, and interconnecting equipment to maintain the operating, protection, and power quality requirements of the EPS with the connection of the DR. In some cases, these requirements cannot be met. It then must be determined if the DR can be connected at all or if the requirements can be modified for this case.

Detailed Approach

A more detailed approach is presented as an additional aid to the analysis process.

The protection and planning engineers should be familiar with all interconnection guidelines that apply. This will include all corporate and state-mandated requirements. Any references to IEEE 1547 apply. Any requirement not properly addressed during the planning stage of the DR interconnection facility that later requires design or actual construction revisions can be very costly to the utility and the DR.

Steps:

1. Obtain information noted in Appendix A1, "Information Required to Evaluate a Request From a Generating Customer to Install Facilities on the Distribution System."

2. Determine the DR category from the list below. The interconnection guidelines may permit a simplified interconnection for the specific case.

    - Parallel or not parallel
    - Momentary parallel only
    - Sellback or not sellback
    - Unit sizes, aggregate size, and generator type (i.e., synchronous, induction, inverter)
    - Stand-by or base-load operation.

3. As appropriate from the DR category above, model the DR in a load flow and fault analysis study tool (program) to determine the effect of the DR on fault current, load current, and voltage profile for all applicable conditions.

Protection Engineer

1. Determine if existing protective devices will be desensitized beyond permissible limits as discussed in EEI Issue 1 "Improper Coordination – Reduced Fault Detection Sensitivity." Recommend protective device modifications as required.

2. Determine if any protective devices will become overloaded because of the DR operation. Recommend protective device modifications as required.

3. Determine if any protective devices become inselective as discussed in EEI Issue 2, EEI Issue 16, and EEI Issue 27.

4. Determine if protective device operation is likely to create an islanded system fed from the DR. Make appropriate recommendations such as installing transfer tripping equipment.

5. Determine if the additional fault current contribution from the DR subjects any devices to fault current duty beyond its capability (i.e., interrupting, momentary, and fault closing ratings).

Planning Engineer

1. Determine if DR operation creates an unacceptable voltage profile on the EPS. Recommend required changes.

2. Determine if operation of the DR creates any overload situations. Recommend required changes.

Appendix J: List of Remaining Work for Future Study

- Develop penetration limit curves using phase angle for summation of system fault current and DR fault current through substation breaker. Present method assumes currents are in phase.

- Develop penetration limit curve software to include issues 1, 2, 16, and 27.

- Perform similar studies with full complement of relays at the DR. Include the operation of these relays and the effects on the system. Include IEEE Standard P1547 requirements such as over/under voltage or reverse power relays.

- Perform studies for issues 1 and 2 for line-to-ground fault conditions.

- Perform studies for issues 16 and 27 introducing fault impedance. A value of zero was used for fault impedance for this study.

- Perform studies that simulate the decreasing fault current from a synchronous generator based on Xd", Td", Xd', Td', and Xs (synchronous reactance).

- Develop low-cost standard transfer trip equipment implementation.

- Develop phase angle/torque stability method for determining islanded condition.

    - This would include the possible radio transmission of system phase angle for comparison with local phase angle.

    - This could also include the use of the TV phasing system used by Detroit Edison.

- Take actual measurements on the Pioneer and Argo circuits to verify the voltage profile and harmonic studies. A proposed project has been submitted to DOE/NREL.

Appendix K: Definitions

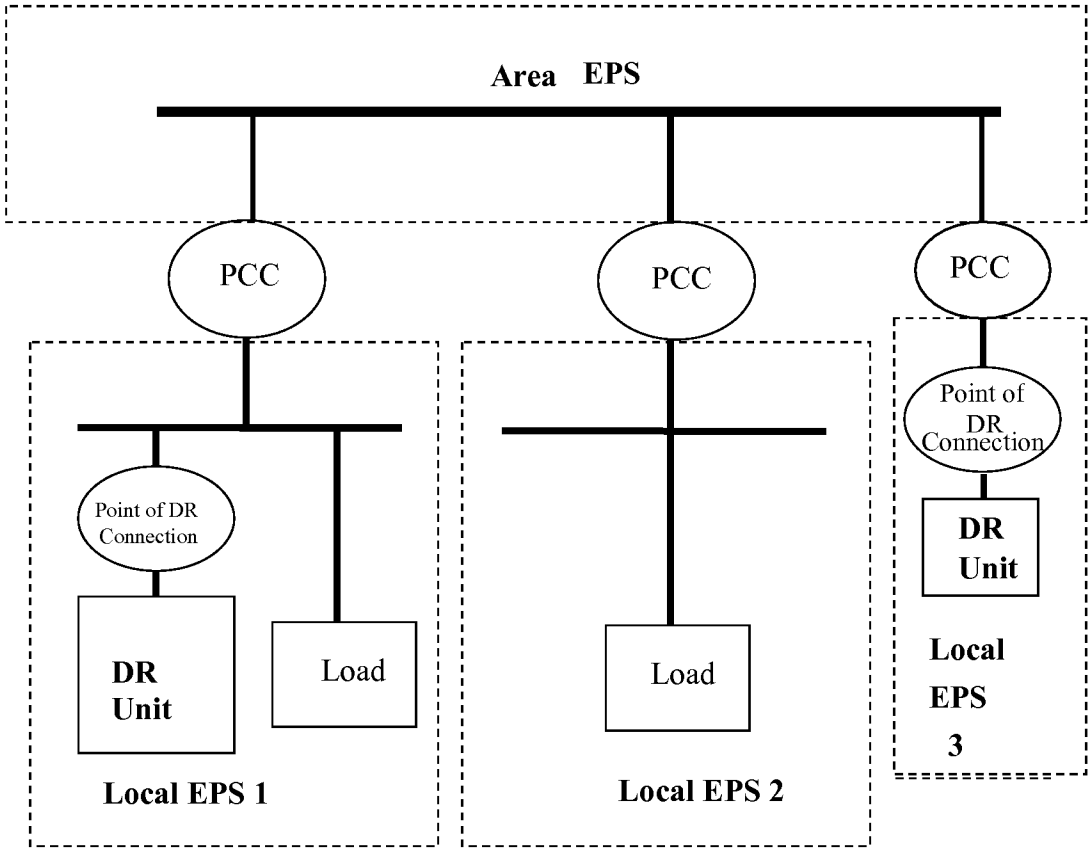

Note: Dotted lines are EPS boundaries. There can be any number of local EPSs.

Figure K-1. Relationship of Area EPS to Local EPS and DR unit

1. **Distributed generation (DG)**: electric generation facilities connected to an Area EPS through a PCC; a subset of DR.

2. **Distributed resources (DR)**: sources of electric power that are not directly connected to a bulk power transmission system. DR include both generators and energy storage technologies.

3. **DR operator**: the organization or company that is responsible for designing, building, operating, and maintaining the DR as part of the local EPS.

4. **DR zone**: the local EPS to which the DR is connected.

5. **Electric power system (EPS)**: facilities that deliver electric power to a load. (Note: This can include generation units.) See Figure K-1.

6. **Electric power system, area (Area EPS)**: an EPS that serves Local EPSs. (Note: Typically, an Area EPS enjoys benefits such as primary access to public rights-of-way, priority crossing of property boundaries, etc., and is subject to regulatory oversight.) See Figure K-1.

7. **Electric power system, local (Local EPS):** an EPS contained entirely within a single premises or group of premises. See Figure K-1.

8. **EPS**: electric power system.

9. **Point of common coupling (PCC)**: the point at which a Local EPS is connected to an Area EPS.

10. **Stiffness ratio**: the stiffness ratio is calculated at the PCC, except when there is a transformer dedicated to one customer — in which case the stiffness ratio is calculated on the high-voltage side of the dedicated transformer(s).

$$\text{stiffness ratio} = \frac{\text{SC kVA (Area EPS)} + \text{SC kVA (DR)}}{\text{SC kVA (DR)}}$$

Where:
SC kVA (Area EPS) = the short-circuit contribution in kVA of the Area EPS
and SC kVA (DR) = the short-circuit contribution in kVA of the DR.

11. **Upstream:** Electrically closer to the normal utility source for the Area EPS. Applies to radial circuits only.

12. **Downstream:** Electrically more remote from the normal utility source for the Area EPS. This term applies to radial circuits only.

Appendix L: References

1. Elmore, W.A., ed. *Protective Relay Theory and Applications*. Allentown, PA: ABB Power T&D Company Inc., 1994. ISBN 0-8247-9152-5.

2. Cooper Power Systems. *Overcurrent Protection.* R240-30-3.

3. IEEE Standards Coordinating Committee 21. *IEEE P1547 Draft 7 Draft Standard for Interconnecting Distributed Resources with Electric Power Systems*. New York: Institute of Electrical and Electronics Engineers Inc., February 2001.

4. Mason, C.R. "Transformer Protection," Chapter 11. *The Art and Science of Protective Relaying*. http://www.geindustrial.com/pm/notes/artsci/art11.pdf.

5. EPRI. *Integration of Distributed Resources in Electric Utility Distribution Systems: Distribution System Behavior Analysis for Suburban Feeder*. TR-111490. Palo Alto, CA: EPRI, November 1998.

6. EPRI. *Integration of Distributed Resources in Electric Utility Distribution Systems: Distribution System Behavior Analysis for Urban and Rural Feeders*. TR-112737. Palo Alto, CA: EPRI, November 1999.

7. Canadian Electrical Association. *Connecting Small Generators to Utility Distribution Systems*. 128 D 767. A.B. Sturton Consultants Inc. and Acres International Ltd, June 1994.

8. Stevenson, W.D. *Elements of Power System Analysis*. New York: McGraw Hill Education - Europe, 1955.

REPORT DOCUMENTATION PAGE

Form Approved
OMB NO. 0704-0188

1. AGENCY USE ONLY (Leave blank)	2. REPORT DATE	3. REPORT TYPE AND DATES COVERED
	July 2003	Subcontract Report

4. TITLE AND SUBTITLE
Distributed and Electric Power System Aggregation Model and Field Configuration Equivalency Validation Testing

5. FUNDING NUMBERS
DP03.1001
AAD-0-30605-09

6. AUTHOR(S)
M. Davis, D. Costyk, A. Narang

7. PERFORMING ORGANIZATION NAME(S) AND ADDRESS(ES)
DTE Energy Technologies
37849 Interchange Dr.
Farmington Hills MI 48335

Kinectrics, Inc.
800 Kipling Ave, KL 204
Toronto, ON, CANADA M8Z 6C4

8. PERFORMING ORGANIZATION REPORT NUMBER

9. SPONSORING/MONITORING AGENCY NAME(S) AND ADDRESS(ES)
National Renewable Energy Laboratory
1617 Cole Blvd.
Golden, CO 80401-3393

10. SPONSORING/MONITORING AGENCY REPORT NUMBER
NREL/SR-560-33909

11. SUPPLEMENTARY NOTES
NREL Technical Monitor: T.S. Basso

12a. DISTRIBUTION/AVAILABILITY STATEMENT
National Technical Information Service
U.S. Department of Commerce
5285 Port Royal Road
Springfield, VA 22161

12b. DISTRIBUTION CODE

13. ABSTRACT *(Maximum 200 words)*
This report details the research undertaken by DTE Energy Technologies, DTE Energy, and Kinectrics under contract to the National Renewable Energy Laboratory. The focus of this study was to determine the magnitude of distributed resources that can be added to a distribution circuit without causing undesirable voltage regulation, power quality, stability, or reliability conditions or equipment damage.

14. SUBJECT TERMS
distributed power; distributed resources; distributed generation; interconnection; aggregation; electric power system; DTE; Kinectrics; National Renewable Energy Laboratory; NREL

15. NUMBER OF PAGES

16. PRICE CODE

17. SECURITY CLASSIFICATION OF REPORT	18. SECURITY CLASSIFICATION OF THIS PAGE	19. SECURITY CLASSIFICATION OF ABSTRACT	20. LIMITATION OF ABSTRACT
Unclassified	Unclassified	Unclassified	UL

US007096175B2

(12) **United States Patent**
Rehtanz et al.

(10) **Patent No.: US 7,096,175 B2**
(45) **Date of Patent: Aug. 22, 2006**

(54) **STABILITY PREDICTION FOR AN ELECTRIC POWER NETWORK**

(75) Inventors: **Christian Rehtanz**, Baden-Dättwil (CH); **Valentin Bürgler**, Endingen (CH); **Joachim Bertsch**, Baden-Dättwil (CH)

(73) Assignee: **ABB Research LTD**, Zurich (CH)

(*) Notice: Subject to any disclaimer, the term of this patent is extended or adjusted under 35 U.S.C. 154(b) by 822 days.

(21) Appl. No.: **10/144,069**

(22) Filed: **May 14, 2002**

(65) **Prior Publication Data**

US 2003/0040846 A1 Feb. 27, 2003

(30) **Foreign Application Priority Data**

May 21, 2001 (EP) 01112354

(51) **Int. Cl.**
G06G 7/54 (2006.01)

(52) **U.S. Cl.** **703/18**; 700/293

(58) **Field of Classification Search** ..... 703/2, 703/18; 700/286, 293; 307/102, 20, 31, 307/38, 132 EA
See application file for complete search history.

(56) **References Cited**

U.S. PATENT DOCUMENTS

5,566,085 A 10/1996 Marceau et al.
5,625,751 A * 4/1997 Brandwajn et al. 706/20
5,638,297 A * 6/1997 Mansour et al. 700/286
5,719,787 A * 2/1998 Chiang et al. 700/293
6,202,041 B1 * 3/2001 Tse et al. 703/13

OTHER PUBLICATIONS

Chiou, et al., "Development of a Micro-processor-based Transient Data Recording System for Load Behavior Analysis", IEEE Transactions on Power Systems 8, No. 1, Feb. 1993, New York, USA, pp. 16-22.
Vu, et al., "Use of Local Measurements to Estimate Voltage-Stability Margin", IEEE 1997, pp. 318-323.
Liu, et al., "Application of synchronised phasor measurements to real-time transient stability prediction", IEEE Proc.-Gener. Transm. Distrib., vol. 142, No. 4, Jul. 1995, pp. 355-360.
Quintana, et al., "Voltage stability as affected by discrete changes in the topology of power networks", IEEE Proc.-Gener. Transm. Distrib., vol. 141, No. 4, Jul. 1994, pp. 346-352.
Karlsson, et al., "Modelling and identification of nonlinear dynamic loads in power systems", IEEE Transactions on Power Systems, vol. 9, No. 1, Feb. 1994, pp. 157-163.

* cited by examiner

Primary Examiner—Albert W. Paladini
(74) *Attorney, Agent, or Firm*—Buchanan Ingersoll PC

(57) **ABSTRACT**

A method, device and computer program product for the prediction of the stability of an electric power network, where the method is executed after a fault or contingency has occurred, and comprises the steps of (a) during a time interval in which the network is in a transient condition, determining for at least one load connected to the electric power network, at least one parameter describing an estimated steady state behavior of the load, (b) executing a load flow calculation for the electric power network using the least one parameter describing the estimated steady state behavior the at least one load, (c) determining, if the load flow calculation indicates stability has a solution, that a future stability of the electrical power network exists, or, if the load flow calculation indicates instability does not have a solution, that a future stability of the electrical power network does not exist.

11 Claims, 2 Drawing Sheets

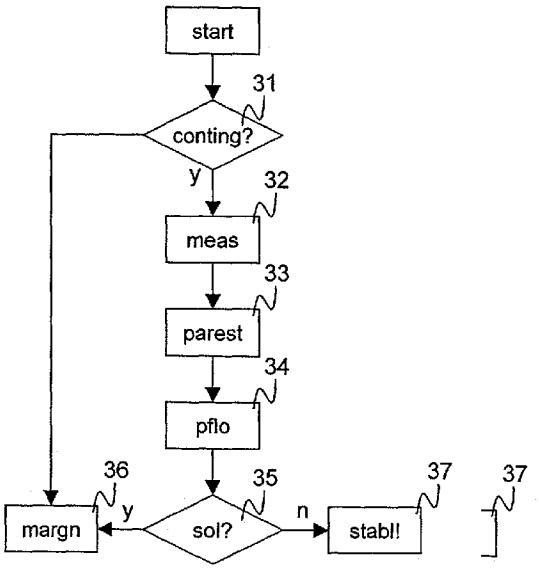

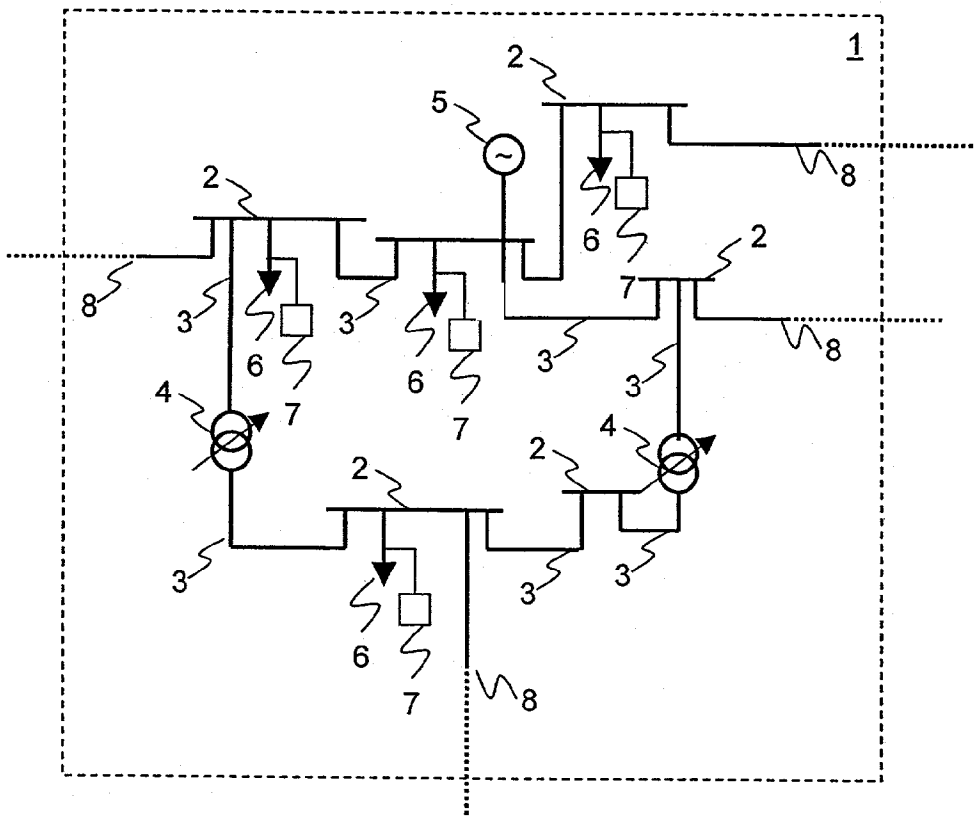

Fig. 1

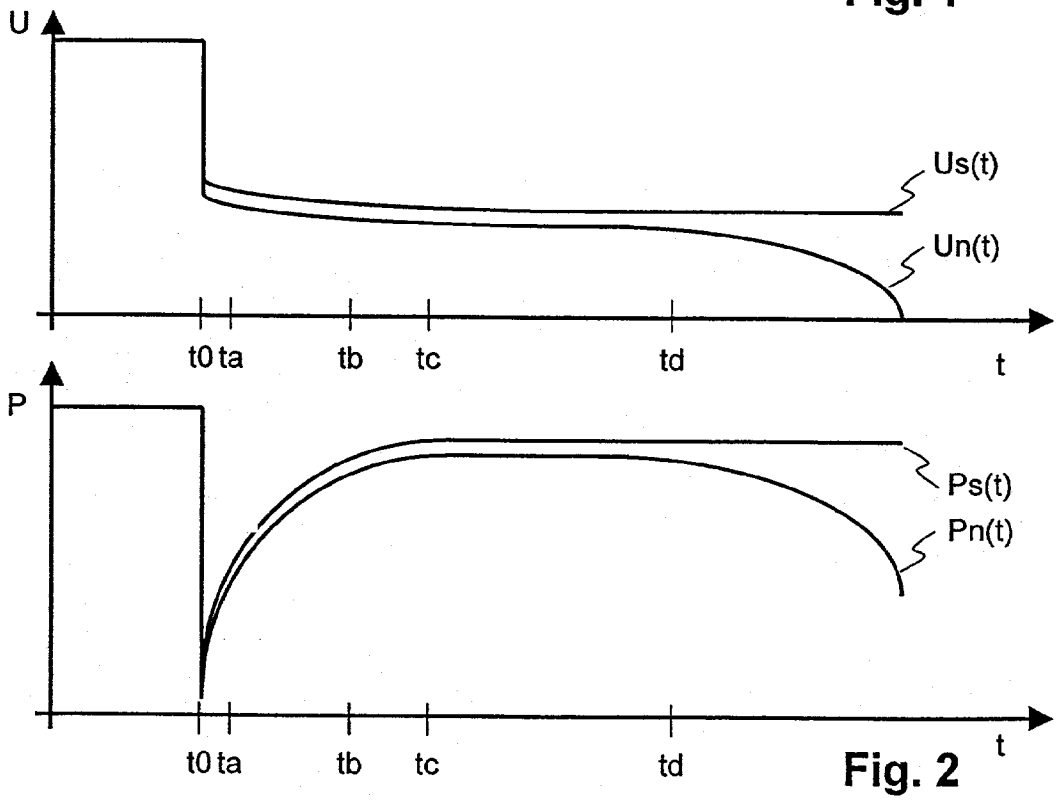

Fig. 2

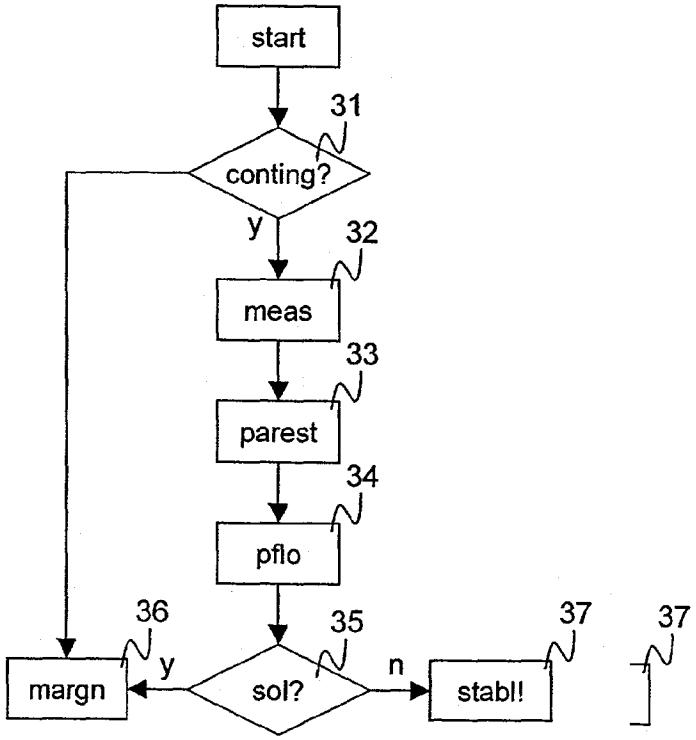
start
31
conting?
y
32
meas
33
parest
34
pflo
36
35
37
37
margn
y
sol?
n
stabl!

Fig. 3

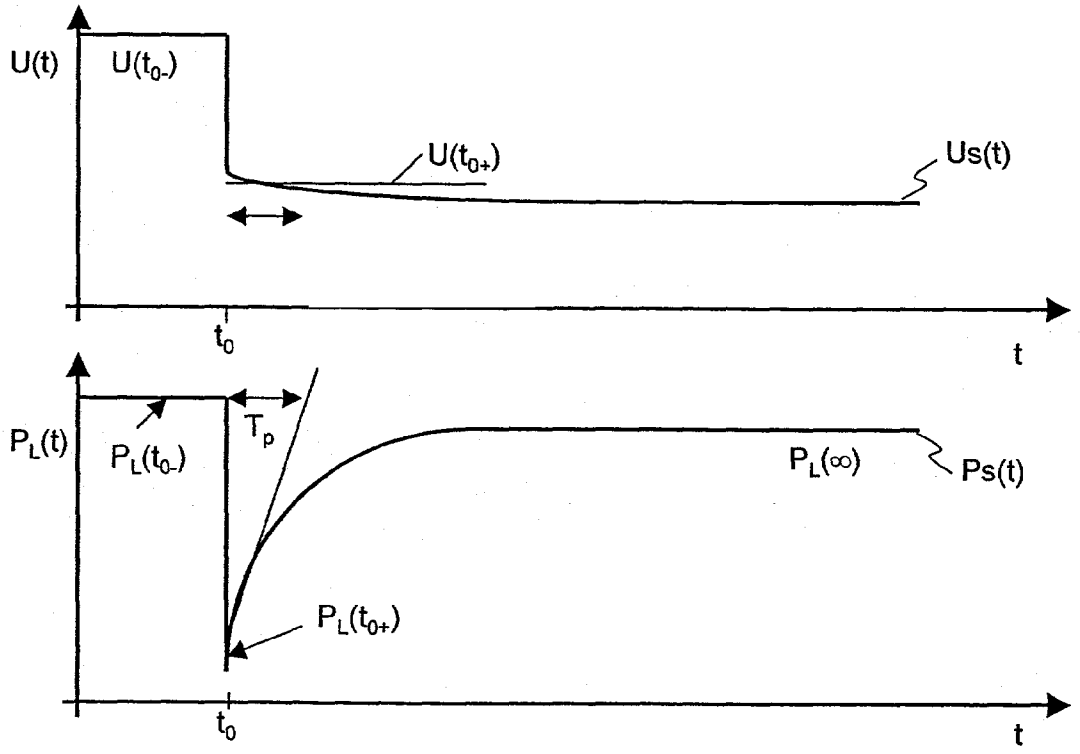
U(t)
U(t0-)
U(t0+)
Us(t)
t0
t
PL(t)
PL(t0-)
Tp
PL(∞)
Ps(t)
PL(t0+)
t0
t

Fig. 4

STABILITY PREDICTION FOR AN ELECTRIC POWER NETWORK

FIELD OF THE INVENTION

The invention relates to the field of electric power transmission networks, and, more particularly, to a method, computer program product and device for the prediction of the stability of an electric power network as described in the preamble of claims **1**, **10** and **11**, respectively.

BACKGROUND OF THE INVENTION

An electric power transmission network comprises high-voltage tie lines and substations for transforming voltages and for switching connections between lines. Loads and power generating plants are connected to the network. An important issue when controlling power generation and load flow is to keep the network stable, i.e. to avoid voltage collapse and swings. Existing SCADA (Supervisory control and data acquisition) systems provide estimates about the stability of a network. However, such an estimate is based on the assumption that the network is in a steady state condition. Consequently, it is not valid if it is obtained during a transient condition, i.e. in the time after a fault or contingency has occurred and before the network is back in a seemingly steady state. It often happens that the network seems to be in a steady state after a contingency, however, an instability caused by the contingency develops unnoticed. The instability is detected by the SCADA system only when the network voltages are severely affected. At this point in time, remedial actions such as load shedding must be drastic, if complete collapse of the network is to be avoided. It therefore is desirable to obtain, after a contingency is detected, an early estimate of the future stability of a network, such that remedial actions can be executed before the effects of the instability become too large.

U.S. Pat. No. 5,638,297 shows a method of on-line transient stability assessment of an electrical power system. A computer model is used to simulate an effect of an artificially introduced study contingency. The simulation uses a step-by-step integration method and predicts future effects of the contingency on the network, in particular on network stability. However, the method requires a full model of dynamic behavior of the network and a significant computational effort for the simulation. The algorithm uses pre-calculations that are made before a given contingency occurs. If a contingency was not pre-calculated or if cascaded contingencies occur, the algorithm fails. If applied to voltage stability, the algorithm would fail as well for cascaded contingencies since an exhaustive pre-calculation of combinations of contingencies is not practicable.

SUMMARY OF THE INVENTION

It is therefore an object of the invention to create a method and computer program product for the prediction of the stability of an electric power network of the type mentioned initially, which overcome the disadvantages mentioned above.

These objects are achieved by a method, computer program product and device for the prediction of the stability of an electric power network according to the claims **1**, **10** and **11**.

In the method for the prediction of the stability of an electric power network according to the invention, the method is executed after a contingency has occurred, and comprises the steps of

a) during a time interval in which the network is in a transient condition, determining, for at least one load connected to the electric power network, at least one parameter describing an estimated steady state behavior of the load,

b) executing a load flow calculation for determining a steady state equilibrium of the electric power network, using the least one parameter describing the estimated steady state behavior the at least one load,

c) determining, if the load flow calculation indicates stability, i.e. if it has a solution, that a future stability of the electrical power network exists, or, if the load flow calculation indicates instability, i.e. if it does not have a solution, that a future stability of the electrical power network does not exist.

The inventive method thus determines, during a transient state of the network, one or more parameters relevant to the network's future steady state or stationary behavior. The future steady state equilibrium of the dynamic system is then determined without any need for a simulation over time. Modeling and computation effort is therefore reduced significantly, as compared to a dynamic simulation of network behavior, but nevertheless the behavior of the complete system around the equilibrium point is determined. Since calculations are necessary only after a contingency occurs, the algorithm is independent from any pre-calculations and is applicable to any contingency or combination of contingencies.

In a preferred embodiment of the invention, the load flow calculation is a so-called extended load flow calculation that includes steady state behavior of a variety of elements of the power system, in particular of under load tap changers and of power generators.

The computer program product for the prediction of the stability of an electric power network according to the invention is loadable into an internal memory of a digital computer, and comprises computer program code means to make, when said computer program code means is loaded in the computer, the computer execute the method according to the invention. In a preferred embodiment of the invention, the computer program product comprises a computer readable medium, having the computer program code means recorded thereon.

The device for the prediction of the stability of an electric power network after a contingency has occurred comprises

a) means for storing values of voltage and power measurements made at the load,

b) means for detecting an occurrence of a contingency,

c) means for determining at least one parameter, where the parameter describes an estimated steady state behavior of the load, from the stored voltage and power values and from measurement values that are obtained when the network is in a transient condition after the contingency has occurred.

Further preferred embodiments are evident from the dependent patent claims.

BRIEF DESCRIPTION OF THE DRAWINGS

The subject matter of the invention will be explained in more detail in the following text with reference to preferred exemplary embodiments which are illustrated in the attached drawings, in which:

FIG. **1** schematically shows part of an electrical power transmission network;

FIG. **2** shows a time history with typical values of voltage and power flow at a load connection after a contingency occurs;

FIG. **3** shows a flow diagram of the inventive method; and

FIG. **4** shows a time history of voltage and power flow and its relation to parameters of a load model.

The reference symbols used in the drawings, and their meanings, are listed in summary form in the list of reference symbols. In principle, identical parts are provided with the same reference symbols in the figures.

DETAILED DESCRIPTION OF THE INVENTION

FIG. **1** schematically shows a part **1** of an electric power network. Buses **2** are connected by lines **3** which may comprise under load tap changers (ULTC) **4**. An under load tap changer is a transformer whose voltage ratio may be switched in discrete steps. Also connected to buses **2** are generators **5** such as single generators or complete power plants and loads **6**. Loads **6** are consumers of power or other networks, e.g. at a lower voltage level. Each load **6** is connected to the network by a load connection which is, for example a feeder leading to a power consumer. When the section of electric power network under consideration is a high voltage transmission network, the feeder may lead to a high of medium voltage distribution network. At least one phasor measurement unit **7** is connected to a bus **2** or to a feeder. Interface lines **8** lead to neighboring networks.

The phasor measurement unit **7** measures phasors of voltage at and current through an electric connection such as a feeder or line or busbar. The phasor data represents a phasor and may be a polar number, the absolute value of which corresponds to either the real magnitude or the RMS value of a quantity, and the phase argument to the phase angle at zero time. Alternatively, the phasor may be a complex number having real and imaginary parts or the phasor may use rectangular or exponential notation. Phasors may be used to represent quantities such as the voltage, current, power or energy associated with a phase conductor or an electronic circuit. By contrast, conventional sensing devices used in power networks generally measure only scalar, average representations, such as the RMS value of a voltage, current etc. In a three-phase power system whose phases are in a balanced state, phasors from all three phases may be represented by a single common phasor.

The phasor measurement units **7** are used for three reasons. First, the measurements are taken with short time intervals of approximately 20 to 100 milliseconds. This gives a view on the system with a high resolution over time. Second, the provided phasor information requires an installation of phasor measurement units **7** at only about each third or forth station or bus for an area that is to be observed. Third, synchronized time-triggered and time-stamped measurements from the entirety of phasor measurement units **7** together form a dynamic snapshot of the system state. The first reason is related to the parameter determination of the load parameter, the second and third reason are related to the dynamic observation of the critical area and the determination of the equilibrium of the system model.

FIG. **2** shows a time history over time t with typical values of voltage U and power flow P at a load connection after a contingency occurs. A contingency is an unexpected event such as, for example, a line **3** tripping, a generator **5** tripping, an extreme change in load or a feeder opening. While FIG. **2** shows the effects of an unexpected voltage drop at a load connection, similar effects occur for voltage increases, and the invention is applicable as well.

At time t**0**, the contingency occurs, causing the voltage U to drop. Such unexpected voltage drops or increases typically are in the range of a few percent to 10% percent of a nominal voltage. The voltage drop causes the power flow P to the load **6** to decrease as well. Due to the decrease in power P, local controllers of the load **6** try to draw more power in order to reach a nominal power consumption or operating point. This increase in power flow P in turn causes the voltage U to drop even more. At time tc the values for voltage U and power P have reached a seemingly steady state. However, only one of the two curves corresponds to a steady state while the other one corresponds to an unstable state, due to long term dynamic effects of the load, the ULTCs and the generators. "Long-term" in this context refers to time ranges of several seconds to several tens or hundreds of seconds.

If the state is stable, the voltage U and power P remain approximately constant, as shown by the trajectories Us(t) and Ps(t). At a later time, an increase in generated power or a reduction of power consumption will cause the voltage U and power P to return to nominal values. In the unstable case, after a time td the voltage U and with it the power P will further decrease, as shown by the trajectories Un(t) and Pn(t). Whether the situation is stable or unstable is a property of the entire network, not just of the load **6** itself. However, the dynamic behavior of each load **6** influences the network and its stability. It therefore is necessary to analyze the interplay between the network and all loads, as well as generators. This interplay between the loads, the generators and the network is described with a set of static equations called load flow equations or power flow equations. These equations express the relation between the voltages at the connections of the elements and the power they consume or generate. Methods to solve such an equation system are well known as "load flow calculation" or "load flow analysis" and use, for example a Newton-Raphson algorithm.

In order to determine the stability of the network, said equations are combined and the resulting set of equations is solved using load flow analysis. If the power network comprises ULTCs **4**, their controlled behavior is described by step functions that represent a voltage ratio as a function of one of the transformer voltages. The extended load flow analysis in this case incorporates a representation or model of the ULTCs behavior, as shown in "Voltage Stability of Electric Power Systems", Vournas, C.; Van Cutsem, T., Kluwer Academic Publishers, Boston, 1998. The load flow analysis uses an optimization technique that determines a steady state solution that satisfies all equations including the ULTC equations.

Modeling of a generator **5** or power generating unit such as a power plant may be simplified to the point that a behavior of a generator **5** is described only by the maximum reactive power that it is allowed to generate continuously, i.e. in a steady state. These values are known in advance from the operational diagram of the generator. The maximum influences the load flow calculation by giving a boundary condition on the space of solutions to the load flow problem. In a preferred embodiment of the invention, the voltage controller of generator **5** is represented by the static relationship between generator power output and generator voltage. This represents the steady state part of a voltage controller and excitation system of the generator model.

The behavior of neighboring networks connected to the network under consideration by interface lines **8** is modeled by static or dynamic relationships such as constant power or

current on the interface line, representation as constant impedance or as a Thevenin equivalent of the neighboring network.

The resulting equation system contains the load flow equations, extended by steady state or static representations of all the elements of the power system which influence the stability. The solution of this equation system is a stable equilibrium and therefore a steady state solution of a complete dynamic representation of the power system. Therefore it is valid to determine the future equilibrium or steady-state solution with the load flow calculation with the embedded static models instead of executing a dynamic simulation over time. This solution of the extended set of equations is called extended load flow calculation.

If the load flow calculation reaches a solution, then the network is stable, if not, then the network is unstable. The load flow calculation requires a number of network, generator and load parameters. Some of these are constant, some may be determined prior to a contingency, but some remain unknown at the time the contingency occurs. In particular, the voltage/power characteristics of the loads **6** change slowly, that is with time constants in the range of hours. These characteristics can, in general, not be measured or identified as long as the power network is in its normal and nominal steady state, since unchanging values do not provide enough information. However, since the contingency causes changes in voltage U and power P to each of the loads **6**, it is possible to identify load parameters for each load **6** immediately after a contingency occurs.

According to the invention, measurement data obtained in a transient phase between t**0** and tc is used to identify the load parameters. A further aspect of the invention is that only load parameters relevant to a static or stationary behavior of each load **6** are identified. Since these parameters change only slowly with respect to the seconds or minutes between the contingency at t**0** and the manifestation of the instability at td, the parameters are used in a static load flow calculation to determine the stability of the network, i.e. of the part of the network under consideration. The stability can therefore be assessed long before an instability manifests itself visibly, as it does after td.

FIG. **3** shows a flow diagram of the inventive method. In step **31**, voltages and currents at load connections are measured by phasor measurement units **7**, each of which is associated to one load **6** whose behavior is to be identified. From these measurements, steady state absolute voltages U_0, steady state active power P_0 and steady state reactive power Q_0 are continuously updated. Network topology is updated from a known or measured state of switches and breakers. If no contingency is detected, execution continues in step **36**, where a stability margin is computed in a known fashion. When a contingency is detected by known means, e.g. when a large and fast voltage change occurs at at least one load **6**, execution proceeds to step **32**. In step **32**, a sequence of voltage and power values is measured at the load connections. Based on these measured values, in step **33**, for each load **6** whose behavior is to be identified, at least one parameter describing the stationary behavior of the load is estimated. In step **34**, the extended load flow calculation is performed, using among others said load parameters. In step **35** it is checked whether the extended load flow calculation has arrived at a solution. If it has, then in step **36** a stability margin is computed on the base of the found solution in a known fashion, taking also into account the steady-state models which are included in the extended load flow calculation. The stability margin is optionally communicated to an operator. If it has not, then in step **37** remedial actions such as shedding loads are taken in order to achieve stability. Other remedial actions are, for example reactive power increase, blocking of ULTC-tapping, control of FACTS-devices, Automatic Generation Control (AGC), Secondary Voltage Control, change of voltage set values of controllable devices or controlled islanding.

In a preferred embodiment of the invention, the load model implicitly used in step **33** is a so-called Hill and Karlsson model, described in "Modelling and identification of nonlinear dynamic loads in power systems"; Hill, D. J. and Karlsson, D., IEEE Trans. on Power Systems, Vol. 9, No. 1, pp. 157–163, 1994. The model describes the behavior of a load as seen from a feeder of a high voltage system by a differential equation

$$-T_p\dot{P} + P_0\left(\frac{U}{U_0}\right)^{\alpha_S} + \frac{P_0}{U_0}\dot{U}\ T_p\ \alpha_t\left(\frac{U}{U_0}\right)^{\alpha_S - 1} = P \tag{1}$$

The equation gives the dynamic relation between the voltage U at and the power P through a connection to the load. U_0 and P_0 are a nominal voltage and nominal active power, respectively, as measured prior to the contingency. It is assumed that P_0 does not change stepwise and remains essentially unchanged for the purposes of the invention, i.e. during and after the transient phase caused by a contingency. $\dot{P}$ and $\dot{U}$ are time derivatives and are preferably determined as mean values of gradients determined from a series of measurement points. Voltage values considered in the context of the invention are absolute voltage values of voltage phasors representing a three-phase system. Parameters are a time constant T_P and exponents α_S and α_t. These parameters are to be determined, since they change during a day and over the seasons. Steady state behavior is determined by α_S. Typical values for α_S can be expected to lie between approximately 0 and 2 for active power. If the same analysis is done for the reactive power part of the load, typical values of a corresponding exponent β_S are 0 to 4. T_p is typically between 20 and 300 seconds and α_t between 0 and 5. Detailed measured values are given in the reference on the Hill and Karlsson Model cited above.

In a first preferred embodiment of the invention, the parameters are determined as follows: For a step change in voltage, the solution of Eq. (1) is, for t>t**0**, given by

$$P_L(t) = P_L(\infty) + [P_L(t_{0+}) - P_L(\infty)] \cdot e^{\frac{-(t-t_0)}{T_p}} \tag{2}$$

where $P_L(t_{0+})$ is the power immediately after the contingency. In a preferred embodiment of the invention, $P_L(t_{0+})$ is determined as the lowest power value measured after a contingency. $P_L(\infty)$ is a steady state power value reached after a transient phase.

FIG. **4** shows time histories of voltage U and power P representing a step change in voltage followed by a trajectory according to Eq. (2). $U(t_{0-})$ and $P_L(t_{0-})$ are the voltage and the power prior to the contingency occurring at time t_0. A gradient of $P_L(t)$ determines the time constant T_p. The desired value $P_L(\infty)$ can now be determined by solving equation (2) for $P_L(\infty)$ with the measured load $P_L(t)$ at the time t. This value can be updated over time.

$U(t_{0+})$ is the voltage after the contingency. From the steady state part of (1), i.e. by setting $\dot{P}$ and $\dot{U}$ to zero, it follows that

$$\frac{P_L(\infty)}{P_L(t_{0-})} = \left(\frac{U(t_{0+})}{U(t_{0-})}\right)^{\alpha_S} \tag{3}$$

since $P_L(t_{0-})=P_0$ and $U(t_{0-})=U_0$, α_S is determined by Eq. (3). From Eq. (1) it can be seen that α_S influences a stationary part of the expression, whereas α_t is associated with a dynamic part and becomes irrelevant when derivatives over time are zero.

In summary, in the first preferred embodiment of the invention, α_S is determined by the following steps:

1. From the power $P_L(t_{0+})$ immediately after the contingency and a sequence of Power measurements $P_L(t)$, determine the time constant T_p and $P_L(\infty)$ from Eq. (2).

2. From $P_L(\infty)$, a measurement of $U(t_{0+})$ and power and voltage values made prior to the contingency, determine α_S from Eq. (3).

For practical purposes, $U(t_{0+})$ is determined as a minimum of values obtained by filtering voltage measurements that are measured from immediately after the contingency has been detected for approximately 1 to 5 seconds. For example, a sliding window is moved over the measurements, for every window position, an average of values in the window is determined as a filtered value, and a minimum of filtered values is taken to be $U(t_{0+})$.

The load flow calculation uses

either the constant value $P_L(\infty)$ for the load flow, which gives approximate results, or

the expression

$$P_L = P_L(t_{0-})\left(\frac{U}{U(t_{0-})}\right)^{\alpha_S} \tag{4}$$

derived from Eq. (3), which determines the load flow P in function of the voltage U measured immediately after the contingency, giving more accurate results.

The above method showed how to determine load characteristics for active power after a contingency. Characteristics describing reactive power consumption of the load are determined in the same fashion, replacing in all the measurements and equations mentioned above the active power P by reactive power Q. A variable β_S corresponding to α_S is then determined which determines the steady state relationship between voltage and reactive power.

In a second preferred embodiment of the invention, not just a single pair but a plurality of voltage and power measurements is used to estimate α_S. In a sliding window of measurements, a series of measurements of voltage U and power P as well as their derivatives are obtained. For more than three measurement points, an over-determined set of nonlinear equations, i.e. several times Eq. (1), results, where each instance of Eq. (1) holds for a different measurement point. The set of equations can be solved for the parameters, in particular for α_S.

In a third preferred embodiment of the invention, Eq. (1) is rewritten as

$$-x_1\dot{P} + P_0\,x_2 + \frac{P_0}{U_0}\dot{U}\,x_3 = P \tag{5}$$

where the variable of interest α_S is contained in

$$x_2 = \left(\frac{\overline{U}}{U_0}\right)^{\alpha_S} \tag{6}$$

where $\overline{U}$ is a mean of voltages measured in the sliding measurement window. Assuming the voltage U to be constant for the purpose of transforming Eq. (1) to the form of Eq. (5) is an approximation, and is only valid for small changes in the voltage U within the sliding window. Since the change in voltage U decreases after the contingency, the accuracy of the approximation increases from time t**0** to tb. The measurements in the sliding window, made at times t**1**, t**2**, t**3**, . . . tn define an over-determined linear system of equations

$$A\cdot x = b \text{ with } A = \begin{bmatrix} -\dot{P}(t_1) & P_0 & \frac{P_0}{U_0}\dot{U}(t_1) \\ -\dot{P}(t_2) & P_0 & \frac{P_0}{U_0}\dot{U}(t_2) \\ -\dot{P}(t_3) & P_0 & \frac{P_0}{U_0}\dot{U}(t_3) \\ \cdots & \cdots & \cdots \\ -\dot{P}(t_n) & P_0 & \frac{P_0}{U_0}\dot{U}(t_n) \end{bmatrix} b = \begin{bmatrix} P(t_1) \\ P(t_2) \\ P(t_3) \\ \cdots \\ P(t_n) \end{bmatrix}$$

which can be solved e.g. by the least squares approach. From x_2, α_S is immediately determined.

In the preferred embodiments of the invention, measurement values providing good estimates of the steady state parameters are obtained starting at a time ta which lies from ca. 5 to 15 seconds after the time t**0** at which the contingency occurs, since the approximation inherent in Eqs. (5) and (6) improves with time. The short-term transients of voltage and power in the first ca. 2 to 5 seconds after the contingency must have subsided before the sliding window can start to collect data. A typical length of the sliding window is between 3 and 10 seconds. Therefore the starting time plus the sliding window results in the above values of about 5 to 15 seconds after which the first results are available.

After this time, α_S should have been estimated, so that the remaining steps of the method can be executed and enough time remains for remedial actions.

Beginning with the results from the first sliding window, the extended load flow calculation can be started. In order to increase robustness at the expense of speed, the average of several following results from the sliding window can be taken. In a preferred embodiment of the invention, averages are taken over up to approximately 5 seconds. For a continuous supervision of the stability, an average of the last results is taken for continuous calculations of stability. In order to schedule and execute stabilizing actions as soon as possible, the first results available are preferably used.

In summary, the method according to the invention comprises the steps of, after a contingency has been detected,

a) During a time interval in which the network is in a transient condition, determining for at least one load connected to the electric power network, at least one parameter α_S that describes an estimated steady state, i.e. stationary behavior of the load.

b) Executing a load flow calculation for the electric power network using the least one parameter α_S that describes the estimated steady state behavior at the at least one load. The load flow calculation is also based on values that characterize the state of the network prior to the contingency, such as power and voltage at the at least one load.

c) Determining, if the load flow calculation indicates stability, i.e. if it has a solution, that a future stability of the electrical power network exists, or, if the load flow calculation indicates instability, i.e. if it does not have a solution, that a future stability of the electrical power network does not exist.

In a preferred embodiment of the invention, the step a) of determining, for one load connected by a load connection to the electric power network, the at least one parameter describing the estimated steady state behavior of the load, comprises measuring a voltage and a power flow from phasor measurements at the load connection, where measurement intervals, i.e. the time between measurements are approximately 20 to 250 milliseconds.

In a further preferred embodiment of the invention, the load flow calculation is extended by the steady state behavior of all elements of the power system. This means that the solution of the load flow calculation is the equilibrium or steady-state solution of the full dynamic system.

A device for the prediction of the stability of an electric power network according to the invention comprises means for determining, after a contingency has occurred and during a time interval in which the network is in a transient condition, for one load associated with the device, at least one parameter that describes an estimated steady state behavior of the load. In a preferred embodiment of the invention, the device determines the parameter α_S according to one of the first, second or third preferred embodiments of the invention described above.

The device comprises

- means for storing values of voltage and power measurements made at the load,
- means for locally detecting an occurrence of a contingency, preferably by detecting a voltage drop of, for example, 2%.,
- means for determining the at least one parameter α_S, where the parameter describes an estimated steady state behavior of the load, from the stored voltage and power values and from measurement values that are obtained when the network is in a transient condition after the contingency has occurred, and, in a preferred embodiment,
- means for transmitting the parameter α_S to a remote device.

Such an inventive device is preferably a phasor measurement unit **7** itself, or a device associated with a phasor measurement unit **7**. The values of parameter α_S obtained by a plurality of such devices are transmitted by each device to the remote device, for example to a central data processor, in which the load flow analysis and further steps of the inventive method are performed.

List of designations

1	section of electric power network
2	bus
3	line
4	ULTC (under load tap changer)
5	generator
6	load
7	phasor measurement unit
8	interface line
31	"conting?", check for contingency
32	"meas", perform measurements
33	"parest", estimate parameters
34	"pflo", perform load flow calculation
35	"sol?", check existence of solution
36	"marg", compute power margin
37	"stabl!", perform stabilizing actions

The invention claimed is:

1. A method for the prediction of the stability of an electric power network, where said method is executed after a contingency has occurred, wherein the method comprises the steps of

a) during a time interval in which the network is in a transient condition, determining for at least one load connected to the electric power network, at least one parameter that describes an estimated steady state behavior of the at least one load,

b) executing a load flow calculation for determining a steady state equilibrium of the electric power network, using the least one parameter,

c) determining, if the load flow calculation has a solution, that a future stability of the electrical power network exists, or, if the load flow calculation does not have a solution, that a future stability of the electrical power network does not exist.

2. Method according to claim **1**, wherein the method comprises the step of determining a power margin of the electric power network, using the at least one parameter describing the estimated steady state behavior of the at least one load.

3. Method according to claim **1**, wherein the method comprises the step of taking a remedial action in order to prevent a predicted instability from occurring.

4. Method according to claim **1**, wherein determining, for one load connected by a load connection to the electric power network, the at least one parameter describing the estimated steady state behavior of the load, comprises measuring a voltage and a power flow at the load connection, where measurement intervals are approximately 20 to 250 milliseconds.

5. Method according to claim **1**, wherein a time interval in which the at least one parameter describing the estimated steady state behavior of the at least one load is determined begins at the time when a contingency is detected and has a length of approximately 1 to 20 seconds.

6. Method according to claim **1**, wherein the at least one load is modeled by the equation

$$-T_p\dot{P}+P_0\left(\frac{U}{U_0}\right)^{\alpha_S}+\frac{P_0}{U_0}\dot{U}\,T_p\,\alpha_t\left(\frac{U}{U_0}\right)^{\alpha_S-1}=P$$

where

U is a voltage at and P a power flow through a connection to the load,

$\dot{U}$ and $\dot{P}$ are their derivatives over time,

U_0 and P_0 are a nominal voltage and nominal active power, respectively,

T_p is a time constant,

and where α_S is the parameter describing the estimated steady state behavior.

7. Method according to claim **1**, wherein the load flow is an extended load flow calculation that incorporates at least one of models for under load tap changers and models that describe the behavior of at least one power generating unit.

8. Method according to claim **7**, wherein at least one of the power generating units is described by the maximum steady state reactive power that said power generating unit may provide in a steady state.

9. Method according to claim **1**, wherein the load flow calculation incorporates network parameters that are obtained prior to the occurrence of the contingency, and where said network parameters are a nominal voltage U_0 and a nominal active power measured prior to the contingency.

10. Computer program product for the prediction of the stability of an electric power network according to the invention that is loadable into an internal memory of a digital computer, and comprises computer program code means to make, when said computer program code means is loaded in the computer, the computer execute the method according to claim **1**.

11. Method according to claim **1**, wherein determining, for the at least one load connected by a load connection to the electric power network, the at least one parameter describing the estimated steady state behaviour of the at least one load, comprises measuring a voltage and a power flow at the load connection by means of a phasor measurement unit.

* * * * *

Distribution System Modeling and Analysis

by William H. Kersting

ISBN 0-8493-0812-7